



TITLE:

Synthesis, Structure, and Reactivity of Novel Zerovalent Ruthenium Complexes(Dissertation_全文)

AUTHOR(S):

Shiotsuki, Masashi

CITATION:

Shiotsuki, Masashi. Synthesis, Structure, and Reactivity of Novel Zerovalent Ruthenium Complexes. 京都大学, 2003, 博士(工学)

ISSUE DATE:

2003-03-24

URL:

<https://doi.org/10.14989/doctor.k10172>

RIGHT:

新制
工
1266

Synthesis, Structure, and Reactivity of Novel Zerovalent Ruthenium Complexes

Masashi SHIOTSUKI

2003

Synthesis, Structure, and Reactivity of Novel Zerovalent Ruthenium Complexes

Masashi SHIOTSUKI

**Department of Energy and Hydrocarbon Chemistry
Graduate School of Engineering
Kyoto University**

2003

Acknowledgment

The studies presented in this thesis are the summary of the author's work carried out during 1998–2003 at the Department of Energy and Hydrocarbon Chemistry, Graduate School of Engineering, Kyoto University.

The author wishes to express his sincerest gratitude to Professor Take-aki Mitsudo for providing a chance to study at his laboratory and for his invaluable guidance, suggestions, and innumerable instructions throughout the course of these studies. He is also grateful to Professor Sakae Uemura and Professor Masahiro Murakami for their valuable comments and discussions. He deeply thanks Associate Professor Teruyuki Kondo, Dr. Kenji Wada, and Dr. Yasuyuki Ura for their helpful discussions, valuable suggestions, and advices. Thanks are due to Mr. Toshiaki Hattori for his hearty encouragement.

The author wishes to express his appreciation to Professor Masakazu Yamashita of Doshisha University. It is his great pleasure to thank Dr. Toshiaki Suzuki, Dr. Yasuhiro Morisaki, Dr. Takumi Okada, and Dr. Takashi Mino for their hearty encouragement.

Heartfelt thanks go to Messrs. Kazuo Iida, Hiroshi Miyai, Yoshitaka Sato, and Kazuo Sadaoka for their valuable collaboration in this work. He is indebted to all the members of the research group of Professor Take-aki Mitsudo.

The author is deeply grateful to the Research Fellowship of the Japan Society for the Promotion of Science for Young Scientists from April 2000.

Finally, the author would like to give his greatest thanks to his parents, brothers, and my fiancée Chisa Naomoto for their understanding and continuous encouragement throughout the study.

January 2003

Masashi Shiotsuki

Contents

General Introduction		1
Chapter 1	Reaction of Ru(1-6- η -cyclooctatriene)(η^2 -dimethyl fumarate) ₂ with Monodentate and Bidentate Phosphines: A Model Reaction of Catalytic Dimerization of Alkenes	13
Chapter 2	Synthesis, Structure, and Reactivity of a Stable Zerovalent Ruthenium Aqua Complex	47
Chapter 3	Synthesis and Structure of Novel Zerovalent Ruthenium Complexes with Three Pyridine Ligands or Tridentate Pyridyl Ligands	67
Chapter 4	Synthesis and Structures of Novel Zerovalent Ruthenium <i>p</i> -Quinone Complexes and a Bimetallic <i>p</i> -Biquinone Complex	95
Chapter 5	Synthesis of Novel Zerovalent Ruthenium η^6 -Arene Complexes via Direct Displacement of a 1,3,5-Cyclooctatriene Ligand by Arenes	117
General Conclusion		137
List of Publications		141

General Introduction

Since the discovery of the Oxo process (hydroformylation of alkenes) in 1938,¹ organometallic chemistry has been extensively studied.² A variety of homogeneous catalytic processes such as the Reppe process (Ni),³ polymerization of alkenes by Ziegler-Natta (Ti/Al)⁴ or Kaminsky (Zr/Al)⁵ catalyst, Wacker process (Pd/Cu),⁶ and Monsanto process (Rh),⁷ have been investigated so far to produce large amounts of industrial materials.

As the base for homogeneous catalytic processes, stoichiometric reactions of organometallic compounds have received much attention. They have greatly contributed to the development of the catalytic processes² as well as the growth of organic syntheses.^{2c} The catalytic processes described above consist of combinations of fundamental reactions of organometallic complexes, represented by oxidative addition, reductive elimination, insertion, transmetalation, metathesis of alkenes, and σ -bond metathesis. Elucidation of these reactions is essential for understanding the mechanism of catalytic reactions, especially together with the kinetic and theoretical studies. The fruit of the study could enable one to design a more suited catalyst and a new catalytic system. Wilkinson and co-workers, for a typical example, studied the detailed reactivity of a rhodium complex, $\text{RhCl}(\text{PPh}_3)_3$, and elucidated the mechanism of hydrogenation of olefinic compounds using the rhodium catalyst.⁸ Up to the present, there have been numerous reports on the isolation of the intermediates of catalytic reactions, which contribute to clarify the mechanism of the reactions.⁹⁻²⁶

With respect to both catalytic and stoichiometric reactions, ruthenium chemistry has been one of major topics in organometallic chemistry for the past 20 years,²⁷ although it has lagged behind the chemistry of other transition metals such as palladium and rhodium because of its peculiarity. In a laboratory scale, various ruthenium-catalyzed reactions such as C-H, C-C, C-N, C-O, and C-S

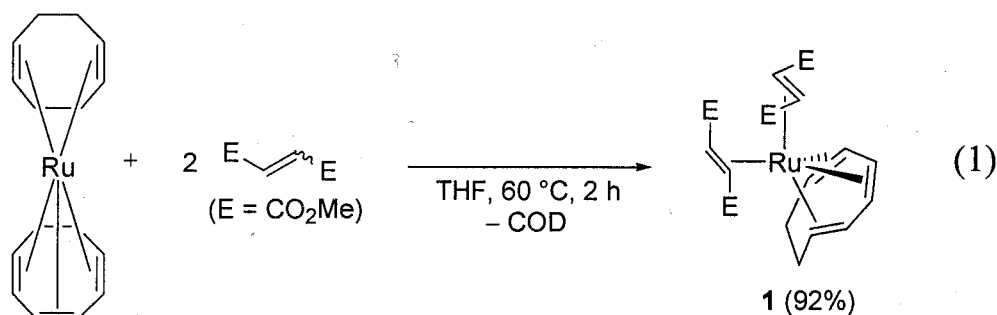
bond forming reactions have been found,²⁸ and recently catalytic cleavage reactions of these covalent bonds have also been developed.²⁸⁻³¹ In most of these reactions, the employed ruthenium catalysts are di- or higher valent complexes. It is worth noting that *zerovalent* ruthenium complexes without a CO ligand were rarely investigated in both catalytic and stoichiometric reactions until recently.³²⁻³⁹ Zerovalent ruthenium complexes are usually unstable to air and moisture due to their high reactivity, and thus the isolation and treatment of the complexes are difficult. Further, examples of zerovalent ruthenium complexes have been limited in number with the exception of a zerovalent ruthenium carbonyl cluster, $\text{Ru}_3(\text{CO})_{12}$,⁴⁰ which is commercially available and used in some catalytic reactions.^{27,41}

What is expected of zerovalent ruthenium complexes? First, the zerovalent complexes are generally conceivable to have higher reactivity due to the higher levels of the *d* orbital so that electrons become more available.⁴² Second, the zerovalent complexes tend to accept oxidative addition of various bonds because the ruthenium center of the complex has relatively condensed electron density.⁴² On the contrary, the reductive elimination from the divalent ruthenium complex giving a zerovalent one is hard to proceed. These facts suggest that the isolation of divalent ruthenium intermediates of a catalytic reaction could be achieved, in which oxidative addition of substrates is the key step. In fact, it is known that a covalent bond such as C-H,⁴³ C-O,^{43,44} C-S,⁴⁵ and O-H^{43,46} bond, can be cleaved by a zerovalent ruthenium complex via oxidative addition to form an isolable divalent ruthenium complex.

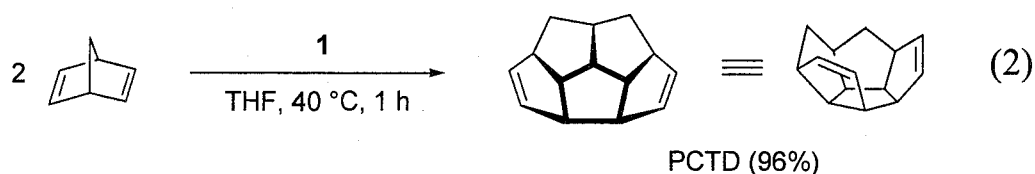
It is very important to control the high reactivity of a zerovalent ruthenium complex. Low-valent complexes are known to be stabilized by the coordination of a strong π -acid ligand,^{42,43a} and hence it is necessary to design a ligand that has suitable π -acidity and occupies an appropriate number of vacant sites of the zerovalent ruthenium complex. The coordination number of a zerovalent ruthenium complex is usually five, which is less than that of higher valent

ruthenium complexes; six for a divalent and seven for a tetravalent ruthenium complex.

Recently, we found that a novel zerovalent ruthenium complex, $\text{Ru}(\eta^6\text{-cot})(\text{dimethyl fumarate})_2$ [**1**; cot = 1,3,5-cyclooctatriene], is formed readily by the reaction of $\text{Ru}(\eta^4\text{-cod})(\eta^6\text{-cot})$ [cod = 1,5-cyclooctadiene] with dimethyl fumarate or dimethyl maleate (eq 1).^{32a} Complex **1** is the first example derived from $\text{Ru}(\eta^4\text{-cod})(\eta^6\text{-cot})$ by replacement of the $\eta^4\text{-cod}$ ligand, not the $\eta^6\text{-cot}$ ligand, by two moles of an olefin. Complex **1** possesses two electron-deficient olefins and a tridentate olefinic ligand. It is known that the cot ligand is labile and displays a versatile coordination mode. The coordination mode of the cot ligand in zerovalent ruthenium complexes varies from η^6 to η^4 , η^5 , $\eta^1\text{:}\eta^3$, etc., during reactions.⁴⁷⁻⁵⁰ This tendency is of particular interest, and may also play a crucial role in determining catalytic reactivity by controlling the access of a reagent to the metal center.



Indeed, complex **1** showed excellent catalytic activity in the unusual dimerization of bicyclo[2.2.1]hepta-2,5-diene (2,5-norbornadiene) to give pentacyclo[6.6.0.0^{2,6}.0^{3,13}.0^{10,14}]tetradeca-4,11-diene (PCTD) involving C–C bond cleavage and reconstruction of a novel carbon skeleton under very mild conditions (eq 2).^{32a}



In this thesis, the synthesis of various low-valent, especially zerovalent, ruthenium complexes using **1** as the starting material is discussed. In response to the type of ligand, complex **1** shows diverse reactivity to generate novel complexes by ligand exchange or bond activation. Corresponding to the high and unique catalytic reactivity of **1**, the complexes derived from **1** are expected to show specific features in both catalytic and stoichiometric reactions.

In Chapter 1, the reactions of **1** with mono- or bidentate phosphorus ligands are described. Complex **1** reacts with monodentate tertiary phosphine ligands to give novel zerovalent ruthenium phosphine complexes, $\text{Ru}(\eta^6\text{-cot})(\text{dimethyl fumarate})(\text{L})$ [L = tertiary phosphine], in high yields. These complexes show fluxionality based on the rotation of the cot ligand, which was elucidated by the NMR spectra and the X-ray crystallography. The preparation of novel bidentate phosphine complexes, $\text{Ru}(\text{dimethyl fumarate})(\text{dppe})_2$ and $\text{Ru}(\text{alkenyl})(\text{alkyl})(\text{dppe})$ [dppe = 1,2-bis(diphenylphosphino)ethane], is discussed, which are obtained by the reaction of **1** with dppe. $\text{Ru}(\text{alkenyl})(\text{alkyl})(\text{dppe})$ is generated through the activation of the sp^2 carbon–hydrogen bond of dimethyl fumarate, and then the insertion of the other dimethyl fumarate into the formed ruthenium–hydrogen bond. The treatment of $\text{Ru}(\text{alkenyl})(\text{alkyl})(\text{dppe})$ with 60 atm of carbon monoxide (CO) gives dimers of dimethyl fumarate and $\text{Ru}(\text{CO})_3(\text{dppe})$ via reductive elimination. A series of the reactions is considered as model reactions of catalytic dimerization of olefinic compounds.

Chapter 2 deals with the synthesis of a zerovalent ruthenium aqua complex. The reaction of **1** with dppe in 1,2-dichloroethane/water affords $\text{Ru}(\text{dimethyl fumarate})_2(\text{dppe})(\text{H}_2\text{O})$, which is the first example of a stable and isolable zerovalent ruthenium aqua complex. The X-ray crystallography of this complex indicates that the coordination of a water molecule to the ruthenium center is stabilized by two hydrogen bonds with the carbonyl oxygen atoms of the dimethyl fumarate ligands. The reactivity of $\text{Ru}(\text{dimethyl fumarate})_2(\text{dppe})(\text{H}_2\text{O})$ toward CO is examined.

Chapter 3 presents the synthesis and structure of novel zerovalent ruthenium complexes with three pyridine ligands or tridentate pyridyl ligands. Complex **1** reacts with an excess amount of pyridine to give a novel ruthenium zerovalent complex, $\text{Ru}(\text{dmfm})_2(\text{pyridine})_3$. The reaction of **1** with a tridentate pyridyl ligand (N-N'-N) such as 2,2':6',2''-terpyridine (terpy), 2,6-bis(imino)pyridyl ligands, and 2,6-bis[(4*S*)-(-)-isopropyl-2-oxazolin-2-yl]pyridine (*i*-Pr-Pybox) gives novel zerovalent ruthenium complexes, $\text{Ru}(\text{dmfm})_2(\text{N-N'-N})$. The obtained complexes are the first example of an isolable zerovalent ruthenium complex having tridentate nitrogen ligands.

Chapter 4 describes the synthesis of novel zerovalent ruthenium complexes with *p*-quinone derivatives, $\text{Ru}(\eta^6\text{-cot})(p\text{-quinone})$ via the reaction of **1** with *p*-quinones. The reaction of **1** with *p*-biquinone gives a novel binuclear zerovalent complex $\{\text{Ru}(\eta^6\text{-cot})\}_2(p\text{-biquinone})$ in which *p*-biquinone coordinates to two isolated $\text{Ru}(\text{cot})$ moieties and the two $\text{Ru}(\text{cot})$ groups are located at endo positions.

In Chapter 5, the synthesis of novel zerovalent arene complexes bearing two dimethyl fumarate ligands, $\text{Ru}(\eta^6\text{-arene})(\text{dimethyl fumarate})_2$ (arene = benzene, toluene, *p*-xylene, mesitylene, etc.), is discussed in detail. Although some additives are essential for the conventional synthesis of zerovalent ruthenium arene complexes, this chapter provides a direct synthetic method of these complexes via the ligand exchange of **1** with arenes.

Thus, the synthesis, structure, and reactivity of novel zerovalent ruthenium complexes derived from **1** are fully discussed.

References

- (1) (a) Rölen, O. German Patent 849548, 1938. (b) Rölen, O. *Angew. Chem.* **1948**, 60, 62. (c) Rölen, O. *ChEd Chem. Exp. Didakt.* **1977**, 3, 119. (d) Cornils, B.; Herrmann, W. A.; Rasch, M. *Angew. Chem., Int. Ed. Engl.* **1994**, 33, 2144. (e) Pruetz, R. L. *Adv. Organomet. Chem.* **1979**, 17, 1.
- (2) (a) Hegedus, L. S. *Transition Metals in the Synthesis of Complex Organic Molecules*; University Science Books: Mill Valley, CA, 1994. (b) Collman, J. P.; Hegedus, L. S.; Norton, J. R.; Finke, R. G. *Principle and Applications of Organotransition Metal Chemistry*; University Science Books: Mill Valley, CA, 1987. (c) Beller, M.; Bolm, C. *Transition Metals for Organic Synthesis*; WILEY-VCH: Weinheim, Germany, 1998. (d) *Applied Homogeneous Catalysis with Organometallic Compounds*; Cornils, B.; Herrmann, W. A. Eds.; VCH Publishers: New York, NY, 1996; Vol. 1 and 2. (e) Gerlovh, M.; Constable, E. C. *Transition Metal Chemistry*; VCH Publishers: New York, NY, 1994. (f) Elschenbroich, C.; Salzer, A. *Organometallics*, 2nd ed.; VCH Publishers: New York, NY, 1992. (g) Komiya, S. *Synthesis of Organometallic Compounds*; JOHN WILEY & SONS: Chichester, U. K., 1997. (h) Brandsma, L.; Vasilevsky, S. F.; Verkruijsse, H. D. *Application of Transition Metal Catalysts in Organic Synthesis*; Springer: Berlin, Germany, 1998.
- (3) (a) Reppe, W. German Patent 855110, 1939. (b) Reppe, W. *Neue Entwicklungen auf dem Gebiete der Chemie des Acetylens und des Kohlenoxyds*; Springer: New York, NY, 1949. (c) Reppe, W. *Liebigs Ann. Chem.* **1953**, 582, 1. (d) Reppe, W.; Kröper, H. *Liebigs Ann. Chem.* **1953**, 582, 38. (e) Reppe, W.; Kröper, H.; von Kutepow, N.; Pistor, H. J. *Liebigs Ann. Chem.* **1953**, 582, 72. (f) Reppe, W.; Kröper, H.; Pistor, H. J. Weissbarth, O. *Liebigs Ann. Chem.* **1953**, 582, 87. (g) Reppe, W.; Vetter, H. *Liebigs Ann. Chem.* **1953**, 582, 133.

- (4) (a) Ziegler, K. In *Advances in Organometallic Chemistry*; Academic Press: New York, NY, 1968; Vol. 6, p 1. (b) Natta, G. *Scientific American* **1961**, 205, 33. (c) Ziegler, K.; Natta, G. *Angew. Chem.* **1964**, 76, 545.
- (5) (a) Sinn, H.; Kaminsky, W. *Adv. Organomet. Chem.* **1980**, 18, 99. (b) Sinn, H.; Kaminsky, W.; Vollmer, H. J.; Woldt, R. *Angew. Chem.* **1980**, 92, 396.
- (6) (a) Shmidt, J.; Hafner, W.; Jira, R.; Sieber, R.; Sedlmeier, J.; Sabel, A. *Angew. Chem., Int. Ed. Engl.* **1962**, 1, 80. (b) Shmidt, J. *J. Chem. and Ind.* **1962**, 54.
- (7) (a) Forster, D. *Adv. Organomet. Chem.* **1979**, 17, 255. (b) Roth, J. F.; Craddock, J. H.; Hershman, A.; Paulik, F. E. *CHEMTECH* **1971**, 347.
- (8) (a) Jordan, R. B. *Reaction Mechanisms of Inorganic and Organometallic Systems*, Oxford University Press: Oxford, U.K. 1991. (b) Harpern, J. In *Organotransition Metal Chemistry*; Ishii, Y.; Tsutsui, M. Eds.; Plenum: New York, NY, 1975; p 109. (c) Osborn, J. A.; Jardine, F. H.; Young, J. F.; Wilkinson, G. *J. Chem. Soc. A* **1966**, 1711.
- (9) Allegra, G.; Natta, G. *Chem. Commun.* **1967**, 1263.
- (10) Wilke, G. *Angew. Chem.* **1963**, 75, 10.
- (11) Matsumoto, T.; Furukawa, J. *J. Polymer Sci.* **1968**, B6, 896; **1969**, B7, 541.
- (12) James, B. R.; Rattray, A. D.; Wang, D. K. W. *J. Chem. Soc., Chem. Commun.* **1976**, 792.
- (13) Hills, J.; Francis, J.; Ori, M.; Tsutsui, M. *J. Am. Chem. Soc.* **1974**, 96, 4800.
- (14) (a) Komiya, S.; Yamamoto, A. *Chem. Lett.* **1975**, 475. (b) Komiya, S.; Ito, T.; Cowie, M.; Yamamoto, A.; Ibers, J. A. *J. Am. Chem. Soc.* **1976**, 98, 3874.
- (15) (a) McLain, S. J.; Schrock, R. R. *J. Am. Chem. Soc.* **1978**, 100, 1315. (b) McLain, S. J.; Sancho, J. Schrock, R. R. *J. Am. Chem. Soc.* **1980**, 102, 560.

- (16) Brookhart, M.; Sabo-Etienne, S. *J. Am. Chem. Soc.* **1991**, *113*, 2777.
- (17) Bianchini, C.; Casares, J.; Peruzzini, M.; Romerosa, A.; Zanobini, F. *J. Am. Chem. Soc.* **1996**, *118*, 4585.
- (18) Kondo, T.; Uenoyama, S.; Fujita, K.; Mitsudo, T. *J. Am. Chem. Soc.* **1999**, *121*, 482.
- (19) (a) Nishibayashi, Y.; Wakiji, I.; Hidai, M. *J. Am. Chem. Soc.* **2000**, *122*, 11019. (b) Nishibayashi, Y.; Wakiji, I.; Ishii, Y.; Uemura, S.; Hidai, M. *J. Am. Chem. Soc.* **2001**, *123*, 3393. (c) Nishibayashi, Y.; Inada, Y.; Hidai, M.; Uemura, S. *J. Am. Chem. Soc.* **2002**, *124*, 7900. (d) Nishibayashi, Y.; Yoshikawa, M.; Hidai, M.; Uemura, S. *J. Am. Chem. Soc.* **2002**, *124*, 11846.
- (20) Brunel, J. M.; Hirlemann, M.-H.; Heumann, A.; Buono, G. *Chem. Commun.* **2000**, 1869.
- (21) Sessanta o Santi, A.; Milani, B.; Zangrando, E.; Mestroni, G. *Eur. J. Inorg. Chem.* **2000**, 2351.
- (22) Smith, P. D.; Millar, A. J.; Young, C. G.; Ghosh, A.; Basu, P. *J. Am. Chem. Soc.* **2000**, *122*, 9298.
- (23) del Río, I.; van Koten, G.; Lutz, M.; Spek, A. L. *Organometallics* **2000**, *19*, 361.
- (24) Mino, T.; Shiotsuki, M.; Yamamoto, N.; Suenaga, T.; Sakamoto, M.; Fujita, T.; Yamashita, M. *J. Org. Chem.* **2001**, *66*, 1795.
- (25) Minglana, J. J. G.; Okazaki, M.; Tobita, H.; Ogino, H. *Chem. Lett.* **2002**, 406.
- (26) Ricci, A.; Angelucci, F.; Bassetti, M.; Lo Sterzo, C. *J. Am. Chem. Soc.* **2002**, *124*, 1060.
- (27) (a) Bennett, M. A.; Matheson, T. W. In *Comprehensive Organometallic Chemistry*; Wilkinson, G., Stone, F. G. A., Abel, E. W., Eds.; Pergamon Press: Oxford, U.K. 1982; Vol. 4, p 931. (b) Shriver, D. F.; Bruce, M. I. In *Comprehensive Organometallic Chemistry II*; Abel, E. W., Stone, F. G. A.;

- Wilkinson, G, Eds.; Pergamon Press: Oxford, U.K. 1995; vol. 7.
- (28) For reviews: (a) Trost, B. M.; Toste, F. D.; Pinkerton, A. B. *Chem. Rev.* **2001**, *101*, 2067. (b) Kondo, T.; Mitsudo, T. *Chem. Rev.* **2000**, *100*, 3205. (c) Naota, T.; Takaya, H.; Murahashi, S. *Chem. Rev.* **1998**, *98*, 2599. (d) Mitsudo, T.; Hori, Y.; Watanabe, Y. *J. Organomet. Chem.* **1987**, *334*, 157.
- (29) (a) *Activation of Unreactive Bonds and Organic Synthesis*; Murai, S., Ed.; Springer: New York, 1999. (b) Hill, C. L *Activation and Funtionalization of Alkanes*; JOHN WILEY & SONS: Chichester, U. K., 1989.
- (30) (a) Ritleng, V.; Sirlin, C.; Pfeffer, M. *Chem. Rev.* **2002**, *102*, 1731. (b) Kakiuchi, F.; Murai, S. *Acc. Chem. Res.* **2002**, *35*, 826.
- (31) (a) Mitsudo, T.; Kondo, T. *Synlett*, **2000**, 309. (b) Jennings, P. W.; Johnson, L. L. *Chem. Rev.* **1994**, *94*, 2241. (c) Crabtree, R. H. *Chem. Rev.* **1985**, *85*, 245. (d) Bishop, K. C., III. *Chem. Rev.* **1976**, *76*, 461.
- (32) (a) Mitsudo, T.; Suzuki, T.; Zhang, S.-W.; Imai, D.; Fujita, K.; Manabe, T.; Shiotsuki, M.; Watanabe, Y.; Wada, K.; Kondo, T. *J. Am. Chem. Soc.* **1999**, *121*, 1839. (b) Suzuki, T.; Shiotsuki, M.; Wada, K.; Kondo, T.; Mitsudo, T. *Organometallics* **1999**, *18*, 3671. (c) Suzuki, T.; Shiotsuki, M.; Wada, K.; Kondo, T.; Mitsudo, T. *J. Chem. Soc., Dalton Trans.* **1999**, 4231. (d) Shiotsuki, M.; Suzuki, T.; Kondo, T.; Wada, K.; Mitsudo, T. *Organometallics* **2000**, *19*, 5733. (e) Shiotsuki, M.; Miyai, H.; Ura, Y.; Suzuki, T.; Kondo, T.; Mitsudo, T. *Organometallics* **2002**, *21*, 4960.
- (33) (a) Mitsudo, T.; Kokuryo, K.; Takegami, Y. *J. Chem. Soc., Chem. Commun.* **1976**, 722. (b) Mitsudo, T.; Watanabe, Y. *J. Organomet. Chem.* **1987**, *334*, 157. review (c) Mitsudo, T.; Zhang, S.-W.; Nagao, M.; Watanabe, Y. *Chem. Commun.* **1991**, 598. (d) Mitsudo, T.; Zhang, S.-W.; Satake, N.; Kondo, T.; Watanabe, Y. *Tetrahedron Lett.* **1992**, *33*, 5533. (e) Mitsudo, T.; Takagi, M.; Zhang, S.-W.; Watanabe, Y. *J. Organomet. Chem.* **1992**, *423*, 405. (f) Mitsudo, T.; Zhang, S.-W.; Kondo, T.; Watanabe, Y. *Tetrahedron Lett.* **1992**, *33*, 341. (g) Zhang, S.-W.; Mitsudo, T.; Kondo, T.;

- Watanabe, Y. *J. Org. Chem.* **1993**, 450, 197. (h) Kondo, T.; Hiraishi, N.; Morisaki, Y.; Wada, K.; Watanabe, Y.; Mitsudo, T. *Organometallics* **1998**, 17, 2131. (i) Kondo, T.; Okada, T.; Suzuki, T.; Mitsudo, T. *J. Organomet. Chem.* **2001**, 622, 149.
- (34) (a) Fukuoka, A.; Nagano, T.; Furuta, S.; Yoshizawa, M.; Hirano, M.; Komiya, S. *Bull. Chem. Soc. Jpn.* **1998**, 71, 1409. (b) Alvarez, S. G.; Hasegawa, S.; Hirano, M.; Komiya, S. *Tetrahedron Lett.* **1998**, 39, 5209. (c) Sato, T.; Komine, N.; Hirano, M.; Komiya, S. *Chem. Lett.* **1999**, 441. (d) Hirano, M.; Takenaka, A.; Mizuho, Y.; Hiraoka, M.; Komiya, S. *J. Chem. Soc., Dalton Trans.* **1999**, 3209. (e) Hirano, M.; Kiyota, S.; Imoto, M.; Komiya, S. *Chem. Commun.* **2000**, 1679.
- (35) (a) Bouachir, F.; Chaudret, B.; Neibecker, D.; Tkatchenko, I. *Angew. Chem.* **1985**, 97, 347. (b) Chaudret, B.; Poiblan, R. *Organometallics* **1985**, 4, 1722. (c) Bouachir, F.; Chaudret, B.; Tkatchenko, I. *J. Chem. Soc., Chem. Commun.* **1986**, 94. (d) Bouachir, F.; Chaudret, B.; Dahan, F.; Agbossou, F.; Tkatcheko, I. *Organometallics* **1991**, 10, 455. (e) Pan, C.; Pelzer, K.; Philippot, K.; Chaudret, B.; Dassenoy, F.; Lecante, P.; Casanove, M.-J. *J. Am. Chem. Soc.* **2001**, 123, 7584.
- (36) Airoidi, M.; Deganello, G.; Gennaro, G. *J. Organomet. Chem.* **1980**, 187, 391.
- (37) (a) Pertici, P.; Vitulli, G.; Bigelli, C.; Lazzaroni, R. *J. Organomet. Chem.* **1984**, 2775, 113. (b) Bennett, M. A.; Neumann, H.; Thomas, M.; Wang, X. Q.; Pertici, P.; Salvadori, P.; Vitulli, G. *Organometallics* **1991**, 10, 3237.
- (38) Murata, M.; Kawakita, K.; Asana, T.; Watanabe, S.; Masuda, Y. *Bull. Chem. Soc. Jpn.* **2002**, 75, 825.
- (39) Wiles, J. A.; Bergens, S. H.; Vanhessche, K. P. M.; Dobbs, D. A.; Rautenstrauch, V. *Angew. Chem., Int. Ed.* **2002**, 40, 914.
- (40) (a) Eady, C. R.; Jackson, P. F.; Johnson, B. F. G.; Lewis, J.; Malatesta, M. C.; McPartlin, M.; Nelson, W. J. H. *J. Chem. Soc., Dalton Trans.* **1980**,

383. (b) Bruce, M. I.; Jensen, C. M.; Jones, N. L. *Inorg. Chem. Synth.* **1989**, 26, 259. (c) James, B. R.; Rempel, G. L.; Teo, W. K. *Inorg. Chem. Synth.* **1976**, 16, 45. (d) Churchill, M. R.; Hollander, F. J.; Hutchinson, J. P. *Inorg. Chem.* **1977**, 16, 2655.
- (41) For recent leading papers, e.g. (a) Choi, J. H.; Kim, Y. H.; Nam, S. H.; Shin, S. T.; Kim, M.-J.; Park, J. *Angew. Chem., Int. Ed.* **2002**, 41, 2373. (b) Kakiuchi, F.; Igi, K.; Matsumoto, M.; Hayamizu, T.; Chatani, N.; Murai, S. *Chem. Lett.* **2002**, 396. (c) Kang, S.-K.; Kim, K.-J.; Hong, Y.-T. *Angew. Chem., Int. Ed.* **2002**, 41, 1584. (d) Kondo, T.; Kaneko, T.; Taguchi, Y.; Nakamura, A.; Okada, T.; Shiotsuki, M.; Ura, Y.; Wada, K.; Mitsudo, T. *J. Am. Chem. Soc.* **2002**, 124, 6824. (e) Ko, S.; Na, Y.; Chang, S. *J. Am. Chem. Soc.* **2002**, 124, 750. (f) Chatani, N.; Asaumi, T.; Yorimitsu, S.; Ikeda, T.; Kakiuchi, F.; Murai, S. *J. Am. Chem. Soc.* **2001**, 123, 10935. (g) Ragaini, S.; Cenini, S.; Gasperini, M. *J. Mol. Catal. A Chem.* **2001**, 174, 51. (h) Yoneda, E.; Zhang, S.-W.; Onitsuka, K.; Takahashi, S. *Tetrahedron Lett.* **2001**, 42, 5459. (i) Ragaini, F.; Cenini, S.; Dompé, M.; Gallo, E.; Moret, M. *Organometallics* **2001**, 20, 3390. (j) Kondo, T.; Nakamura, A.; Okada, T.; Suzuki, N.; Wada, K.; Mitsudo, T. *J. Am. Chem. Soc.* **2000**, 122, 6319.
- (42) Crabtree, R. H. *The Organometallic Chemistry of the Transition Metals, Third Edition*; Wiley-Interscience: New York, 2001; pp 38.
- (43) For example of C–H bond cleavage by Ru(0), see: (a) Chatt, J.; Davidson, J. M. *J. Chem. Soc.* **1965**, 843. (b) Hsu, G. C.; Kosar, W. P.; Jones, W. D. *Organometallics* **1994**, 13, 385. (c) Ozawa, F.; Yamagami, I.; Yamamoto, A. *J. Organomet. Chem.* **1994**, 473, 265. (d) Bianchini, C.; Casares, J. A.; Osman, R.; Pattison, D. I.; Peruzzini, M.; Perutz, R. N.; Zonobini, F. *Organometallics* **1997**, 16, 4611. (e) Hirano, M.; Kurata, N.; Marumo, T.; Komiya, S. *Organometallics* **1998**, 17, 501. (f) Hartwig, J. F.; Bergman, R. G.; Andersen, R. A. *J. Am. Chem. Soc.* **1991**, 113, 3404.

- (44) For example of C–O bond cleavage by Ru(0), see: (a) Komiya, S.; Suzuki, J.; Miki, K.; Kasai, N. *Chem. Lett.* **1987**, 1287. (b) Komiya, S.; Srivastava, R. S.; Yamamoto, A.; Yamamoto, T. *Organometallics* **1985**, *4*, 1504.
- (45) For example of C–S bond cleavage by Ru(0), see: (a) Planas, J. G.; Hirano, M.; Komiya, S. *Chem. Commun.* **1999**, 1793. (b) Planas, J. G.; Hirano, M.; Komiya, S. *Chem. Lett.* **1998**, 123. (c) Planas, J. G.; Marumo, T.; Ichikawa, Y.; Hirano, M.; Komiya, S. *J. Chem. Soc., Dalton Trans.* **2000**, 2613.
- (46) For example of O–H bond cleavage by Ru(0), see: (a) Burn, M. J.; Bergman, R. G. *J. Organomet. Chem.* **1994**, *472*, 43. (b) Burn, M. J.; Fickes, M. G.; Hartwig, J. F.; Hollander, F. J.; Bergman, R. G. *J. Am. Chem. Soc.* **1993**, *115*, 5875.
- (47) Komiya, S.; Planas, J. G.; Onuki, K.; Lu, Z.; Hirano, M. *Organometallics* **2000**, *19*, 4051.
- (48) Deganello, G.; Mantovani, A.; Sandrini, P. L.; Pertici, P.; Vitulli, G. *J. Organomet. Chem.* **1977**, *135*, 215.
- (49) Pertici, P.; Vitulli, G.; Porzio, W.; Zocchi, M.; Barili, P. L.; Deganello, G. *J. Chem. Soc., Dalton Trans.* **1983**, 1553.
- (50) Chaudret, B.; Commenges, G.; Poilblanc, R. *J. Chem. Soc., Chem. Commun.* **1982**, 1388.

Chapter 1

Reaction of Ru(1-6- η -cyclooctatriene)(η^2 -dimethyl fumarate)₂ with Monodentate and Bidentate Phosphines: A Model Reaction of Catalytic Dimerization of Alkenes

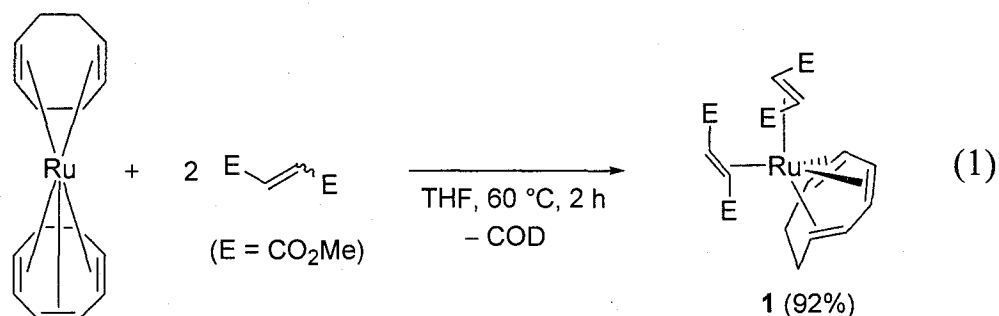
Abstract

Ru(η^6 -cot)(η^2 -dimethyl fumarate)₂ [**1**; cot = 1,3,5-cyclooctatriene] reacts with monodentate tertiary phosphine ligands, PPh₃, PMePh₂, PMe₂Ph, and PEt₃, to give novel ruthenium(0) phosphine complexes, Ru(η^6 -cot)(η^2 -dimethyl fumarate)(L) [L = PPh₃ (**2a**), PMePh₂ (**2b**), PMe₂Ph (**2c**), and PEt₃ (**2d**)], in high yields. The structures of **2b**, **2c**, and **2d** were determined by X-ray analysis. The coordination geometry of the complexes around the central ruthenium atom is a highly distorted trigonal bipyramid, but the orientation of coordination of the cot ligand differs from each other. Complexes **2a–d** show dynamic behavior in solution involving the rotation of the cyclooctatriene ligand around the axis, which lies between the ruthenium metal and the center of the cot ligand. Novel bidentate phosphine complexes, Ru(η^2 -dimethyl fumarate)(dppe)₂ (**4**) and Ru[C(CO₂CH₃)=CHC(O)OCH₃][CH(CO₂CH₃)CH₂C(O)OCH₃](dppe) (**5**) [dppe = 1,2-bis(diphenylphosphino)ethane] were prepared by the reaction of **1** with dppe in high yields. The structures of **4** and **5** were determined by single-crystal X-ray diffraction. Complex **5** is generated through the activation of the sp² carbon-hydrogen bond of dimethyl fumarate and then the insertion of the other dimethyl fumarate into the formed ruthenium–hydrogen bond, followed by the coordination of the two carbonyl groups of the esters. The treatment of **5** with 1 atm of carbon monoxide afforded Ru[C(CO₂CH₃)=CHC(O)OCH₃][CH(CO₂-CH₃)CH₂C(O)OCH₃](CO)(dppe) (**6**), the structure of which was confirmed by

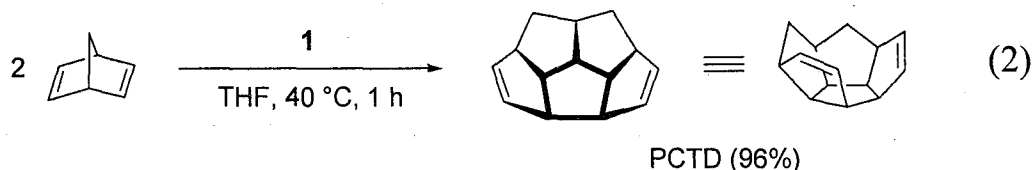
X-ray analysis. Complex **5** reacted with 60 atm of carbon monoxide to give dimers of dimethyl fumarate and $\text{Ru}(\text{CO})_3(\text{dppe})$ via reductive elimination.

Introduction

Over the past 20 years, the chemistry of ruthenium complexes has been developed extensively.¹ Especially, low-valent ruthenium complexes whose oxidation state is 0 or II, such as $\text{Ru}(1\text{-}2:5\text{-}6\text{-}\eta\text{-cod})(\eta^6\text{-cot})$ [cod = 1,5-cyclooctadiene, cot = 1,3,5-cyclooctatriene],^{2,3} $\text{Ru}_3(\text{CO})_{12}$,^{1c,4} $\text{RuH}_2(\text{PPh}_3)_4$,^{5,6} and $\text{RuH}_2(\text{CO})(\text{PPh}_3)_3$,^{7,8} have attracted much attention due to their high reactivity in both stoichiometric and catalytic reactions. Quite recently, we have found a novel zerovalent complex, $\text{Ru}(\eta^6\text{-cot})(\text{dmfm})_2$ [**1**; dmfm = dimethyl fumarate], which is readily prepared by the reaction of $\text{Ru}(1\text{-}2:5\text{-}6\text{-}\eta\text{-cod})(\eta^6\text{-cot})$ with dimethyl fumarate or dimethyl maleate (eq 1).⁹ Complex **1** shows



high catalytic reactivity for a unique dimerization of 2,5-norbornadiene to afford a novel half-cage compound, pentacyclo[6.6.0.0^{2,6}.0^{3,13}.0^{10,14}]tetradeca-4,11-diene (PCTD), via carbon-carbon bond cleavage and reconstruction of the carbon skeleton under very mild reaction conditions (eq 2).⁹

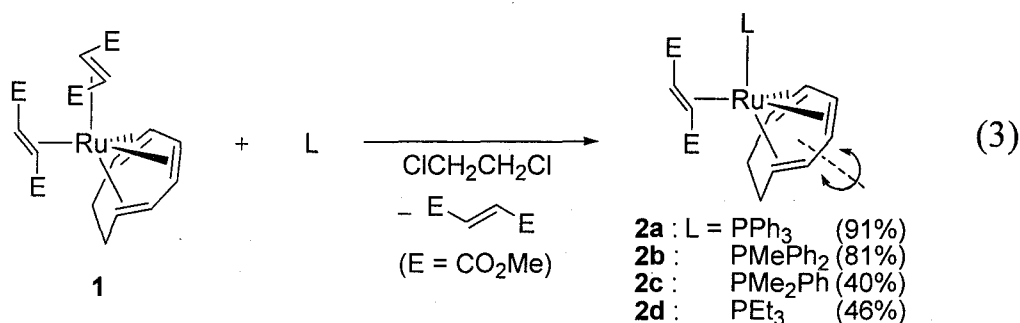


Complex **1** can be regarded as a new starting material for zerovalent ruthenium complexes. It reacts with mono- or bidentate amine ligands to give first examples of completely characterized and isolated zerovalent ruthenium complexes with amine ligands.^{10,11}

Studies on the reactivity and the catalytic activity of **1** led us to examine the character of the related ruthenium complexes having phosphine ligands. Here we report the synthesis and the structures of novel zero- or divalent ruthenium complexes with mono- and bidentate phosphine ligands derived from **1**.

Results and Discussion

Reaction of $\text{Ru}(\eta^6\text{-cot})(\text{dmfm})_2$ (1**) with Monodentate Phosphine Ligands.** $\text{Ru}(\eta^6\text{-cot})(\text{dmfm})_2$ (**1**) readily reacted with monodentate phosphine ligands (L) in 1,2-dichloroethane at room temperature to give novel zerovalent ruthenium complexes, $\text{Ru}(\eta^6\text{-cot})(\text{dmfm})(\text{L})$ [L = PPh_3 (**2a**), PMePh_2 (**2b**), PMe_2Ph (**2c**), and PEt_3 (**2d**)], in good to high yields by the substitution of one of the dimethyl fumarates with L (eq 3).



The structures of **2b–d** in solid-state were determined by single-crystal X-ray diffraction (Figures 1–3). Crystal data and the details of data collection of **2b–d** are given in Table 1, and lists of the selected bond distances and bond angles of **2b–d** are provided in Tables 2 and 3, respectively. The structure of each complex can be rationalized as a distorted trigonal bipyramid in which the

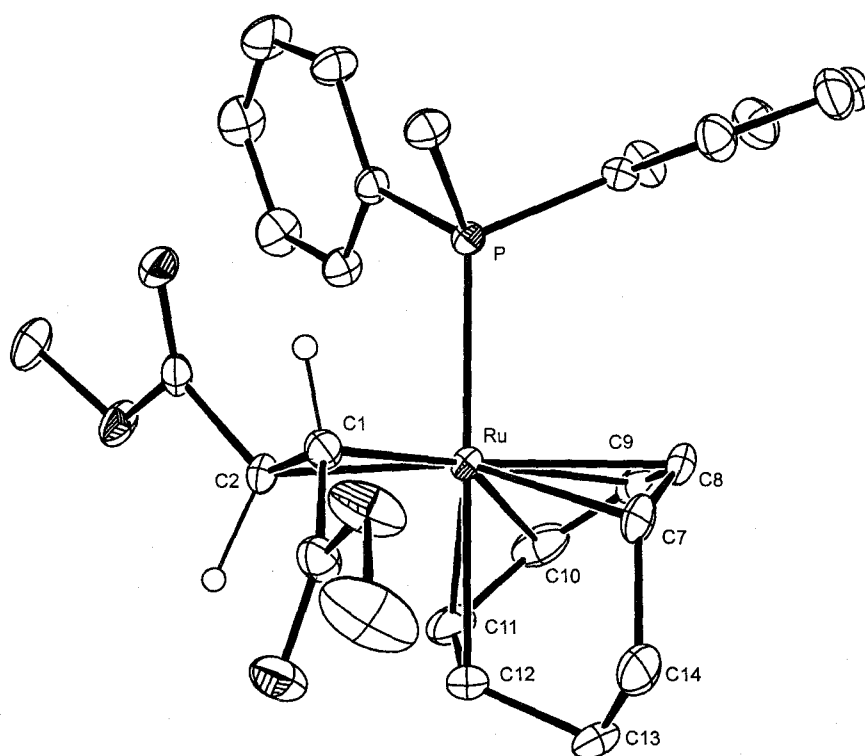


Figure 1. ORTEP drawing of the structure of **2b**. A part of hydrogen atoms are omitted for clarity.

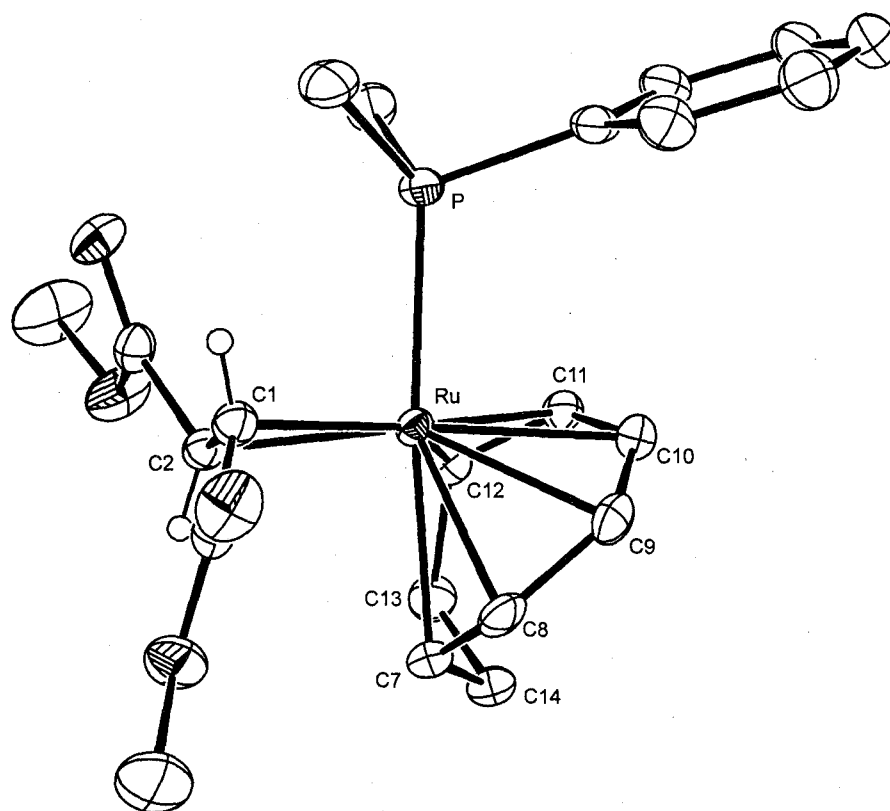


Figure 2. ORTEP drawing of the structure of **2c**. A part of hydrogen atoms are omitted for clarity.

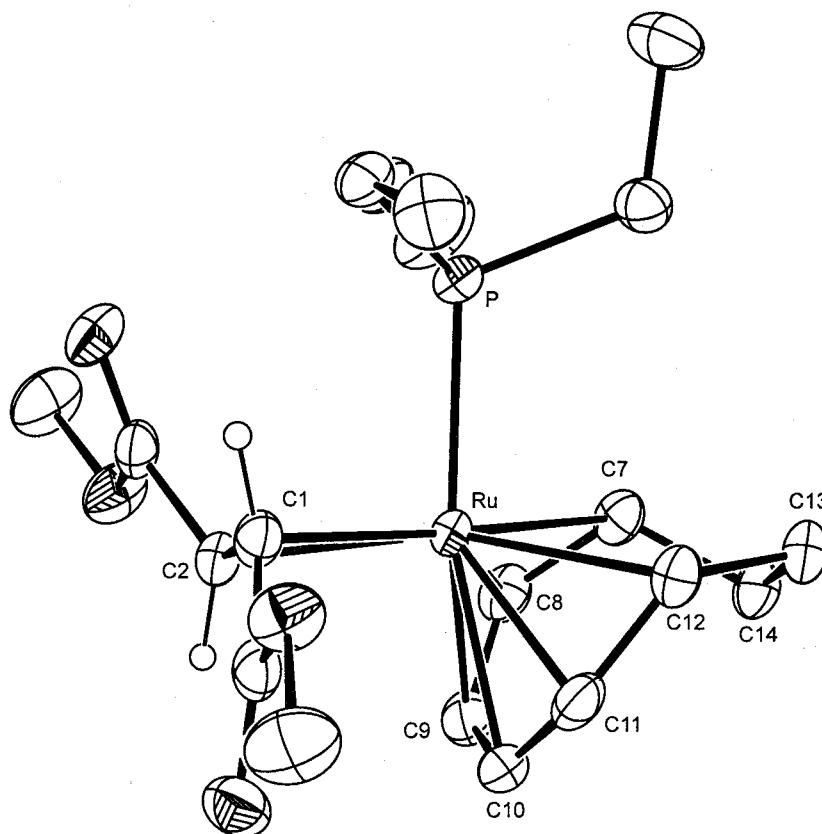


Figure 3. ORTEP drawing of the structure of **2d**. A part of hydrogen atoms are omitted for clarity.

phosphine and one of the olefinic bonds of cot occupy two axial positions, and dimethyl fumarate and the other two olefinic bonds of cot occupy the equatorial positions. The molecular structures of **2b–d** are apparently similar to each other, but it should be noted that the cot ligand of each complex coordinates in a different way. In Figure 1, the olefinic carbons of cyclooctatriene located at the axial position in **2b** are C(11) and C(12), but in Figure 2, those in **2c** are C(7) and C(8). Figure 3 shows that the olefinic carbons C(9) and C(10) in **2d** occupy the axial position.

In the solid-state ^{13}C NMR (CP-MAS) and ^{31}P NMR (MASGHD) spectra of **2b–d**, all peaks were consistent with the structures shown in the X-ray analyses. However, the solid-state ^{13}C (CP-MAS) and ^{31}P NMR (MASGHD) spectra of **2a** were complicated; the latter spectrum showed at least three broad peaks. This result will be discussed below.

Table 1. Summary of Crystal Data, Collection Data, and Refinement of **2b**, **2c**, and **2d**

	2b	2c	2d
formula	C ₂₇ H ₃₁ O ₄ PRu	C ₂₂ H ₂₉ O ₄ PRu	C ₂₀ H ₃₃ O ₄ PRu
fw	551.58	489.51	469.52
crystal color	yellow	orange	orange
crystal system	monoclinic	monoclinic	triclinic
space group	<i>P</i> 2 ₁ / <i>c</i>	<i>P</i> 2 ₁ / <i>a</i>	<i>P</i> $\bar{1}$
<i>a</i> (Å)	11.656(9)	14.814(8)	9.637(8)
<i>b</i> (Å)	22.27(2)	9.180(6)	13.189(6)
<i>c</i> (Å)	10.812(5)	16.121(8)	8.749(3)
α (deg)	90	90	92.25(3)
β (deg)	62.47(5)	100.83(4)	103.35(4)
γ (deg)	90	90	77.07(4)
<i>V</i> (Å ³)	2489(3)	2153(1)	1054(1)
<i>Z</i>	4	4	2
<i>D</i> _{calcd} (g/cm ³)	1.472	1.510	1.479
μ (Mo K α) (cm ⁻¹)	7.25	8.27	8.41
<i>T</i> (°C)	23.0	23.0	23.0
2 θ _{max} (deg)	55.0	55.0	55.0
no. of measd rflns	11519	5126	5130
no. of obsd rflns	5034	4272	4056
residuals: <i>R</i> ; <i>R</i> _w	0.037; 0.055	0.030; 0.036	0.028; 0.030
GOF	2.12	1.71	0.72

Table 2. Selected Bond Distances for **2b**, **2c**, and **2d**

	bond distances (Å)		
	2b	2c	2d
Ru–P	2.387(2)	2.3653(9)	2.3483(9)
Ru–C(1)	2.145(5)	2.133(3)	2.189(3)
Ru–C(2)	2.152(4)	2.119(3)	2.181(3)
Ru–C(7)	2.243(5)	2.312(3)	2.266(3)
Ru–C(8)	2.228(5)	2.205(3)	2.166(3)
Ru–C(9)	2.266(5)	2.268(3)	2.229(3)
Ru–C(10)	2.277(6)	2.258(3)	2.220(3)
Ru–C(11)	2.198(5)	2.207(3)	2.164(3)
Ru–C(12)	2.274(5)	2.216(4)	2.341(3)
C(1)–C(2)	1.450(6)	1.434(5)	1.441(4)
C(7)–C(8)	1.425(9)	1.403(5)	1.402(5)
C(8)–C(9)	1.434(10)	1.424(5)	1.414(5)
C(9)–C(10)	1.422(10)	1.408(5)	1.412(5)
C(10)–C(11)	1.425(9)	1.430(5)	1.430(5)
C(11)–C(12)	1.390(8)	1.412(5)	1.409(5)
C(12)–C(13)	1.514(7)	1.507(5)	1.503(4)
C(13)–C(14)	1.52(1)	1.509(6)	1.495(5)
C(14)–C(7)	1.515(8)	1.500(5)	1.525(4)

Table 3. Selected Bond Angles for **2b**, **2c**, and **2d**^a

	bond angles (deg)		
	2b	2c	2d
P–Ru–C(1)	90.5(1)	88.72(10)	89.81(9)
P–Ru–C(2)	93.8(1)	97.63(9)	97.79(9)
P–Ru–C(7)	107.4(2)	174.37(9)	88.22(9)
P–Ru–C(8)	90.3(1)	141.2(1)	109.7(1)
P–Ru–C(9)	92.2(2)	110.2(1)	147.0(1)
P–Ru–C(10)	108.0(2)	91.48(9)	165.23(9)
P–Ru–C(11)	137.0(2)	86.68(9)	129.7(1)
P–Ru–C(12)	173.0(2)	102.34(10)	96.04(9)
P–Ru–Ctr(1–2)	92.3	93.3	94.0
P–Ru–Ctr(7–8)	99.2	159.4	99.0
P–Ru–Ctr(9–10)	100.6	101.3	162.1
P–Ru–Ctr(11–12)	155.4	94.7	112.3
Ctr(1–2)–Ru–Ctr(7–8)	131.0	97.2	139.5
Ctr(1–2)–Ru–Ctr(9–10)	154.5	151.9	100.7
Ctr(1–2)–Ru–Ctr(11–12)	97.7	134.1	119.3
Ctr(7–8)–Ru–Ctr(9–10)	68.8	62.6	63.1
Ctr(7–8)–Ru–Ctr(11–12)	91.1	90.6	90.6
Ctr(9–10)–Ru–Ctr(11–12)	62.4	68.8	68.9

^a Definitions: Ctr(1–2), the center of C(1) and C(2); Ctr(7–8), the center of C(7) and C(8); Ctr(9–10), the center of C(9) and C(10); Ctr(11–12), the center of C(11) and C(12).

The ¹H NMR spectra of **2a–d** in solution showed reversible temperature dependence exhibiting fluxional behavior of these complexes. The spectra of **2b** are representative (Figure 4). At room temperature, two sets of broad peaks were observed, showing the presence of at least two species. The species with smaller and larger peaks are assigned to **A** and **B**, respectively. It is noteworthy that these two sets of peaks were observed even when a single crystal of **2b** was dissolved in CDCl₃ or CD₂Cl₂. The spectra for **A** have shown very characteristic peaks of methylene protons of cyclooctatriene at very high field (ca. –1 and 0 ppm), while the spectrum of **B** has no such signals at high field. At –40 °C, the signals of **A** became sharper and the signals for the methylene groups shifted to higher field, while the peaks for **B** became very broad, and the signals for the cyclooctatriene ligand of **B** almost disappeared. At –70 °C, the peaks for **A** mostly remained with some broadening, and two sets of broad peaks appeared,

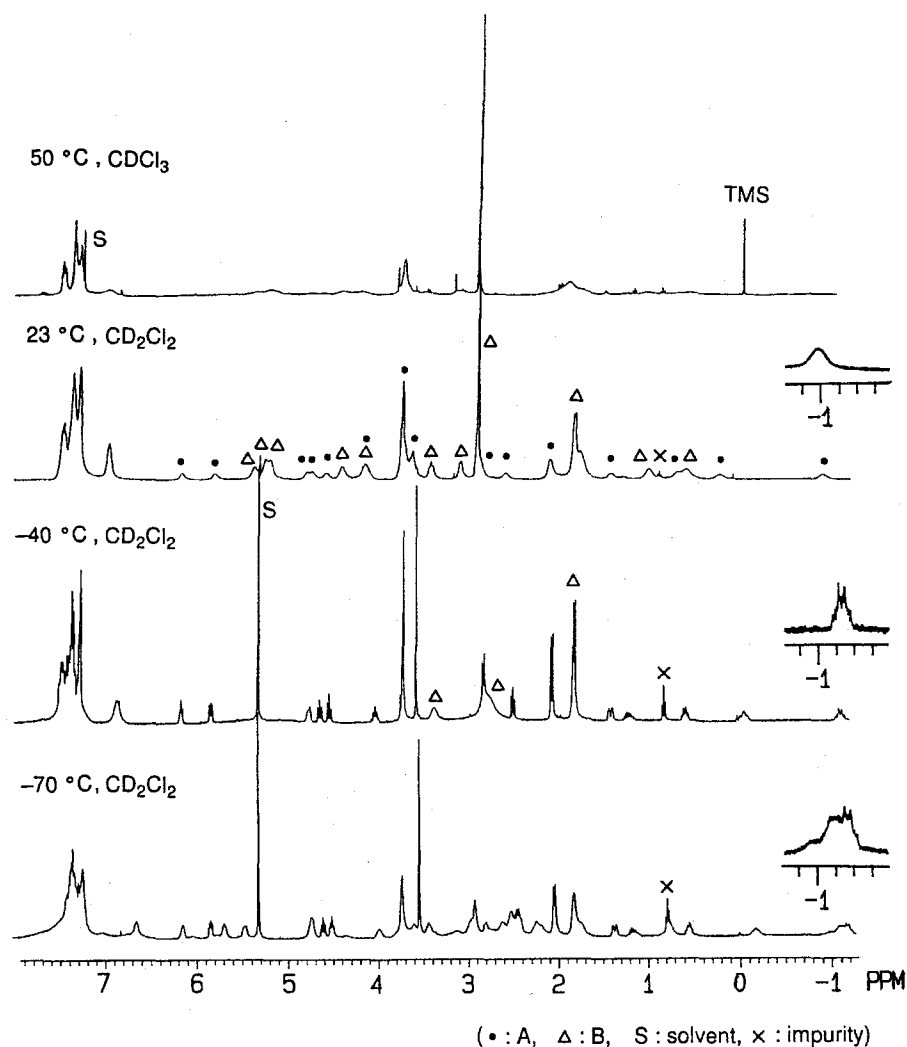


Figure 4. Variable-temperature ^1H NMR spectra of **2b**.

suggesting the rate of conversion between two isomers, **C** and **D** (see $^{31}\text{P}\{^1\text{H}\}$ NMR spectra in Figure 5), became slow. On the other hand, at 50 °C all peaks became broad. Unfortunately, the dynamic process at the higher temperatures could not be studied in detail because these complexes decomposed irreversibly.

The $^{13}\text{C}\{^1\text{H}\}$ NMR spectra of **2b–d** in solution at room temperature showed two sets of peaks (see Experimental Section). One of them was sharper and the other was broader, which correspond to the ^1H NMR spectra. Variable-temperature ^{13}C NMR spectra were not informative because of their complexity.

Variable-temperature $^{31}\text{P}\{^1\text{H}\}$ NMR spectra of **2a–d** in solution were very informative. The representative spectra for **2b** are shown in Figure 5. The signal for the free phosphine was not detected. As one peak corresponds to one

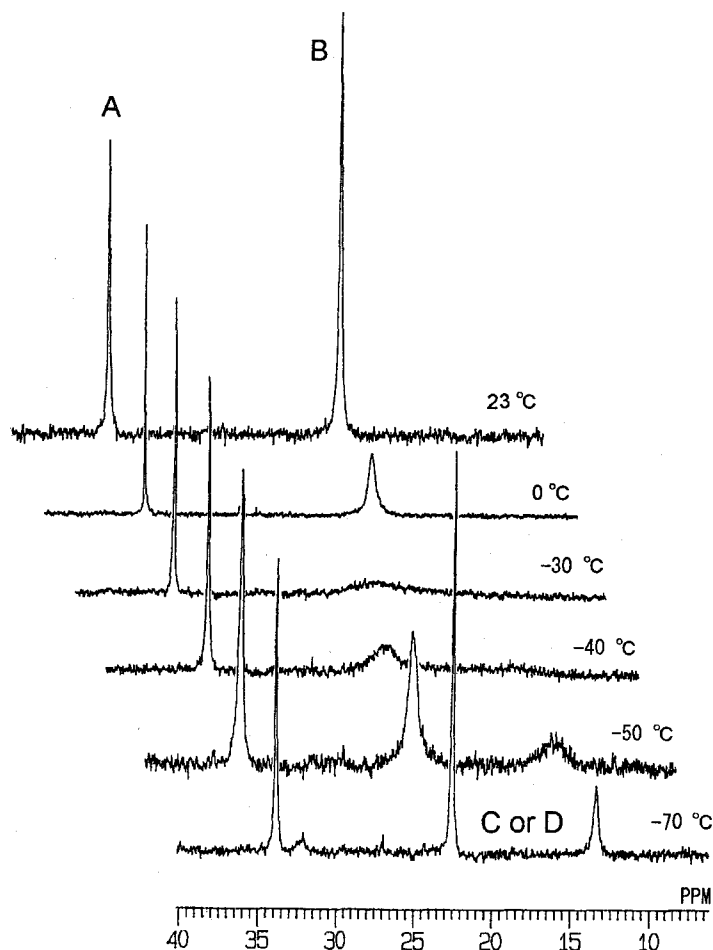
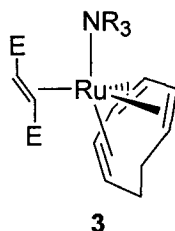


Figure 5. Variable-temperature ^{31}P NMR spectra of **2b**.

complex, the results in Figure 5 clearly show that at room temperature two species **A** and **B** ($= \text{C} + \text{D}$) are present in the solution. At $-30 \sim -40\text{ }^{\circ}\text{C}$, the broader peak almost disappeared and the signals of **A** remained. At $-70\text{ }^{\circ}\text{C}$, three peaks, which correspond to **A**, **C**, and **D**, were observed. These results are fully consistent with those observed in the ^1H NMR study for **2b**. The fluxional behavior between **C** and **D** is not frozen completely even at $-70\text{ }^{\circ}\text{C}$.

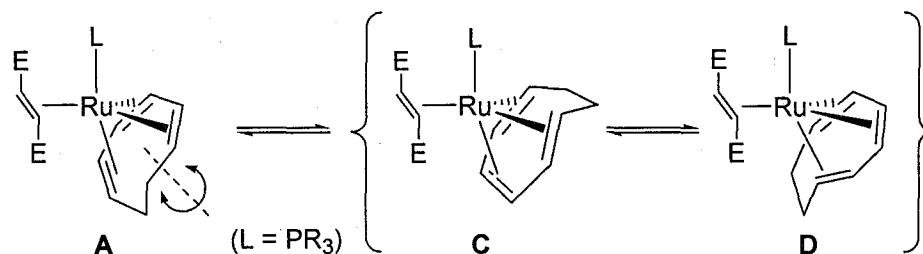
The phenomenon that the signals assigned to the methylene protons of the coordinated cot appear at higher field at lower than $-70\text{ }^{\circ}\text{C}$ can be reasonably explained by the partial freezing of the conformers of the two methylene groups.¹²

Taking into account the ^1H NMR spectrum of the amine complex **3**,¹¹ which shows the methylene signals at higher fields (-0.98 and 0.85 ppm), the structure of **A** was deduced to be that shown in Scheme 1. The disappearance of the peaks



for the other cot ligand in **2b** isomer at $-40\text{ }^{\circ}\text{C}$ could be explained by the coalescence of the signals for the structures **C** and **D** in Scheme 1. The structures of **A**, **C**, and **D** correspond to those of **2c**, **2b**, and **2d**, respectively.

Scheme 1. A Possible Mechanism for the Isomerization of **2a–d**



The solid-state ^{31}P NMR (MASGHD) spectrum of **2a** showed three broad peaks (vide supra) and this is because the cot ligand of **2a** would not be fixed in only one orientation even in solid state. The amine complex **3** does not show fluxionality even at over $50\text{ }^{\circ}\text{C}$, and its coordination mode of cot corresponds to that of **A** in Scheme 1.¹¹ Hence, the present isomerization of **2a–d** is due to the weakness of the bond between Ru and cot, which is attributed to the π -back bonding to both the phosphorus and the dimethyl fumarate ligands from the ruthenium center.

The rotation of the coordinated dimethyl fumarate should be considered.¹³ Figure 4 shows that the coalescence of the two methoxy peaks due to the rotation of the dimethyl fumarate in **2b-A** is observed around at room temperature and those in **2b-C** and **2b-D** at over $-40\text{ }^{\circ}\text{C}$.

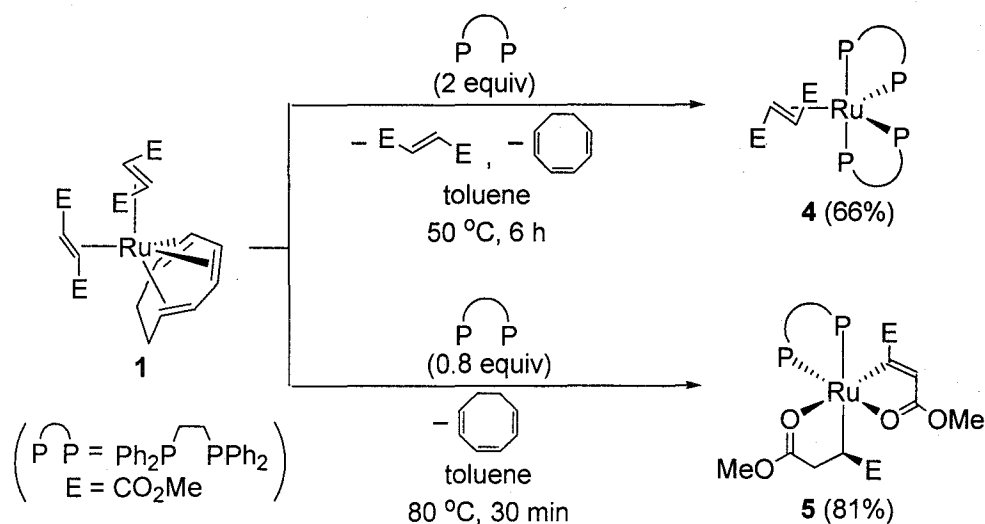
The possibility of the substitution of the coordinated dimethyl fumarate was examined. The rate of the formation of $\text{Ru}(\eta^6\text{-cot})(\text{H}_3\text{CO}_2\text{CCD}=\text{CDCO}_2\text{CH}_3)\text{-(PMePh}_2\text{)}$ (**2b-d₂**) on mixing **2b** and $\text{H}_3\text{CO}_2\text{CCD}=\text{CDCO}_2\text{CH}_3$ (dimethyl

fumarate- d_2) in CD_2Cl_2 was proved to be comparatively slow; only 8.9% of the dimethyl fumarate was substituted after 30 min at room temperature (see Experimental Section). The result indicates that the dissociation and recoordination of dimethyl fumarate in **2b** is essentially indifferent to the isomerization of **2b**.

The ^1H and ^{31}P NMR spectra of **2a**, **2c**, and **2d** in solution also showed principally the same behavior as those of **2b**. At $-30 \sim -40\text{ }^\circ\text{C}$, the ^1H NMR spectra of these complexes showed the signals only for the structure **A** with the characteristic signals of the methylene protons at high magnetic field. The ^{31}P NMR spectra of **2a**, **2c**, and **2d** in solution showed two peaks at room temperature and three peaks at $-70\text{ }^\circ\text{C}$. These results show that these complexes exhibit similar fluxional behavior to that of **2b** in solution independently on the structures in solid state.

Reaction of $\text{Ru}(\eta^6\text{-cot})(\text{dmfm})_2$ (1**) with a Bidentate Phosphine Ligand, 1,2-Bis(diphenylphosphino)ethane.** The reaction of $\text{Ru}(\eta^6\text{-cot})(\text{dmfm})_2$ (**1**) with 2 equiv of 1,2-bis(diphenylphosphino)ethane [dppe] in toluene at $50\text{ }^\circ\text{C}$ for 6 h afforded a new complex, $\text{Ru}(\text{dmfm})(\text{dppe})_2$ (**4**) in 66% yield (Scheme 2).

Scheme 2. Reactions of $\text{Ru}(\eta^6\text{-cot})(\text{dmfm})_2$ (**1**) with dppe



On the other hand, the treatment of **1** with 0.8 equiv of dppe in toluene at 80 °C for 30 min gave a novel complex $\text{Ru}[\text{C}(\text{CO}_2\text{CH}_3)=\text{CHC}(\text{O})\text{OCH}_3][\text{CH}(\text{CO}_2\text{CH}_3)\text{CH}_2\text{C}(\text{O})\text{OCH}_3](\text{dppe})$ (**5**) in 81% yield (Scheme 2). The structures of **4** and **5** were deduced on the basis of ^1H and $^{13}\text{C}\{^1\text{H}\}$ NMR and IR spectra and were exactly confirmed by X-ray analysis. The X-ray structures of **4** and **5** are shown in Figures 6 and 7. Crystal data and the details of data collection of **4** and **5** are given in Table 4, and lists of the selected bond distances and bond angles of **4** and **5** are provided in Tables 5 and 6, respectively.

The structure of **4** is represented by a trigonal bipyramid, in which dimethyl fumarate occupies an equatorial position. The two phosphorus atoms of dppe occupy an axial and an equatorial position, respectively, and the other dppe coordinates in the same way. Figure 6 shows that the geometry of the structure of **4** is C_2 symmetry. Complex **4** is an analogue of the known complex, $\text{Ru}\{1,2\text{-bis}(\text{dimethylphosphino})\text{ethane}\}(\eta^2\text{-ethylene})$.¹⁴

Table 4. Summary of Crystal Data, Collection Data, and Refinement of **4**, **5**, and **6**

	4	5	6
formula	$\text{C}_{38}\text{H}_{56}\text{O}_4\text{P}_4\text{Ru}$	$\text{C}_{38}\text{H}_{40}\text{O}_8\text{P}_2\text{Ru}$	$\text{C}_{39}\text{H}_{40}\text{O}_9\text{P}_2\text{Ru}$
fw	1042.04	787.75	815.76
crystal color	yellow	orange	yellow
crystal system	monoclinic	monoclinic	monoclinic
space group	$P2_1/n$	$P2_1/n$	$P2_1/n$
a (Å)	12.85(1)	10.38(3)	13.198(6)
b (Å)	19.48(2)	19.95(3)	20.720(4)
c (Å)	19.77(1)	17.40(4)	13.837(3)
β (deg)	93.03(6)	94.7(2)	96.13(3)
V (Å ³)	4940(6)	3593(12)	3762(1)
Z	4	4	4
D_{calcd} (g/cm ³)	1.401	1.456	1.440
μ (Mo $K\alpha$) (cm ⁻¹)	4.95	5.77	5.56
T (°C)	23.0	23.0	23.0
$2\theta_{\text{max}}$ (deg)	55.0	55.2	55.0
no. of measd reflections	11670	8751	8995
no. of obsd reflections	4107	6781	5015
residuals: R ; R_w	0.052; 0.061	0.031; 0.033	0.038; 0.040
GOF	0.73	2.83	0.64

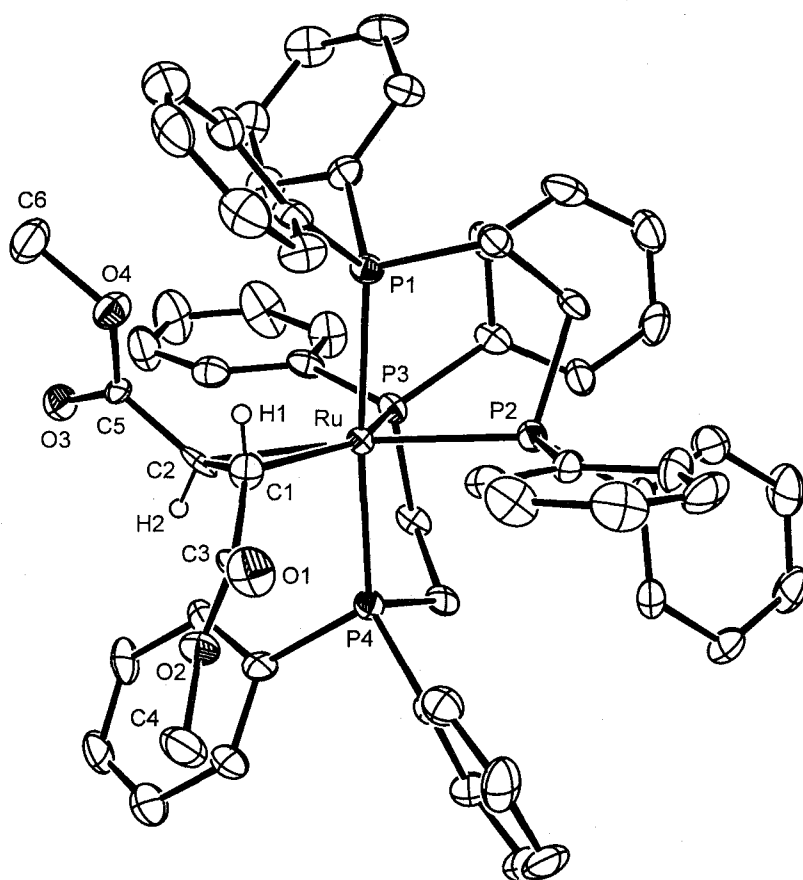


Figure 6. ORTEP drawing of the structure of **4**. Some hydrogen atoms are omitted for clarity.

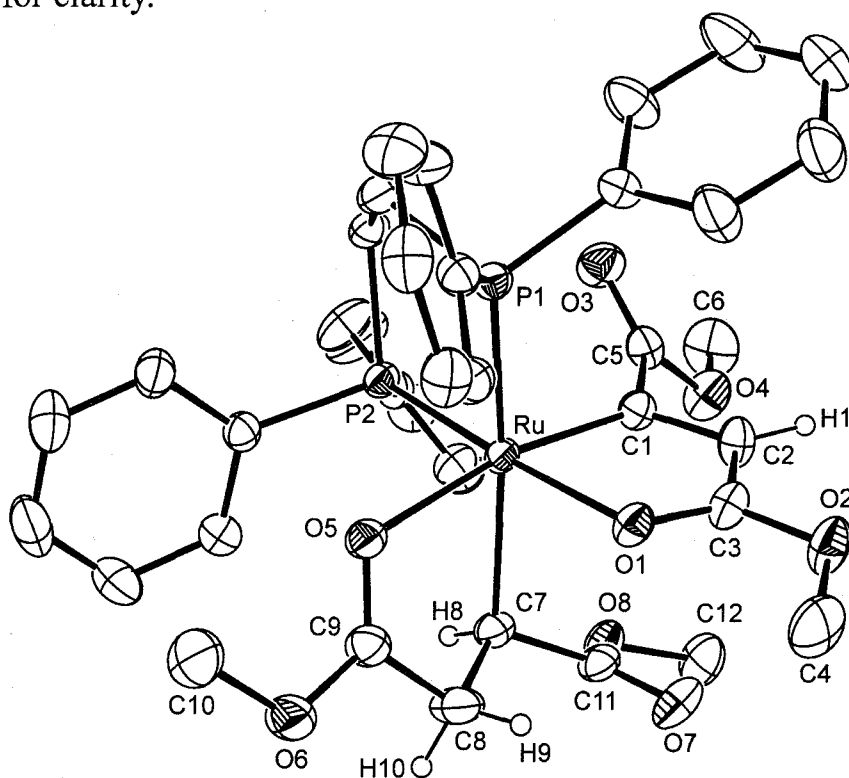


Figure 7. ORTEP drawing of the structure of **5**. Hydrogen atoms of methyl groups and dppe are omitted for clarity.

Table 5. Selected Bond Distances and Angles for **4**^a

bond distances (Å)			
Ru–C(1)	2.218(10)	Ru–C(2)	2.192(10)
Ru–P(1)	2.411(3)	Ru–P(2)	2.377(3)
Ru–P(3)	2.372(3)	Ru–P(4)	2.355(3)
bond angles (deg)			
P(1)–Ru–P(2)	81.28(9)	P(1)–Ru–P(3)	97.1(1)
P(1)–Ru–P(4)	175.10(10)	P(2)–Ru–P(3)	95.67(9)
P(2)–Ru–P(4)	93.88(10)	P(3)–Ru–P(4)	82.6(1)
Ctr(1–2)–Ru–P(1)	91.8	Ctr(1–2)–Ru–P(2)	134.4
Ctr(1–2)–Ru–P(3)	130.0	Ctr(1–2)–Ru–P(4)	92.2

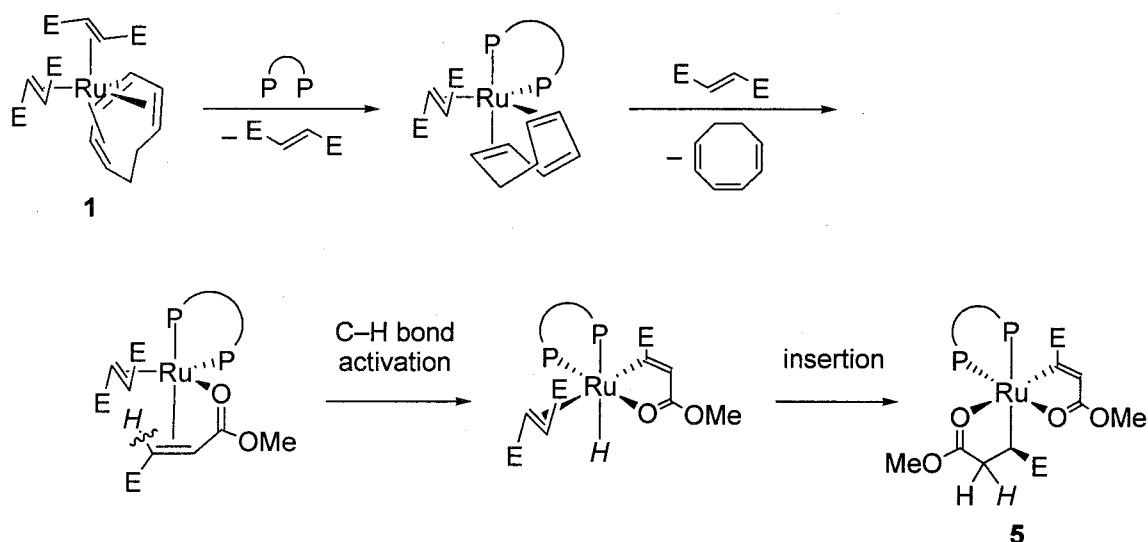
^a Definitions: Ctr(1–2), the center of C(1) and C(2).

Table 6. Selected Bond Distances and Angles for **5**

bond distances (Å)			
Ru–P(1)	2.289(3)	Ru–P(2)	2.230(4)
Ru–O(1)	2.181(4)	Ru–O(5)	2.235(2)
Ru–C(1)	1.979(3)	Ru–C(7)	2.241(4)
C(1)–C(2)	1.365(5)	C(1)–C(5)	1.494(4)
C(2)–C(3)	1.425(4)	C(7)–C(8)	1.525(4)
C(8)–C(9)	1.478(5)		
bond angles (deg)			
P(1)–Ru–P(2)	84.2(2)	P(1)–Ru–O(1)	92.8(2)
P(1)–Ru–O(5)	93.63(8)	P(1)–Ru–C(1)	91.3(1)
P(1)–Ru–C(7)	169.58(8)	P(2)–Ru–O(1)	176.50(6)
P(2)–Ru–O(5)	93.08(8)	P(2)–Ru–C(1)	99.3(1)
P(2)–Ru–C(7)	99.2(2)	O(1)–Ru–O(5)	88.86(9)
O(1)–Ru–C(1)	79.0(1)	O(1)–Ru–C(7)	84.1(2)
O(5)–Ru–C(1)	167.10(9)	O(5)–Ru–C(7)	76.4(1)
C(1)–Ru–C(7)	97.9(2)		

As Figure 7 shows, the structure of **5** is represented by an octahedral. Complex **5** has β -methoxycarbonylalkenyl and β -methoxycarbonylalkyl chelate ligands. The β -methoxycarbonylalkenyl group coordinates to the ruthenium center with an sp^2 carbon atom C(1) and a carbonyl oxygen atom O(1). This ligand can be generated by the activation of the sp^2 C–H bond of the dimethyl fumarate in **1**. The β -methoxycarbonylalkyl group coordinates with C(7) and a carbonyl oxygen atom O(5). This ligand is derived from the dimethyl fumarate

Scheme 3. A Plausible Mechanism of the Formation of **5**



that inserted into the formed Ru-H bond. Since C(7) and the ruthenium center in **5** are chiral, the formation of several diastereomers is expected. The NMR data of **5**, however, revealed that no diastereomer was formed. Reactions of **1** with other bidentate phosphines such as bis(diphenylphosphino)methane [dppm], 1,3-bis(diphenylphosphino)propane [dppp] and 1,4-bis(diphenylphosphino)butane [dppb] were attempted, but no isolable complex was formed. A plausible mechanism of the formation of **5** is shown in Scheme 3. The dimethyl fumarate ligand and one of the olefinic bonds of cyclooctatriene in **1** dissociate, and then dppe coordinates with both phosphorus atoms to generate an intermediate, an analogue of the reported zerovalent ruthenium bidentate nitrogen complex, $\text{Ru}(1\text{-}2:5\text{-}6\text{-}\eta\text{-cot})(\text{dmfm})(\text{L}_2)$ [$\text{L}_2 = 2,2'$ -bipyridyl or 1,10-phenanthroline] which is readily prepared by the reaction of **1** with bidentate nitrogen ligands.¹⁰ Then the cyclooctatriene ligand dissociates and the removed dimethyl fumarate coordinates again. The activation of the sp^2 C-H bond of the dimethyl fumarate ligand occurs, followed by the insertion of the other dimethyl fumarate into the formed Ru-H bond to form **5**.

Complex **5** readily reacts with 1 atm of carbon monoxide to give **6** (eq 4). The reductive elimination to afford the dimer of dimethyl fumarate did not occur under the condition. The structure of **6** was deduced on the basis of

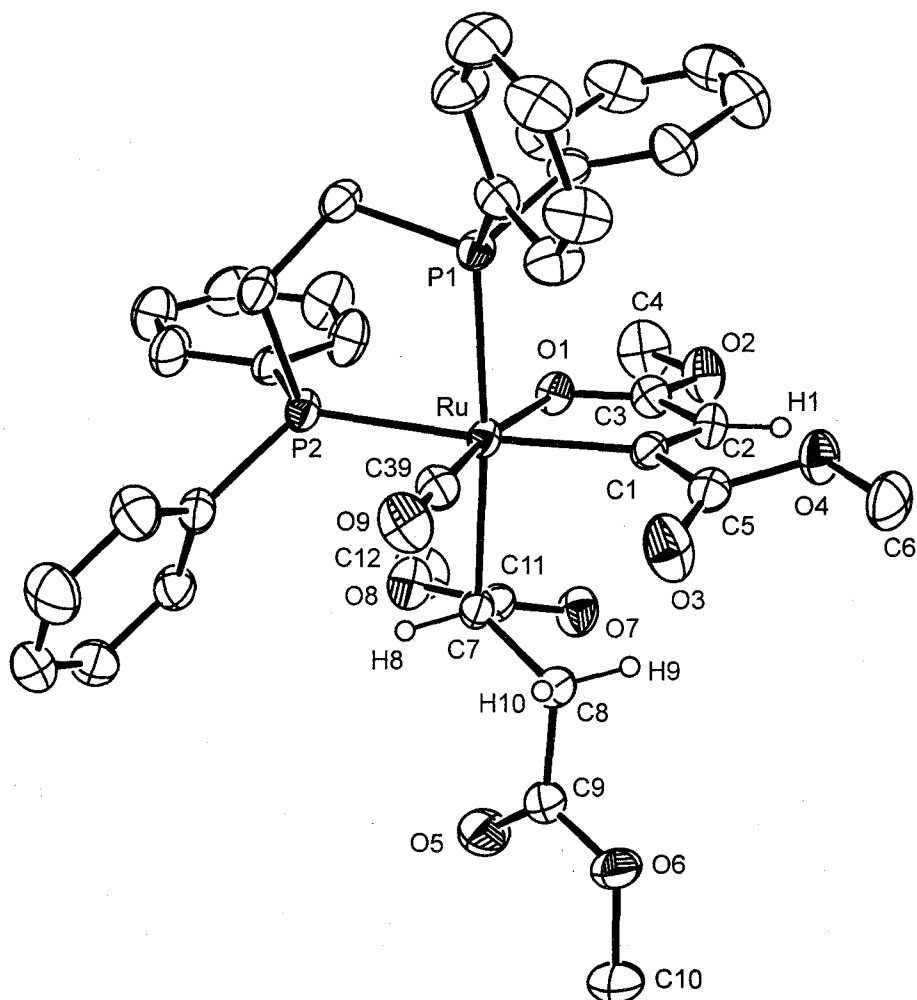
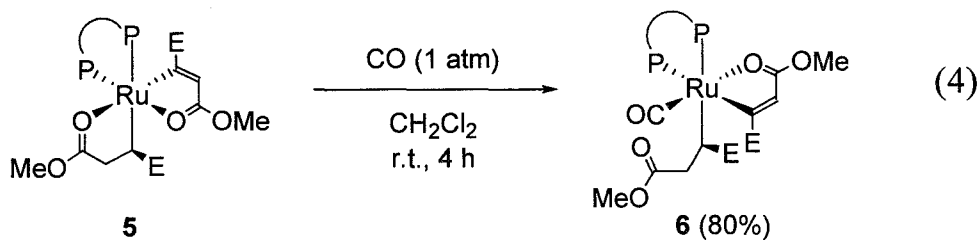


Figure 8. ORTEP drawing of the structure of **6**. Hydrogen atoms of methyl groups and the dppe ligand are omitted for clarity.

^1H and $^{13}\text{C}\{^1\text{H}\}$ NMR and IR spectra and exactly confirmed by X-ray analysis.

The structure of **6** is shown in Figure 8. Crystal data and the details of data collection of **6** are given in Table 4, and lists of the selected bond distances and bond angles of **6** are provided in Table 7. The reaction appears to be a direct substitution reaction of the coordinated methoxy carbonyl group with carbon

Table 7. Selected Bond Distances and Angles for **6**

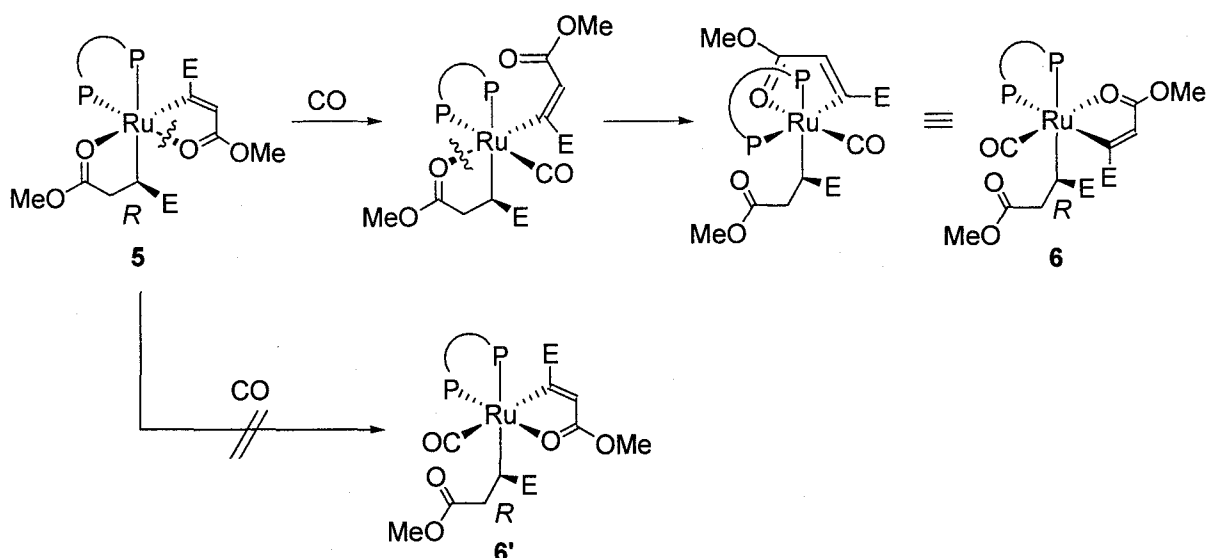
bond distances (Å)			
Ru–P(1)	2.369(1)	Ru–P(2)	2.392(1)
Ru–O(1)	2.179(3)	Ru–C(1)	2.072(4)
Ru–C(7)	2.237(4)	Ru–C(39)	1.820(5)
C(1)–C(2)	1.344(6)	C(1)–C(5)	1.509(6)
C(2)–C(3)	1.430(6)	C(7)–C(8)	1.516(6)
C(8)–C(9)	1.515(6)		
bond angles (deg)			
P(1)–Ru–P(2)	82.53(4)	P(1)–Ru–O(1)	88.25(8)
P(1)–Ru–C(1)	94.2(1)	P(1)–Ru–C(7)	173.4(1)
P(1)–Ru–C(13)	94.9(1)	P(2)–Ru–O(1)	98.48(8)
P(2)–Ru–C(1)	173.9(1)	P(2)–Ru–C(7)	91.6(1)
P(2)–Ru–C(13)	88.1(1)	O(1)–Ru–C(1)	76.2(1)
O(1)–Ru–C(7)	89.7(1)	O(1)–Ru–C(39)	173.1(2)
C(1)–Ru–C(7)	91.4(1)	C(1)–Ru–C(39)	97.3(2)
C(7)–Ru–C(39)	87.9(2)		

monoxide; however, the reaction was not simple. The product was not **6'** (Scheme 4), which could be derived via simple substitution of **5**, but **6**. If it is assumed that the configuration C(7) in **5** is overall retention through the reaction, the C(1) in **6**, which had coordinated to the ruthenium center at the cis position of both phosphorus atoms of dppe in **5**, changed the relative position. In complex **6**, the carbon atom is located at the trans position of one of the phosphorus atoms of dppe.

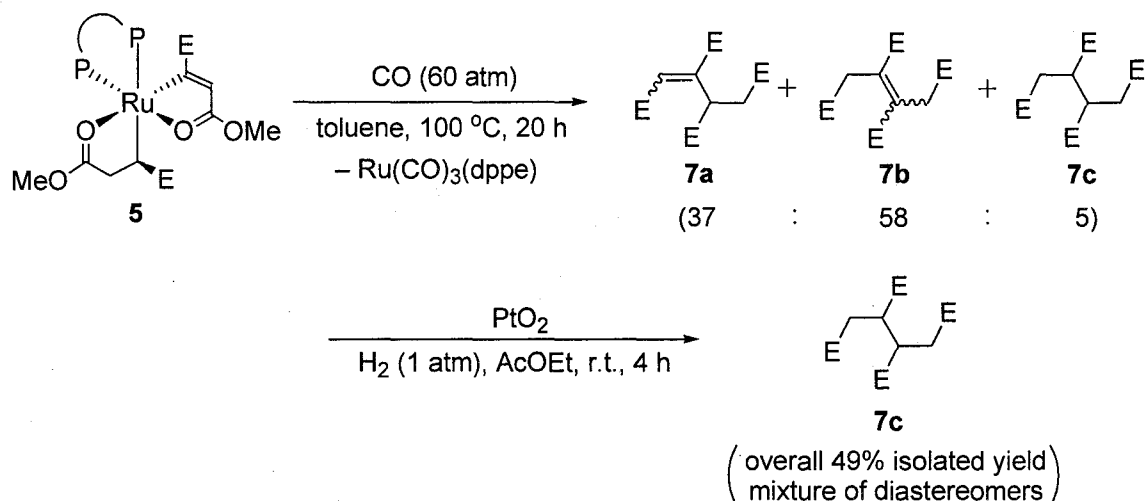
A plausible mechanism of the formation of **6** is shown in Scheme 4. First, the dissociation of O(1) in **5** would occur, and then carbon monoxide coordinates at the vacant site formed. The carbonyl oxygen atom O(5) dissociates to result in the immigration of one of the phosphorus atoms of dppe, which had coordinated at the trans position toward the carbon monoxide. Then the carbonyl oxygen atom O(1) coordinates again at the formed vacant site to afford **6**.

Complex **5** was treated under 60 atm of carbon monoxide at 100 °C to give dimers of dimethyl fumarate **7a–c** (**7a**:**7b**:**7c** = 37:58:5) and Ru(CO)₃(dppe)¹⁵ via reductive elimination (Scheme 5). Hydrogenation of the mixture of **7a–c** by

Scheme 4. A Plausible Mechanism of the Formation of **6**



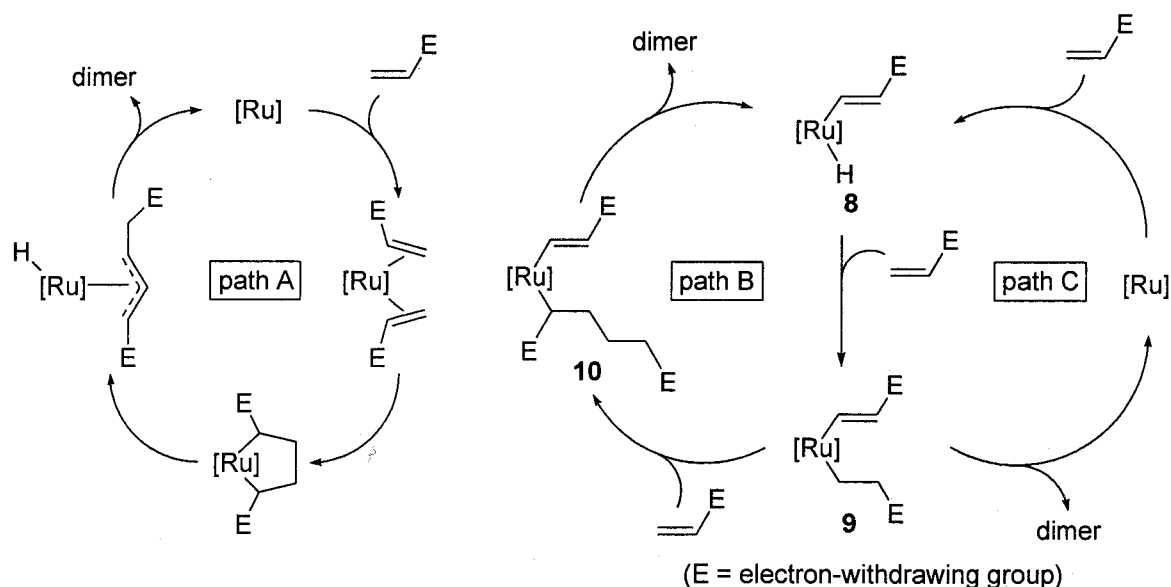
Scheme 5. Reaction of **5** with Carbon Monoxide



the PtO_2 catalyst afforded **7c** in 49% yield based on **5**.

Although the hydrodimerization of dialkyl fumarate has been performed by electrolytic reductive coupling,¹⁶ the present reactions are the first example of the stepwise dimerization of dimethyl fumarate mediated by a transition metal and can be regarded as a model of catalytic dimerization of a general olefinic compound. The catalytic dimerization of an olefinic compound with an electron-withdrawing group, such as methyl acrylate,^{17–20} acrylonitrile,²¹ and acrolein,²² has been achieved by using ruthenium and other transition metal complexes. Various mechanisms for these dimerization reactions were proposed

Scheme 6. Proposed Catalytic Cycles for the Dimerization of an Olefin with an Electron-Withdrawing Group



and they are roughly divided into three paths, A, B, and C in Scheme 6.

Path A is the oxidative cyclization of $\text{Ru}(\text{olefin})_2\text{L}_n$ to form a ruthenacyclopentane, followed by β -hydride elimination to form a hydrido η^3 -allyl complex. The reductive elimination of the complex gives the dimer and catalytically active species.

In paths B and C, the formation of an alkenylhydridoruthenium complex **8** via oxidative addition of the olefinic C–H bond would be the first step of the catalytic cycle. A model complex of **8** derived from $\text{RuH}_2(\text{PPh}_3)_4$ and alkyl methacrylate has been reported by Komiya et al.^{5d,5f} The presence of an intermediate that has both alkenyl and alkyl groups such as **9** has also been suggested in various reactions.^{17b,17f,17g} To the best of our knowledge, complex **5** is the first evidence of the oxidative addition of the vinyl C–H bond followed by the insertion of another olefinic compound.

In path B, the dimer is formed by the insertion of another olefinic compound into the Ru–C(alkyl) bond of **9**, followed by β -H elimination. Sustmann and coworkers suggested this mechanism for the dimerization of methyl acrylate on the basis of the study by means of cyclic voltammetry.^{17g} Further treatment of **5** with dimethyl fumarate gave no dimer.

Path C shows that the dimer is generated from **9** by reductive elimination. The reaction of **5** with carbon monoxide shown in Scheme 5 indicates that a catalytic dimerization of dimethyl fumarate via path C could be designed.

Conclusion

The reactions of $\text{Ru}(\eta^6\text{-cot})(\text{dmfm})_2$ (**1**) with various tertiary phosphine ligands provide new routes to novel low-valent ruthenium complexes. In the reaction with monodentate phosphine ligands, new ruthenium zerovalent complexes, $\text{Ru}(\text{cot})(\text{dmfm})(\text{L})$ (**2a–d**) [$\text{L} = \text{PPh}_3$, PMePh_2 , PMe_2Ph , and PEt_3], were formed by the substitution of one of the dimethyl fumarates in **1** with the phosphine ligand. In contrast to the amine complexes, these phosphine complexes were fluxional in solution via changing the orientation of the coordination of the cyclooctatriene ligand. The reaction of **1** with a bidentate phosphine ligand, dppe, gave a novel ruthenium(II) complex **5** via sp^2 C–H bond activation of dimethyl fumarate followed by insertion of the other dimethyl fumarate. This complex **5** would be a model complex of the intermediate of catalytic dimerization of olefinic compounds. These results would shed some light on the chemistry of the low-valent ruthenium and the catalysis of the complexes.

Experimental Section

Materials or Methods. All manipulations were performed under an argon atmosphere by standard Schlenk techniques. All solvents were distilled under argon over appropriate drying reagents (sodium, calcium chloride, or calcium hydride). $\text{Ru}(\eta^6\text{-cot})(\text{dmfm})_2$ ⁹ and $\text{H}_3\text{CO}_2\text{CCD}=\text{CDCO}_2\text{CH}_3$ (dimethyl fumarate- d_2)²³ were synthesized as described in the literature. PPh_3 , PMePh_2 , PMe_2Ph , PEt_3 , carbon monoxide and 1,2-bis(diphenylphosphino)ethane were

obtained commercially and used without further purification.

Physical and Analytical Measurements. NMR spectra were recorded on either a JEOL GSX-270 [FT, 270 MHz (^1H), 68 MHz (^{13}C), 109 MHz (^{31}P)] or a JEOL EX-400 [FT, 400 MHz (^1H), 100 MHz (^{13}C), 162 MHz (^{31}P)] instrument. Chemical shifts (δ) for ^1H and ^{13}C are referenced to internal solvent resonances and reported relative to SiMe_4 . Chemical shifts for ^{31}P are referenced to an external $\text{P}(\text{OMe})_3$ resonance and reported relative to H_3PO_4 . Solid-state ^{13}C (CP-MAS) and ^{31}P NMR (MASGHD) spectra were recorded on a JEOL GSX-270 with DOTY DSI-698 5 mm MAS probe. IR spectra were recorded using a Nicolet Impact 410 FT-IR spectrometer. GC-MS studies were conducted on a Shimadzu GCMS-QP5000 instrument with 70-eV electron impact ionization. Elemental analyses were performed at the Microanalytical Center of Kyoto University. Analytical gas chromatography was performed on a Shimadzu GC-14B gas chromatograph with FID detection using a 3.2-mm i.d. \times 3 m column with 2% (w/w) silicone OV-17 liquid phase on a Chromosorb W(AW DMCS) support in 60/80 mesh.

Synthesis of $\text{Ru}(\eta^6\text{-cot})(\text{dmfm})(\text{PPh}_3)$ (2a**).** To a solution of $\text{Ru}(\eta^6\text{-cot})(\text{dmfm})_2$ [**1**; 0.26 g, 0.52 mmol] in 1.0 mL of 1,2-dichloroethane was added a solution of PPh_3 (0.14 g, 0.53 mmol) in 1.0 mL of 1,2-dichloroethane, and the mixture was stirred at room temperature. Yellow microcrystals precipitated immediately; after 15 min, the product was separated by filtration, washed with CH_2Cl_2 , and dried under vacuum to give **2a** (0.29 g, 91%). Satisfactory elemental analysis data were obtained without recrystallization.

Complex **2a**: yellow crystals, mp 186–187 °C dec. Anal. Calcd for $\text{C}_{32}\text{H}_{33}\text{O}_4\text{PRu}$: C, 62.63; H, 5.42. Found: C, 62.48; H, 5.49. IR (KBr disk): 1686, 1675, 1438, 1247, 1155 cm^{-1} . ^1H NMR (400 MHz, CDCl_3 , -40°C): δ 7.50–7.30 (H_{Ar}), 6.26 (CH of cot), 5.88 (CH of cot), 5.09 (CH of cot), 4.83 (CH of cot), 4.68 (CH of cot), 4.14 (CH of cot), 3.78 (s, OCH_3), 3.65 (s, OCH_3), 2.87 (CH of dmfm), 1.97 (CH of dmfm), 1.48 (CHH of cot), 0.68 (CHH of cot), 0.00 (CHH

of cot), -0.97 (CHH of cot). ^{31}P NMR (162 MHz, CD_2Cl_2 , $-40\text{ }^\circ\text{C}$): δ 53.90 (s). Because of low solubility of **2a**, the sufficient ^{13}C NMR spectrum in solution could not be obtained.

Synthesis of $\text{Ru}(\eta^6\text{-cot})(\text{dmfm})(\text{PMePh}_2)$ (2b**).** To a solution of $\text{Ru}(\eta^6\text{-cot})(\text{dmfm})_2$ [**1**; 0.55 g, 1.1 mmol] in 5 mL of 1,2-dichloroethane was added PMePh_2 (0.22 g, 1.1 mmol), and the mixture was stirred at room temperature for 2 h and then chromatographed on alumina. Elution with chloroform gave a yellow solution, from which the solvent was evaporated. The yellow residue was recrystallized from chloroform/pentane to give **2b** (0.49 g, 81%).

Complex **2b**: yellow solid, mp $151\text{ }^\circ\text{C}$ dec. Anal. Calcd for $\text{C}_{27}\text{H}_{31}\text{O}_4\text{PRu}$: C, 58.79; H, 5.66. Found: C, 58.61; H, 5.56. IR (KBr disk): 1691, 1681, 1459, 1432, 1297, 1163 cm^{-1} . Solid-state ^{13}C NMR (68 MHz, CP-MAS): δ 180.57, 176.42, 139.36–128.04, 105.58, 96.08, 93.10, 92.10, 86.23, 77.73, 53.31, 49.77, 43.72, 42.00, 38.89, 21.18, 11.93. Solid-state ^{31}P NMR (109 MHz, MASGHD): δ 27.00. ^1H NMR (400 MHz, CD_2Cl_2 , $-40\text{ }^\circ\text{C}$): for isomer A: δ 7.5–6.8 (H_{Ar}), 6.14 (t, $J = 6.4\text{ Hz}$, CH of cot), 5.81 (dd, $J = 8.8\text{ Hz}$, $J = 5.4\text{ Hz}$, CH of cot), 4.74 (br, CH of cot), 4.63 (t, $J = 7.8\text{ Hz}$, CH of cot), 4.52 (t, $J = 7.8\text{ Hz}$, CH of cot), 4.01 (quintet, $J = 7.3\text{ Hz}$, CH of cot), 3.70 (s, OCH_3), 3.55 (s, OCH_3), 2.79 (t, $J = 9.3\text{ Hz}$, CH of dmfm), 2.47 (t, $J = 8.3$, CH of dmfm), 2.04 (d, $J = 7.8\text{ Hz}$, PCH_3), 1.40 (d, CHH of cot), 0.56 (m, CHH of cot), -0.07 (br, CHH of cot), -1.12 (m, CHH of cot), and for the other isomers: δ 2.68 (br), 1.79 (d, $J = 7.8\text{ Hz}$, PCH_3). ^{31}P NMR (162 MHz, CD_2Cl_2 , $-40\text{ }^\circ\text{C}$): δ 33.16 (s). ^{13}C NMR (100 MHz, CD_2Cl_2 , $23\text{ }^\circ\text{C}$): δ 179.4, 178.0, 177.4, 161.2, 139.9–128.0, 103.6, 102.7, 100.2, 99.6, 96.5, 95.2, 94.4, 88.8, 85.0, 82.3, 80.8, 76.8, 50.7, 50.5, 50.3, 40.5, 39.5, 35.4, 32.3, 31.8, 29.8, 24.2, 16.8, 13.5 (d, $J_{\text{CP}} = 23.9\text{ Hz}$).

Synthesis of $\text{Ru}(\eta^6\text{-cot})(\text{dmfm})(\text{PMe}_2\text{Ph})$ (2c**).** To a solution of $\text{Ru}(\eta^6\text{-cot})(\text{dmfm})_2$ [**1**; 0.59 g, 1.2 mmol] in 5 mL of 1,2-dichloroethane was added PMe_2Ph (0.17 g, 1.2 mmol), and the mixture was stirred at room

temperature for 2 h and then chromatographed on alumina. Elution with chloroform gave a yellow solution, from which the solvent was evaporated. The yellow residue was recrystallized from chloroform/pentane to give **2c** (0.235 g, 40%).

Complex **2c**: yellow solid, mp 141–142 °C dec. Anal. Calcd for $C_{22}H_{29}O_4PRu$: C, 53.98; H, 5.97. Found: C, 53.79; H, 5.96. IR (KBr disk): 1687, 1672, 1450, 1433, 1295, 1260, 1156 cm^{-1} . Solid-state ^{13}C NMR (68 MHz, CP-MAS): δ 181.93, 180.03, 141.84–129.58, 110.92, 97.44, 92.00, 90.10, 82.67, 78.78, 51.65, 40.33, 34.63, 21.76, 14.94, 9.155. Solid-state ^{31}P NMR (109 MHz, MASGHD): δ 4.897. 1H NMR (400 MHz, CD_2Cl_2 , $-20\text{ }^\circ C$): for isomer **A**: δ 7.5–7.24 (H_{Ar}), 5.76 (t, $J = 6.8$ Hz, CH of cot), 5.68 (t, $J = 5.4$ Hz, CH of cot), 4.82 (br, CH of cot), 4.58 (t, $J = 7.8$ Hz, CH of cot), 4.50 (t, $J = 8.3$ Hz, CH of cot), 3.97 (quintet, $J = 8.3$ Hz, CH of cot), 3.58 (s, OCH_3), 3.52 (s, OCH_3), 2.67 (d, $J = 8.8$ Hz, CH of dmfm), 2.38 (t, $J = 8.8$ Hz, CH of dmfm), 1.71 (d, $J = 9.3$ Hz, PCH_3), 1.58 (d, $J = 8.3$ Hz, CHH of cot), 1.19 (br, CHH of cot), 1.01 (d, $J =$ Hz, PCH_3), 0.90 (br, CHH of cot), -0.78 (br, CHH of cot), and for the other isomers: δ 6.81 (m), 4.31 (t, $J = 6.6$ Hz), 4.22 (br), 3.52 (s), 3.15 (s), 3.13 (t, $J = 10.25$ Hz), 1.53 (d, $J = 8.8$ Hz, PCH_3), 1.28 (d, $J = 8.8$ Hz, PCH_3). ^{31}P NMR (162 MHz, CD_2Cl_2 , $-20\text{ }^\circ C$): δ 13.28 (s), 1.81 (s). ^{13}C NMR (100 MHz, CD_2Cl_2 , $23\text{ }^\circ C$): δ 180.2, 179.3, 177.6, 176.9, 141.0–128.2, 107.2, 103.5, 102.6, 97.8, 96.3, 92.7, 91.7, 85.2, 84.8, 83.2, 79.3, 78.8, 78.2 50.9, 50.6, 50.3, 38.8, 38.5, 38.1, 36.5, 35.5, 32.7, 26.0, 23.6, 18.3, 15.9 (d, $J_{CP} = 23.9$ Hz), 11.0 (d, $J_{CP} = 23.9$ Hz).

Synthesis of $Ru(\eta^6\text{-cot})(dmfm)(PEt_3)$ (2d**).** To a solution of $Ru(\eta^6\text{-cot})(dmfm)_2$ [**1**; 0.38 g, 0.78 mmol] in 5 mL of 1,2-dichloroethane was added PEt_3 (93 mg, 0.79 mmol), and the mixture was stirred at room temperature for 2 h and then chromatographed on alumina. Elution with chloroform gave a yellow solution, from which the solvent was evaporated. The orange residue was recrystallized from chloroform/pentane to give **2d** (0.17 g,

46%).

Complex **2d**: orange solid, mp 107–108 °C dec. Anal. Calcd for $C_{20}H_{33}O_4PRu$: C, 51.16; H, 7.08. Found: C, 51.08; H, 7.12. IR (KBr disk): 1683, 1676, 1476, 1458, 1451, 1431, 1297, 1150, 1044, 1038 cm^{-1} . Solid-state ^{13}C NMR (68 MHz, CP-MAS): δ 177.52, 104.26, 99.08, 83.10, 75.58, 53.55, 52.00, 40.94, 38.87, 32.39, 25.73, 22.45, 17.35, 14.59, 10.10, 8.89, 8.11. Solid-state ^{31}P NMR (109 MHz, MASGHD): δ 27.18. 1H NMR (400 MHz, CD_2Cl_2 , 0 °C): for isomer A: δ 5.98 (t, $J = 6.4$ Hz, CH of cot), 5.56 (dd, $J = 8.8$ Hz, $J = 5.3$ Hz, CH of cot), 5.07 (br, CH of cot), 4.64 (t, $J = 7.8$ Hz, CH of cot), 4.52 (t, $J = 8.8$ Hz, CH of cot), 4.35 (m, CH of cot), 3.61 (s, OCH_3), 3.41 (s, OCH_3), 2.64 (d, $J = 9.3$ Hz, CH of dmfm), 2.33 (m, CHH of cot), 2.14 (t, $J = 7.3$ Hz, CH of dmfm), 1.81 (d, $J = 15.6$ Hz, CHH of cot), 1.36 (br, CHH of cot), 1.25 (m, PCH_2), 0.78 (m, CH_3 of PEt), -0.78 (m, CHH of cot), and for the other isomers: δ 6.04 (br), 5.90 (br), 4.95 (br), 3.63 (s, OCH_3), 3.51 (s, OCH_3), 3.23 (br, CH of dmfm), 2.93 (t, $J = 9.7$ Hz, CH of dmfm), 1.75–1.64 (m), 0.76 (m, CH_3 of PEt). ^{31}P NMR (162 MHz, CD_2Cl_2 , 0 °C): δ 25.91 (s, isomer A), 9.66 (br). ^{13}C NMR (100 MHz, CD_2Cl_2 , 23 °C): δ 179.7, 179.5, 177.9, 177.8, 105.2, 102.5, 99.8, 95.3, 94.6, 93.9, 92.0, 83.7, 82.4, 80.9, 79.8, 76.5, 50.6, 50.4, 50.0, 38.5, 37.6, 37.5, 37.2, 33.6, 31.3, 28.0, 25.9, 16.8 (d, $J_{CP} = 25.7$ Hz), 13.8 (d, $J_{CP} = 20.3$ Hz), 7.5 (d, $J_{CP} = 25.7$ Hz)

Synthesis of $Ru(dmfm)(dppe)_2$ (4). To a suspension of $Ru(\eta^6\text{-cot})(dmfm)_2$ [**1**; 0.11 g, 0.23 mmol] in 2.0 mL of toluene was added a solution of dppe (0.19 g, 0.47 mmol) in 2.0 mL of toluene, and the mixture was stirred at 50 °C. Yellow microcrystals precipitated immediately; after 6 h, the product was separated by filtration, washed with toluene, and dried under vacuum to give **4** (0.16 g, 66%).

Complex **4**: yellow crystals, mp 235–236 °C dec. Anal. Calcd for $C_{58}H_{56}O_4P_4Ru$: C, 66.85; H, 5.42. Found: C, 66.60; H, 5.51. IR (KBr disk): 1686, 1655, 1432, 1262, 1207, 1139 cm^{-1} . 1H NMR (400 MHz, CD_2Cl_2): δ 7.95–5.94 (H_{Ar}), 3.34 (s, 6H, CH_3), 2.79 (m, 2H, CH of dmfm), 1.80 (br, 4H, PCH_2), 1.52

(br, 4H, PCH₂). ³¹P NMR (162 MHz, CDCl₃): δ 60.61 (t, *J* = 18.3 Hz), 56.73 (t, *J* = 18.3 Hz). Because of low solubility of **4**, the sufficient ¹³C NMR spectrum could not be obtained.

Synthesis of Ru[C(CO₂CH₃)=CHC(O)OCH₃][CH(CO₂CH₃)CH₂C(O)OCH₃](dppe) (5**).** To a suspension of Ru(*η*⁶-cot)(dmfm)₂ [**1**; 1.7 g, 3.4 mmol] in 100 mL of toluene was added a solution of 1,2-bis(diphenylphosphino)ethane [dppe; 1.1 g, 2.8 mmol] in 2.0 mL of toluene. The mixture was stirred at 80 °C for 30 min and then chromatographed on alumina. Elution with chloroform gave an orange solution from which the solvent was evaporated. The orange residue was recrystallized from chloroform/pentane to give **5** (1.8 g, 81% based on dppe).

Complex **5**: orange crystals, mp 192–194 °C dec. Anal. Calcd for C₃₈H₄₀O₈P₂Ru: C, 57.94; H, 5.12. Found: C, 57.78; H, 5.03. IR (KBr disk): 1708, 1701, 1669, 1659, 1562, 1434, 1351 cm⁻¹. ¹H NMR(400 MHz, CD₂Cl₂): δ 8.06–6.92 (H_{Ar}), 5.80 (t, *J* = 1.5 Hz, 1H, CH of alkenyl group), 3.93 (s, 3H, CH₃), 3.42 (s, 3H, CH₃), 3.35 (m, 1H, Ru–CH of alkyl group), 3.23 (m, 1H, PCHH), 3.20 (m, 1H, CHH of alkyl group), 3.08 (s, 3H, CH₃), 2.89 (m, 2H, PCH₂), 2.73 (s, 3H, CH₃), 2.51 (m, 1H, CHH of alkyl group), 2.47 (m, 1H, PCHH). ¹³C NMR (100 MHz, CD₂Cl₂): δ 223.29 (m, Ru–C(alkenyl group)), 188.27 (s, C=O), 188.20 (s, C=O), 178.21 (s, C=O), 176.35 (s, C=O), 141.14–127.39 (C_{Ar}), 117.86 (s, CH of alkenyl group), 53.27 (s, CH₃), 53.14 (s, CH₃), 49.87 (s, CH₃), 49.17 (s, CH₃), 36.41 (d, *J* = 3.7 Hz, CH₂ of alkyl group), 30.39 (dd, *J* = 33.1 Hz, *J* = 11.1 Hz, PCH₂), 27.79 (dd, *J* = 42.3 Hz, *J* = 5.6 Hz, Ru–CH), 26.70 (dd, *J* = 29.4 Hz, *J* = 18.3 Hz, PCH₂). ³¹P NMR (162 MHz, CD₂Cl₂): δ 87.28 (d, *J* = 12.2 Hz), 61.63 (d, *J* = 12.2 Hz).

Synthesis of Ru[C(CO₂CH₃)=CHC(O)OCH₃][CH(CO₂CH₃)CH₂C(O)OCH₃](CO)(dppe) (6**).** In a 20 mL Pyrex flask with a stirring bar, **5** (0.10 g, 0.13 mmol) was placed under a carbon monoxide atmosphere. Then 1.5 mL of CH₂Cl₂ was added and the solution was magnetically stirred at room

temperature. After 4 h, 10 mL of pentane was added and yellow microcrystals were precipitated. The product was separated by filtration and dried under vacuum to give **6** (0.085 g, 80%).

Complex 6: yellow solid, mp 178–181 °C dec. Anal. Calcd for $C_{39}H_{40}O_9P_2Ru$: C, 57.42; H, 4.94. Found: C, 57.44; H, 4.93. IR (KBr disk): 1930, 1731, 1698, 1692, 1582, 1444, 1434, 1350 cm^{-1} . 1H NMR (400 MHz, $CDCl_3$): δ 7.80–6.86 (H_{Ar}), 6.41 (dd, 1H, $J = 8.3$ Hz, $J = 2.0$ Hz, =CH–), 3.70 (s, 3H, CH_3), 3.37 (s, 3H, CH_3), 3.36 (s, 3H, CH_3), 3.06 (s, 3H, CH_3), 2.86 (m, 1H, Ru–CH), 2.80 (m, 1H, CHH of alkyl group), 2.49 (m, 2H, PCH_2), 2.19 (m, 2H, PCH_2), 2.04 (m, 1H, CHH of alkyl group). ^{13}C NMR (100 MHz, $CDCl_3$): δ 219.68 (dd, $J = 75.4$ Hz, $J = 9.2$ Hz, carbon monoxide), 205.88 (t, $J = 11.0$ Hz, Ru–C(alkenyl group)), 181.05 (d, $J = 9.2$ Hz, C=O of ester), 180.25 (s, C=O of ester), 176.02 (d, $J = 5.5$ Hz, C=O of ester), 174.44 (s, C=O of ester), 134.52–128.12 (C_{Ar}), 122.50 (s, =CH of alkenyl group), 52.92 (s, CH_3), 51.18 (s, CH_3), 50.59 (s, CH_3), 48.82 (s, CH_3), 39.25 (s, CH_2 of alkyl group), 29.93 (dd, $J = 28.5$ Hz, $J = 16.6$ Hz, PCH_2), 26.15 (dd, $J = 27.6$ Hz, $J = 14.7$ Hz, PCH_2), 22.03 (dd, $J = 43.2$ Hz, $J = 4.6$ Hz, Ru–CH). ^{31}P NMR (162 MHz, $CDCl_3$): δ 55.44 (s), 44.55 (s).

Reaction of 5 with carbon monoxide to give dimethyl fumarate dimers, and subsequent hydrogenation of dimers. A suspension of **5** (0.20 g, 0.25 mmol) in 10 mL of toluene was placed in a 50 mL stainless steel autoclave under a flow of argon. Carbon monoxide was then pressured to 60 atm at room temperature, and the mixture was magnetically stirred at 100 °C for 20 h. After cooling, the mixture of dimethyl fumarate dimer was isolated by Kugelrohr distillation and placed in a 20 mL Pyrex flask under a hydrogen atmosphere. Then 2 mL of ethyl acetate was added, and the solution was magnetically stirred at room temperature. After 4 h, the product was isolated by Kugelrohr distillation (overall 49% yield). The ratio of the isomers was determined by 1H NMR spectra.²⁴

Reaction of 2b with H₃CO₂CCD=CDCO₂CH₃ (Dimethyl Fumarate-*d*₂).

Complex **2b** (10.3 mg, 0.019 mmol) and dimethyl fumarate-*d*₂ (3.8 mg, 0.026 mmol) were placed in an NMR tube and then CD₂Cl₂ (0.7 mL) was added. The ¹H NMR spectra of this sample were measured at 30 min, 3 h, 6 h and 24 h. It was proved that the exchange ratios against the coordinated dimethyl fumarate were 0.089, 0.365, 0.618 and 1.184 and that after 24 h some disproportionation occurred.

Crystallographic study of complexes 2b, 2c, 2d, 4, 5, and 6. Single crystals of complexes **2b–d**, **4**, **5**, and **6** obtained by recrystallization from CH₂Cl₂/pentane were subjected to X-ray crystallographic analysis. The crystal data and experimental details for **2b**, **2c** and **2d** are summarized in Table 1 and for **4**, **5** and **6** in Table 4. All measurements were made on a Rigaku AFC7R diffractometer with graphite-monochromated Mo K α radiation (λ = 0.71069 Å) and a rotating anode generator. The reflection intensities were monitored by three standard reflections at every 150 measurements. No decay correction was applied. Reflection data were corrected for Lorentz and polarization effects. Azimuthal scans of several reflections indicated no need for an absorption correction. The structures were solved by direct methods using SIR92²⁵ for **2c**, **2d**, **4**, **5**, **6** and SHELXS86²⁶ for **2b**, expanded using Fourier techniques, DIRDIF94,²⁷ and refined anisotropically for non-hydrogen atoms by full-matrix least-squares calculations. Atomic scattering factors and anomalous dispersion terms were taken from the literature.^{28–30} Hydrogen atoms were found except for the hydrogens on C(4), C(6), C(14), C(18), C(19), C(21), C(23), and C(24) for **2b** and on C(4), C(12), C(24), C(29), C(31), C(32), and C(35) for **6**, and all protons for **4**. The hydrogens' positions in **2b**, **4**, and **6** were not refined, and isotropic *B* values were refined. Hydrogens in **2c**, **2d**, and **5** were refined isotropically. The calculations were performed on an Silicone Graphics O₂ computer using the program system teXsan.³¹ In Figures 1–3 and 6–8, thermal ellipsoids are shown at the 30% probability level.

References

- (1) (a) Bennett, M. A.; Matheson, T. W. In *Comprehensive Organometallic Chemistry*; Wilkinson, G., Stone, F. G. A., Abel, E. W., Eds.; Pergamon Press: Oxford, U.K. 1982; Vol. 4, p 931. (b) Shriver, D. F.; Bruce, M. I. In *Comprehensive Organometallic Chemistry II*; Abel, E. W., Stone, F. G. A.; Wilkinson, G., Eds.; Pergamon Press: Oxford, U.K. 1995; vol. 7. (c) Naota, T.; Takaya, H.; Murahashi, S.-I. *Chem. Rev.* **1998**, *98*, 2599. (d) Mitsudo, T.; Kondo, T. *Synlett*, **2000**, 309.
- (2) For recent leading papers, e.g., (a) Airoidi, M.; Deganello, G.; Dia, G.; Gennaro, G. *J. Organomet. Chem.* **1980**, *187*, 391. (b) Mitsudo, T.; Nakagawa, Y.; Watanabe, K.; Hori, Y.; Misawa, H.; Watanabe, H.; Watanabe, Y. *J. Org. Chem.* **1985**, *50*, 565. (c) Maruyama, Y.; Sezaki, T.; Tekawa, M.; Sakamoto, T.; Shimizu, I.; Yamamoto, A. *J. Organomet. Chem.* **1994**, *473*, 257. (d) Hori, Y.; Mitsudo, T.; Watanabe, Y. *Bull. Chem. Soc. Jpn.* **1988**, *61*, 3011. (e) Mitsudo, T.; Takagi, M.; Zhang, S.-W.; Watanabe, Y. *J. Organomet. Chem.* **1992**, *423*, 405. (f) Fukuoka, A.; Nagano, T.; Furuta, S.; Yoshizawa, M.; Hirano, M.; Komiya, S. *Bull. Chem. Soc. Jpn.* **1998**, *71*, 1409. (g) Kondo, T.; Uenoyama, S.; Fujita, K.; Mitsudo, T. *J. Am. Chem. Soc.* **1999**, *121*, 482.
- (3) (a) Deganello, G.; Mantovani, A.; Sandrini, P. L.; Pertici, P.; Vitulli, G. *J. Organomet. Chem.* **1977**, *135*, 215. (b) Chaudret, B.; Commenges, G.; Poilblanc, R. *J. Chem. Soc., Chem. Commun.* **1982**, 1388. (c) Itoh, K.; Mukai, K.; Nagashima, H.; Nishiyama, H. *Chem. Lett.* **1983**, 499. (d) Pertici, P.; Vitulli, G.; Porzio, W.; Zocchi, M.; Barili, P. L.; Deganello, G. *J. Chem. Soc., Dalton Trans.* **1983**, 1553. (e) Bouachir, F.; Chaudret, B.; Tkatchenko, I. *J. Chem. Soc., Chem. Commun.* **1986**, 94. (f) Komiya, S.; Suzuki, J.; Miki, K.; Kasai, N. *Chem. Lett.* **1987**, 1287. (g) Bouachir, F.; Chaudret, B.; Dahan, F.; Agbossou, F.; Tkatchenko, I. *Organometallics*

- 1991, 10, 455. (h) Komiya, S.; Kabasawa, T.; Yamashita, K.; Hirano, M.; Fukuoka, A. *J. Organomet. Chem.* **1994**, 471, C6. (i) Hirano, M.; Marumo, T.; Miyasaka, T.; Fukuoka, A.; Komiya, S. *Chem. Lett.* **1997**, 297. (j) Hirano, M.; Kurata, T.; Marumo, T.; Komiya, S. *Organometallics* **1998**, 27, 501. (k) Planas, J. G.; Marumo, T.; Ichikawa, Y.; Hirano, M.; Komiya, S. *Chem. Lett.* **1998**, 123. (l) Planas, J. G.; Hirano, M.; Komiya, S. *Chem. Lett.* **1999**, 953.
- (4) For recent leading papers, e.g., (a) Moore, E. J.; Pretzer, W. R.; O'Connell, T. J.; Harris, J.; LaBounty, L.; Chou, L.; Grimmer, S. S. *J. Am. Chem. Soc.* **1992**, 114, 5888. (b) Lavigne, G.; Lugan, N.; Kalck, P.; Soulié, J. M.; Lerouge, O.; Salliard, J. Y.; Halet, J. F. *J. Am. Chem. Soc.* **1992**, 114, 10669. (c) Valli, V. L. K.; Alper, H. *J. Am. Chem. Soc.* **1993**, 115, 3778. (d) Lugan, N.; Lavigne, G.; Soulié, J. M.; Fabre, S.; Kalck, P.; Saillard, J. Y.; Halet, J. F. *Organometallics* **1995**, 14, 1712. (e) Chatani, N.; Fukuyama, T.; Kakiuchi, F.; Murai, S. *J. Am. Chem. Soc.* **1996**, 118, 493. (f) Cenini, S.; Ragaini, F.; Tollari, S.; Paone, D. *J. Am. Chem. Soc.* **1996**, 118, 11964. (g) Chatani, N.; Ie, Y.; Kakiuchi, F.; Murai, S. *J. Org. Chem.* **1997**, 62, 2604. (h) Fukuyama, T.; Chatani, N.; Kakiuchi, F.; Murai, S. *J. Org. Chem.* **1997**, 62, 5647. (i) Kondo, T.; Suzuki, N.; Okada, T.; Mitsudo, T. *J. Am. Chem. Soc.* **1997**, 119, 6187.
- (5) (a) Knoth, W. H. *J. Am. Chem. Soc.* **1972**, 94, 104. (b) Komiya, S.; Yamamoto, A.; Ikeda, S. *J. Organomet. Chem.* **1972**, 42, C65. (c) Komiya, S.; Yamamoto, A.; Ikeda, S. *Bull. Chem. Soc. Jpn.* **1975**, 48, 101. (d) Komiya, S.; Yamamoto, A. *Chem. Lett.* **1975**, 475. (e) Komiya, S.; Yamamoto, A. *Bull. Chem. Soc. Jpn.* **1976**, 49, 784. (f) Komiya, S.; Ito, T.; Cowie, M.; Yamamoto, A.; Ibers, J. A. *J. Am. Chem. Soc.* **1976**, 98, 3874. (g) McGuiggan, M. F.; Pignolet, L. H. *Inorg. Chem.* **1982**, 21, 2523. (h) Osakada, K.; Ohshiro, K.; Yamamoto, A. *Organometallics* **1991**, 10, 404. (i) Komiya, S.; Aoki, Y.; Mizuho, Y.; Oyasato, N. *J. Organomet.*

Chem. **1993**, 463, 179.

- (6) (a) Mitsudo, T.; Kokuryo, K.; Takegami, Y. *J. Chem. Soc., Chem. Commun.* **1976**, 722. (b) Horino, H.; Ito, T.; Yamamoto, A. *Chem. Lett.* **1978**, 17. (c) Naota, T.; Taki, H.; Mizuno, M.; Murahashi, S. *J. Am. Chem. Soc.* **1989**, 111, 5954. (d) Murahashi, S.-I.; Naota, T.; Taki, H.; Mizuno, M.; Takaya, H.; Komiya, S.; Mizuho, Y.; Oyasato, N.; Hiraoka, M.; Hirano, M.; Fukuoka, A. *J. Am. Chem. Soc.* **1995**, 117, 12436.
- (7) (a) Yamazaki, H. *J. Chem. Soc., Chem. Commun.* **1976**, 841. (b) Wakatsuki, Y.; Yamazaki, H.; Kumegawa, N.; Satoh, Y.; Satoh J. Y. *J. Am. Chem. Soc.* **1991**, 113, 5453.
- (8) (a) Murai, S.; Kakiuchi, F.; Sekine, S.; Tanaka, Y.; Kamatani, A.; Sonoda, M.; Chatani, N. *Nature* **1993**, 366, 529. (b) Murai, S.; Kakiuchi, F.; Sekine, S.; Tanaka, Y.; Kamatani, A.; Sonoda, M.; Chatani, N. *Pure Appl. Chem.* **1994**, 66, 1527. (c) Kakiuchi, F.; Sekine, S.; Tanaka, Y.; Kamatani, A.; Sonoda, M.; Chatani, N.; Murai, S. *Bull. Chem. Soc. Jpn.* **1995**, 68, 62.
- (9) Mitsudo, T.; Suzuki, T.; Zhang, S.-W.; Imai, D.; Fujita, K.; Manabe, T.; Shiotsuki, M.; Watanabe, Y.; Wada, K.; Kondo, T. *J. Am. Chem. Soc.* **1999**, 121, 1839.
- (10) Suzuki, T.; Shiotsuki, M.; Wada, K.; Kondo, T.; Mitsudo, T. *Organometallics* **1999**, 18, 3671.
- (11) Suzuki, T.; Shiotsuki, M.; Wada, K.; Kondo, T.; Mitsudo, T. *J. Chem. Soc., Dalton Trans.* **1999**, 4231.
- (12) Kreiter, C. G.; Lang, M.; Strack, H. *Chem. Ber.* **1975**, 108, 1502.
- (13) (a) Kruczynski, L.; Martin, J. L.; Takats, J. *J. Organomet. Chem.* **1974**, 80, C9. (b) Frühauf, H.-W.; Pein, I.; Seils, F. *Organometallics* **1987**, 6, 1613. (c) Helliwell, M.; Vessey, J. D.; Mawby, R. J. *J. Chem. Soc., Dalton Trans.* **1994**, 1193. (d) de Klerk-Engels, B.; Delis, J. G. P.; Ernsting, J.-M.; Elsevier, C. J.; Frühauf, H.-W.; Stufkens, D. J.; Vrieze, K.; Goubitz, K.;

- Fraanje, J. *Inorg. Chim. Acta.* **1995**, *240*, 273. (e) van Wijnkoop, M.; de Lange, P. P. M.; Frühauf, H.-W.; Vrieze, K. *Organometallics* **1995**, *14*, 4781.
- (14) Tolman, C. A.; Ittel, S. D.; English, A. D.; Jesson, J. P. *J. Am. Chem. Soc.* **1978**, *100*, 4080.
- (15) (a) Sanchez-Delgado, R. A.; Bradley, J. S.; Wilkinson, G.; *J. Chem. Soc., Dalton Trans.* **1976**, 399. (b) Skoog, S. J.; Jorgenson, A. L.; Campbell, J. P.; Douskey, M. L.; Munson, E.; Gladfelter, W. L. *J. Organomet. Chem.* **1998**, *557*, 13.
- (16) White, D. A. *Org. Synth.* **1981**, *60*, 58 and references therein.
- (17) Ru-based acrylate dimerization catalysts: (a) Alderson, T.; Jenner, E. L.; Lindsey, R. V. *J. Am. Chem. Soc.* **1965**, *87*, 5638. (b) McKinney, R. J.; Colton, M. C. *Organometallics* **1986**, *5*, 1080. (c) McKinney, R. J. *Organometallics* **1986**, *5*, 1752. (d) Ren, C. Y.; Cheng, W. C.; Chan, W. C.; Yeung, C. H.; Lau, C. P. *J. Mol. Catal.* **1990**, *59*, L1. (e) Sustmann, R.; Hornung, H. J.; Schupp, T.; Patzke, B. *J. Mol. Catal.* **1993**, *85*, 149. (f) Pertici, P.; Ballantini, V.; Salvadori, P.; Bennett, M. A. *Organometallics* **1995**, *14*, 2565. (g) Strehblow, C.; Schupp, T.; Sustmann, R. *J. Organomet. Chem.* **1998**, *561*, 181.
- (18) Pd-based acrylate dimerization catalysts: (a) Barlow, M. G.; Bryant, M. J.; Haszeldine, R. N.; Mackie, A. G. *J. Organomet. Chem.* **1970**, *21*, 215. (b) Oehme, G.; Pracejus, H. Z. *Chem.* **1974**, *14*, 24. (c) Milstein, D.; Stille, J. K. *J. Am. Chem. Soc.* **1979**, *101*, 4981 and 4992. (d) Oehme, G.; Pracejus, H. J. *Prakt. Chem.* **1980**, *322*, 798. (e) Oehme, G. *J. Prakt. Chem.* **1984**, *326*, 779. (f) Oehme, G.; Grassert, I.; Baudisch, H.; Mennenga, H. *J. Mol. Catal.* **1986**, *37*, 53. (g) Guibert, I.; Neibecker, D.; Tkatchenko, I. *J. Chem. Soc., Chem. Commun.* **1989**, 1850.
- (19) Rh-based acrylate dimerization catalysts: (a) Nugent, W. A.; McKinney, R. J. *J. Mol. Catal.* **1985**, *29*, 65. (b) Brookhart, M.; Sabo-Etienne, S. *J. Am.*

- Chem. Soc.* **1991**, *113*, 2777. (c) Brookhart, M.; Hauptman, E. *J. Am. Chem. Soc.* **1992**, *114*, 4437. (d) Hauptman, E.; Sabo-Etienne, S.; White, P. S.; Brookhart, M.; Garner, J. M.; Fagan, P. J.; Calabrese, J. C. *J. Am. Chem. Soc.* **1994**, *116*, 8038.
- (20) Ni-based acrylate dimerization catalysts: (a) Wilke, G. *Angew. Chem., Int. Ed. Engl.* **1988**, *27*, 185. (b) Lehmkuhl, H.; Naydowski, C. *J. Organomet. Chem.* **1984**, *277*, C18. (c) Grubbs, R. H.; Miyashita, A. *J. Am. Chem. Soc.* **1978**, *100*, 1300.
- (21) Ru-based acrylonitrile dimerization catalysts: (a) Rhone-Poulenc, Netherland Patent 6,603,115,1966; *Chem. Abstr.* **1967**, *66*, 85483. (b) Misono, A.; Uchida, Y.; Hidai, M.; Kanai, H. *Chem. Commun.* **1967**, 357. (c) McClure, J. D.; Owyang, R.; Slaugh, L. H. *J. Organomet. Chem.* **1968**, *12*, 8. (d) Billing, E.; Strow, C. B.; Pruett, R. L. *Chem. Commun.* **1968**, 1307. (e) Misono, A.; Uchida, Y.; Hidai, M.; Shinohara, H.; Watanabe, Y. *Bull. Chem. Soc. Jpn.* **1968**, *41*, 396. (f) Misono, A.; Uchida, Y.; Hidai, M.; Inomata, I. *Chem. Commun.* **1968**, 704. (g) Strohmeier, W.; Kaiser, A. *J. Organomet. Chem.* **1976**, *114*, 273. (h) Tsou, D. T.; Burrington, J. D.; Maher, E. A.; Grasselli, R. K. *J. Mol. Catal.* **1985**, *30*, 219. (i) Kashiwagi, K.; Sugise, R.; Shimakawa, T.; Matuura, T.; Shirai, M.; Kakiuchi, F.; Murai, S. *Organometallics* **1997**, *16*, 2233. (j) Fukuoka, A.; Nagano, T.; Furuta, S.; Yoshizawa, M.; Hirano, M.; Komiya, S. *Bull. Chem. Soc. Jpn.* **1998**, *71*, 1409.
- (22) Ohgomori, Y.; Ichikawa, S.; Sumitani, N. *Organometallics* **1994**, *13*, 3758.
- (23) Richards, E. M.; Tebby, J. C.; Ward, R. S.; Williams, D. H. *J. Chem. Soc. C* **1969**, 1542.
- (24) (a) Cuppen, Th. J. H. M.; Laarhoven, W. H. *J. Am. Chem. Soc.* **1972**, *94*, 5914. (b) Ito, S.; Hirata, Y. *Bull. Chem. Soc. Jpn.* **1977**, *50*, 1813. (c) de Lange, P. P. M.; de Boer, R. P.; van Wijnkoop, M.; Ernsting, J. M.;

- Frühauf, H.-W.; Vrieze, K. *Organometallics* **1993**, *12*, 440.
- (25) *SIR92*: Altomare, A.; Burla, M. C.; Camalli, M.; Cascarano, M.; Giacovazzo, C.; Guagliardi, A.; Polidori, G. *J. Appl. Crystallogr.* **1994**, *27*, 435.
- (26) *SHELXS86*: Sheldrick, G. M. *Crystallographic Computing 3*; Sheldrick, G. M.; Kruger, C.; Goddard, R., Eds.; Oxford University Press: Oxford, U.K., 1985; pp 175–189.
- (27) *DIRDIF94*: Beurskens, P. T.; Admiraal, G.; Beurskens, G.; Bosman, W. P.; de Gelder, R.; Israel, R.; Smits, J. M. M. *The DIRDIF-94 program system*; Technical Report of the Crystallography Laboratory; University of Nijmegen: The Netherlands, 1994.
- (28) Cromer, D. T.; Waber, J. T. *International Tables for X-ray Crystallography*; Kynoch: Birmingham, U.K. 1974; Vol. IV.
- (29) Ibers, J. A.; Hamilton, W. C. *Acta Crystallogr.* **1964**, *17*, 781.
- (30) (a) Creagh, D. C.; McAuley, W. J. *International Tables for Crystallography*; Wilson, A. J. C., Ed.; Kluwer Academic Publishers: Boston, MA, 1992; Vol. C, pp 219–222. (b) Creagh, D. C.; Hubbell, J. H. *International Tables for Crystallography*; Wilson, A. J. C., Ed.; Kluwer Academic Publishers: Boston, MA, 1992; Vol. C, pp 200–206.
- (31) *teXsan: Crystal Structure Analysis Package*; Molecular Structure Corp.: the Woodlands, TX, 1985 and 1992.

Chapter 2

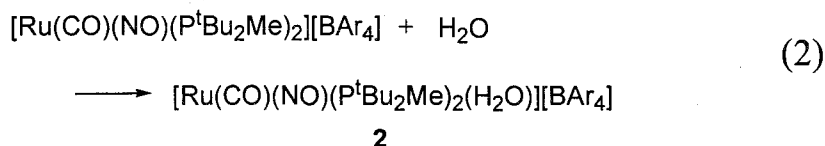
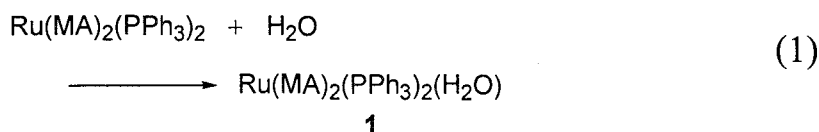
Synthesis, Structure, and Reactivity of a Stable Zerovalent Ruthenium Aqua Complex

Abstract

A novel ruthenium(0) aqua complex, $\text{Ru}(\text{dimethyl fumarate})_2(\text{dppe})(\text{H}_2\text{O})$ (**4**), was synthesized via the reaction of $\text{Ru}(\eta^6\text{-cot})(\text{dimethyl fumarate})_2$ [**3**; cot = 1,3,5-cyclooctatriene] with dppe in 1,2-dichloroethane/water, which is a quite rare example of a stable and isolable ruthenium(0) aqua complex. The X-ray crystallography of **4** indicated that coordination of a water molecule to the ruthenium center was stabilized by two hydrogen bonds with the carbonyl oxygen atoms of dimethyl fumarate ligands.

Introduction

Investigation of the reactivity of transition metal complexes toward H₂O is very important because H₂O is an extremely attractive reagent in transition metal-catalyzed organic reactions; for example, hydration of alkynes,¹⁻³ dienes⁴ and nitriles,⁵ and, in particular, anti-Markovnikov hydration of terminal alkynes^{6,7} and alkenes.⁸ With respect to one activation reaction of water by transition metals, the first step would be the coordination of H₂O to a metal center and then the oxidative addition to afford a hydrido hydroxo complex. A number of examples of transition-metal aqua complexes⁹⁻¹¹ and hydrido hydroxo complexes¹²⁻¹⁶ have been found. As for ruthenium complexes, although many examples for divalent or trivalent complexes having H₂O ligands have been reported,^{7,9,10} *zerovalent* ruthenium aqua complexes have been investigated by only two groups. Sustmann et al. showed the formation of Ru(MA)₂(PPh₃)₂(H₂O) [**1**; MA = methyl acrylate] by the reaction of the coordinatively unsaturated ruthenium(0) complex Ru(MA)₂(PPh₃)₂ with H₂O (eq 1).^{11a} The structure of **1** was confirmed by X-ray analysis. Ogasawara et al. synthesized the ruthenium(0) aqua nitrosyl complex [Ru(CO)(NO)(P^tBu₂Me)₂(H₂O)][BAR₄] [**2**; Ar = C₆H₃-3,5-(CF₃)₂] from [Ru(CO)(NO)(P^tBu₂Me)₂][BAR₄] and H₂O (eq 2).^{11b} Although both complexes are claimed to be formed in high yields *in solution* on the basis of their NMR spectra, neither the procedure of the isolation of the products nor the isolated yields have been reported. These zerovalent ruthenium complexes are apparently unstable, and



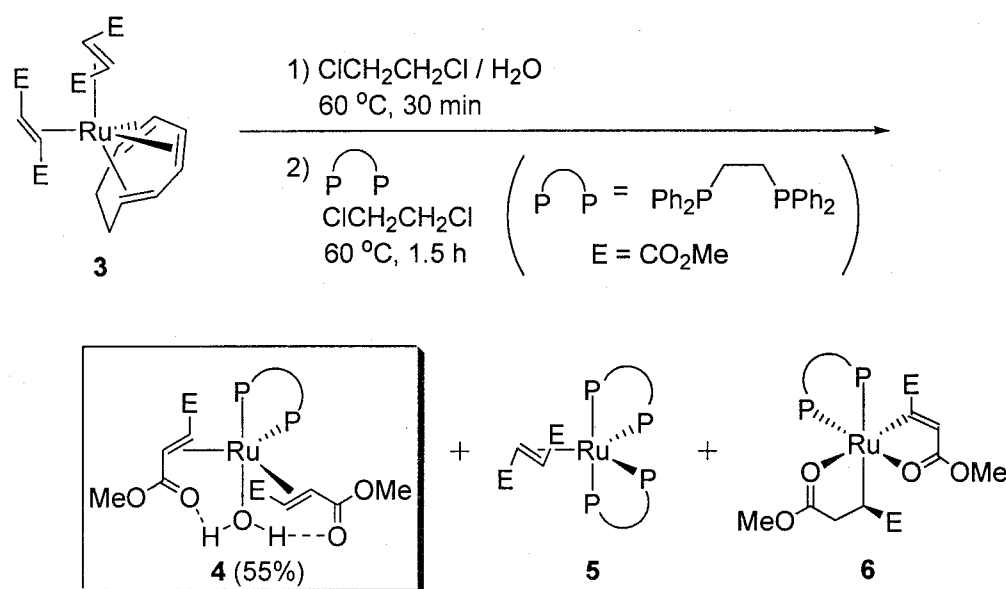
they do not tolerate the isolation procedures. It was claimed that an attempt to isolate **2** in pure form under vacuum gave $[\text{Ru}(\text{CO})(\text{NO})(\text{P}^t\text{Bu}_2\text{Me})_2][\text{BAr}_4]$ via dissociation of the H_2O ligand.

In this study, the synthesis and characterization of an isolable zerovalent ruthenium complex, $\text{Ru}(\text{dimethyl fumarate})_2(\text{dppe})(\text{H}_2\text{O})$ [dppe = 1,2-bis(di-phenylphosphino)ethane], was examined, and we found that the coordination of a water molecule in the ruthenium aqua complex is stabilized by two hydrogen bonds with the carbonyl oxygen atoms of dimethyl fumarate ligands.

Results and Discussion

$\text{Ru}(\eta^6\text{-cot})(\text{dmfm})_2$ [**3**;¹⁷ cot = 1,3,5-cyclooctatriene, dmfm = dimethyl fumarate] in 1,2-dichloroethane/ H_2O was treated with dppe at 60°C . From the reaction solution, a novel ruthenium(0) aqua complex, $\text{Ru}(\text{dmfm})_2(\text{dppe})(\text{H}_2\text{O})$ (**4**), was isolated in 55% yield as a pale yellow, relatively air-stable powder (Scheme 1). Simultaneously, two known complexes, **5** and **6**,¹⁸ were also obtained as byproducts. The reaction of **3** with other phosphine ligands such as

Scheme 1. Synthesis of a Ruthenium Aqua Complex, **4**



1,2-bis(diethylphosphino)ethane, bis(diphenylphosphino)methane, 1,3-bis(diphenylphosphino)propane, 1,4-bis(diphenylphosphino)butane, and triphenylphosphine did not give an analogue of **4**.

As mentioned in the Introduction, there have been only two reports on the synthesis of zerovalent ruthenium aqua complexes; however, their isolated yields have not been reported. Thus, complex **4** is the first example of a zerovalent ruthenium aqua complex suitable for large-scale synthesis and further investigation of the reactivity.

The ^1H , ^{13}C , and ^{31}P NMR spectra of **4** at room temperature showed very broad peaks, which suggests that **4** is fluxional in solution. At $-20\text{ }^\circ\text{C}$, all signals were sharpened, and the results are summarized in Table 1. In the ^1H NMR spectrum, the four singlet signals (3.90, 3.38, 3.00, and 2.82 ppm) for the methyl groups of dmfm were observed, showing that neither the mirror plane nor the symmetry axis exists in **4**; in other words, both of the two dmfm ligands coordinate with the same enantioface, not with a combination of (*re*, *re*) and (*si*, *si*) faces. In contrast to this result, Sustmann's complex **1**, $\text{Ru}(\text{MA})_2(\text{PPh}_3)_2(\text{H}_2\text{O})$, has a mirror plane; two methyl acrylates coordinate to the ruthenium center with a combination of *re* and *si* faces. Although it was revealed that **1** in solution isomerizes into two isomeric complexes in the geometry around ruthenium, complex **4** was revealed to be a single isomer based on the variable-temperature ^1H and ^{31}P NMR spectroscopy (-55 to $50\text{ }^\circ\text{C}$).

The solid-state structure of **4** was confirmed by X-ray analysis, and the result is shown in Figure 1. Single crystals of $\text{4}\cdot\text{C}_6\text{H}_5\text{Cl}$ for X-ray analysis were obtained by recrystallization from $\text{C}_6\text{H}_5\text{Cl}$ /pentane. The crystal data and the details are given in Table 2, and lists of the selected bond angles and bond lengths of **4** are given in Tables 3 and 4, respectively. The structure of **4** can be rationalized as a distorted trigonal bipyramid in which H_2O and one of the phosphorus atoms of dppe occupy two axial positions, and two dimethyl fumarate molecules and the other phosphine moiety of dppe hold equatorial

Table 1. ^1H , ^{13}C , and ^{31}P NMR Spectra of **4** (δ)^a

¹ H		¹³ C	
dimethyl fumarate			
=CH	3.82 (m)	=CH	53.95
	2.74 (d, 10.6)		51.16
	2.41 (dd, 9.6, 4.4)		47.12
	3.21 (d, 9.6)		45.87
Me	3.90 (s)	Me	51.78 (2C)
	3.38 (s)		50.85
	3.00 (s)		50.30
	2.82 (s)	C=O	182.59
			182.43
			176.84
			179.26
dppe			
Ph	7.93–6.83 (m)	Ph	139.24–127.11
PCH ₂	3.00 (br)	PCH ₂	29.20 (dd, 136.8, 87.6)
	2.81 (br)		18.26 (d, 78.8)
	2.30 (br d, 7.6)		
	1.91 (br)		
H ₂ O			
	4.72 (br s)		
³¹ P			
dppe		73.9 (d, 12.2)	
		42.7 (d, 12.2)	

^a Measured in CDCl_3 solution at $-20\text{ }^\circ\text{C}$. Legend: s = singlet, d = doublet, m = multiplet, br = broad. Values in parentheses are the coupling constants J (Hz).

positions. The X-ray analysis reveals that both dmfm ligands coordinate to the ruthenium center with the same enantioface, which coincides with the results of the NMR spectra (vide supra). The structure showed that the water molecule was fixed by two hydrogen bonds to the carbonyl oxygen atoms of each dmfm ligand. In complex **1**, $\text{Ru}(\text{MA})_2(\text{PPh}_3)_2(\text{H}_2\text{O})$, the H_2O molecule is also held by two hydrogen bonds with the carbonyl oxygen atoms of methyl acrylate. However, the orientations of the two hydrogen bonds are somewhat different. In complex **1**, since the two methoxy carbonyl groups are oriented to the same side, the

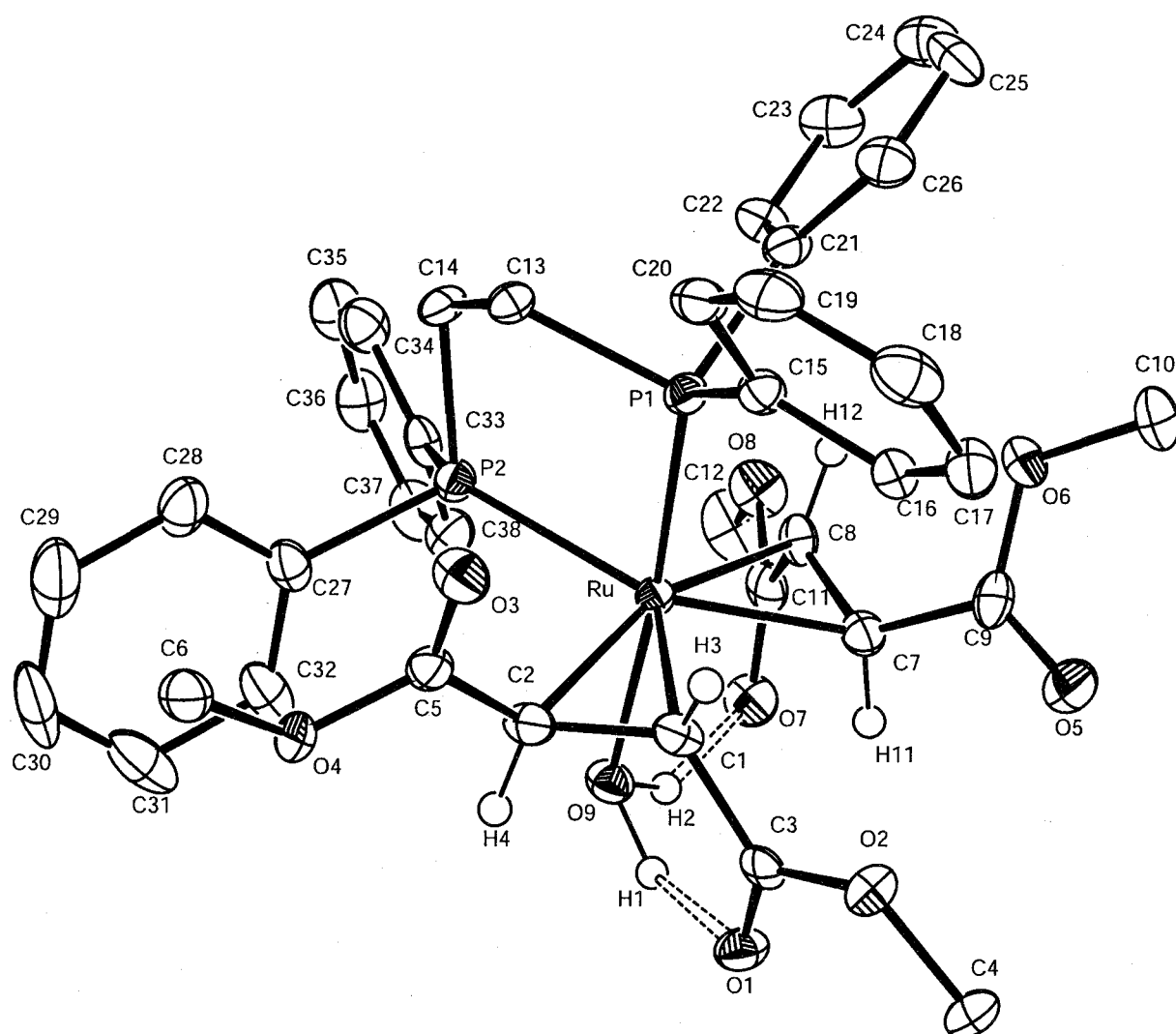


Figure 1. Structure of $4 \cdot \text{C}_6\text{H}_5\text{Cl}$. Some hydrogen atoms and $\text{C}_6\text{H}_5\text{Cl}$ molecules are omitted for clarity. Ellipsoids are given at the 50% probability level.

Chart 1. Partial Structures of **1** and **4**

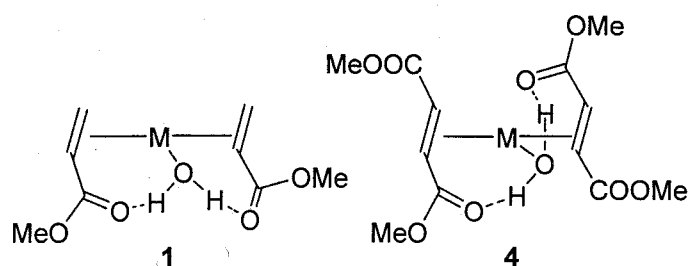


Table 2. Crystal Data of **4·C₆H₅Cl** and **7-dppm**

	4·C₆H₅Cl	7-dppm
empirical formula	C ₃₈ H ₄₂ O ₉ P ₂ Ru·C ₆ H ₅ Cl	C ₃₉ H ₄₀ O ₄ P ₂ Ru
fw	918.32	735.76
crystal system	orthorhombic	monoclinic
space group	<i>P</i> 2 ₁ 2 ₁ 2 ₁ (#19)	<i>P</i> 2 ₁ /n (#14)
<i>a</i> (Å)	8.9235(1)	11.810(3)
<i>b</i> (Å)	12.7964(3)	15.917(3)
<i>c</i> (Å)	36.6115(7)	18.031(2)
β (deg)	90	99.43(1)
<i>V</i> (Å ³)	4180.6(1)	3343.8(1)
<i>Z</i>	4	4
<i>D</i> _{calcd} (g/cm ³)	1.459	1.461
<i>F</i> ₀₀₀	1896.00	1520.00
μ (Mo K α) (cm ⁻¹)	5.71	6.06
<i>T</i> (°C)	-130	23.0
2 θ _{max} (deg)	55.0	55.0
no. of measd rflns	19557	8353
no. of unique rflns	4947 (<i>R</i> _{int} = 0.056)	7689 (<i>R</i> _{int} = 0.058)
residuals: <i>R</i> ; <i>R</i> _w	0.040; 0.051	0.040; 0.041
GOF	1.05	0.60

Table 3. Selected Bond Angles (deg) for **4**

P(1)–Ru–P(2)	82.60(6)	P(1)–Ru–O(9)	175.5(1)
P(1)–Ru–C(1)	92.2(2)	P(1)–Ru–C(2)	99.5(2)
P(1)–Ru–C(7)	100.5(2)	P(1)–Ru–C(8)	95.7(2)
P(2)–Ru–O(9)	93.2(1)	P(2)–Ru–C(1)	126.8(2)
P(2)–Ru–C(2)	90.0(2)	P(2)–Ru–C(7)	140.6(2)
P(2)–Ru–C(8)	101.9(2)	O(9)–Ru–C(1)	89.0(2)
O(9)–Ru–C(2)	78.8(2)	O(9)–Ru–C(7)	83.8(2)
O(9)–Ru–C(8)	86.7(2)	C(1)–Ru–C(2)	38.5(2)
C(1)–Ru–C(7)	92.5(2)	C(1)–Ru–C(8)	131.3(2)
C(2)–Ru–C(7)	127.3(2)	C(2)–Ru–C(8)	161.8(2)
C(7)–Ru–C(8)	38.8(2)	Ru–C(1)–C(2)	71.9(4)
Ru–C(1)–C(3)	113.8(4)	Ru–C(2)–C(1)	69.6(4)
Ru–C(2)–C(5)	126.1(4)	Ru–C(7)–C(8)	72.3(4)
Ru–C(7)–C(9)	124.8(4)	Ru–C(8)–C(7)	68.9(3)
Ru–C(8)–C(11)	117.4(4)	Ru–O(9)–H(1)	116.6(6)
Ru–O(9)–H(2)	115.6(4)	P(1)–C(13)–C(14)	108.8(5)
P(2)–C(14)–C(13)	109.3(5)	C(1)–C(2)–C(5)	115.3(5)
C(2)–C(1)–C(3)	121.9(6)	C(7)–C(8)–C(11)	118.8(6)
C(8)–C(7)–C(9)	123.0(6)	H(1)–O(9)–H(2)	86.5(7)
O(9)–H(1)–O(1)	136.6(89)	O(9)–H(2)–O(7)	144.6(68)

Table 4. Selected Bond Lengths (Å) for **4**

Ru–P(1)	2.269(2)	Ru–P(2)	2.389(2)
Ru–O(9)	2.241(5)	Ru–C(1)	2.147(6)
Ru–C(2)	2.177(6)	Ru–C(7)	2.158(6)
Ru–C(8)	2.203(6)	P(1)–C(13)	1.852(7)
P(1)–C(15)	1.831(6)	P(1)–C(21)	1.871(7)
P(2)–C(14)	1.852(6)	P(2)–C(27)	1.830(7)
P(2)–C(33)	1.835(6)	O(1)–C(3)	1.221(8)
O(2)–C(3)	1.339(8)	O(2)–C(4)	1.454(7)
O(3)–C(5)	1.211(8)	O(4)–C(5)	1.354(8)
O(4)–C(6)	1.445(7)	O(5)–C(9)	1.206(8)
O(6)–C(9)	1.353(8)	O(6)–C(10)	1.446(8)
O(7)–C(11)	1.230(8)	O(8)–C(11)	1.357(8)
O(8)–C(12)	1.455(8)	C(1)–C(2)	1.425(9)
C(1)–C(3)	1.476(9)	C(2)–C(5)	1.484(8)
C(7)–C(8)	1.449(9)	C(7)–C(9)	1.469(9)
C(8)–C(11)	1.462(9)	C(13)–C(14)	1.524(8)
C(15)–C(16)	1.401(9)	C(15)–C(20)	1.397(9)
C(16)–C(17)	1.385(9)	C(17)–C(18)	1.42(1)
C(18)–C(19)	1.36(1)	C(19)–C(20)	1.394(9)
C(21)–C(22)	1.394(9)	C(21)–C(26)	1.388(9)
C(22)–C(23)	1.38(1)	C(23)–C(24)	1.38(1)
C(24)–C(25)	1.38(1)	C(25)–C(26)	1.36(1)
C(27)–C(28)	1.39(1)	C(27)–C(32)	1.38(1)
C(28)–C(29)	1.39(1)	C(29)–C(30)	1.36(1)
C(30)–C(31)	1.38(1)	C(31)–C(32)	1.40(1)
C(33)–C(34)	1.39(1)	C(33)–C(38)	1.404(9)
C(34)–C(35)	1.39(1)	C(35)–C(36)	1.37(1)
C(36)–C(37)	1.38(1)	C(37)–C(38)	1.391(9)
O(1)–O(9)	2.668(6)	O(7)–O(9)	2.643(7)
H(1)–O(1)	1.84(11)	H(1)–O(9)	1.01(11)
H(2)–O(7)	1.73(8)	H(2)–O(9)	1.03(8)

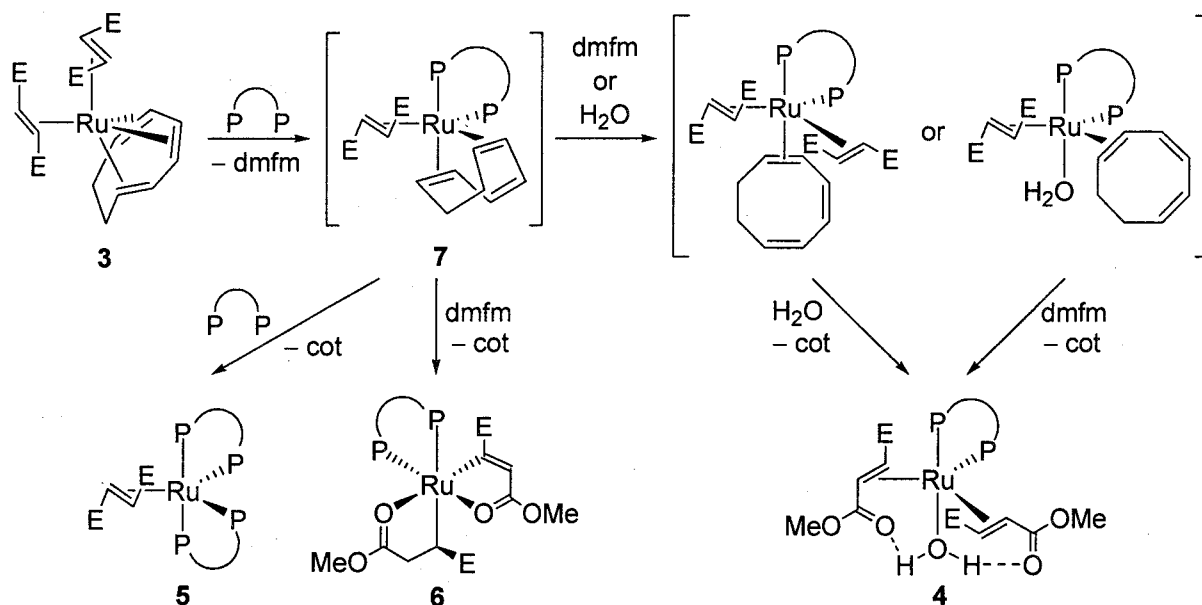
hydrogen bonds are formed with the adjacent carbonyl groups. On the other hand, in complex **4**, hydrogen bonds are formed between distant carbonyl groups (Chart 1). In solution, complex **2**, [Ru(CO)(NO)(P^tBu₂Me)₂(H₂O)][BAr₄], is stable, but the H₂O ligand, having no hydrogen bond, is only weakly coordinated. Removal of the solvent in vacuo gives the starting unsaturated ruthenium(0) complex.^{11b} Thus, the hydrogen bonds in **4** and the stronger π -acid, dimethyl fumarate, would stabilize the coordination of H₂O to form an isolable zerovalent ruthenium complex.

Preparation of $\text{Ru}(\text{dmfm})_2(\text{dppe})(\text{D}_2\text{O})$ (**4-d₂**) was attempted. Unfortunately, the isolation of pure **4-d₂** was unsuccessful. Formation of **4-d₂** was confirmed in the reaction of **3** with D_2O and dppe; however, ligand exchange between the coordinated D_2O and the adsorbed H_2O on alumina occurred during the isolation procedure of chromatography on alumina. When a drop of D_2O was added to **4** in CDCl_3 , the intensity of the ^1H NMR signal for H_2O decreased to 1/10, which means that **4-d₂** was formed in situ. Another synthesis of **4-d₂** was attempted as follows. Complex **4** was treated with D_2O in dichloromethane. After the biphasic solution was stirred for 15 min at room temperature, the solvent and D_2O were evaporated under reduced pressure. These procedures were repeated three times, and then the residue was dissolved in CDCl_3 and the ^1H NMR spectrum revealed that up to 69% of the water hydrogens were exchanged with D.

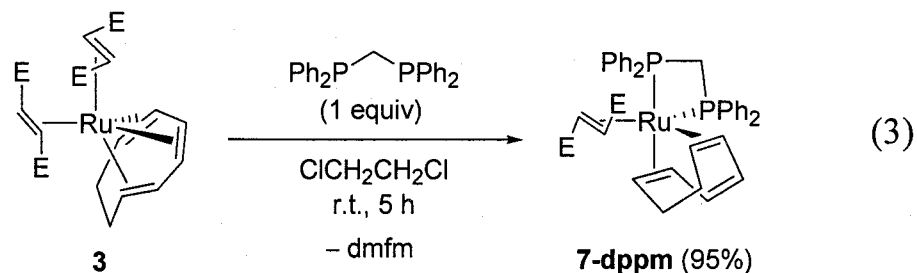
Complex **4** was reacted with another molecule of dppe in 1,2-dichloroethane at 60 °C for 2 h to give **5**. The reaction of **5** with water did not give the aqua complex **4**. While the interconversion from **6** to **4** was not observed, the transformation of **4** into **6** occurred by heating **4** in solution with a drying reagent, molecular sieves 3A (see Experimental Section).

A plausible mechanism of the formation of the aqua complex **4** is as follows (Scheme 2). We have already reported that one of the dmfm ligands and one of the olefinic moieties of the cot ligand in **3** are replaced by a bidentate nitrogen ligand in the reaction of complex **3** with 2,2'-bipyridyl or 1,10-phenanthroline.¹⁹ Considering this ligand exchange reaction, an intermediate **7** would be formed at an early stage by the reaction of **3** with a bidentate phosphine ligand, dppe. Successive replacement of the coordinated olefin moieties of cot by dmfm and H_2O will lead to the formation of **4** along with the liberation of cot. The formation of **5** may be explained by the ligand exchange of the cot moiety of **7** with dppe. In the case of the formation of **6**, sp^2 C–H bond activation of dmfm and successive insertion of another molecule of dmfm into a Ru–H bond are involved.

Scheme 2. A Plausible Mechanism of the Formation of **4**, **5**, and **6**



An analogue of the intermediate **7**, Ru(1-2:5-6- η -cot)(dmfm)(dppm) [**7-dppm**; dppm = bis(diphenylphosphino)methane] in eq 3, was obtained by the reaction of **3** with dppm in 1,2-dichloroethane. Even in the presence of water as a solvent, the product was not an aqua complex such as Ru(dmfm)₂(dppm)(H₂O) but **7-dppm**. The structure of **7-dppm** was determined by X-ray analysis (Figure 2). The crystal data and experimental details of **7-dppm** are given in Table 2, and lists of the selected bond lengths and bond angles of **7-dppm** are given in Tables 5 and 6, respectively. Complex **7-dppm** seemed to be very stable, and further ligand exchange reactions did not occur.



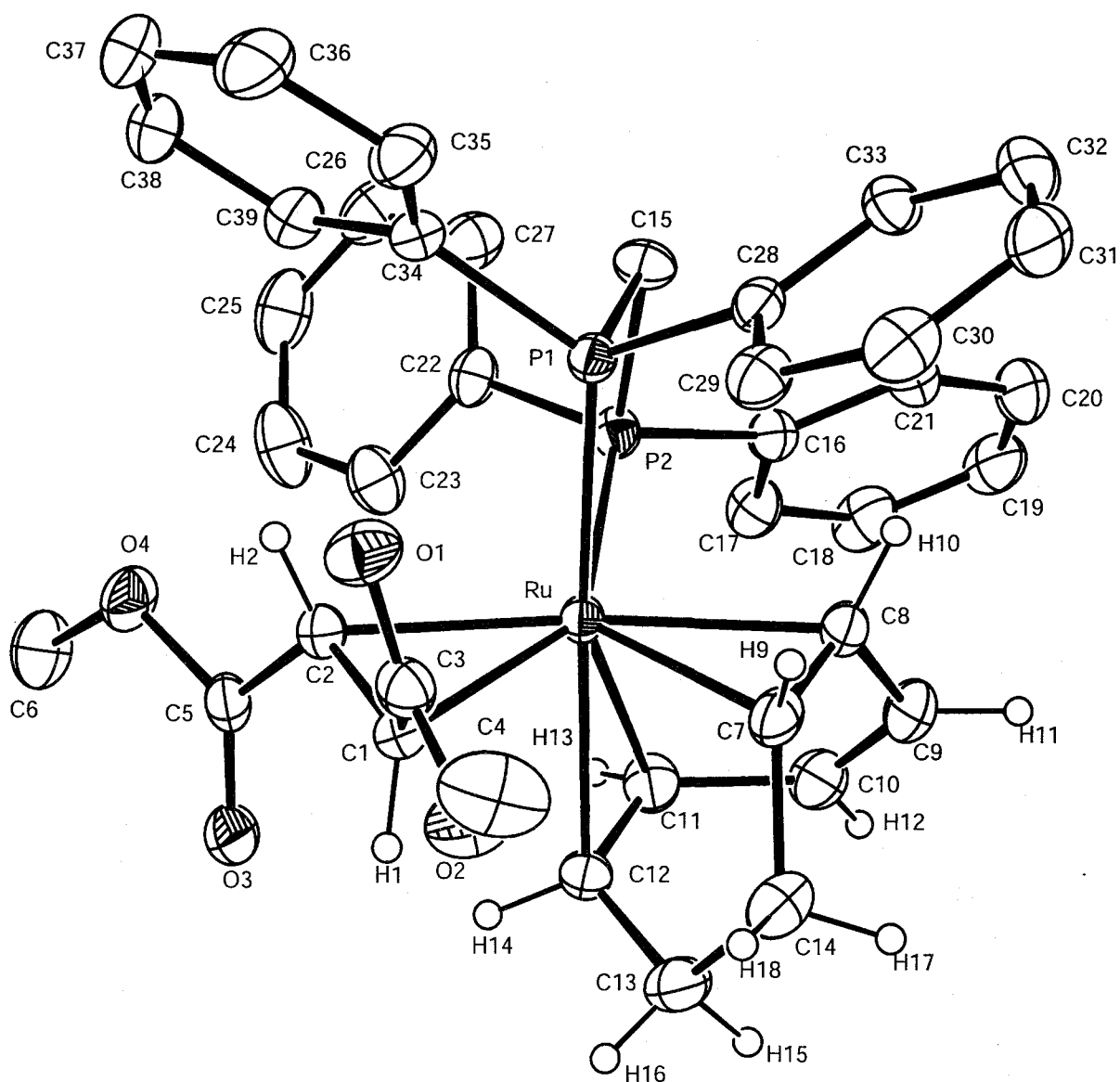


Figure 2. Structure of **7-dppm**. Some hydrogen atoms are omitted for clarity. Ellipsoids are given at the 30% probability level.

The reaction of **4** with carbon monoxide (1 atm) gave $\text{Ru}(\text{CO})_2(\text{dmfm})\text{-(dppe)}$ (**8**) via the dissociation of H_2O and one of the dmfm ligands followed by the coordination of two carbon monoxide molecules (Scheme 3). The NMR spectra of **8** in solution show the fluxionality. In the ^{31}P NMR, a slightly broadened singlet signal (57.9 ppm) and a pair of the doublet signals (62.9 and 60.0 ppm, $J = 18.3$ Hz) are observed. This result indicates the presence of two isomeric forms, **8a** and **8b**, which are different in the position of one carbon

Table 5. Selected Bond Lengths (Å) for **7-dppm**

Ru–P(1)	2.371(1)	Ru–P(2)	2.364(1)
Ru–C(1)	2.174(4)	Ru–C(2)	2.226(4)
Ru–C(7)	2.162(4)	Ru–C(8)	2.221(4)
Ru–C(11)	2.325(4)	Ru–C(12)	2.293(4)
P(1)–C(15)	1.839(5)	P(1)–C(28)	1.839(4)
P(1)–C(34)	1.838(4)	P(2)–C(15)	1.830(4)
P(2)–C(16)	1.831(5)	P(2)–C(22)	1.839(5)
O(1)–C(3)	1.203(5)	O(2)–C(3)	1.345(6)
O(2)–C(4)	1.435(6)	O(3)–C(5)	1.219(6)
O(4)–C(5)	1.355(5)	O(4)–C(6)	1.432(6)
C(1)–C(2)	1.447(5)	C(1)–C(3)	1.473(6)
C(2)–C(5)	1.454(6)	C(7)–C(8)	1.413(6)
C(7)–C(14)	1.521(6)	C(8)–C(9)	1.485(6)
C(9)–C(10)	1.326(7)	C(10)–C(11)	1.489(7)
C(11)–C(12)	1.394(7)	C(12)–C(13)	1.503(7)
C(13)–C(14)	1.509(7)	C(16)–C(17)	1.392(7)
C(16)–C(21)	1.395(6)	C(17)–C(18)	1.390(7)
C(18)–C(19)	1.373(8)	C(19)–C(20)	1.366(9)
C(20)–C(21)	1.396(7)	C(22)–C(23)	1.383(7)
C(22)–C(27)	1.378(7)	C(23)–C(24)	1.377(8)
C(24)–C(25)	1.381(9)	C(25)–C(26)	1.376(9)
C(26)–C(27)	1.388(7)	C(28)–C(29)	1.397(6)
C(28)–C(33)	1.393(6)	C(29)–C(30)	1.391(7)
C(30)–C(31)	1.377(8)	C(31)–C(32)	1.372(8)
C(32)–C(33)	1.377(6)	C(34)–C(35)	1.390(7)
C(34)–C(39)	1.383(7)	C(35)–C(36)	1.386(7)
C(36)–C(37)	1.370(9)	C(37)–C(38)	1.386(9)
C(38)–C(39)	1.388(7)		

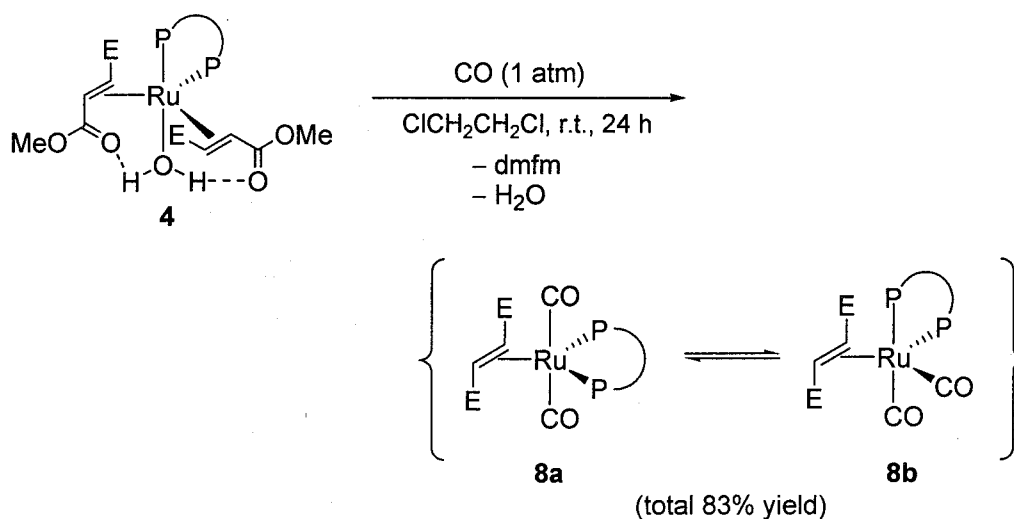
Scheme 3. Reaction of **4** with Carbon Monoxide

Table 6. Selected Bond Angles (deg) for **7-dppm**

P(1)–Ru–P(2)	70.68(4)	P(1)–Ru–C(1)	98.9(1)
P(1)–Ru–C(2)	90.6(1)	P(1)–Ru–C(7)	93.7(1)
P(1)–Ru–C(8)	88.0(1)	P(1)–Ru–C(11)	150.1(1)
P(1)–Ru–C(12)	171.6(1)	P(2)–Ru–C(1)	143.3(1)
P(2)–Ru–C(2)	105.3(1)	P(2)–Ru–C(7)	124.2(1)
P(2)–Ru–C(8)	87.4(1)	P(2)–Ru–C(11)	83.0(1)
P(2)–Ru–C(12)	116.7(1)	C(1)–Ru–C(2)	38.4(1)
C(1)–Ru–C(7)	90.7(2)	C(1)–Ru–C(8)	128.2(2)
C(1)–Ru–C(11)	110.8(2)	C(1)–Ru–C(12)	77.5(2)
C(2)–Ru–C(7)	128.8(2)	C(2)–Ru–C(8)	166.0(2)
C(2)–Ru–C(11)	110.3(2)	C(2)–Ru–C(12)	91.1(2)
C(7)–Ru–C(8)	37.6(2)	C(7)–Ru–C(11)	89.5(2)
C(7)–Ru–C(12)	78.9(2)	C(8)–Ru–C(11)	76.5(2)
C(8)–Ru–C(12)	88.3(2)	C(11)–Ru–C(12)	35.1(2)
C(7)–C(8)–C(9)	121.1(4)	C(8)–C(9)–C(10)	120.5(4)
C(9)–C(10)–C(11)	119.7(5)	C(10)–C(11)–C(12)	120.3(5)
C(12)–C(13)–C(14)	116.8(4)	C(7)–C(14)–C(13)	115.1(4)

monoxide and one phosphine moiety. The singlet in the ^{31}P NMR spectrum is consistent with **8a** and the pair of doublets is in accord with **8b**. Helliwell et al. reported that an analogous complex, $\text{Ru}(\text{CO})_2(\text{dmfm})(\text{PMe}_2\text{Ph})_2$,²⁰ shows fluxionality in solution on the basis of the Berry pseudorotation²¹ and the rotation of the dmfm ligand. At room temperature the ratio of **8a** to **8b** was 1:1.6 on the basis of the ^1H NMR spectrum. As the temperature was lowered, the equilibrium inclined to **8b**; actually, at $-55\text{ }^\circ\text{C}$ the ratio of **8a** to **8b** became 1:2.6.

Conclusion

The synthesis and reactivity of a zerovalent ruthenium aqua complex were discussed in detail. The reaction of **3** with dppe in the presence of excess water affords $\text{Ru}(\text{dmfm})_2(\text{dppe})(\text{H}_2\text{O})$ (**4**), which is a quite rare example of a stable and isolable ruthenium(0) aqua complex. The X-ray crystallography of **4** indicates that coordination of a water molecule to the ruthenium center is stabilized by

two hydrogen bonds with the carbonyl oxygen atoms of the dmfm ligands. In case of the reaction of **3** with dppm [dppm = bis(diphenylphosphino)methane], the product was not an aqua complex such as $\text{Ru}(\text{dmfm})_2(\text{dppm})(\text{H}_2\text{O})$ even in the presence of excess water, but a novel zerovalent complex, $\text{Ru}(\eta^4\text{-cot})\text{-(dmfm)(dppe)}$ was obtained via the dissociation of one of dmfm and one of cot's olefinic bond and then the coordination of dppm. This complex is considered as a model complex of the intermediate in the formation reaction of **4**. Further studies on the reactivity of **4** are currently in progress.

Experimental Section

Materials or Methods. All manipulations were performed under an argon atmosphere using standard Schlenk techniques. All solvents were distilled under argon over appropriate drying reagents (sodium, calcium chloride, or calcium hydride). $\text{Ru}(\eta^6\text{-cot})(\text{dmfm})_2$ (**3**) was synthesized as described in the literature.¹⁷ 1,2-Bis(diphenylphosphino)ethane, 1,2-bis(diethylphosphino)ethane, bis(diphenylphosphino)methane, 1,3-bis(diphenylphosphino)propane, 1,4-bis(diphenylphosphino)butane, triphenylphosphine, and carbon monoxide were obtained commercially and used without further purification.

Physical and Analytical Measurements. NMR spectra were recorded on a JEOL EX-400 (FT, 400 MHz (^1H), 100 MHz (^{13}C), 162 MHz (^{31}P)) instrument. Chemical shifts (δ) for ^1H and ^{13}C are referenced to internal solvent signals and reported relative to SiMe_4 . Chemical shifts for ^{31}P are referenced to an external $\text{P}(\text{OMe})_3$ resonance and reported relative to H_3PO_4 . IR spectra were recorded using a Nicolet Impact 410 FT-IR spectrometer. Elemental analyses were performed at the Microanalytical Center of Kyoto University.

Synthesis of $\text{Ru}(\text{dmfm})_2(\text{dppe})(\text{H}_2\text{O})$ (4**).** $\text{Ru}(\eta^6\text{-cot})(\text{dmfm})_2$ [**3**; 1.11 g, 2.2 mmol] in a 1,2-dichloroethane (6 mL) / H_2O (9 mL) solution was stirred at 60 °C for 30 min. Then dppe (894 mg, 2.24 mmol) in 1,2-dichloroethane (9 mL)

was added dropwise and the mixture was stirred at 60 °C for 1.5 h. After the solvent and water were evaporated, the orange-yellow solid was dissolved into chloroform and then chromatographed on alumina (Merck, No. 1.01097, activity II-III). Elution with chloroform gave a yellow solution, from which the solvent was evaporated. The yellow residue was recrystallized from chloroform/pentane to give **4** as pale yellow microcrystals (988 mg, 55%). Preparation of single crystals of **4**·C₆H₅Cl will be described later.

Complex 4: pale yellow crystals, mp 127–129 °C dec. Anal. Calcd for C₃₈H₄₂O₉P₂Ru: C, 56.64; H, 5.25. Found: C, 56.64; H, 5.24. IR spectrum (KBr disk): 3406, 1707, 1685, 1642 cm⁻¹.

Reaction of 4 with dppe. Complex **4** (50 mg, 0.10 mmol) and dppe (48 mg, 0.1 mmol) were reacted in 1,2-dichloroethane at 60 °C for 2 h. After the solvent was evaporated, the ¹H NMR spectrum of the residue in CDCl₃ revealed that 40% of **4** was converted into **5**.

Attempt to Synthesize 4 from 6. Complex **6** and water (excess) were reacted in 1,2-dichloroethane at 60 °C for 2 h. After the solvent and water were evaporated, the ¹H NMR spectrum of the residue in CDCl₃ revealed the complete recovery of **6**.

Synthesis of 6 from 4. Complex **4** (22 mg, 27 μmol) was heated in 1,2-dichloroethane (3 mL) with molecular sieves 3A (230 mg) at 60 °C for 2 h. After the solvent was evaporated, the ¹H NMR spectrum of the residue in CDCl₃ was measured. The spectrum revealed the complete transformation of **4** into **6**.

Synthesis of Ru(cot)(dmfm)(dppm) (7-dppm). In a 50 mL Pyrex flask with a stirring bar, complex **3** (296 mg, 0.60 mmol) and dppm (229 mg, 0.60 mmol) were placed under an argon atmosphere. Then 1,2-dichloroethane (3 mL) was added and the mixture was stirred at room temperature for 5 h. The product was separated by filtration. The yellow residue was recrystallized from dichloromethane/pentane to give **7-dppm** (420 mg, 95%). The ¹³C NMR spectrum of **7-dppm** could not be measured because of its poor solubility.

Complex **7-dppm**: pale yellow crystals, mp 211–213 °C dec. Anal. Calcd for $C_{39}H_{40}O_4P_2Ru$: C, 63.67; H, 5.48. Found: C, 63.75; H, 5.65. IR spectrum (KBr disk): 1683, 1656, 1465, 1432, 1304, 1157 cm^{-1} . 1H NMR (400 MHz, $CDCl_3$): δ 7.85–6.68 (m, 20H, H_{Ar}), 5.10 (dd, 1H, $J = 3.6$ Hz, $J = 8.0$ Hz, olefin of cot), 4.88 (dt, 1H, $J = 10.4$ Hz, $J = 15.2$ Hz, olefin of cot), 4.48 (m, 1H, olefin of cot), 4.47 (d, 1H, $J = 10.0$ Hz, olefin of cot), 4.22 (dt, 1H, $J = 8.8$ Hz, $J = 7.4$ Hz, olefin of cot), 4.17 (m, 1H, olefin of cot), 4.02 (m, 1H, olefin of dmfm), 3.79 (m, 1H, CH_2 of cot), 3.69 (s, 3H, OCH_3 of dmfm), 3.54 (s, 3H, OCH_3 of dmfm), 3.53 (m, 2H, PCH_2), 2.97 (dd, 1H, $J = 6.8$ Hz, $J = 8.8$ Hz, olefin of dmfm), 2.59 (m, 1H, CHH of cot), 2.45 (m, 2H, CH_2 of cot), 1.85 (br, 1H, CHH of cot). ^{31}P NMR (162 MHz, $CDCl_3$, -20 °C): δ -0.90 (d, $J = 48.8$ Hz), -11.1 (d, $J = 48.8$ Hz).

Synthesis of $Ru(CO)_2(dmfm)(dppe)$ (8). In a 50 mL Pyrex flask with a stirring bar, complex **4** (188 mg, 0.23 mmol) was placed under a carbon monoxide atmosphere (1 atm). 1,2-Dichloroethane (5 mL) was added, and the solution was magnetically stirred at room temperature. After 24 h, the solution was chromatographed on alumina. Elution with chloroform gave a pale yellow solution from which the solvent was evaporated to give **8** as pale yellow microcrystals (131 mg, 83%).

Complex **8**: pale yellow crystals, mp 228–230 °C dec. Anal. Calcd for $C_{34}H_{32}O_6P_2Ru$: C, 58.37; H, 4.61. Found: C, 58.27; H, 4.61. IR spectrum (KBr disk): 2013, 1975, 1948, 1677, 1434 1296 cm^{-1} . For the isomer **8a**: 1H NMR (400 MHz, $CDCl_3$) δ 7.91–7.15 (H_{Ar}), 3.67 (s, 2H, =CH), 3.63 (s, 6H, 2MeO), 3.09 (dd, 1H, $J = 20.8$ Hz, $J = 9.2$ Hz, $PCHH$), 2.36 (m, 1H, $PCHH$). ^{13}C NMR (100 MHz, $CDCl_3$): δ 198.2 (m, $Ru-CO$), 178.4 ($C=O$), 138.7–125.1 (C_{Ar}), 50.5 (OMe), 29.2 (m, =CH), 28.8 (t, $J = 22.1$ Hz, PCH_2). ^{31}P NMR (162 MHz, $CDCl_3$): δ 57.9 (s). For the isomer **8b**: 1H NMR (400 MHz, $CDCl_3$): δ 7.91–7.15 (H_{Ar}), 3.63 (br, 1H, =CH), 3.53 (s, 3H, OMe), 3.29 (s, 3H, OMe), 2.76 (m, 1H, $PCHH$), 2.57 (m, 1H, $PCHH$), 2.53 (m, 1H, $PCHH$), 2.37 (br, 1H, =CH), 2.10

(m, 1H, PCHH); ^{13}C NMR (100 MHz, CDCl_3): δ 201.5 (m, Ru–CO), 197.1 (m, Ru–CO), 179.2 (s, C=O), 178.2 (s, C=O), 138.7–125.1 (C_{Ar}), 50.5 (OMe), 50.3 (OMe), 37.8 (s, =CH), 34.4 (dd, $J = 32.5$ Hz, $J = 20.0$ Hz, PCH_2), 32.2 (d, $J = 16.7$ Hz, =CH), 29.6 (dd, $J = 25.8$ Hz, $J = 10.8$ Hz, PCH_2). ^{31}P NMR (162 MHz, CDCl_3): δ 62.9 (d, $J = 18.3$ Hz), 60.0 (d, $J = 18.3$ Hz).

Crystallographic Study. Single crystals of **4** and **7-dppm** obtained by recrystallization from chlorobenzene/pentane and dichloromethane/pentane, respectively, were subjected to X-ray crystallographic analyses. Measurements were made on a Rigaku RAXIS imaging plate area detector with graphite-monochromated Mo $\text{K}\alpha$ radiation for **4** and a Rigaku AFC7R diffractometer with graphite-monochromated Mo $\text{K}\alpha$ radiation ($\lambda = 0.71069$ Å) and a rotating anode generator for **7-dppm**. The structures were solved by direct methods using SIR92²² for **4** and **7-dppm** expanded using Fourier techniques, DIRDIF99,²³ and were refined anisotropically for non-hydrogen atoms by full-matrix least-squares calculations. Hydrogen atoms except for the H_2O ligand and the solvent in **4** and all hydrogen atoms in **7-dppm** were placed at their geometrically calculated positions. The hydrogen atoms of the H_2O ligand in **4**, H(1) and H(2), were located from Fourier maps and refined about xyz and B_{iso} . On the disordered solvent molecule, chlorobenzene, the hydrogen atoms were not located. The calculations were performed using the Crystal Structure of Rigaku Corp. and Molecular Structure Corp.

References

- (1) Ru catalyst: (a) Halpern, J.; James, B. R.; Kemp, A. L. W. *J. Am. Chem. Soc.* **1961**, 83, 4097. (b) Khan, M. M. T.; Halligudi, S. B.; Shukla, S. J. *Mol. Catal.* **1990**, 58, 299.
- (2) Pt catalyst: (a) Hiscox, W.; Jennings, J. W. *Organometallics* **1990**, 9, 1997. (b) Hartman, J. W.; Hiscox, W. C.; Jennings, P. W. *J. Org. Chem.* **1993**, 58,

7613. (c) Jennings, P. W.; Hartman, J. W.; Hiscox, W. C. *Inorg. Chim. Acta*. **1994**, 222, 317. (d) Baidossi, W.; Lahav, M.; Blum, J. *J. Org. Chem.* **1997**, 62, 669.
- (3) Rh catalyst: (a) Blum, J.; Huminer, H.; Alper, H. *J. Mol. Catal.* **1992**, 75, 153. (b) Setty-Fichman, M.; Sasson, Y.; Blum, J. *J. Mol. Catal. A: Chem.* **1997**, 126, 27.
- (4) Manyik, R. M.; Atkins, K. E.; Walker, W. E. *J. Chem. Soc. D* **1971**, 330.
- (5) (a) Jensen, C. M.; Trogler, W. C. *J. Am. Chem. Soc.* **1986**, 108, 723. (b) Murahashi, S.; Naota, T.; Saito, E. *J. Am. Chem. Soc.* **1986**, 108, 7846. (c) Murahashi, S.; Sasao, S.; Saito, E.; Naota, T. *J. Org. Chem.* **1992**, 57, 2521. (d) Murahashi, S.; Takaya, H. *Acc. Chem. Res.* **2000**, 33, 225.
- (6) (a) Tokunaga, M.; Wakatsuki, Y. *Angew. Chem.* **1998**, 110, 3024; *Angew. Chem., Int. Ed. Engl.* **1998**, 37, 2867. (b) Suzuki, T.; Tokunaga, M.; Wakatsuki, Y. *Org. Lett.* **2001**, 3, 735. (c) Tokunaga, M.; Suzuki, T.; Koga, N.; Fukushima, T.; Horiuchi, A.; Wakatsuki, Y. *J. Am. Chem. Soc.* **2001**, 123, 11917.
- (7) Grotjahn, D.; Incarvito, C. D.; Rheingold, A. *Angew. Chem., Int. Ed.* **2001**, 40, 3884.
- (8) Jensen, C. M.; Trogler, W. C. *Science* **1986**, 233, 1069.
- (9) Shriver, D. F.; Bruce, M. I. In *Comprehensive Organometallic Chemistry II*; Abel, E. W., Stone, F. G. A., Wilkinson, G., Eds.; Pergamon Press: Oxford, U.K., 1995; Vols. 6–9.
- (10) For recent leading papers, e.g., (a) Grundler, P. V.; Laurenczy, G.; Merbach, A. E. *Helv. Chim. Acta* **2001**, 84, 2854. (b) Kanaya, S.; Komine, N.; Hirano, M.; Komiya, S. *Chem. Lett.* **2001**, 1284.
- (11) (a) Sustmann, R.; Patzke, B.; Boese, R. *J. Organomet. Chem.* **1994**, 470, 191. (b) Ogasawara, M.; Huang, D.; Streib, W. E.; Huffman, J. C.; Gallego-Planas, N.; Maseras, F.; Eisenstein, O.; Caulton, K. G. *J. Am. Chem. Soc.* **1997**, 119, 8642.

- (12) Ru complex: (a) Gould, R. O.; Jones, C. L.; Robertson, D. R.; Tocher, D. A.; Stephenson, T. A. *J. Organomet. Chem.* **1982**, 226, 199. (b) Gould, R. O.; Jones, C. L.; Stephenson, T. A.; Tocher, D. A. *J. Organomet. Chem.* **1984**, 263, 375. (c) Burn, M. J.; Fickes, M. G.; Hartwig, J. F.; Hollander, F. J.; Bergman, R. G. *J. Am. Chem. Soc.* **1993**, 115, 5875. (d) Wada, T.; Tsuge, K.; Tanaka, K. *Angew. Chem., Int. Ed.* **2000**, 39, 1479.
- (13) Ir complex: (a) Milstein, D.; Calabrese, J. C.; Williams, I. D. *J. Am. Chem. Soc.* **1986**, 108, 6387. (b) Stevens, R. C.; Bau, R.; Milstein, D.; Blum, O.; Koetzle, T. F. *J. Chem. Soc., Dalton Trans.* **1990**, 1429. (c) Tani, K.; Iseki, A.; Yamagata, T. *Angew. Chem., Int. Ed.* **1998**, 37, 3381. (d) Morales-Morales, D.; Lee, D. W.; Wang, Z.; Jensen, C. M. *Organometallics* **2001**, 20, 1144. (e) Dorta, R.; Rozenberg, H.; Shimon, L. J. W.; Milstein, D. *J. Am. Chem. Soc.* **2002**, 124, 188.
- (14) Pt complex: (a) Gerlach, D. H.; Kane, A. R.; Parshall, G. W.; Jesson, J. P.; Muetterties, E. L. *J. Am. Chem. Soc.* **1971**, 93, 3543. (b) Yoshida, T.; Matsuda, T.; Okano, T.; Kitani, T.; Otsuka, S. *J. Am. Chem. Soc.* **1979**, 101, 2027.
- (15) Os complex: Eady, C. R.; Johnson, B. F. G.; Lewis, J. *J. Chem. Soc., Dalton Trans.* **1977**, 838.
- (16) Rh complex: Gillard, R. D.; Heaton, B. T.; Vaughan, D. H. *J. Chem. Soc. A* **1970**, 3126.
- (17) Mitsudo, T.; Suzuki, T.; Zhang, S.-W.; Imai, D.; Fujita, K.; Manabe, T.; Shiotsuki, M.; Watanabe, Y.; Wada, K.; Kondo, T. *J. Am. Chem. Soc.* **1999**, 121, 1839.
- (18) Shiotsuki, M.; Suzuki, T.; Kondo, T.; Wada, K.; Mitsudo, T. *Organometallics* **2000**, 19, 5733.
- (19) Suzuki, T.; Shiotsuki, M.; Wada, K.; Kondo, T.; Mitsudo, T. *Organometallics* **1999**, 18, 3671.
- (20) Helliwell, M.; Vessey, J. D.; Mawby, R. J. *J. Chem. Soc., Dalton Trans.*

1994, 1193.

- (21) Berry, R. S. *J. Chem. Phys.* **1960**, 32, 933.
- (22) *SIR92*: Altomare, A.; Cascarano, G.; Giacovazzo, C.; Guagliardi, A.; Burla, M.; Polidori, G.; Camalli, M. *J. Appl. Cryst.*, **1994**, 27, 435.
- (23) *DIRDIF99*: Beurskens, P. T.; Admiraal, G.; Beurskens, G.; Bosman, W. P.; de Gelder, R.; Israel, R.; Smits, J. M. M. *The DIRDIF-99 program system*; Technical Report of the Crystallography Laboratory; University of Nijmegen, Nijmegen, The Netherlands, 1999.

Chapter 3

Synthesis and Structure of Novel Zerovalent Ruthenium Complexes with Three Pyridine Ligands or Tridentate Pyridyl Ligands

Abstract

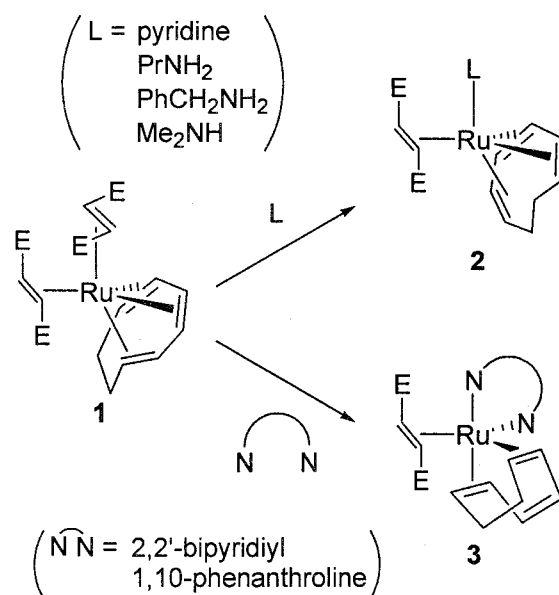
$\text{Ru}(\eta^6\text{-cot})(\text{dmfm})_2$ [**1**; cot = 1,3,5-cyclooctatriene, dmfm = dimethyl fumarate] reacted with an excess amount of pyridine to give a novel ruthenium(0) complex, $\text{Ru}(\text{dmfm})_2(\text{pyridine})_3$ (**4**). The reaction of **1** with tridentate pyridyl ligands (N-N'-N) gave novel ruthenium(0) complexes, $\text{Ru}(\text{dmfm})_2(\text{N-N'-N})$ [N-N'-N = 2,2':6',2''-terpyridine (terpy), 2,6-bis(imino)-pyridyl ligands, and 2,6-bis{(4*S*)-(-)-isopropyl-2-oxazolin-2-yl}pyridine (*i*-Pr-Pybox)]. The products are mixtures of two isomers, respectively, one of which is different from the other by the coordinating enantioface of a dmfm ligand. The structure of **4**, one isomer of $\text{Ru}(\text{dmfm})_2(\text{terpy})$ (**5**) and $\text{Ru}(\text{dmfm})_2(\textit{i}\text{-Pr-Pybox})$ (**8**) were elucidated by X-ray analysis.

Introduction

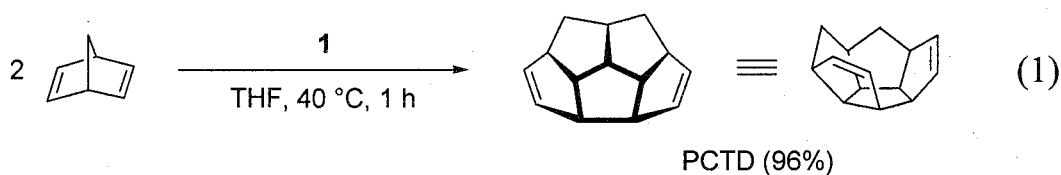
Strong σ -donor nitrogen ligands have been revealed to be congenial to transition metals. Particularly, transition metal complexes bearing pyridine-based ligands have been thoroughly studied. As for ruthenium, various complexes with polypyridyl ligands (for instance; 2,2':6',2''-terpyridine and its derivatives¹) have been well investigated because of their interesting photochemical and redox properties.² Other tridentate ligands such as 2,6-bis(imino)pyridine and Pincer-type ligand have been disclosed to form ruthenium complexes,³⁻⁹ some of which show catalytic activity in many important reactions such as epoxidation of cyclohexene,⁷ cyclopropanation of styrene,⁸ N-alkylation of aromatic amines with diols,⁹ ring-opening metathesis polymerization of 2-norbornene,¹⁰ and DNA cleavage.¹¹ An asymmetric tridentate nitrogen ligand, 2,6-bis[(4*S*)-(-)-isopropyl-2-oxazolin-2-yl]pyridine (*i*-Pr-Pybox) is known to form ruthenium complexes which catalyze an asymmetric cyclopropanation of olefinic compounds with diazoacetates¹² and polymerization of ethylene.¹³ It should be noted that these complexes are divalent or tetravalent ruthenium complexes, and, to the best of our knowledge, isolable mononuclear *zerovalent* ruthenium complexes with tridentate nitrogen ligands have not been reported, which are expected to have unique reactivity.

Recently, we reported the first example of zerovalent ruthenium complexes with mono- and bidentate nitrogen ligands (L^1 and L^2 , respectively) such as $Ru(\eta^6\text{-cot})(\text{dmfm})(L^1)$ [**2**;¹⁴ L^1 = pyridine, propylamine, benzylamine, or dimethylamine; cot = 1,3,5-cyclooctatriene; dmfm = dimethyl fumarate] and $Ru(1\text{-}2:5\text{-}6\text{-}\eta\text{-cot})(\text{dmfm})(L^2)$ [**3**;¹⁵ L^2 = 2,2'-bipyridyl or 1,10-phenanthroline]. Complexes **2** and **3** are easily derived from $Ru(\eta^6\text{-cot})(\text{dmfm})_2$ (**1**)¹⁶ (Scheme 1). Complex **1** shows excellent catalytic activity in unusual dimerization of 2,5-norbornadiene to give pentacyclo[6.6.0.0^{2,6}.0^{3,13}.0^{10,14}]tetradeca-4,11-diene (PCTD) involving carbon-carbon bond cleavage and reconstruction of a novel

Scheme 1. Reactions of **1** with Mono- or Bidentate Nitrogen Ligands



carbon skeleton under very mild conditions (eq 1).¹⁶ Complex **1** has been revealed to be a versatile starting material for preparation of various Ru(0) complexes.^{14,15,17,18} We now report a series of novel zerovalent ruthenium complexes with three pyridine ligands and those with tridentate pyridyl ligands derived from **1**.



Results and Discussion

A pyridine solution of Ru(η^6 -cot)(dmfm)₂ (**1**) was refluxed for 2 h to give Ru(dmfm)₂(pyridine)₃ (**4**) in 58% yield via the dissociation of the cot ligand in **1** followed by the coordination of three pyridine molecules (eq 2). It is noteworthy that no stereoisomer was included in the product of this reaction. Complex **4** is a zerovalent ruthenium complex with both σ -donor and π -acceptor ligands, and

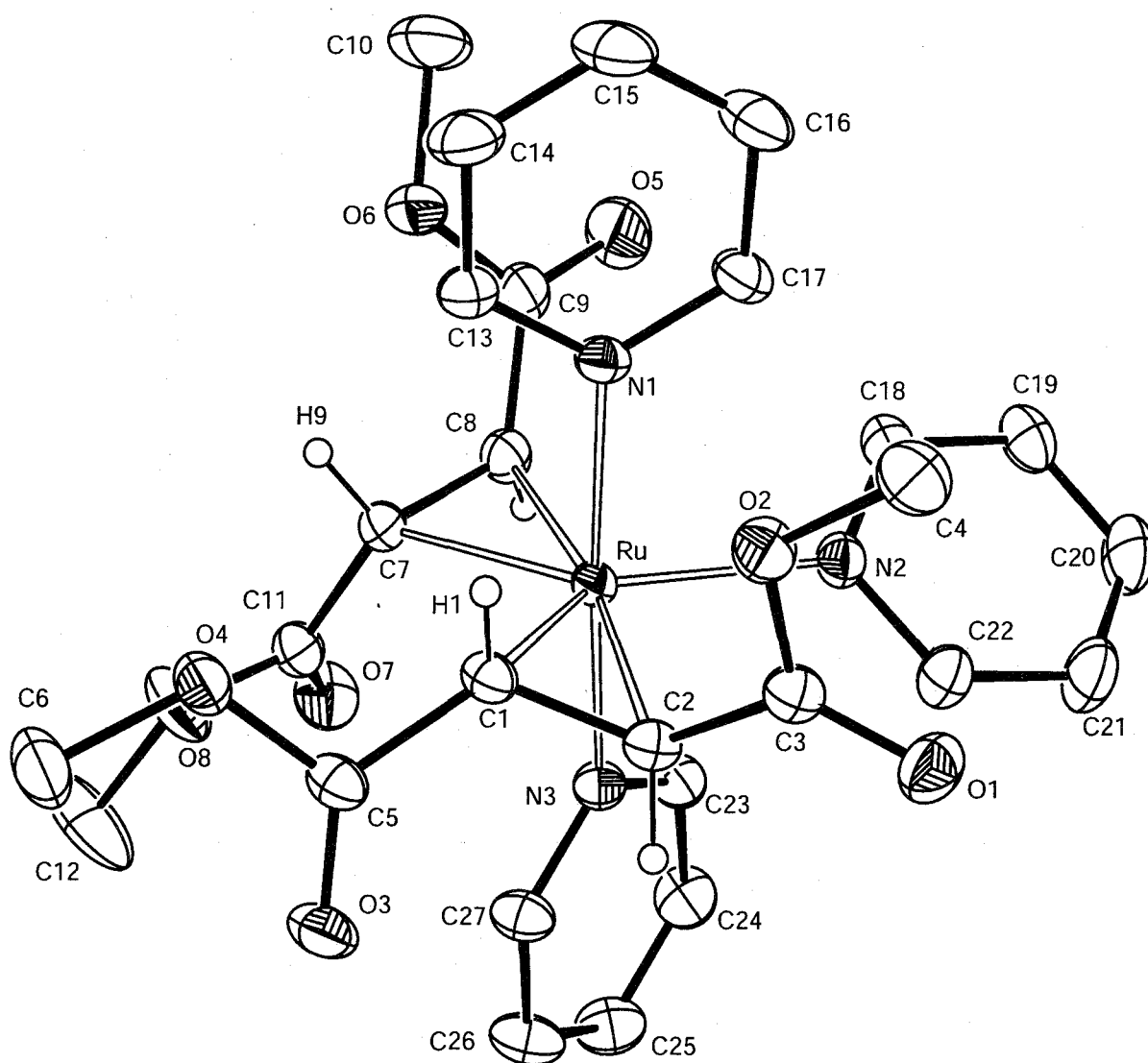
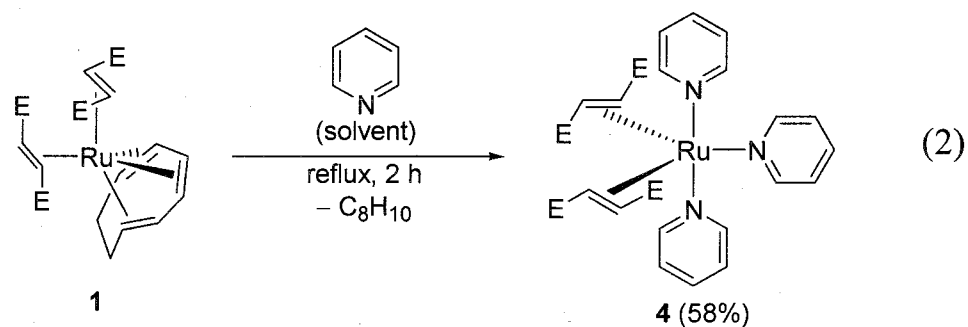


Figure 1. Structure of $\text{Ru}(\text{dmfm})_2(\text{pyridine})_3 \cdot \text{CH}_2\text{Cl}_2$ ($4 \cdot \text{CH}_2\text{Cl}_2$). CH_2Cl_2 and some hydrogen atoms are omitted for clarity. Thermal ellipsoids are given at 30% probability level.

Table 1. Summary of Crystal Data, Collection Data, and Refinement of **4**, **5b**, and **10a**

	4 ·CH ₂ Cl ₂	5b ·2{(CH ₃) ₂ CO}	10a
empirical formula	C ₂₇ H ₃₁ N ₃ O ₈ Ru·CH ₂ Cl ₂	C ₂₇ H ₂₇ N ₃ O ₈ Ru·2{(CH ₃) ₂ CO}	C ₂₉ H ₃₉ N ₃ O ₁₀ Ru
fw	711.56	738.76	690.71
crystal color	brown	brown	black
crystal system	triclinic	monoclinic	monoclinic
space group	<i>P</i> $\bar{1}$ (#2)	<i>P</i> 2 ₁ /c (#14)	<i>P</i> 2 ₁ (#4)
<i>a</i> (Å)	10.830(6)	13.6929(9)	9.064(9)
<i>b</i> (Å)	15.52(1)	14.027(1)	17.019(5)
<i>c</i> (Å)	10.035(6)	18.8621(2)	10.776(5)
α (deg)	104.38(6)	90	90
β (deg)	105.46(5)	111.98(1)	110.86(4)
γ (deg)	82.78(5)	90	90
<i>V</i> (Å ³)	1571.8(2)	3359.4(5)	1553.3(2)
<i>Z</i>	2	4	2
<i>D</i> _{calcd} (g/cm ³)	1.503	1.461	1.477
μ (Mo K α) (cm ⁻¹)	7.20	5.27	5.64
<i>T</i> (°C)	23.0	-160.0	23.0
2 θ _{max} (deg)	55.0	55.0	55.0
no. of measd reflns	7581	35799	3991
no. of obsd reflns	7199	7531	3680
residuals: <i>R</i> ; <i>R</i> _w	0.028; 0.030	0.054; 0.100	0.085; 0.099
GOF	1.40	1.21	1.20

follows the 18-electron rule. The ¹H NMR spectrum of **4** exhibited two singlets (δ 3.36 and 2.98) corresponding to the methoxy groups of dmfm and an AB quartet (δ 4.23 and 3.97, *J* = 8.6 Hz) corresponding to the olefinic protons of dmfm. In the ¹H NMR spectrum of **4**, eleven non-equivalent protons for pyridine ligands were observed for these 15 protons, which means that two axial pyridine ligands are not equivalent each other. Therefore, the structure of **4** in solution could be *C*_s symmetry; one of two dmfm ligands in **4** coordinates with (*re, re*) enantioface and the other with (*si, si*) enantioface. This means that one of the dmfm ligands must dissociate once and re-coordinate to the ruthenium center through the formation reaction of **4**.

Table 2. Selected Bond Distances (Å) for **4**

Ru–N(1)	2.133(2)	Ru–N(2)	2.221(2)
Ru–N(3)	2.135(2)	Ru–C(1)	2.148(3)
Ru–C(2)	2.194(3)	Ru–C(7)	2.129(3)
Ru–C(8)	2.172(3)	O(1)–C(3)	1.216(3)
O(2)–C(3)	1.347(3)	O(2)–C(4)	1.443(3)
O(3)–C(5)	1.211(3)	O(4)–C(5)	1.355(3)
O(4)–C(6)	1.435(3)	O(5)–C(9)	1.211(3)
O(6)–C(9)	1.352(4)	O(6)–C(10)	1.434(3)
O(7)–C(11)	1.209(3)	O(8)–C(11)	1.345(3)
O(8)–C(12)	1.440(4)	N(1)–C(13)	1.343(3)
N(1)–C(17)	1.346(3)	N(2)–C(18)	1.347(3)
N(2)–C(22)	1.341(3)	N(3)–C(23)	1.348(3)
N(3)–C(27)	1.339(3)	C(1)–C(2)	1.437(3)
C(1)–C(5)	1.468(3)	C(2)–C(3)	1.462(3)
C(7)–C(8)	1.437(3)	C(7)–C(11)	1.475(3)
C(8)–C(9)	1.459(4)	C(13)–C(14)	1.382(3)
C(14)–C(15)	1.372(4)	C(15)–C(16)	1.373(4)
C(16)–C(17)	1.387(4)	C(18)–C(19)	1.372(4)
C(19)–C(20)	1.376(4)	C(20)–C(21)	1.366(5)
C(21)–C(22)	1.379(4)	C(23)–C(24)	1.382(4)
C(24)–C(25)	1.373(4)	C(25)–C(26)	1.371(4)
C(26)–C(27)	1.386(3)		

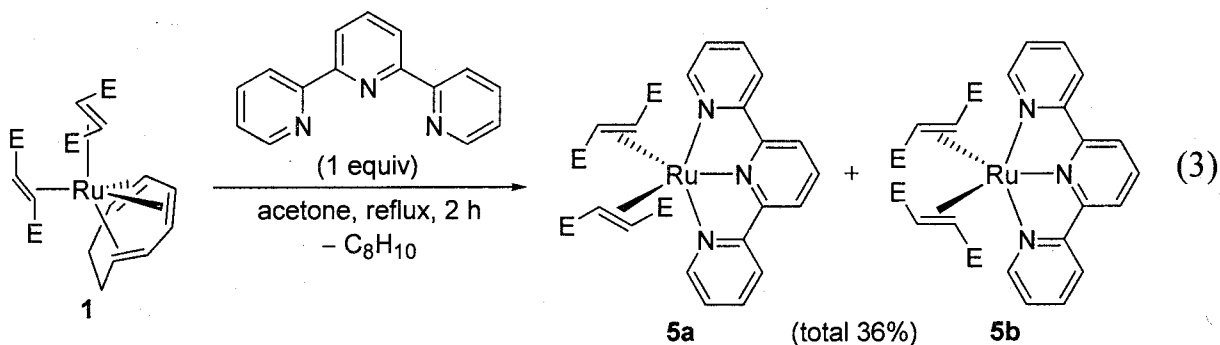
The structure of **4** was exactly confirmed by X-ray analysis (Figure 1). The crystal data and the details are summarized in Table 1. The selected bond distances and angles of **4** are given in Tables 2 and 3, respectively. The structure of **4** is rationalized as a distorted trigonal bipyramid, in which three molecules of pyridine occupy two axial and one equatorial positions, and two dmfm ligands are held in equatorial positions. The olefinic double bonds of the dmfm ligands lie in the equatorial plane. There is a mirror plane including N(1), N(2), N(3) and Ru atoms, which makes complex **4** C_s symmetric as discussed above. The angle of N(1)–Ru–N(3) is 175.40(8)°, which implies that the coordinated N(1) and N(3) of the σ -donor ligands occupy axial positions. The axial Ru–N bond

Table 3. Selected Bond Angles (deg) for **4**

N(1)–Ru–N(2)	92.2(1)	N(1)–Ru–N(3)	175.40(8)
N(1)–Ru–C(1)	82.1(1)	N(1)–Ru–C(2)	94.9(1)
N(1)–Ru–C(7)	93.1(1)	N(1)–Ru–C(8)	88.6(1)
N(2)–Ru–N(3)	83.9(1)	N(2)–Ru–C(1)	130.01(9)
N(2)–Ru–C(2)	93.4(1)	N(2)–Ru–C(7)	133.89(9)
N(2)–Ru–C(8)	95.4(1)	N(3)–Ru–C(1)	102.3(1)
N(3)–Ru–C(2)	87.8(1)	N(3)–Ru–C(7)	87.8(1)
N(3)–Ru–C(8)	89.2(1)	C(1)–Ru–C(2)	38.63(9)
C(1)–Ru–C(7)	96.1(1)	C(1)–Ru–C(8)	133.7(1)
C(2)–Ru–C(7)	131.6(1)	C(2)–Ru–C(8)	170.36(9)
C(7)–Ru–C(8)	39.03(9)	Ru–N(1)–C(13)	121.8(2)
Ru–N(1)–C(17)	121.8(2)	Ru–N(2)–C(18)	122.7(2)
Ru–N(2)–C(22)	120.0(2)	Ru–N(3)–C(23)	120.5(2)
Ru–N(3)–C(27)	123.1(2)	Ru–C(1)–C(2)	72.4(1)
Ru–C(1)–C(5)	125.4(2)	Ru–C(2)–C(1)	69.0(1)
Ru–C(2)–C(3)	116.7(2)	Ru–C(7)–C(8)	72.1(1)
Ru–C(7)–C(11)	118.8(2)	Ru–C(8)–C(7)	68.9(1)
Ru–C(8)–C(9)	120.6(2)	N(1)–C(13)–C(14)	123.6(3)
N(1)–C(17)–C(16)	123.2(3)	N(2)–C(18)–C(19)	123.2(3)
N(2)–C(22)–C(21)	122.7(3)	N(3)–C(23)–C(24)	123.2(3)
N(3)–C(27)–C(26)	123.2(3)	O(1)–C(3)–O(2)	121.8(2)
O(1)–C(3)–C(2)	124.3(2)	O(2)–C(3)–C(2)	113.8(2)
O(3)–C(5)–O(4)	121.7(2)	O(3)–C(5)–C(1)	129.0(2)
O(4)–C(5)–C(1)	109.3(2)	C(5)–O(4)–C(6)	116.9(2)
O(5)–C(9)–O(6)	121.2(3)	C(1)–C(2)–C(3)	122.6(2)
O(6)–C(9)–C(8)	113.5(2)	O(5)–C(9)–C(8)	125.3(3)
O(7)–C(11)–C(7)	126.4(3)	O(7)–C(11)–O(8)	122.1(2)
O(8)–C(11)–C(7)	111.5(2)	C(2)–C(1)–C(5)	123.6(2)
C(3)–O(2)–C(4)	116.2(2)	C(7)–C(8)–C(9)	122.2(2)
C(8)–C(7)–C(11)	117.6(2)	C(9)–O(6)–C(10)	117.2(3)
C(11)–O(8)–C(12)	116.2(3)	C(13)–N(1)–C(17)	116.4(2)
C(13)–C(14)–C(15)	119.1(3)	C(14)–C(15)–C(16)	118.7(3)
C(15)–C(16)–C(17)	119.1(3)	C(18)–N(2)–C(22)	116.9(2)
C(18)–C(19)–C(20)	119.2(3)	C(19)–C(20)–C(21)	118.4(3)
C(20)–C(21)–C(22)	119.7(3)	C(23)–N(3)–C(27)	116.5(2)
C(23)–C(24)–C(25)	119.4(3)	C(24)–C(25)–C(26)	118.2(3)
C(25)–C(26)–C(27)	119.5(3)		

distances [Ru–N(1) = 2.133(2) and Ru–N(3) = 2.135(2) Å] are shorter than that of a monopyridine ruthenium(0) complex, **2** [Ru–N = 2.175(3) Å],¹⁴ but are in the typical range for the Ru–N(pyridine) σ -bond of ruthenium complexes bearing three pyridine ligands.¹⁹ The equatorial Ru–N bond distance [Ru–N(2) = 2.221(2) Å] is exceptionally longer than the axial Ru–N bond distances. One reason for this difference would be the decrease of the electron density on the ruthenium atom by back donation to the dmfm ligands. The same tendency was observed in the result of X-ray analysis of the reported bipyridyl ruthenium(0) complex, **3**.¹⁵

A tridentate nitrogen ligand, 2,2':6',2''-terpyridine (terpy), was reacted with **1** in acetone under reflux for 2 h to afford a mixture of stereoisomers of a novel ruthenium(0) complex, Ru(dmfm)₂(terpy) (**5**) in 36% yield via the substitution between the cot ligand and terpy. In this reaction, the starting complex was completely consumed. The ¹H NMR spectrum of the reaction mixture showed that the selective formation of **5** was unsuccessful and a mixture of various complexes was formed. Using column chromatography, only complex **5** could be isolated. The obtained complexes were revealed to be a mixture of two stereoisomers, **5a** and **5b** in eq 3, based on the NMR spectra and the ratio of **5a** to **5b** was 2.5:1. The structure of **5a** resembles that of **4**, but that of **5b** is different from those of **4** and **5a**; in **5a**, two dmfm ligands coordinate with (*re, re*) and (*si, si*) enantiofaces, respectively, but in **5b**, both of the dmfm ligands coordinate with the same enantiofaces, (*si, si*) and (*si, si*) [or (*re, re*) and (*re, re*) in the enantiomer]. Thus, **5a** has a mirror plane containing all nitrogen atoms



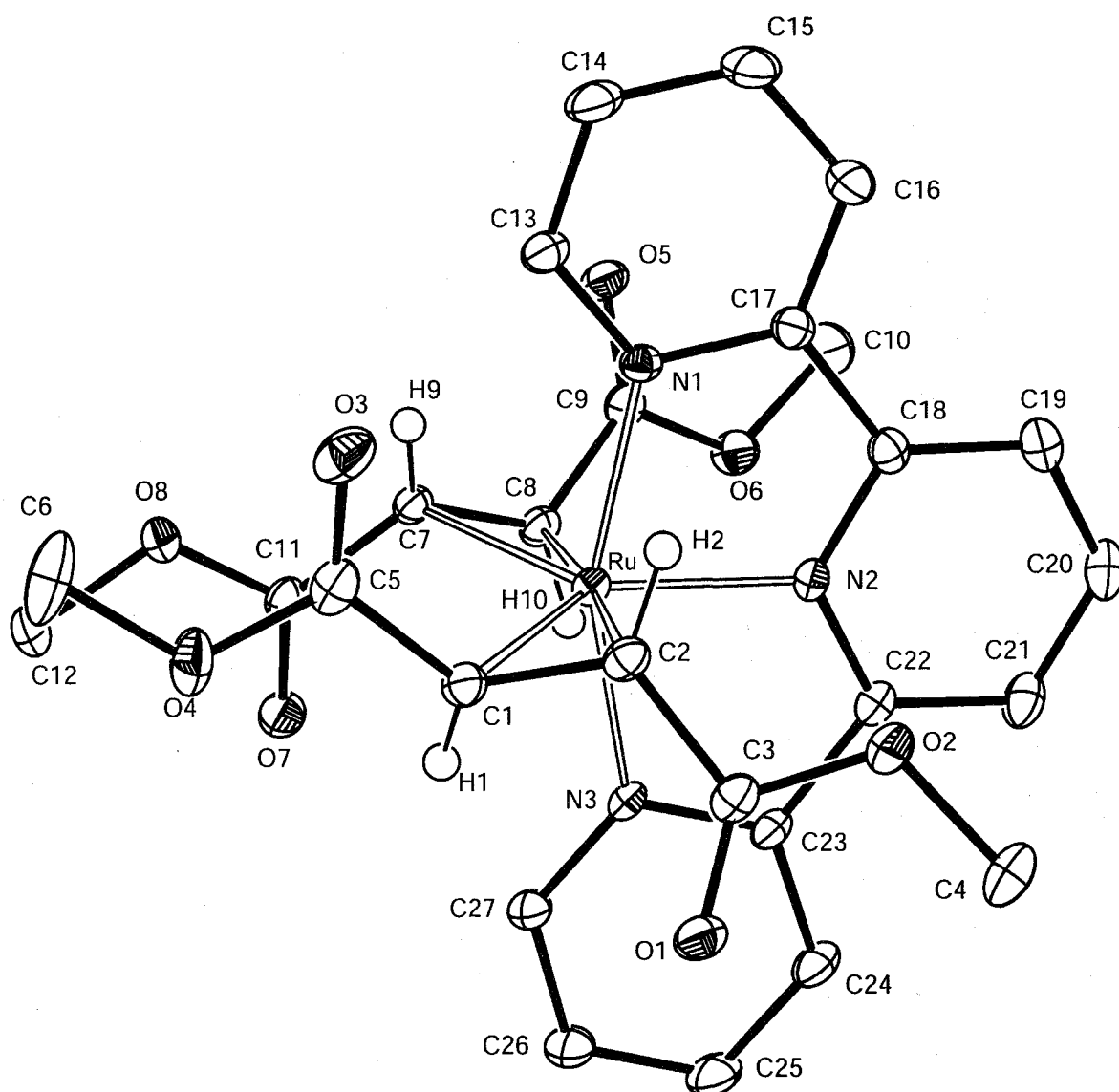


Figure 2. Structure of $\text{Ru}(\text{dmfm})_2(\text{terpy}) \cdot 2\{(\text{CH}_3)_2\text{CO}\}$ [**5b**·2{ $(\text{CH}_3)_2\text{CO}$ }]. Two molecules of acetone [$(\text{CH}_3)_2\text{CO}$] and some hydrogen atoms are omitted for clarity. Thermal ellipsoids are given at 50% probability level.

and the Ru center, while complex **5b** has a C_2 symmetry axis involving the Ru–N(central) bonds.

A number of ruthenium(II) complexes having a terpy ligand were reported so far.² Although the selective formation of one of the stereoisomers has not been achieved, **5a** and **5b** are the first example of an isolable mononuclear zerovalent ruthenium complex with a tridentate nitrogen ligand.

The structure of **5b** was confirmed by X-ray analysis. Single crystals of **5b**

Table 4. Selected Bond Distances (Å) for **5b**

Ru–N(1)	2.078(1)	Ru–N(2)	2.002(1)
Ru–N(3)	2.072(1)	Ru–C(1)	2.163(2)
Ru–C(2)	2.159(2)	Ru–C(7)	2.154(2)
Ru–C(8)	2.159(2)	O(1)–C(3)	1.213(2)
O(2)–C(3)	1.356(2)	O(2)–C(4)	1.441(2)
O(3)–C(5)	1.217(2)	O(4)–C(5)	1.355(2)
O(4)–C(6)	1.442(2)	O(5)–C(9)	1.221(2)
O(6)–C(9)	1.357(2)	O(6)–C(10)	1.444(2)
O(7)–C(11)	1.225(2)	O(8)–C(11)	1.360(2)
O(8)–C(12)	1.442(2)	N(1)–C(13)	1.345(2)
N(1)–C(17)	1.376(2)	N(2)–C(18)	1.345(2)
N(2)–C(22)	1.343(2)	N(3)–C(23)	1.373(2)
N(3)–C(27)	1.341(2)	C(1)–C(2)	1.441(3)
C(1)–C(5)	1.465(2)	C(2)–C(3)	1.473(2)
C(7)–C(8)	1.437(2)	C(7)–C(11)	1.459(2)
C(8)–C(9)	1.462(2)	C(13)–C(14)	1.387(3)
C(14)–C(15)	1.384(3)	C(15)–C(16)	1.387(3)
C(16)–C(17)	1.390(2)	C(17)–C(18)	1.481(2)
C(18)–C(19)	1.396(2)	C(19)–C(20)	1.390(3)
C(20)–C(21)	1.394(3)	C(21)–C(22)	1.390(2)
C(22)–C(23)	1.447(2)	C(23)–C(24)	1.387(3)
C(24)–C(25)	1.384(3)	C(25)–C(26)	1.385(3)
C(26)–C(27)	1.395(2)		

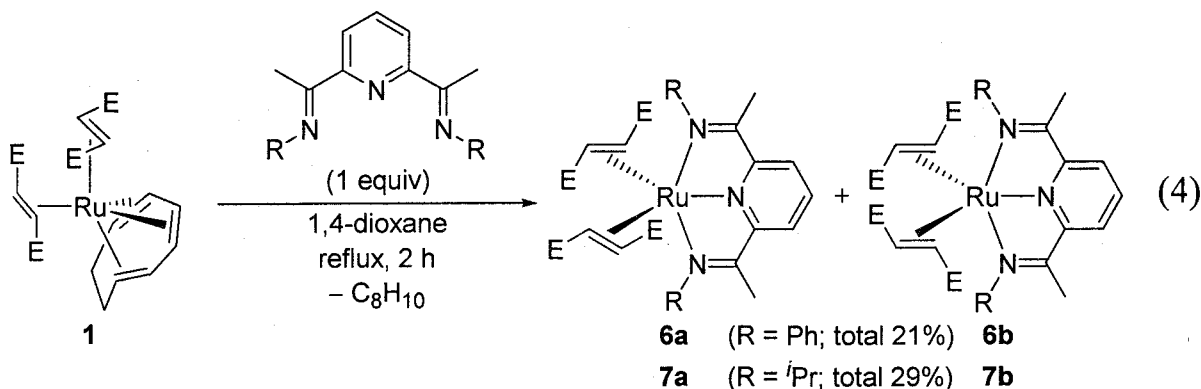
were obtained by recrystallization of the mixture of **5a** and **5b** from acetone/pentane. The ORTEP drawing of **5b** is displayed in Figure 2. The crystal data and the details are summarized in Table 1. The selected bond distances and angles of **5b** are given in Tables 4 and 5, respectively. The structure of **5b** is rationalized as a distorted trigonal bipyramid, in which the outer pyridyl moieties of terpy occupy axial coordination sites, and the central one is placed at an equatorial position. Both of the dmfm ligands are held in equatorial positions. These results indicate that the coordination number of **5b** is five, and complex **5b** is a zerovalent ruthenium complex following the 18-electron rule. Three pyridyl rings are almost on the same plane. The bond angle of N(1)–Ru–N(3) is 158.23(6)°, which is within the range [156.9(5) to 159.8(1)°] observed for other ruthenium(II) complexes having a terpy ligand.^{19c,20} The equatorial Ru–N bond

Table 5. Selected Bond Angles (deg) for **5b**

N(1)–Ru–N(2)	79.10(6)	N(1)–Ru–N(3)	158.23(6)
N(2)–Ru–N(3)	79.12(6)	N(1)–Ru–C(1)	103.85(6)
N(1)–Ru–C(2)	87.95(6)	N(1)–Ru–C(7)	89.52(6)
N(1)–Ru–C(8)	90.01(6)	N(2)–Ru–C(1)	129.33(6)
N(2)–Ru–C(2)	91.79(6)	N(2)–Ru–C(7)	130.15(6)
N(2)–Ru–C(8)	93.17(6)	N(3)–Ru–C(1)	89.93(6)
N(3)–Ru–C(2)	92.94(6)	N(3)–Ru–C(7)	104.66(6)
N(3)–Ru–C(8)	87.28(6)	C(2)–Ru–C(7)	136.55(7)
C(1)–Ru–C(2)	38.97(7)	C(1)–Ru–C(7)	100.52(6)
C(1)–Ru–C(8)	135.96(8)	C(2)–Ru–C(8)	174.92(7)
C(7)–Ru–C(8)	38.93(6)	Ru–N(1)–C(13)	128.6(1)
Ru–N(1)–C(17)	113.6(1)	Ru–N(2)–C(18)	118.7(1)
Ru–N(2)–C(22)	118.3(1)	Ru–N(3)–C(23)	113.9(1)
Ru–N(3)–C(27)	128.4(0)	Ru–C(1)–C(2)	70.38(10)
Ru–C(1)–C(5)	117.6(1)	Ru–C(2)–C(1)	70.66(9)
Ru–C(2)–C(3)	112.4(1)	Ru–C(7)–C(8)	70.71(9)
Ru–C(7)–C(11)	117.3(1)	Ru–C(8)–C(7)	70.36(10)
Ru–C(8)–C(9)	110.6(1)	N(1)–C(13)–C(14)	122.9(2)
N(1)–C(17)–C(16)	121.8(2)	N(1)–C(17)–C(18)	115.4(1)
N(2)–C(18)–C(17)	127.0(2)	N(2)–C(18)–C(19)	119.8(2)
N(2)–C(22)–C(21)	119.6(2)	N(2)–C(22)–C(23)	113.5(1)
N(3)–C(23)–C(24)	115.1(1)	N(3)–C(23)–C(24)	121.8(2)
N(3)–C(27)–C(26)	123.1(2)	O(1)–C(3)–O(2)	122.1(2)
O(1)–C(3)–C(2)	127.1(2)	O(2)–C(3)–C(2)	110.8(2)
C(3)–O(2)–C(4)	115.6(1)	O(3)–C(5)–C(1)	127.5(2)
O(3)–C(5)–O(4)	122.5(2)	O(4)–C(5)–C(1)	110.1(2)
O(5)–C(9)–O(6)	122.0(2)	O(5)–C(9)–C(8)	127.4(2)
O(6)–C(9)–C(8)	110.6(1)	O(7)–C(11)–O(8)	121.9(2)
O(7)–C(11)–C(7)	120.7(2)	C(7)–C(8)–C(9)	121.0(1)
O(8)–C(11)–C(7)	111.1(1)	C(1)–C(2)–C(3)	119.8(2)
C(2)–C(1)–C(5)	120.8(2)	C(8)–C(7)–C(11)	120.9(2)
C(5)–O(4)–C(6)	115.5(2)	C(9)–O(6)–C(10)	115.4(1)
C(11)–O(8)–C(12)	114.9(1)	C(13)–N(1)–C(17)	117.7(1)
C(13)–C(14)–C(15)	119.2(2)	C(14)–C(15)–C(16)	119.1(2)
C(15)–C(16)–C(17)	119.3(2)	C(16)–C(17)–C(18)	122.8(2)
C(17)–C(18)–C(19)	120.7(2)	C(18)–N(2)–C(22)	122.9(1)
C(18)–C(19)–C(20)	118.4(2)	C(19)–C(20)–C(21)	120.6(2)
C(20)–C(21)–C(22)	118.6(2)	C(21)–C(22)–C(23)	126.9(2)
C(22)–C(23)–C(24)	123.1(2)	C(23)–N(3)–C(27)	117.7(1)
C(23)–C(24)–C(25)	119.5(2)	C(24)–C(25)–C(26)	119.1(2)
C(25)–C(26)–C(27)	118.7(2)		

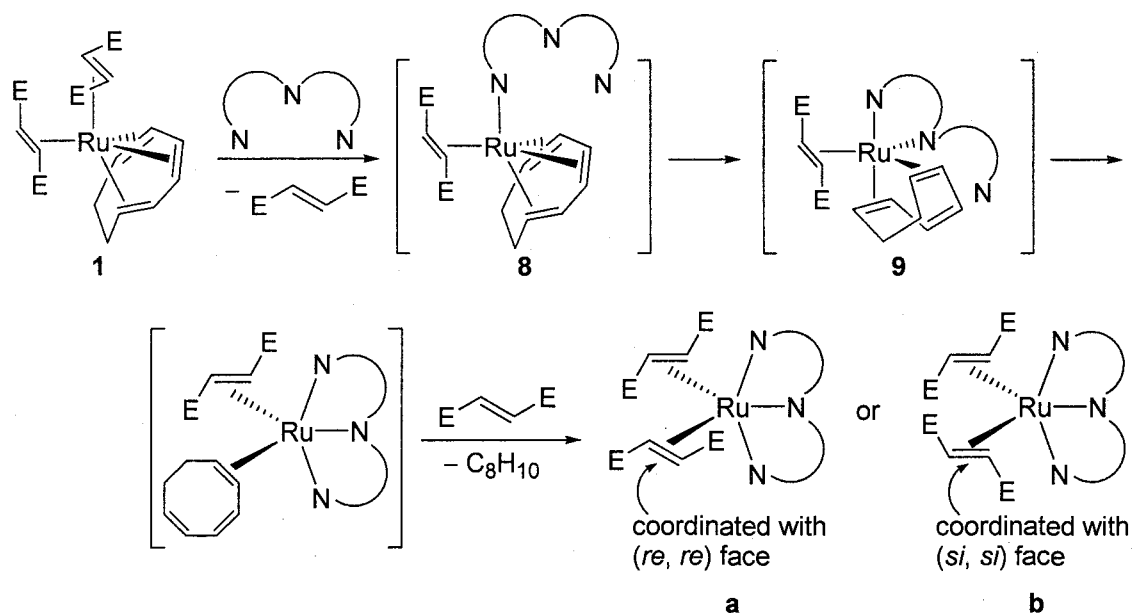
distance [Ru–N(2) = 2.002(1) Å] was shorter than that of the axial Ru–N bond [Ru–N(1) = 2.078(1) and Ru–N(3) = 2.072(1) Å], but is typical of Ru^{II}(terpy) complexes. This deviation is attributed to the geometrical constraints of the terpy backbone. These results point out that terpy holds the Ru atom tightly, and the ligand does not tend to dissociate from the Ru center.

A strong tridentate σ -donor ligand, 2,6-bis(imino)pyridine (NN'N) such as 2,6-bis{1-(phenylimino)ethyl}pyridine, was reacted with **1** in 1,4-dioxane under reflux for 2 h to give Ru(dmfm)₂(NN'N) (**6**) in 21% yield (eq 4). In a similar manner, 2,6-bis{(1-isopropylimino)ethyl}pyridine reacted with **1** to afford an analogue **7** in 29% yield (eq 4). The products of these reactions were also a mixture of stereoisomers; one of which has two dmfm ligands coordinated with a combination of same enantiofaces, and the other has two dmfm ligands coordinate with a combination of (*si*, *si*) and (*re*, *re*) faces. The isolation of each isomer has not been achieved. The ratio of **6a** to **6b** was revealed to be 5.6:1, and that of **7a** to **7b** to be 3.7:1 by the ¹H NMR spectra.



Switching the coordinative enantioface of one of the dmfm ligands through this reaction suggests that the reaction would begin with the dissociation of the dmfm ligand (Scheme 2). The generated vacant site would be occupied by one of the terminal imine moieties to give an intermediate **8**. This is supposed on the basis of our report on the formation of ruthenium(0) complexes with

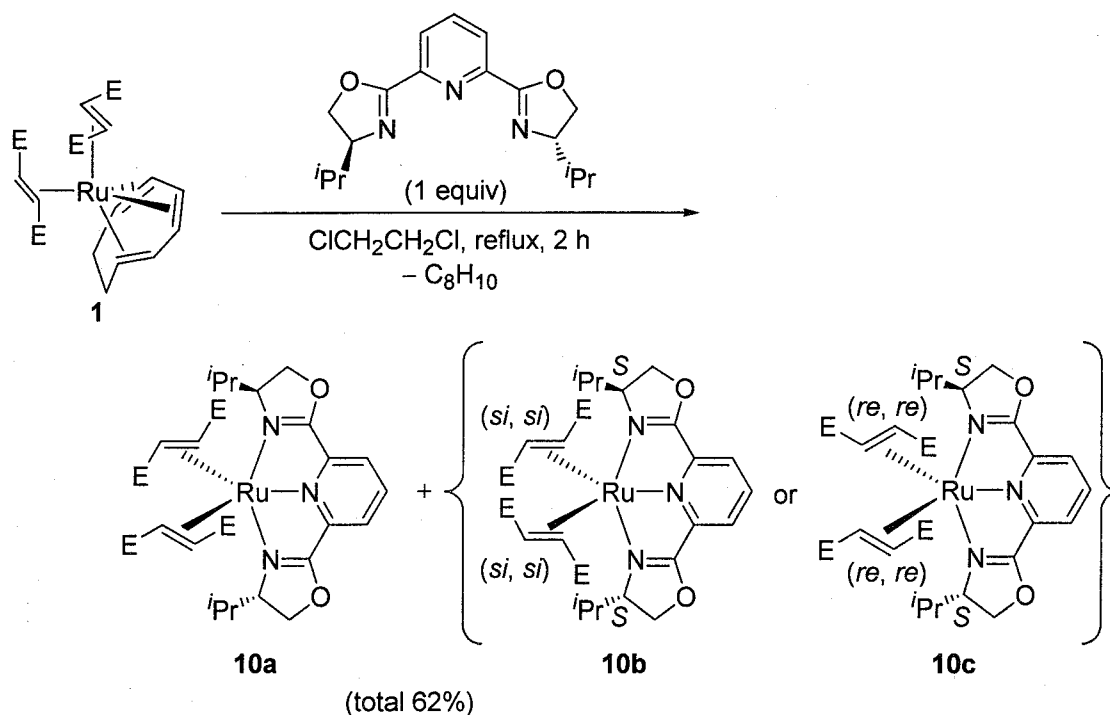
Scheme 2. Mechanism of the Formation of a Tridentate Nitrogen Complex



monodentate nitrogen ligands.¹⁴ Then the dissociation of the central olefinic group of the cot ligand is followed by the coordination of the central pyridyl group of the tridentate ligand to afford an intermediate **9**, according to the reported reaction pathway to form ruthenium(0) complexes having bidentate nitrogen ligands.¹⁵ The complete dissociation of the cot ligand and the coordination of the last nitrogen moiety formed the Ru(N-N'-N) species. Finally, the dissociated dmfm coordinates again in the place of the cot ligand with the (*si*, *si*) or (*re*, *re*) enantioface, which would produce stereoisomers such as **a** and **b** in Scheme 2. The cot ligand is not directly substituted by a tridentate nitrogen ligand. This mechanism would be able to explain the formation of the analogous complexes reported in this paper. In case of **4**, however, the reason why only one isomer could be obtained has not been clarified.

By using an asymmetric tridentate nitrogen ligand, 2,6-bis(oxazolinyl)-pyridine (Pybox), successful enantioface-selective coordination of dmfm or *trans*-cyclooctene to ruthenium(II) was reported by Nishiyama et al.^{21,22} Complex **1** reacted with 2,6-bis[(4*S*)-(-)-isopropyl-2-oxazolin-2-yl]pyridine (*i*-Pr-Pybox) in 1,2-dichloroethane under reflux for 2 h to afford a mixture of two stereoisomers of Ru(dmfm)₂(*i*-Pr-Pybox) (**10a**, and **10b** or **10c**) in good

Scheme 3. Reaction of **1** with *i*-Pr-Pybox



yield (Scheme 3). Although the selective formation of only one stereoisomer could not be achieved, the formation of the one isomer (**10b** or **10c**) could be successfully prevented. The ratio of **10a** to **10b** (or **10c**) was revealed to be 1:1 by the ^1H NMR spectrum. The structures of the products were deduced on the basis of ^1H , ^{13}C NMR and IR spectra. The structure of **10a** was confirmed by X-ray analysis. The used single crystals of **10a** were obtained by the recrystallization of the mixture of **10a** and **10b** (or **10c**) from acetone/pentane. The ORTEP drawing of **10a** is shown in Figure 3. The crystal data and the details are given in Table 1. The selected bond distances and angles of complex **10a** are given in Tables 6 and 7, respectively. The coordination number of **10a** is five and it is also a zerovalent ruthenium complex satisfying the 18-electron rule. The structure of **10a** is represented by a trigonal bipyramid. The nitrogen atoms of the oxazolinyl group occupy axial positions, and the pyridyl moiety of *i*-Pr-Pybox and two dmfm ligands coordinated at equatorial positions. One of the dmfm ligands coordinates to the ruthenium center with the (*si*, *si*) face and the

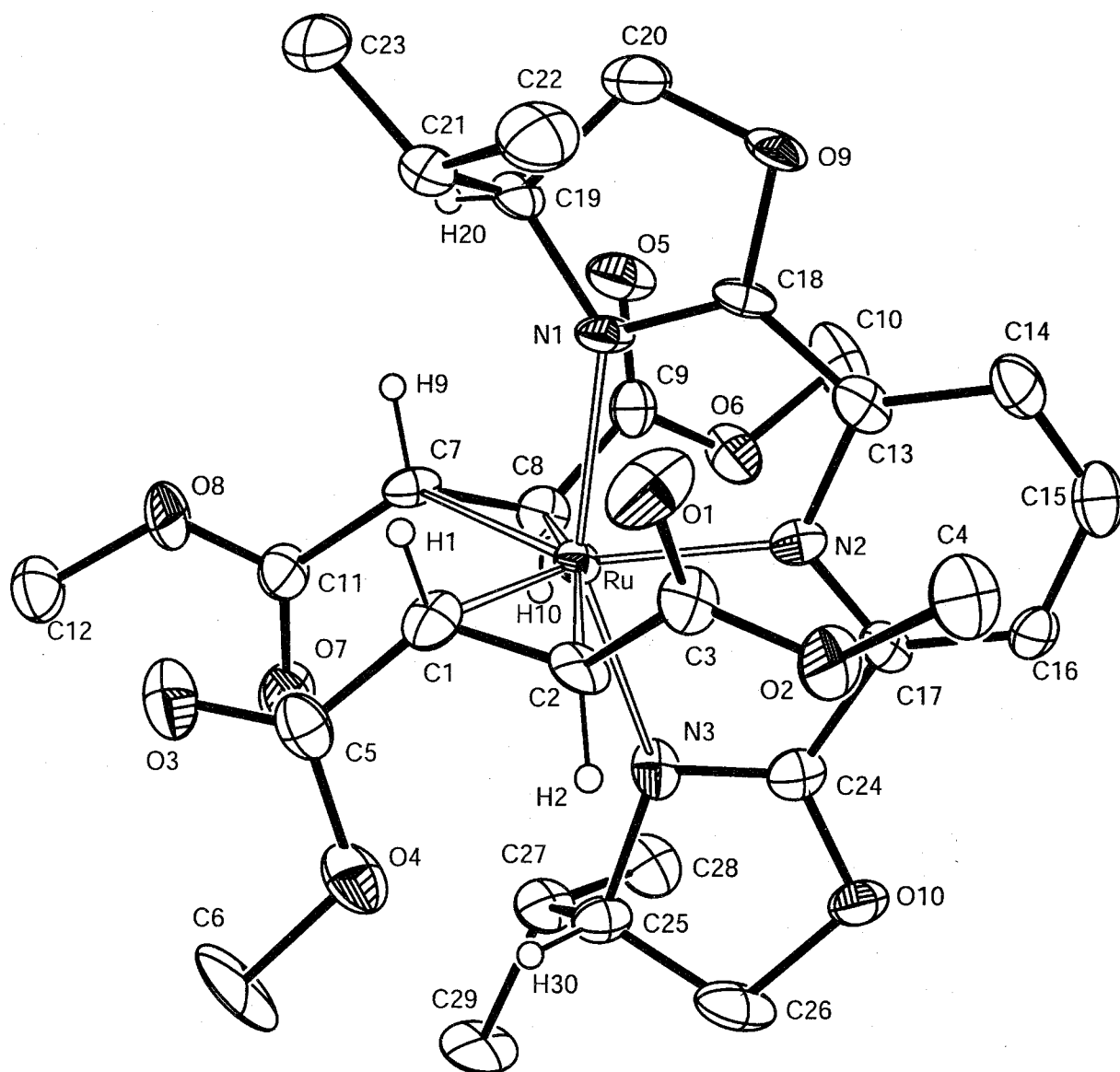


Figure 3. ORTEP drawing of $\text{Ru}(\text{dmfm})_2(i\text{-Pr-Pybox})$ (**10a**). Some hydrogen atoms are omitted for clarity. Thermal ellipsoids are given at 30% probability level.

other with the (*re, re*) face. Thus, any atoms in **10a** could not be equivalent with each other in the NMR spectra.

Unfortunately, it could not be achieved to elucidate which isomer, **10b** or **10c**, was formed. Both **10b** and **10c** have a symmetry axis including the bond between Ru and the nitrogen atom of the central pyridyl group. Thus, the results of NMR spectra of these complexes must be very similar.

Considering the steric repulsion between *i*-Pr of Pybox and the ester groups

Table 6. Selected Bond Distances (Å) for **10a**

Ru(1)–N(1)	2.13(2)	Ru(1)–N(2)	2.02(1)
Ru(1)–N(3)	2.16(2)	Ru(1)–C(1)	2.11(2)
Ru(1)–C(2)	2.13(2)	Ru(1)–C(7)	2.19(2)
Ru(1)–C(8)	2.20(2)	O(1)–C(3)	1.22(2)
O(2)–C(3)	1.30(3)	O(2)–C(4)	1.46(2)
O(3)–C(5)	1.19(3)	O(4)–C(5)	1.40(3)
O(4)–C(6)	1.45(2)	O(5)–C(9)	1.30(3)
O(6)–C(9)	1.28(3)	O(6)–C(10)	1.42(3)
O(7)–C(11)	1.27(3)	O(8)–C(11)	1.24(2)
O(8)–C(12)	1.42(2)	O(9)–C(18)	1.37(2)
O(9)–C(20)	1.42(3)	O(10)–C(24)	1.35(2)
O(10)–C(26)	1.48(3)	N(1)–C(18)	1.30(3)
N(1)–C(19)	1.48(3)	N(2)–C(13)	1.38(2)
N(2)–C(17)	1.33(2)	N(3)–C(24)	1.30(3)
N(3)–C(25)	1.52(3)	C(1)–C(2)	1.39(3)
C(1)–C(5)	1.48(3)	C(2)–C(3)	1.46(2)
C(7)–C(8)	1.47(3)	C(7)–C(11)	1.47(3)
C(8)–C(9)	1.38(3)	C(13)–C(14)	1.41(3)
C(13)–C(18)	1.46(3)	C(14)–C(15)	1.32(3)
C(15)–C(16)	1.38(3)	C(16)–C(17)	1.37(3)
C(17)–C(24)	1.46(3)	C(19)–C(20)	1.55(3)
C(19)–C(21)	1.50(3)	C(21)–C(22)	1.55(3)
C(21)–C(23)	1.48(3)	C(25)–C(26)	1.48(3)
C(25)–C(27)	1.56(3)	C(27)–C(28)	1.52(3)
C(27)–C(29)	1.54(3)		

of dmfm, complex **10c** seems to be more stable than **10b**. Nishiyama and coworkers showed that the (*S,S*)-Ph-Pybox coordinated ruthenium(II) complex can select the enantioface of dmfm and the dmfm ligand coordinates by the (*re, re*) face.^{21b} This is the result of the repulsion between Ph groups of Pybox and the ester groups of dmfm. Therefore, it could be possible to say that **10c** is more stable than the other isomers.

The mechanism for the formation of complexes **10** could also be inferred as shown in Scheme 2. This mechanism can explain the prevention of the formation of one isomer, **10b** or **10c**. The starting material **1** has two dimethyl fumarate ligands; one of which would not dissociate during the formation

Table 7. Selected Bond Angles (deg) for **10a**

N(1)–Ru(1)–N(2)	78.5(6)	N(1)–Ru(1)–N(3)	153.3(7)
N(2)–Ru(1)–N(3)	74.8(5)	N(1)–Ru(1)–C(1)	93.8(7)
N(2)–Ru(1)–C(1)	128.1(6)	N(3)–Ru(1)–C(1)	104.0(7)
N(1)–Ru(1)–C(2)	97.8(6)	N(2)–Ru(1)–C(2)	91.4(7)
N(3)–Ru(1)–C(2)	84.8(7)	C(1)–Ru(1)–C(2)	38.3(7)
N(1)–Ru(1)–C(7)	87.8(6)	N(2)–Ru(1)–C(7)	133.4(6)
N(3)–Ru(1)–C(7)	109.3(6)	C(1)–Ru(1)–C(7)	96.8(7)
C(2)–Ru(1)–C(7)	134.8(8)	N(1)–Ru(1)–C(8)	95.7(7)
N(2)–Ru(1)–C(8)	97.8(6)	N(3)–Ru(1)–C(8)	86.2(7)
C(1)–Ru(1)–C(8)	134.2(8)	C(2)–Ru(1)–C(8)	165.0(7)
C(7)–Ru(1)–C(8)	39.1(7)	Ru(1)–N(1)–C(19)	140.2(1)
Ru(1)–N(1)–C(18)	109.9(1)	Ru(1)–N(2)–C(13)	118.9(1)
Ru(1)–N(2)–C(17)	123.6(1)	Ru(1)–N(3)–C(24)	112.5(1)
Ru(1)–N(3)–C(25)	140.3(1)	Ru(1)–C(1)–C(2)	71.5(1)
Ru(1)–C(1)–C(5)	119.9(1)	Ru(1)–C(2)–C(1)	70.2(1)
Ru(1)–C(2)–C(3)	115.7(1)	Ru(1)–C(7)–C(8)	70.8(1)
Ru(1)–C(7)–C(11)	121.0(1)	Ru(1)–C(8)–C(7)	70.1(1)
Ru(1)–C(8)–C(9)	109.3(1)	N(1)–C(18)–C(13)	123.5(2)
N(1)–C(19)–C(20)	101.3(2)	N(1)–C(19)–C(21)	114.8(2)
N(2)–C(13)–C(14)	120.6(2)	N(2)–C(13)–C(18)	108.8(2)
N(2)–C(17)–C(16)	123.0(2)	N(2)–C(17)–C(24)	108.1(2)
N(3)–C(24)–C(17)	120.8(2)	N(3)–C(25)–C(26)	100.9(2)
N(3)–C(25)–C(27)	108.2(2)	O(1)–C(3)–O(2)	125.6(2)
O(1)–C(3)–C(2)	121.5(2)	O(2)–C(3)–C(2)	112.8(2)
O(3)–C(5)–O(4)	119.7(2)	O(3)–C(5)–C(1)	128.6(2)
O(4)–C(5)–C(1)	111.6(2)	O(5)–C(9)–O(6)	120.1(2)
O(5)–C(9)–C(8)	125.6(2)	O(8)–C(11)–C(7)	115.9(2)
O(6)–C(9)–C(8)	114.3(2)	O(7)–C(11)–C(7)	123.5(2)
O(7)–C(11)–O(8)	120.7(2)	O(9)–C(18)–N(1)	116.0(2)
O(9)–C(18)–C(13)	120.3(2)	O(9)–C(20)–C(19)	104.6(2)
O(10)–C(24)–N(3)	118.3(2)	O(10)–C(24)–C(17)	120.6(2)
O(10)–C(26)–C(25)	107.9(2)	C(1)–C(2)–C(3)	128.0(2)
C(2)–C(1)–C(5)	124.0(2)	C(3)–O(2)–C(4)	119.4(2)
C(5)–O(4)–C(6)	115.1(2)	C(7)–C(8)–C(9)	124.7(2)
C(8)–C(7)–C(11)	122.4(2)	C(9)–O(6)–C(10)	120.3(2)
C(11)–O(8)–C(12)	121.7(2)	C(13)–N(2)–C(17)	117.1(2)
C(13)–C(14)–C(15)	119.3(2)	C(14)–C(13)–C(18)	130.4(2)
C(14)–C(15)–C(16)	120.2(2)	C(16)–C(17)–C(24)	128.6(2)
C(15)–C(16)–C(17)	119.0(2)	C(18)–N(1)–C(19)	107.7(2)
C(18)–O(9)–C(20)	104.9(2)	C(19)–C(21)–C(22)	111.4(2)
C(19)–C(21)–C(23)	109.2(2)	C(20)–C(19)–C(21)	117.5(2)
C(22)–C(21)–C(23)	111.4(2)	C(24)–N(3)–C(25)	106.6(2)
C(24)–O(10)–C(26)	102.6(2)	C(25)–C(27)–C(28)	114.5(2)
C(25)–C(27)–C(29)	107.4(2)	C(26)–C(25)–C(27)	114.3(2)
C(28)–C(27)–C(29)	110.3(2)		

reaction of **10**, whereas the other would dissociate once and then re-coordinate to the ruthenium center. The enantioface of the former dmfm ligand can be either (*si*, *si*) or (*re*, *re*). On the other hand, the enantioface of the latter dmfm ligand would be selected by (*S,S*)-*i*-Pr-Pybox ligand when it re-coordinates to the ruthenium center. Based on the results reported by Nishiyama et al.,²¹ it seems likely that (*S,S*)-*i*-Pr-Pybox ligand would select the enantioface of the re-coordinated dmfm ligand as (*re*, *re*). If the same selection of the enantioface is performed in the formation of **10**, the formation of **10b** might be difficult.

As for complexes **10**, the substitution of the coordinated dimethyl fumarate ligands with external dimethyl fumarate was examined. A solution of complexes **10** and H₃CO₂CCD=CDCO₂CH₃ (dimethyl fumarate-*d*₂; 8 equiv) in 1,2-dichloroethane was refluxed for 2 h. After solvent was evaporated, the ¹H NMR of the residue in CDCl₃ proved that none of dimethyl fumarate-*d*₂ was incorporated in complexes **10**. This result indicates that the dissociation and re-coordination of the dimethyl fumarate ligands do not occur, and thus there is no equilibrium between complexes **10a** and **10c** (or **10b**).

Conclusion

Complex **1** is revealed to be a parent complex for various zerovalent ruthenium complexes. In contrast to the reaction of **1** with mono- or bidentate nitrogen ligands, in the present reaction with tridentate pyridine ligands, the cot ligand of **1** was dissociated completely to afford a novel series of zerovalent complexes Ru(dmfm)₂(N-N'-N). Complexes **4**, **5**, **6**, **7**, and **10** are interesting complexes possessing both electron-deficient olefinic ligands and electron-rich σ-donor N-ligands. Some of the zerovalent complexes are expected to be valuable catalyst precursors.

Experimental Section

Materials or Methods. All manipulations were performed under an argon atmosphere using standard Schlenk Techniques. All solvents were distilled under argon over appropriate drying reagents (sodium, calcium chloride, and calcium hydride). Complex **1**, 2,6-bis{(1-isopropylimino)ethyl}pyridine, 2,6-bis-{(1-phenylimino)ethyl}pyridine, and $\text{H}_3\text{CO}_2\text{CCD}=\text{CDCO}_2\text{CH}_3$ (dimethyl fumarate- d_2) were synthesized as described in the literature.^{7,16,23} 2,2':6',2''-Terpyridine (terpy), and 2,6-bis[(4*S*)-(-)-isopropyl-2-oxazolin-2-yl]pyridine (*i*-Pr-Pybox) were obtained commercially and used without further purification. All new compounds are characterized below.

Physical and Analytical Measurements. NMR spectra were recorded on a JEOL EX-400 (FT, 400 MHz (^1H), 100 MHz(^{13}C)) instrument. Chemical shifts (δ) for ^1H and ^{13}C are referenced to internal solvent resonances and reported relative to SiMe_4 . IR spectra were recorded using a Nicolet Impact 410 FT-IR spectrometer. HR-MS spectra were recorded on JEOL SX102A spectrometers with *m*-nitrobenzyl alcohol (*m*-NBA) as a matrix. Elemental analyses of the complexes except for **6** were performed at the Microanalytical Center of Kyoto University. Elemental analysis of **6** was performed using PerkinElmer PE 2400 series II CHNS/O analyzer.

Synthesis of $\text{Ru}(\text{dmfm})_2(\text{pyridine})_3$ (4**).** In a 20 mL two-necked flask equipped with a reflux condenser and a stirring bar, $\text{Ru}(\eta^6\text{-cot})(\text{dmfm})_2$ (**1**; 0.50 g, 1.0 mmol) was placed under an argon atmosphere. Then 5.0 mL of pyridine was added and the mixture was refluxed for 2 h. The solution was chromatographed on alumina (activity II-III). Elution with hexane-pyridine (50:50) gave an orange solution, from which the solvent was evaporated. The orange residue was recrystallized from CH_2Cl_2 /pentane to give complex $4 \cdot \text{CH}_2\text{Cl}_2$ (0.416 g, 58% yield).

Complex **4**·CH₂Cl₂: Orange crystals, mp 100–102 °C dec. Anal. Calcd for C₂₇H₃₁N₃O₈Ru·CH₂Cl₂: C, 47.26; H, 4.67; N, 5.91; Cl, 9.96. Found: C, 46.99; H, 4.68; N, 5.83; Cl, 9.99. IR (KBr disk): 3047, 2943, 1697, 1659, 1435, 1262, 1169, 1041 cm⁻¹. ¹H NMR (400 MHz, CD₂Cl₂): δ 9.23 (d, 2H, *J* = 4.8 Hz, Py), 8.11 (br, 1H, Py), 8.00 (d, 2H, *J* = 6.1 Hz, Py), 7.80 (t, 1H, *J* = 7.3 Hz, Py), 7.39 (t, 1H, *J* = 7.3 Hz, Py), 7.33 (t, 2H, *J* = 7.3 Hz, Py), 7.28 (t, 1H, *J* = 7.3 Hz, Py), 7.20, (br, 1H, Py), 7.09 (br, 1H, Py), 6.73 (t, 2H, *J* = 7.3 Hz, Py), 6.58 (br, 1H, Py), 4.23 (d, 2H, *J* = 8.6 Hz, =CH), 3.97 (d, 2H, *J* = 8.6 Hz, =CH), 3.36 (s, 6H, OMe), 2.98 (s, 6H, OMe). ¹³C NMR (100 MHz, CD₂Cl₂): δ 180.0 (C=O), 177.5 (C=O), 157.9 (Py), 155.6 (Py), 134.6 (Py), 134.6 (Py), 125.7 (Py), 123.2 (Py), 52.3 (=CH), 50.7 (OMe), 49.9 (OMe), 48.5 (=CH).

Synthesis of Ru(dmfm)₂(terpy) (5a and 5b). In a 20 mL two-necked flask equipped with a reflux condenser and a stirring bar, Ru(*η*⁶-cot)(dmfm)₂ (**1**; 1.0 g, 2.0 mmol) and terpy (0.49 g, 2.1 mmol) were placed under an argon atmosphere. Acetone (15 mL) was added and the mixture was refluxed with stirring for 2 h. The solution was chromatographed on alumina. Elution with CHCl₃ gave a dark purple solution, from which the solvent was evaporated. The dark purple residue was recrystallized from acetone/pentane and the formed microcrystals were dried under vacuum to give a mixture of complexes **5a** and **5b** (0.45 g, 36% yield).

Mixture of **5a** and **5b**: Dark purple crystals, mp 162–164 °C dec. Anal. Calcd for C₂₇H₂₇N₃O₈Ru: C, 52.09; H, 4.37; N, 6.75. Found: C, 52.52; H, 4.62; N, 6.49. IR spectrum (KBr disk): 2956, 1670, 1446, 1301, 1260, 1148, 1038 cm⁻¹.

Complex **5a**: ¹H NMR (400 MHz, CDCl₃): δ 8.12–7.17 (11H, H_{Py}), 3.97 (d, 2H, *J* = 12.2 Hz, =CH), 3.78 (s, 6H, OMe), 3.57 (d, 2H, *J* = 12.2 Hz, =CH), 2.71

(s, 6H, OMe). ^{13}C NMR (100 MHz, CDCl_3): δ 178.6 (C=O), 174.1 (C=O), 157.6 (Py), 156.7 (Py), 155.8 (Py), 155.6 (Py), 155.2 (Py), 155.2 (Py), 136.3 (Py), 135.5 (Py), 132.9 (Py), 125.5 (Py), 125.4 (Py), 121.0 (Py), 120.6 (Py), 120.0 (Py), 119.6 (Py), 52.6 (=CH), 50.8 (OMe), 49.8 (OMe), 42.9 (=CH).

Complex **5b**: ^1H NMR (400 MHz, CDCl_3): δ 8.12–7.17 (11H, H_{Py}), 3.85 (s, 6H, OMe), 3.76 (d, 2H, $J = 9.3$ Hz, =CH), 3.60 (d, 2H, $J = 9.3$ Hz, =CH), 2.71 (s, 6H, OMe). ^{13}C NMR (100 MHz, CDCl_3): δ 179.6 (C=O), 174.1 (C=O), 157.4 (Py), 156.5 (Py), 154.6 (Py), 135.9 (Py), 134.8 (Py), 125.6 (Py), 121.4 (Py), 119.8 (Py), 50.7 (OMe), 50.6 (=CH), 49.8 (OMe), 42.5 (=CH).

Synthesis of $\text{Ru}(\text{dmfm})_2[2,6\text{-bis}\{(1\text{-phenylimino)ethyl}\}\text{pyridine}]$ (6a** and **6b**).** In a 20 mL two-necked flask equipped with a reflux condenser and a stirring bar, $\text{Ru}(\eta^6\text{-cot})(\text{dmfm})_2$ (**1**; 0.98 g, 2.0 mmol) and 2,6-bis{(1-phenylimino)ethyl}pyridine (0.62 g, 2.0 mmol) were placed under an argon atmosphere. Then 1,4-dioxane was added and the mixture was refluxed with stirring for 2 h. The solution was chromatographed on alumina. Elution with CHCl_3 gave a dark purple solution, from which the solvent was evaporated. The dark purple residue was recrystallized from CHCl_3 /pentane to give a mixture of complexes **6a** and **6b** (0.29 g, 21% yield).

Mixture of **6a** and **6b**: Dark purple crystals, mp 178–181 °C dec. HR-MS FAB^+ (m/z): 704.1522 ($[\text{M} + \text{H}]^+$, calcd 704.1546). IR spectrum (KBr disk): 2951, 1686, 1438, 1280, 1142, 1055 cm^{-1} . Anal. Calcd for $\text{C}_{33}\text{H}_{35}\text{N}_3\text{O}_8\text{Ru}$: C, 56.40; H, 5.02; N, 5.98. Found: C, 56.59; H, 5.45; N, 6.03.

Complex **6a**: ^1H NMR (400 MHz, CDCl_3): δ 8.02–7.88 (3H, H_{Py}), 7.40–6.98 (10H, H_{Ar}), 4.27 (d, 2H, $J = 10.3$ Hz, =CH), 4.14 (d, 2H, $J = 10.3$ Hz, =CH), 3.08 (s, 6H, OMe), 2.86 (s, 6H, OMe), 2.35 (s, 3H, Me), 1.98 (s, 3H, Me). ^{13}C NMR (100 MHz, CDCl_3): δ 175.2 (C=O), 174.0 (C=N), 171.1 (C=O), 165.0

(C=N), 159.1 (Py), 152.7 (Py), 148.5 (Py), 148.3 (Py), 131.4 (Py), 127.9 (Ar), 127.4 (Ar), 125.7 (Ar), 125.4 (Ar), 123.9 (Ar), 122.9 (Ar), 122.7 (Ar), 122.4 (Ar), 54.0 (=CH), 49.5 (OMe), 49.3 (OMe), 46.1 (=CH), 18.7 (Me), 18.1 (Me).

Complex **6b**: ^1H NMR (400 MHz, CDCl_3): δ 8.02–7.88 (3H, H_{Py}), 7.40–7.15 (10H, H_{Ar}), 4.21 (d, 2H, $J = 10.7$ Hz, =CH), 3.72 (d, 2H, $J = 10.7$ Hz, =CH), 3.01 (s, 6H, OMe), 2.99 (s, 6H, OMe), 2.17 (s, 6H, Me). ^{13}C NMR (100 MHz, CDCl_3): δ 175.8 (C=O), 171.4 (C=O), 169.5 (C=N), 155.9 (Py), 148.8 (Py), 132.7 (Py), 127.6 (Ar), 125.3 (Ar), 122.9 (Ar), 122.4 (Ar), 51.3 (=CH), 49.5 (OMe), 49.3 (OMe), 47.8 (=CH), 18.7 (Me),

Synthesis of $\text{Ru}(\text{dmfm})_2[2,6\text{-bis}\{(1\text{-isopropylimino})\text{ethyl}\}\text{pyridine}]$ (7a** and **7b**).** In a 20 mL two-necked flask equipped with a reflux condenser and a stirring bar, $\text{Ru}(\eta^6\text{-cot})(\text{dmfm})_2$ (**1**; 0.15 g, 0.30 mmol) and 2,6-bis{(1-isopropylimino)ethyl}pyridine (0.084 g, 0.34 mmol) were placed under an argon atmosphere. Then 1,4-dioxane was added and the mixture was refluxed with stirring for 2 h. The solution was chromatographed on alumina. Elution with CHCl_3 gave a dark purple solution, from which the solvent was evaporated. The dark purple residue was recrystallized from CHCl_3 /pentane to give a mixture of complexes **7a** and **7b** (0.086 g, 29% yield).

Mixture of **7a** and **7b**: Dark purple crystals, mp 204–206 °C dec. Anal. Calcd for $\text{C}_{27}\text{H}_{39}\text{N}_3\text{O}_8\text{Ru}$: C, 51.09; H, 6.19; N, 6.62. Found: C, 50.65; H, 5.97; N, 6.55. IR spectrum (KBr disk): 2980, 2945, 1693, 1683, 1589, 1578, 1459, 1434 cm^{-1} .

Complex **7a**: ^1H NMR (400 MHz, CDCl_3): δ 7.80–7.65 (3H, H_{Py}), 4.70 (heptet, 1H, $J = 6.8$ Hz, CH of *i*-Pr), 4.16 (d, 2H, $J = 9.6$ Hz, =CH), 3.97 (d, 2H, $J = 9.6$ Hz, =CH), 3.73 (s, 6H, OMe), 3.33 (heptet, 1H, $J = 6.8$ Hz, CH of *i*-Pr), 2.74 (s, 6H, OMe), 2.67 (s, 3H, Me), 2.42 (s, 3H, Me), 1.48 (d, 6H, $J = 6.8$ Hz,

Me of *i*-Pr), 1.41 (d, 6H, $J = 6.8$ Hz, Me of *i*-Pr). ^{13}C NMR (100 MHz, CDCl_3): δ 176.7 (C=O), 171.4 (C=O), 170.0 (C=N), 160.8 (C=N), 160.7 (Py), 155.9 (Py), 130.9 (Py), 122.0 (Py), 120.2 (Py), 61.9 (*i*-Pr), 57.9 (*i*-Pr), 53.6 (=CH), 50.4 (OMe), 49.6 (OMe), 43.7 (=CH), 23.0 (Me of *i*-Pr), 22.3 (Me of *i*-Pr), 19.5 (Me), 19.4 (Me).

Complex **7b**: ^1H NMR (400 MHz, CDCl_3): δ 7.80–7.65 (3H, H_{Py}), 4.22 (d, 2H, $J = 9.6$ Hz, =CH), 3.97 (d, 2H, $J = 9.6$ Hz, =CH), 3.85 (m, 2H, $J = 7.2$ Hz, CH of *i*-Pr), 3.77 (s, 6H, OMe), 2.74 (s, 6H, OMe), 2.54 (s, 6H, Me), 1.45 (d, 6H, $J = 7.2$ Hz, Me of *i*-Pr), 1.41 (d, 6H, $J = 7.2$ Hz, Me of *i*-Pr). ^{13}C NMR (100 MHz, CHCl_3): δ 179.3 (C=O), 172.0 (C=O), 165.4 (C=N), 158.5 (Py), 133.2 (Py), 120.5 (Py), 60.5 (*i*-Pr), 50.7 (=CH), 50.4 (OMe), 49.6 (OMe), 42.8 (=CH), 23.7 (Me of *i*-Pr), 21.9 (Me of *i*-Pr), 19.6 (Me).

Synthesis of $\text{Ru}(\text{dmfm})_2(\textit{i}$ -Pr-Pybox) (10a** and **10b** (or **10c**)).** In a 20 mL two-necked flask equipped with a reflux condenser and a stirring bar, $\text{Ru}(\eta^6\text{-cot})(\text{dmfm})_2$ (**1**; 0.50 g, 1.0 mmol) and *i*-Pr-Pybox (0.31 g, 1.0 mmol) were placed under an argon atmosphere. Then 1,2-dichloroethane was added and the mixture was refluxed with stirring for 2 h. The solution was chromatographed on alumina. Elution with CHCl_3 gave a dark green solution, from which the solvent was evaporated. The dark green residue was recrystallized from CHCl_3 /pentane to give a mixture of complexes **10a** and **10b** or **10c** (0.43 g, 62% yield).

Mixture of **10a** and **10b**: Dark green crystals, mp 90–92 °C dec. Anal. Calcd for $\text{C}_{29}\text{H}_{39}\text{N}_3\text{O}_{10}\text{Ru}$: C, 50.43; H, 5.69; N, 6.08. Found: C, 50.42; H, 5.71; N, 5.80. IR spectrum (KBr disk): 2947, 2869, 2831, 1681, 1387, 1141 cm^{-1} .

Complex **10a**: ^1H NMR (400 MHz, CDCl_3): δ 7.85–7.71 (3H, H_{Py}), 4.59 (dd, 1H, $J = 4.4$ Hz, $J = 8.8$ Hz, OCHH), 4.55 (dd, 1H, $J = 8.8$ Hz, $J = 9.6$ Hz,

OCHH), 4.49 (d, 1H, $J = 10.3$ Hz, =CH), 4.44 (t, 1H, $J = 9.2$ Hz, OCHH), 4.34 (d, 1H, $J = 10.3$ Hz, =CH), 4.18 (dd, 1H, $J = 8.4$ Hz, $J = 12.8$ Hz, OCHH), 3.99 (d, 1H, $J = 9.8$ Hz, =CH), 3.90 (m, 1H, N-CH), 3.83 (m, 1H, N-CH), 3.80 (d, 1H, $J = 9.8$ Hz, =CH), 3.75 (s, 3H, OMe), 3.65 (s, 3H, OMe), 2.92 (s, 3H, OMe), 2.89 (s, 3H, OMe), 2.49 (m, 2H, CH of *i*-Pr), 1.15 (d, 3H, $J = 6.8$ Hz, Me of *i*-Pr), 0.95 (d, 3H, $J = 6.8$ Hz, Me of *i*-Pr), 0.80 (d, 3H, $J = 6.8$ Hz, Me of *i*-Pr), 0.75 (d, 3H, $J = 6.8$ Hz, Me of *i*-Pr). ^{13}C NMR (100 MHz, CDCl_3): δ 178.0 (C=O), 177.8 (C=O), 173.7 (C=O), 173.0 (C=O), 149.8 (C=N), 146.5 (C=N), 150.0 (*ipso*-Py), 146.5 (*ipso*-Py), 133.2 (Py), 122.0 (Py), 121.8 (Py), 71.7 (CH_2), 71.3 (CH_2), 69.8 (=N-CH), 67.1 (=N-CH), 55.8 (=CH), 51.7 (=CH), 50.8 (OMe), 50.3 (OMe), 49.9 (OMe), 49.8 (OMe), 42.5 (=CH), 40.1 (=CH), 26.5 (CH of *i*-Pr), 26.3 (CH of *i*-Pr), 22.4 (Me), 19.6 (Me), 16.7 (Me), 14.3 (Me).

Complex **10b** or **10c**: ^1H NMR(400 MHz, CDCl_3): δ 7.85–7.71 (3H, H_{Py}), 4.52 (m, 2H, OCHH), 4.40 (m, 2H, OCHH), 4.24 (d, 2H, $J = 10.3$ Hz, =CH), 4.12 (d, 2H, $J = 10.3$ Hz, =CH), 3.49 (m, 2H, N-CH), 3.03 (s, 6H, OMe), 2.52 (m, 2H, CH of *i*-Pr), 2.04 (s, 6H, OMe), 0.83 (d, 6H, $J = 6.8$ Hz, Me of *i*-Pr), 0.69 (d, 6H, $J = 6.8$ Hz, Me of *i*-Pr). ^{13}C NMR (100 MHz, CDCl_3): δ 177.9 (C=O), 173.5 (C=O), 161.7 (C=N), 144.4 (*ipso*-Py), 134.0 (Py), 123.0 (Py), 70.8 (CH_2), 67.7 (=N-CH), 50.7 (OMe), 49.9 (OMe), 48.8 (=CH), 42.9 (=CH), 27.3 (CH of *i*-Pr), 19.5 (Me), 14.1 (Me).

Crystallographic Study of 4 and 10a. Single crystals of **4** and **10a** were obtained by recrystallization from CH_2Cl_2 /pentane and acetone/pentane, respectively. The crystal data and experimental details for **4** and **10a** are summarized in Table 1. All measurements were made on a Rigaku AFC7R diffractometer with graphite monochromated Mo $\text{K}\alpha$ radiation ($\lambda = 0.71069$ Å) and a rotating anode generator. The reflection intensities were monitored by three standard reflections at every 150 measurements. No decay correction was

applied. Reflection data were corrected for Lorentz and polarization effects. Azimuthal scans of several reflections indicated no need for an absorption correction. The structures were solved by direct methods using SIR92²⁴ for **4** and **10a**, expanded using Fourier techniques, DIRDIF99,²⁵ and refined anisotropically for non-hydrogen atoms by full-matrix least-squares calculations. All hydrogen atoms in **4** and **10a** were refined using the riding model. The calculations were performed using the program system CrystalStructure crystallographic software package. The final atomic parameters for non-hydrogen atoms of **4** and **10a** are given in the Supporting Information.

Crystallographic Study of 5b. Single crystals of **5b** were obtained by recrystallization from acetone/pentane. The crystal data and experimental details for **5b** are summarized in Table 1. All measurements were made on a Rigaku/MSM Mercury CCD diffractometer with graphite monochromated Mo K α radiation ($\lambda = 0.71069$ Å). The structures were solved by direct methods using SIR97,²⁶ expanded using Fourier techniques, DIRDIF94,²⁷ and refined anisotropically for non-hydrogen atoms by full-matrix least-squares calculations. All hydrogen atoms were included but not refined. The calculations were performed using the program system teXsan crystallographic software package of Molecular Structure Corporation.

References

- (1) For a review of syntheses of polypyridyl ligands, see: Cargill-Tompson, A. M. W. *Coord. Chem. Rev.* **1997**, *160*, 1.
- (2) For reviews of photochemical and redox properties of polypyridyl ligands, see: (a) Kurihara, M.; Nishihara, H. *Coord. Chem. Rev.* **2002**, *226*, 125. (b) De Cola, L.; Belser, P. *Coord. Chem. Rev.* **1998**, *177*, 301. (c) Balzani, V.; Juris, A.; Venturi, M.; Campagna, S.; Serroni, S. *Chem. Rev.* **1996**, *96*, 759. (d) Juris, A.; Balzani, V.; Barigelletti, F.; Campagna, S.; Belser, P.; von

Zelewsky, A. *Coord. Chem. Rev.* **1988**, *84*, 85.

- (3) (a) Dias, E. L.; Brookhart, M.; White, P. S. *Organometallics* **2000**, *19*, 4995. (b) Poon, C.-K.; Che, C.-M. *J. Chem. Soc., Chem. Commun.* **1979**, 861.
- (4) (a) Beerens, H. I.; Wijkens, P.; Jastrzebski, J. T. B. H.; Verpoort, F.; Verdonck, L.; van Koten, G. *J. Organomet. Chem.* **2000**, *603*, 244. (b) del Río, I.; van Koten, G.; Lutz, M.; Spek, A. L. *Organometallics* **2000**, *19*, 361. (c) del Río, I.; Back, S.; Hannu, M. S.; Rheinwald, G.; Lang, H.; van Koten, G. *Inorg. Chim. Acta* **2000**, *300*, 1094. (d) del Río, I.; Gossage, R. A.; Lutz, M.; Spek, A. L.; van Koten, G. *J. Organomet. Chem.* **1999**, *583*, 69. (e) del Río, I.; Gossage, R. A.; Lutz, M.; Spek, A. L.; van Koten, G. *Inorg. Chim. Acta* **1999**, *287*, 113. (f) del Río, I.; Gossage, R. A.; Hannu, M. S.; Lutz, M.; Spek, A. L.; van Koten, G. *Organometallics* **1999**, *18*, 1097. (g) Abbenhuis, R. A. T. M.; del Río, I.; Bergshoef, M. M.; Boersma, J.; Veldman, N.; Spek, A. L.; van Koten, G. *Inorg. Chem.* **1998**, *37*, 1749.
- (5) Gemel, C.; Folting, K.; Caulton, K. G. *Inorg. Chem.* **2000**, *39*, 1593.
- (6) Redmore, S. M.; Rickard, C. E. F.; Webb, S. J.; Wright, L. J. *Inorg. Chem.* **1997**, *36*, 4743.
- (7) Çetinkaya, B.; Çetinkaya, E.; Brookhart, M.; White, P. S. *J. Mol. Catal. A Chem.* **1999**, *142*, 101.
- (8) Bianchini, C.; Lee, H. M. *Organometallics* **2000**, *19*, 1833.
- (9) Abbenhuis, R. A. T. M.; Boersma, J.; van Koten, G. *J. Org. Chem.* **1998**, *63*, 4282.
- (10) del Río, I.; van Koten, G. *Tetrahedron Lett.* **1999**, *40*, 1401.
- (11) Welch, T. W.; Ciftan, S. A.; White, P. S.; Thorp, H. H. *Inorg. Chem.* **1997**, *36*, 4812.
- (12) (a) Doyle, M. P.; Peterson, C. S.; Zhou, Q.-L.; Nishiyama, H. *Chem. Commun.* **1997**, 211. (b) Park, S.-B.; Sakata, N.; Nishiyama, H. *Chem. Eur. J.* **1996**, *2*, 303. (c) Nishiyama, H.; Itoh, Y.; Sugawara, Y.; Matsumoto, H.;

- Aoki, K.; Itoh, K. *Bull. Chem. Soc. Jpn.* **1995**, *68*, 1247. (d) Park, S.-B.; Murata, K.; Matsumoto, H.; Nishiyama, H. *Tetrahedron Asymmetry* **1995**, *6*, 2487. (e) Nishiyama, H.; Itoh, Y.; Matsumoto, H.; Park, S.-B.; Itoh, K. *J. Am. Chem. Soc.* **1994**, *116*, 2223
- (13) (a) Imanishi, Y.; Nomura, K. *J. Polym. Sci. Polym. Chem.* **2000**, *38*, 4613. (b) Nomura, K.; Warit, S.; Imanishi, Y. *Bull. Chem. Soc. Jpn.* **2000**, *73*, 599. (c) Nomura, K.; Warit, S.; Imanishi, Y. *Macromolecules* **1999**, *32*, 4732.
- (14) Suzuki, T.; Shiotsuki, M.; Wada, K.; Kondo, T.; Mitsudo, T. *J. Chem. Soc., Dalton Trans.* **1999**, 4231.
- (15) Suzuki, T.; Shiotsuki, M.; Wada, K.; Kondo, T.; Mitsudo, T. *Organometallics* **1999**, *18*, 3671.
- (16) Mitsudo, T.; Suzuki, T.; Zhang, S.-W.; Imai, D.; Fujita, K.; Manabe, T.; Shiotsuki, M.; Watanabe, Y.; Wada, K.; Kondo, T. *J. Am. Chem. Soc.* **1999**, *121*, 1839.
- (17) Shiotsuki, M.; Suzuki, T.; Kondo, T.; Wada, K.; Mitsudo, T. *Organometallics* **2000**, *19*, 5733.
- (18) Shiotsuki, M.; Miyai, H.; Ura, Y.; Suzuki, T.; Kondo, T.; Mitsudo, T. *Organometallics* **2002**, *21*, 4960.
- (19) For example, see; (a) Roche, S.; Adams, H.; Spey, S. E.; Thomas, J. A. *Inorg. Chem.* **2000**, *39*, 2385. (b) Stern, C.; Franceschi, F.; Solari, E.; Floriani, C.; Re, N.; Scopelliti, R. *J. Organomet. Chem.* **2000**, *593*, 86. (c) Laurent, F.; Plantalech, E.; Donnadiou, B.; Jiménez, A.; Hernández, F.; Martínez-Ripoll, M.; Biner, M.; Llobet, A. *Polyhedron* **1999**, *18*, 3321. (d) Fachinetti, G.; Funaioli, T.; Lecci, L.; Marchetti, F. *Inorg. Chem.* **1996**, *35*, 7217.
- (20) For example, see; (a) Hirano, T.; Ueda, K.; Mukaida, M.; Nagao, H.; Oi, T. *J. Chem. Soc., Dalton Trans.* **2001**, 2341. (b) Hansongnern, K.; Saeteaw, U.; Cheng, J.; Liao, F.-L.; Lu, T.-H. *Acta Cryst.* **2001**, *C57*, 895. (c) Perez, W. J.; Lake, C. H.; See, R. F.; Toomey, L. M.; Churchill, M. R.; Takeuchi,

- K. J.; Radano, C. P.; Boyko, W. J.; Bessel, C. A. *J. Chem. Soc., Dalton Trans.* **1999**, 2281. (d) Heirtzler, F. R.; Neuburger, M.; Zehnder, M.; Bird, S. J.; Orrell, K. G.; Sik, V. *J. Chem. Soc., Dalton Trans.* **1999**, 565. (e) Gibson, D. H.; Sleadd, B. A.; Mashuta, M. S.; Richardson, J. F. *Organometallics* **1997**, *16*, 4421. (f) Sutter, J.-P.; James, S. L.; Steenwinkel, P.; Karlen, T.; Grove, D. M.; Veldman, N.; Smeets, W. J. J.; Spek, A. L.; van Koten, G. *Organometallics* **1996**, *15*, 941. (g) Bardwell, D. A.; Cargill-Thompson, A. M. W.; Jeffery, J. C.; McCleverty, J. A.; Ward, M. D. *J. Chem. Soc., Dalton Trans.* **1996**, 873.
- (21) (a) Motoyama, Y.; Kurihara, O.; Murata, K.; Aoki, K.; Nishiyama, H. *Organometallics* **2000**, *19*, 1025. (b) Motoyama, Y.; Murata, K.; Kurihara, O.; Naitoh, T.; Aoki, K.; Nishiyama, H. *Organometallics* **1998**, *17*, 1251.
- (22) Nishiyama, H.; Naitoh, T.; Motoyama, Y.; Aoki, K. *Chem. Eur. J.* **1999**, *5*, 3509.
- (23) Richards, E. M.; Tebby, J. C.; Ward, R. S.; Williams, D. H. *J. Chem. Soc. C* **1969**, 1542.
- (24) SIR92: Altomare, A.; Cascarano, G.; Giacovazzo, C.; Guagliardi, A.; Burla, M.; Polidori, G.; Camalli, M. *J. Appl. Cryst.*, **1994**, *27*, 435.
- (25) DIRDIF99: Beusken, P. T.; Admiraal, G.; Beurskens, G.; Bosman, W. P.; de Gelder, R.; Israel, R.; Smits, J. M. M. The DIRDIF-99 program system, Technical Report of the Crystallography Laboratory, University of Nijmegen, The Netherlands, 1999.
- (26) SIR97: Altomare, A.; Burla, M. C.; Camali, M.; Cascarano, G. L.; Giacovazzo, C.; Gualardi, A.; Moliterni, A. G. G.; Polidori, G.; Spagna, R. *J. Appl. Cryst.* **1999**, *32*, 115.
- (27) DIRDIF94: Beurskens, P. T.; Admiraal, G.; Beurskens, G.; Bosman, W. P.; de Gelder, R.; Israel R.; Smits, J. M. M. The DIRDIF-94 program system, Technical Report of the Crystallography Laboratory, University of Nijmegen, The Netherlands, 1994.

Chapter 4

Synthesis and Structures of Novel Zerovalent Ruthenium *p*-Quinone Complexes and a Bimetallic *p*-Biquinone Complex

Abstract

$\text{Ru}(\eta^6\text{-cot})(\text{dmfm})_2$ [**1**; cot = 1,3,5-cyclooctatriene, dmfm = dimethyl fumarate] reacted with *p*-quinones to give novel *p*-quinone-coordinated ruthenium(0) complexes, $\text{Ru}(\eta^6\text{-cot})(p\text{-quinone})$ (**2**), in good to high yields via the replacement of two dimethyl fumarates by *p*-quinones. The reaction of **1** with *p*-biquinone gave a novel bimetallic zerovalent complex $\{\text{Ru}(\eta^6\text{-cot})\}_2(p\text{-biquinone})$ (**3**), in which *p*-biquinone coordinates to two isolated “Ru(cot)” moieties with a unique mode and the two Ru(cot) groups are located at endo positions. Complexes **2** and **3** have either *p*-quinone or *p*-biquinone as π -acceptor ligands. The structures of complexes $\text{Ru}(\eta^6\text{-cot})(2,6\text{-dimethoxy-}p\text{-quinone})$ (**2f**) and **3** were determined by X-ray crystallography.

Introduction

Among low-valent transition metal complexes bearing an olefinic π -acceptor ligand, *p*-quinone complexes have been intensively investigated.¹⁻²² The study of *p*-quinone ligands is intriguing not only because of their role in proton/electron transfer but also in view of their strong electron-accepting ability through π -back donation. Since the degree of π -acidity can be controlled by changing the substituents on quinone, the electron density on the metal center is easily adjusted, which is important from the viewpoint of catalytic activity. The first synthesis of a transition metal *p*-quinone complex, $\text{Fe}(\text{CO})_3(\text{duroquinone})$, was accomplished by Sternberg, Markby and Wender in 1958.¹ Several group 9 and 10 metal *p*-quinone complexes have been reported so far.²⁻¹⁶ In contrast, there are very few examples of other metal complexes such as iron(0),^{1,17} ruthenium(II),¹⁸ manganese(-I),¹⁹ and molybdenum(II).²⁰

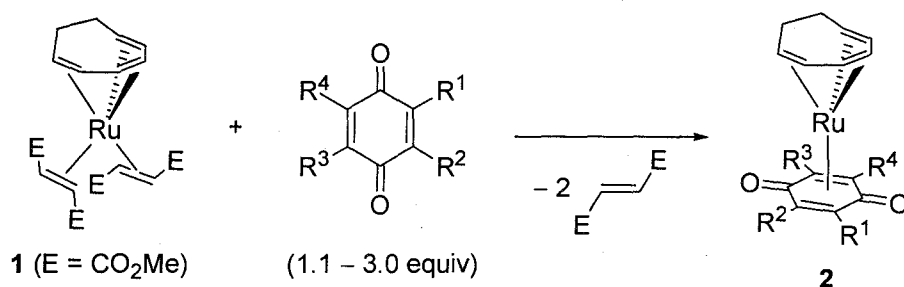
The methods used to prepare *p*-quinone complexes can be divided into four classes: (A) direct ligand exchange of appropriate complexes with *p*-quinones, (B) coupling of alkynes with carbon monoxides on the transition metal, (C) reaction of maleoyl/phthaloylmatal species with an alkyne, and (D) deprotonation of hydroquinone complexes. In the synthesis of *p*-quinone complexes by method A, duroquinone has been frequently used,^{2-5,7,9,11} whereas few examples of other *p*-quinone complexes have been reported.^{10,12,13,16} $\text{Fe}(\text{CO})_3(\text{duroquinone})$,¹ $\text{CpCo}(p\text{-quinone})$,⁸ and $\text{CpMoCl}(\text{CO})(\text{duroquinone})$ ²⁰ have been prepared by method B. Liebeskind and co-workers reported a high-yield synthesis of *p*-quinone cobalt complexes through method C, in which maleoyl/phthaloylmatal species were generated by oxidative addition of cyclobutenedione or benzocyclobutenedione to a low-valent cobalt complex.¹⁴ Iridium and manganese η^6 -hydroquinone complexes have been prepared by Amouri and co-workers^{15,21} and Sweigart and co-workers,^{19,22} respectively, taking advantage of method D; η^5 -semiquinone and η^4 -*p*-quinone complexes are

synthesized.

Recently, we reported a novel zerovalent ruthenium complex $\text{Ru}(\eta^6\text{-cot})\text{-(dmfm)}_2$ [**1**; cot = 1,3,5-cyclooctatriene, dmfm = dimethyl fumarate].²³ Complex **1** was found to be an excellent catalyst for a unique dimerization of 2,5-norbornadiene to afford a novel half-cage compound.²³ In this catalyst, the coordinated dimethyl fumarate was found to be crucial as a π -acceptor ligand. Complex **1** is also a versatile precursor for novel Ru(0) complexes, as we demonstrated previously.²⁴ In the course of our further investigation of the reactivity of **1**, we found that reactions with various *p*-quinones and a *p*-biquinone under mild conditions give novel complexes $\text{Ru}(\eta^6\text{-cot})(p\text{-quinone})$ (**2**) and $\{\text{Ru}(\eta^6\text{-cot})\}_2(p\text{-biquinone})$ (**3**) in high yields via simple and selective ligand exchange (method A) between π -acceptors. We report here the synthesis and structures of a series of novel *p*-quinone ruthenium(0) complexes **2** and a unique *p*-biquinone bimetallic complex **3**.

Results and Discussion

$\text{Ru}(\eta^6\text{-cot})(p\text{-quinone})$ (2**).** As shown in Table 1, the reactions of **1** with *p*-quinones were performed in Et_2O at room temperature for 2 h (entry 1), under reflux for 4 h (entries 2–5, 7) and in toluene at 80 °C for 2 h (entry 6), respectively. The selective ligand exchange between π -acceptors, dimethyl fumarate and *p*-quinone, proceeded smoothly to afford **2** in good to high yield. Several kinds of *p*-quinones with an electron-donating group (entries 2, 3, 6) or an electron-withdrawing group (entries 4, 5) were found to be suitable for this substitution reaction, including *p*-naphthoquinone (entry 7). The reaction with chloranil (tetrachloro-*p*-benzoquinone) also proceeded to give a precipitate; however, spectroscopic characterization was impossible because of the low solubility of the product. The use of DDQ (2,3-dichloro-5,6-dicyano-*p*-benzo-

Table 1. Reactions of **1** with *p*-Quinones

entry	R ¹	R ²	R ³	R ⁴	amount of quinone (equiv)	solvent	reaction condition	product	yield (%) ^a
1	H	H	H	H	1.1	Et ₂ O	r.t., 2 h	2a	98
2	Me	H	H	H	1.1	Et ₂ O	reflux, 4 h	2b	87
3	Me	H	H	Me	2.2	Et ₂ O	reflux, 4 h	2c	94
4	Ph	H	Ph	H	1.2	Et ₂ O	reflux, 4 h	2d	64
5	Cl	H	Cl	H	1.1	Et ₂ O	reflux, 4 h	2e	65
6	OMe	H	H	OMe	1.1	toluene	80 °C, 2 h	2f	60
7	-CH=CH-CH=CH-		H	H	3.0	Et ₂ O	reflux, 4 h	2g	89

^a Isolated yield.

quinone) gave a complex mixture of products.

The structures of **2a–g** were deduced on the basis of ¹H and ¹³C NMR, IR, and mass spectra. The ¹H and ¹³C NMR data for **2a–g** are summarized in Tables 2 and 3, respectively. In the ¹H NMR spectra of **2**, the signals for the olefinic protons of the 1,3,5-cyclooctatriene moiety appear at 6.6–4.1 ppm, and those for the methylene protons appear at 2.8–0.1 ppm. The signals for the olefinic protons of *p*-quinone ligands in **2** appear at 5.0–5.8 ppm, which are shifted to a higher magnetic field than those of the corresponding free *p*-quinones by 1.5–1.8 ppm. The appearance of these signals as singlet peaks, except in **2b**, suggests that cyclooctatriene rotates freely on ruthenium at room temperature in solution. In the ¹³C NMR spectra of **2**, the carbonyl carbons of the coordinated *p*-quinones are observed at 153–159 ppm, which are shifted upfield by ca. 30

Table 2. ^1H NMR Data of **2a–g** (δ , ppm)^a

complex	<i>p</i> -quinone		1,3,5-cyclooctatriene
	=CH	others	
2a	5.02 (s, 4H)		6.33 (m, 2H), 5.56 (br t, 6.8, 2H), 5.04 (m, 2H), 2.22 (m, 2H), 1.00 (m, 2H)
2b	5.16 (s, 1H), 5.00 (m, 2H)	1.82 (s, 3H)	6.20 (m, 2H), 5.42 (br t, 7.4, 1H), 5.38 (br t, 7.4, 1H), 4.90 (m, 2H), 2.19 (m, 2H), 0.95 (m, 2H)
2c	5.09 (s, 2H)	1.82 (s, 6H)	6.04 (dd, 4.9, 2.0, 2H), 5.22 (ddd, 8.3, 4.9, 2.0, 2H), 4.74 (m, 2H), 2.14 (m, 2H), 0.90 (m, 2H)
2d	5.59 (s, 2H)	7.36–7.84 (m, 10H)	5.96 (t, 7.3, 1H), 5.61 (m, 1H), 5.50 (t, 8.0, 1H), 5.35 (t, 8.5, 1H), 5.03 (m, 1H), 4.12 (dd, 13.6, 7.4, 1H), 2.29 (m, 1H), 1.53 (m, 2H), 0.09 (m, 1H)
2e	5.76 (s, 2H)		6.58 (t, 7.4, 1H), 6.19 (t, 8.3, 1H), 5.31 (t, 7.1, 2H), 4.90 (t, 8.8, 1H), 4.80 (dd, 8.0, 14.4, 1H), 2.75 (m, 1H), 1.91 (m, 2H), 0.20 (m, 1H)
2f	5.24 (s, 2H)	3.68 (s, 6H)	6.13 (m, 2H), 5.27 (m, 2H), 4.91 (m, 2H), 2.17 (m, 2H), 0.89 (m, 2H)
2g	5.20 (s, 2H)	8.01 (m, 2H), 7.40 (m, 2H)	5.39 (m, 2H), 4.92 (m, 2H), 4.79 (m, 2H), 1.97 (m, 2H), 0.57 (m, 2H)

^a Measured in CDCl₃ at room temperature and 400 MHz. Legend: s = singlet, d = doublet, t = triplet, m = multiplet, br = broad. Values in parentheses are the coupling constants, $J_{\text{H-H}}$ (Hz).

Table 3. ^{13}C NMR Data of **2a–g** (δ , ppm)^a

complex	<i>p</i> -quinone			1,3,5-cyclooctatriene
	C=C (coordinated)	C=O	others	
2a	83.7	158.6		99.8, 92.6, 91.1, 32.9
2b	99.7, 87.2, 82.4, 82.3	158.1, 157.6	15.7	99.9, 99.7, 94.3, 93.2, 91.8, 90.6, 32.9, 32.6
2c	97.8, 85.7	158.0, 156.8	15.7	99.9, 94.8, 90.8, 32.6
2d	97.7, 81.8	158.6	133.0, 128.8, 128.6, 128.3	102.4, 101.9, 97.7, 95.8, 93.2, 87.7, 34.4, 29.7
2e	103.1, 82.7	154.2		101.5, 101.4, 100.9, 100.8, 98.3, 90.8, 37.6, 28.6
2f	132.3, 68.6	153.4, 141.3	56.4	99.1, 94.7, 91.0, 32.8
2g	109.9, 74.3	157.0	130.2, 125.2	101.8, 95.5, 87.4, 32.0

^a Measured in CDCl₃ at room temperature and 100 MHz.

ppm compared with free *p*-quinones, whereas one of the two carbonyl carbons in **2f** appeared at a higher field (141.3 ppm). The signals for the olefinic carbons of *p*-quinones vary from 68 to 132 ppm depending on their magnetic environment, and most of them are also shifted to higher fields because of π -back bonding from ruthenium.

The molecular structure of Ru(η^6 -cot)(2,6-dimethoxy-*p*-benzoquinone) (**2f**) was confirmed by X-ray crystallography, and the ORTEP drawing is shown in Figure 1. Lists of the selected bond lengths and bond angles of **2f** are given in Tables 4 and 5, respectively. The crystal data and the details are given in Table 6.

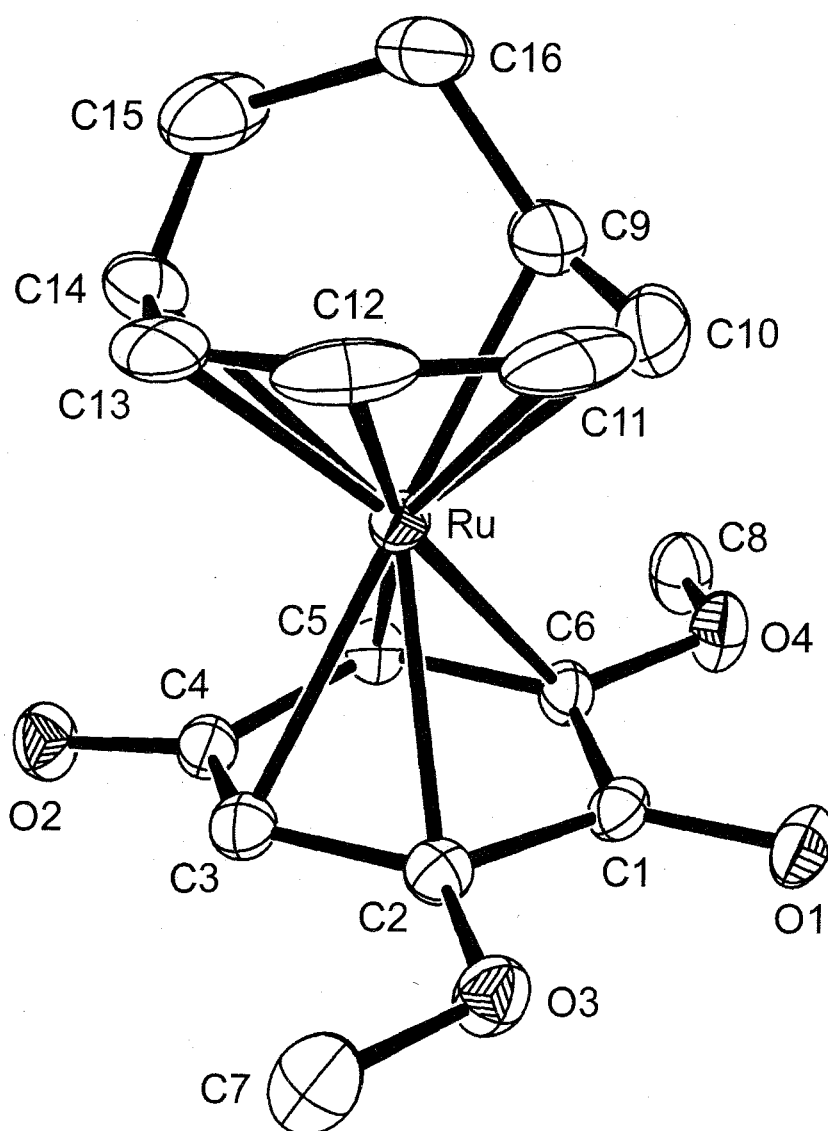


Figure 1. ORTEP drawing of **2f**.

Table 4. Selected Bond Lengths (Å) for **2f**

Ru–C(1)	2.410(4)	Ru–C(2)	2.305(5)
Ru–C(3)	2.238(4)	Ru–C(4)	2.438(4)
Ru–C(5)	2.189(4)	Ru–C(6)	2.246(4)
Ru–C(9)	2.210(6)	Ru–C(10)	2.134(6)
Ru–C(11)	2.185(7)	Ru–C(12)	2.188(6)
Ru–C(13)	2.165(5)	Ru–C(14)	2.227(6)
O(1)–C(1)	1.258(5)	O(2)–C(4)	1.251(5)
O(3)–C(2)	1.349(5)	O(3)–C(7)	1.437(6)
O(4)–C(6)	1.360(5)	O(4)–C(8)	1.441(5)
C(1)–C(2)	1.457(7)	C(1)–C(6)	1.442(7)
C(2)–C(3)	1.400(6)	C(3)–C(4)	1.463(6)
C(4)–C(5)	1.443(6)	C(5)–C(6)	1.416(6)
C(9)–C(10)	1.38(1)	C(9)–C(16)	1.494(8)
C(10)–C(11)	1.38(1)	C(11)–C(12)	1.39(1)
C(12)–C(13)	1.42(1)	C(13)–C(14)	1.360(9)
C(14)–C(15)	1.485(8)	C(15)–C(16)	1.486(8)

Table 5. Selected Bond Angles (deg) for **2f**

C(1)–Ru–C(2)	35.9(2)	C(1)–Ru–C(3)	65.4(2)
C(1)–Ru–C(4)	75.9(1)	C(1)–Ru–C(5)	66.3(2)
C(1)–Ru–C(6)	35.9(2)	C(1)–Ru–C(9)	111.2(2)
C(1)–Ru–C(10)	91.0(2)	C(1)–Ru–C(11)	100.0(3)
C(1)–Ru–C(12)	123.6(3)	C(1)–Ru–C(13)	151.5(2)
C(1)–Ru–C(14)	164.2(2)	C(2)–Ru–C(3)	35.8(2)
C(2)–Ru–C(4)	63.6(2)	C(2)–Ru–C(5)	77.0(2)
C(2)–Ru–C(6)	64.0(2)	C(2)–Ru–C(9)	145.8(2)
C(2)–Ru–C(10)	115.6(3)	C(2)–Ru–C(11)	103.4(2)
C(2)–Ru–C(12)	105.3(2)	C(2)–Ru–C(13)	117.6(2)
C(2)–Ru–C(14)	138.6(2)	C(3)–Ru–C(4)	36.1(2)
C(3)–Ru–C(5)	66.1(2)	C(3)–Ru–C(6)	76.9(2)
C(3)–Ru–C(9)	166.0(2)	C(3)–Ru–C(10)	151.2(3)
C(3)–Ru–C(11)	127.3(3)	C(3)–Ru–C(12)	107.5(2)
C(3)–Ru–C(13)	96.6(2)	C(3)–Ru–C(14)	104.4(2)
C(4)–Ru–C(5)	35.8(2)	C(4)–Ru–C(6)	64.2(2)
C(4)–Ru–C(9)	130.5(2)	C(4)–Ru–C(10)	156.5(3)
C(4)–Ru–C(11)	163.2(3)	C(4)–Ru–C(12)	132.6(3)
C(4)–Ru–C(13)	103.1(2)	C(4)–Ru–C(14)	88.8(2)
C(5)–Ru–C(6)	37.2(2)	C(5)–Ru–C(9)	99.9(2)
C(5)–Ru–C(10)	120.9(3)	C(5)–Ru–C(11)	156.5(4)
C(5)–Ru–C(12)	166.1(3)	C(5)–Ru–C(13)	128.5(2)
C(5)–Ru–C(14)	99.0(2)	C(6)–Ru–C(9)	92.7(2)
C(6)–Ru–C(10)	93.7(3)	C(6)–Ru–C(11)	121.4(3)
C(9)–Ru–C(10)	37.1(3)	C(9)–Ru–C(11)	66.2(3)
C(10)–Ru–C(11)	37.3(3)	C(6)–Ru–C(12)	156.0(3)
C(6)–Ru–C(13)	165.7(2)	C(6)–Ru–C(14)	132.7(2)
C(9)–Ru–C(12)	85.9(3)	C(9)–Ru–C(13)	91.3(2)
C(9)–Ru–C(14)	75.7(2)	C(10)–Ru–C(12)	71.0(3)
C(10)–Ru–C(13)	97.8(3)	C(10)–Ru–C(14)	102.0(2)
C(11)–Ru–C(12)	37.1(3)	C(11)–Ru–C(13)	72.7(3)
C(11)–Ru–C(14)	95.8(3)	C(12)–Ru–C(13)	38.0(3)
C(12)–Ru–C(14)	70.0(3)	C(13)–Ru–C(14)	36.0(2)
C(2)–O(3)–C(7)	118.9(4)	C(6)–O(4)–C(8)	117.7(4)

Table 5. Selected Bond Angles (deg) for **2f** (continued)

Ru–C(1)–O(1)	131.4(3)	Ru–C(1)–C(2)	68.1(2)
Ru–C(1)–C(6)	65.9(2)	Ru–C(2)–O(3)	132.0(3)
Ru–C(2)–C(1)	76.0(3)	Ru–C(2)–C(3)	69.5(3)
Ru–C(3)–C(2)	74.7(3)	Ru–C(3)–C(4)	79.4(3)
Ru–C(4)–O(2)	135.8(3)	Ru–C(4)–C(3)	64.5(2)
Ru–C(4)–C(5)	62.6(2)	Ru–C(5)–C(4)	81.5(3)
Ru–C(5)–C(6)	73.6(3)	Ru–C(6)–O(4)	127.9(3)
Ru–C(6)–C(1)	78.3(3)	Ru–C(6)–C(5)	69.2(3)
Ru–C(9)–C(10)	68.5(4)	Ru–C(9)–C(16)	113.0(4)
Ru–C(10)–C(9)	74.5(4)	Ru–C(10)–C(11)	73.4(4)
Ru–C(11)–C(10)	69.4(4)	Ru–C(11)–C(12)	71.5(4)
Ru–C(12)–C(11)	71.3(4)	Ru–C(12)–C(13)	70.1(3)
Ru–C(13)–C(12)	71.8(4)	Ru–C(13)–C(14)	74.5(4)
Ru–C(14)–C(13)	69.5(4)	Ru–C(14)–C(15)	112.7(4)
O(1)–C(1)–C(2)	123.7(5)	O(1)–C(1)–C(6)	123.3(4)
O(2)–C(4)–C(3)	123.6(4)	C(2)–C(3)–C(4)	121.9(4)
O(2)–C(4)–C(5)	123.4(5)	O(3)–C(2)–C(1)	112.2(4)
O(3)–C(2)–C(3)	124.4(5)	O(4)–C(6)–C(1)	113.4(4)
O(4)–C(6)–C(5)	122.8(4)	C(1)–C(2)–C(3)	123.3(4)
C(1)–C(6)–C(5)	123.8(4)	C(2)–C(1)–C(6)	112.8(4)
C(3)–C(4)–C(5)	112.4(4)	C(4)–C(5)–C(6)	121.6(4)
C(9)–C(10)–C(11)	120.6(7)	C(9)–C(16)–C(15)	107.6(5)
C(10)–C(9)–C(16)	122.3(6)	C(10)–C(11)–C(12)	129.6(7)
C(11)–C(12)–C(13)	132.9(7)	C(13)–C(14)–C(15)	128.7(6)
C(14)–C(15)–C(16)	109.5(5)	C(12)–C(13)–C(14)	131.5(6)

This structure is represented by a highly distorted trigonal bipyramid and is quite similar to that of **1**.²³ Figure 1 shows the η^4 -coordination of the *p*-quinone ligand with olefinic carbons. The axial positions are occupied by an olefinic moiety of 1,3,5-cyclooctatriene [C(9)–C(10)] and an olefinic moiety of 2,5-dimethoxy-*p*-benzoquinone [C(2)–C(3)], which are located diagonally from each other, and other olefinic parts of either cyclooctatriene [C(11)–C(12), C(13)–C(14)] or *p*-quinone [C(5)–C(6)] are located at the three equatorial positions. The average bond distance between Ru and the four olefinic carbons of *p*-quinone is 2.24 Å. On the other hand, the bond lengths between Ru and the carbonyl carbons of quinone, i.e. Ru–C(1) [2.410(4) Å] and Ru–C(4) [2.438(4) Å], are longer than the average distance by ca. 0.2 Å. The bond distances of C(1)–O(1) and C(4)–O(2) are 1.258(5) and 1.251(5) Å, respectively, which are typical lengths in transition metal *p*-quinone complexes.^{5b,14c,15,16,21} A simplified side view of **2f** is shown in Figure 2, where the boat shape of the *p*-quinone

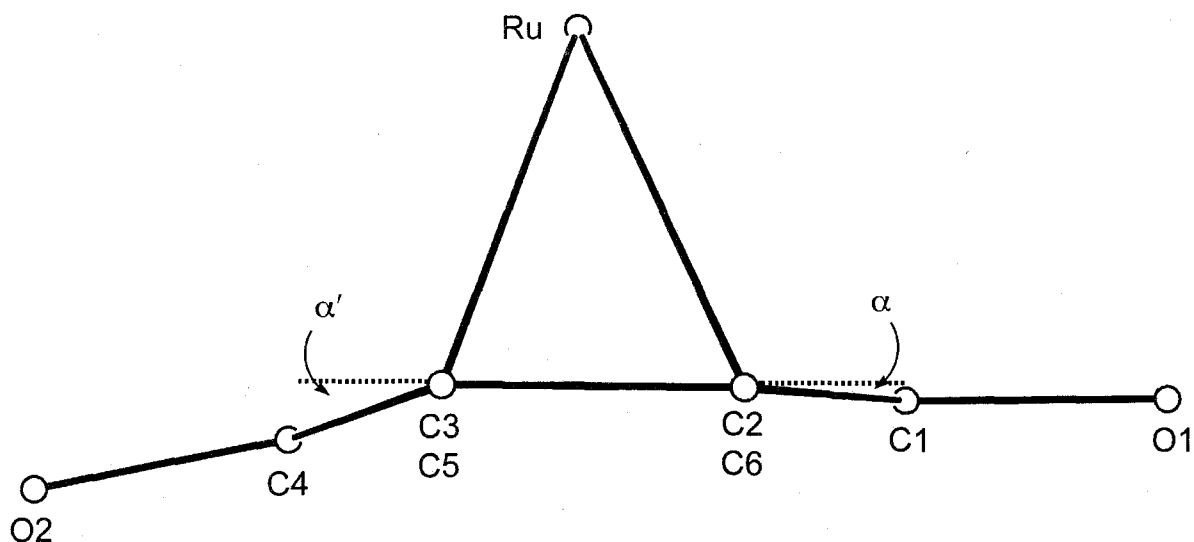


Figure 2. Simplified side view of **2f**. Hydrogen atoms, cyclooctatriene, and two methoxy groups are omitted for clarity. $\alpha = 3.2^\circ$, $\alpha' = 19.0^\circ$.

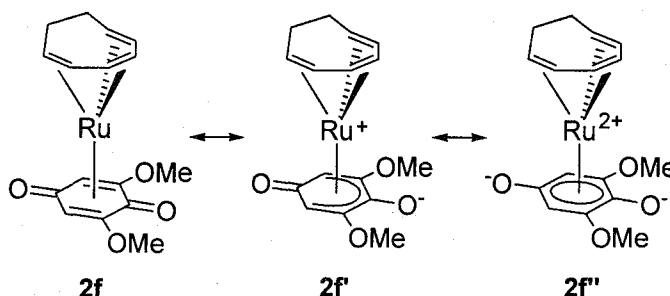
Table 6. Summary of Crystal Data, Collection Data, and Refinement of **2f** and **3**

	2f	3
formula	$\text{C}_{16}\text{H}_{18}\text{O}_4\text{Ru}\cdot\text{H}_2\text{O}$	$\text{C}_{30}\text{H}_{30}\text{O}_6\text{Ru}_2\cdot\text{CH}_2\text{Cl}_2$
fw	393.40	773.64
crystal color	yellow	black
crystal system	orthorhombic	monoclinic
space group	<i>Pbca</i>	<i>P2₁/n</i>
<i>a</i> (Å)	10.5230(3)	10.7583(5)
<i>b</i> (Å)	13.5805(3)	23.2869(9)
<i>c</i> (Å)	20.7004(5)	11.4630(7)
β (deg)	90	103.372(2)
<i>V</i> (Å ³)	2958.2(1)	2793.9(2)
<i>Z</i>	8	4
<i>D</i> _{calcd} (g/cm ³)	1.766	1.839
<i>T</i> (°C)	−50	−130
μ (Mo K α) (cm ^{−1})	10.82	13.18
$2\theta_{\text{max}}$ (deg)	54.9	54.9
no. of measd rflns	28298	24764
no. of obsd rflns	1948	5076
no. of variables	212	403
residuals <i>R</i> ; <i>R</i> _w	0.026; 0.030	0.056; 0.073
GOF	0.43	1.61

ligand can be recognized clearly. The dihedral angles between the plane of four olefinic carbons C(2)–C(3), C(5)–C(6) and the planes that include C(1), C(2), C(6) (α) and C(3), C(4), C(5) (α') are 3.2° and 19.0° , respectively. These angles in transition metal *p*-quinone complexes are normally $\sim 20^\circ$: for example, CpRh(η^4 -duroquinone) (23°),^{5b} (π -C₉H₇)Rh(η^4 -duroquinone) (25°),^{5b} CpCo(η^4 -duroquinone) (21°),⁶ and Cp*Ir(η^4 -*p*-benzoquinone) (16°).¹⁵ Since the smallest reported value is 6.0° in Ni(cod)(duroquinone),⁴ the 3.2° in complex **2f** is quite unusual. Surprisingly, this dihedral angle is even smaller than those of semiquinone complexes such as Ru(η^6 -*p*-MeC₆H₄SO₃-H₂O)(η^6 -*p*-O=C₆Me₄OH) (8.7° , 10°)²⁵ and Mn(η^5 -*p*-O=C₆H₄OH)(CO)₃ (6.7° , 11.3°).^{19b}

The ambiguity of hapticity is often discussed in transition metal *p*-quinone complexes.^{11b,19b} Scheme 1 shows possible resonance structures **2f**–**2f''**. The η^4 -*p*-quinone form (**2f**) basically gives a large contribution because the bond lengths of Ru–C(2), C(3), C(5), C(6) are ca. 0.2 Å shorter than those of Ru–C(1) and C(4). However, the quite small exo-bending ($\alpha = 3.2^\circ$) of the plane that includes C(1), C(2), and C(6) compared to the plane of four olefinic carbons C(2), C(3), C(5), and C(6), as described above, indicates a considerable contribution by an η^5 -*p*-semiquinone coordination mode (**2f'**). The resonance structure of the hydroquinone dianion (**2f''**) also cannot be ruled out, since the carbonyl carbons of *p*-quinones were shifted upfield by ~ 30 ppm in the ¹³C NMR spectrum in **2**, as reported for *p*-quinone complexes.^{9,11a,12a,19b} In the infrared spectra of **2**, the $\nu(\text{C}=\text{O})$ bands of the quinone ligands appeared at

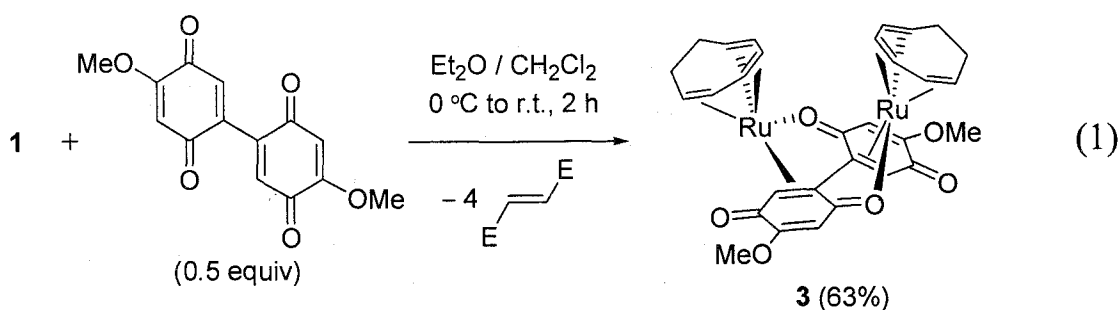
Scheme 1. Possible Resonances in **2f**



1550~1610 cm^{-1} , which are shifted to a lower wavenumber by 50~100 cm^{-1} compared with those of the corresponding free quinones. This shift is attributable to π -back donation from ruthenium metal, and also supports some contribution from the structure **2f''**.

Complexes **2** are the first example of *zerovalent* ruthenium *p*-quinone complexes, whereas Wilkinson and co-workers reported a hydroquinone-bridged divalent ruthenium *p*-quinone complex by reacting $\text{RuH}_2(\text{PPh}_3)_4$ with hydroquinone.¹⁸ Complexes **2** are generally moisture-sensitive due to the highly oxophilic ruthenium center caused by the coordinated *p*-quinones. The reactivity of **2** toward H_2O is dramatically affected by the substituent on the *p*-quinone ligand. For example, complex **2a** was readily decomposed by H_2O in air. On the other hand, complex **2f**, which has two methoxy groups at the 2- and 6-positions, does not react with excess H_2O in dioxane even at a high temperature such as 100 °C.

$\{\text{Ru}(\eta^6\text{-cot})_2(\text{p-biquinone})\}$ (3**).** The reaction of **1** with a 0.5 equiv of *p*-biquinone²⁶ in place of *p*-quinone gave a novel Ru(0) bimetallic complex **3** under very mild conditions, as illustrated in eq 1. η^4 -Coordinated monometallic or bimetallic complexes which are similar to complexes **2** did not form at all in this reaction. X-ray crystallography of **3** was successfully performed, and the ORTEP drawing is shown in Figure 3. Symmetrical patterns can be recognized from the top and side views of **3** (Figure 4). Lists of the selected bond lengths and angles of **3** are given in Tables 7 and 8, respectively.



In complex **3**, the coordination mode of the *p*-quinone moiety is different from that in **2**. One of the two olefinic parts and an oxygen atom of a carbonyl group of each *p*-quinone moiety coordinate to each ruthenium atom to form stable chelate rings. Two ruthenium atoms are located on the same side of the twisted *p*-biquinone framework. Thus, **3** is a C_2 -symmetric compound and the symmetry axis penetrates the center of *p*-biquinone vertically. The distance between the two ruthenium atoms is 4.12 Å, and no metal–metal bond exists. The shorter lengths of Ru(1)–C(2) [2.151(8) Å] and Ru(1)–C(3) [2.145(7) Å] and the greater length of C(2)–C(3) [1.46(1) Å] in **3** compared to those in **2f** reveal that the degree of π -back donation in **3** is much greater than that in **2f**. The C(1)–O(1) bond length in **3** is 1.278(9) Å, which is a little longer than that in **2f**, mainly due to σ -donation from O(1) to Ru(2). The dihedral angle between a *p*-quinone plane [C(1)–C(6)] and a plane containing Ru(1), C(2), and C(3) is 107.7°. Similarly, the dihedral angle between another *p*-quinone plane [C(16)–C(21)] and a plane containing Ru(2), C(17), and C(18) is 108.5°. Thus,

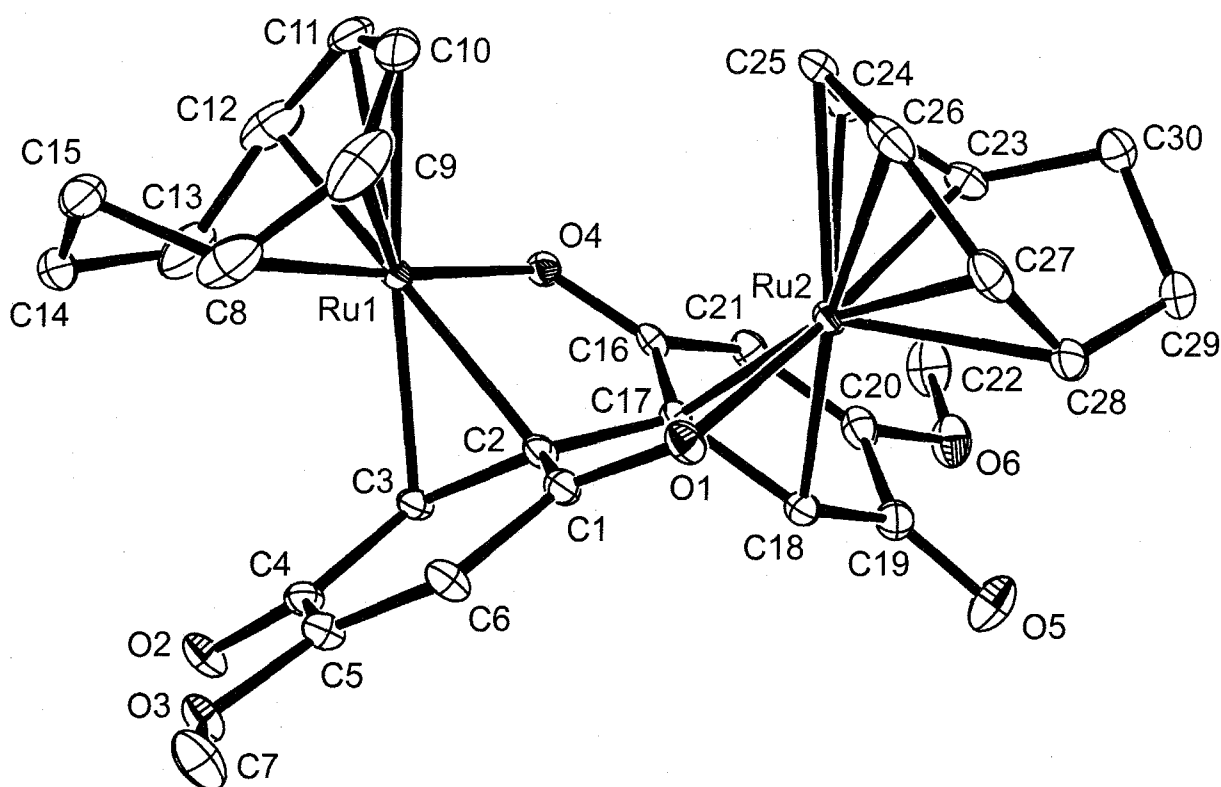


Figure 3. ORTEP drawing of **3**.

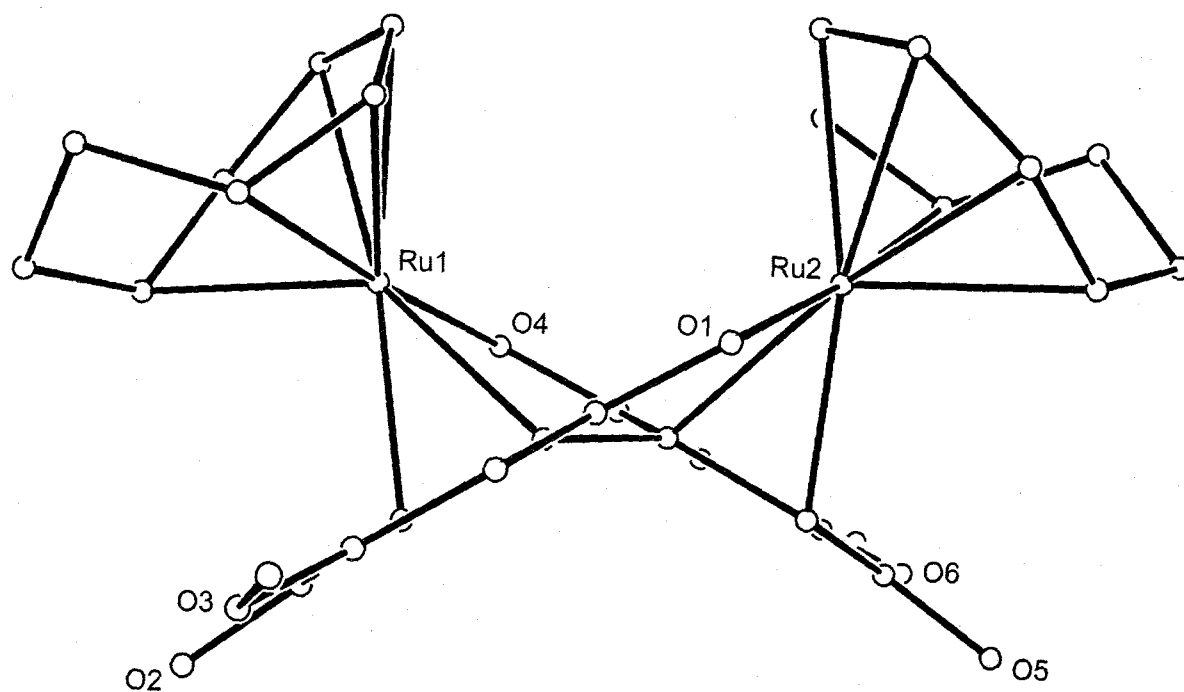
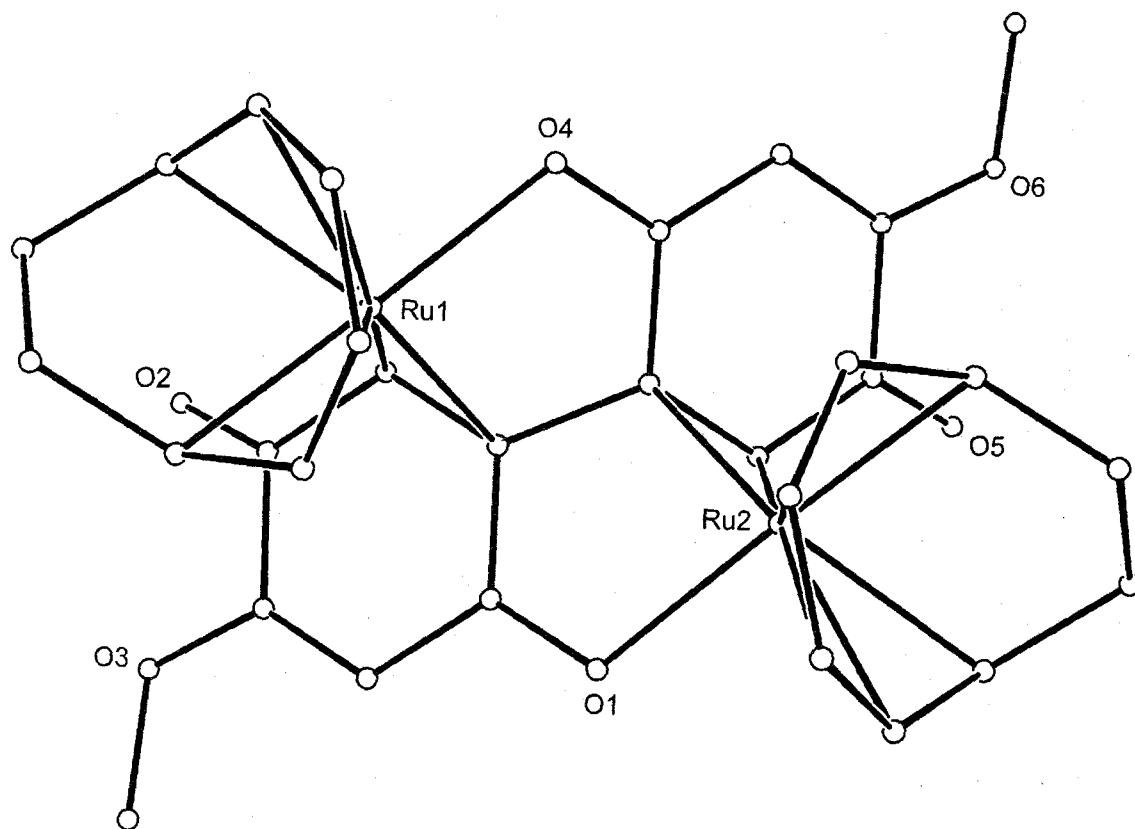


Figure 4. Top and side views of 3.

Table 7. Selected Bond Lengths (Å) for **3**

Ru(1)–O(4)	2.172(6)	Ru(1)–C(2)	2.151(8)
Ru(1)–C(3)	2.145(7)	Ru(1)–C(8)	2.20(1)
Ru(1)–C(9)	2.12(1)	Ru(1)–C(10)	2.236(9)
Ru(1)–C(11)	2.248(9)	Ru(1)–C(12)	2.18(1)
Ru(1)–C(13)	2.20(1)	Ru(2)–O(1)	2.150(5)
Ru(2)–C(17)	2.152(7)	Ru(2)–C(18)	2.146(8)
Ru(2)–C(23)	2.204(8)	Ru(2)–C(24)	2.133(8)
Ru(2)–C(25)	2.260(8)	Ru(2)–C(26)	2.238(8)
Ru(2)–C(27)	2.182(8)	Ru(2)–C(28)	2.224(8)
Cl(1)–C(31)	1.80(2)	Cl(2)–C(31)	1.49(2)
O(1)–C(1)	1.278(9)	O(2)–C(4)	1.225(9)
O(3)–C(5)	1.343(9)	O(3)–C(7)	1.43(1)
O(4)–C(16)	1.275(9)	O(5)–C(19)	1.23(1)
O(6)–C(20)	1.34(1)	O(6)–C(22)	1.42(1)
C(1)–C(2)	1.41(1)	C(1)–C(6)	1.45(1)
C(2)–C(3)	1.45(1)	C(2)–C(17)	1.50(1)
C(3)–C(4)	1.45(1)	C(4)–C(5)	1.50(1)
C(5)–C(6)	1.34(1)	C(8)–C(9)	1.43(2)
C(8)–C(15)	1.52(2)	C(9)–C(10)	1.38(2)
C(10)–C(11)	1.37(2)	C(11)–C(12)	1.42(2)
C(12)–C(13)	1.41(2)	C(13)–C(14)	1.50(2)
C(14)–C(15)	1.45(2)	C(16)–C(17)	1.42(1)
C(16)–C(21)	1.45(1)	C(17)–C(18)	1.45(1)
C(18)–C(19)	1.45(1)	C(19)–C(20)	1.49(1)
C(20)–C(21)	1.35(1)	C(23)–C(24)	1.42(1)
C(23)–C(30)	1.51(1)	C(24)–C(25)	1.42(1)
C(25)–C(26)	1.40(1)	C(26)–C(27)	1.44(1)
C(27)–C(28)	1.41(1)	C(28)–C(29)	1.50(1)
C(29)–C(30)	1.50(1)		

ruthenium atoms are not located over the hexagonal face of quinones. These quinone planes are twisted relative to each other by 119.1°.

In the ¹H NMR spectrum of **3**, the olefinic protons on C(3) and C(18) appear at 3.68 ppm, which are considerably shifted to a higher field. A characteristic downfield signal was observed at 202.2 ppm in ¹³C NMR, which was assignable to carbonyl carbons C(1) and C(16). The olefinic carbons of the *p*-biquinone ligand attached to the ruthenium, C(2), C(17) and C(3), C(18) appeared at 69.3 and 53.6 ppm, respectively.

A couple of chelations in complex **3** cooperate to strengthen the binding of the *p*-biquinone ligand to each ruthenium atom. An attempt to form a monometallic *p*-biquinone complex by reacting **1** with 1 equiv of *p*-biquinone resulted in failure and gave only the bimetallic complex **3**. This is because the

Table 8. Selected Bond Angles (deg) for **3**

O(4)–Ru(1)–C(2)	78.3(3)	O(4)–Ru(1)–C(3)	84.1(3)
C(2)–Ru(1)–C(3)	39.6(3)	O(4)–Ru(1)–C(8)	175.7(3)
C(2)–Ru(1)–C(8)	105.0(3)	C(3)–Ru(1)–C(8)	100.2(4)
O(4)–Ru(1)–C(9)	138.7(4)	C(2)–Ru(1)–C(9)	101.8(4)
C(3)–Ru(1)–C(9)	122.4(4)	C(8)–Ru(1)–C(9)	38.5(5)
O(4)–Ru(1)–C(10)	108.8(4)	C(2)–Ru(1)–C(10)	123.4(4)
C(3)–Ru(1)–C(10)	157.6(4)	C(8)–Ru(1)–C(10)	67.2(5)
C(9)–Ru(1)–C(10)	36.9(5)	O(4)–Ru(1)–C(11)	91.0(3)
C(2)–Ru(1)–C(11)	151.1(4)	C(3)–Ru(1)–C(11)	166.5(4)
C(8)–Ru(1)–C(11)	84.8(4)	C(9)–Ru(1)–C(11)	68.9(5)
O(4)–Ru(1)–C(12)	86.8(3)	C(2)–Ru(1)–C(12)	162.0(4)
C(3)–Ru(1)–C(12)	129.4(4)	C(8)–Ru(1)–C(12)	90.3(4)
C(9)–Ru(1)–C(12)	96.1(4)	O(4)–Ru(1)–C(13)	104.3(4)
C(2)–Ru(1)–C(13)	137.3(4)	C(3)–Ru(1)–C(13)	97.7(4)
C(8)–Ru(1)–C(13)	75.2(5)	C(9)–Ru(1)–C(13)	102.7(4)
C(10)–Ru(1)–C(11)	35.5(5)	C(10)–Ru(1)–C(12)	71.0(5)
C(11)–Ru(1)–C(12)	37.5(5)	C(10)–Ru(1)–C(13)	96.7(4)
C(11)–Ru(1)–C(13)	71.3(5)	C(12)–Ru(1)–C(13)	37.6(5)
O(1)–Ru(2)–C(17)	78.7(3)	O(1)–Ru(2)–C(18)	84.3(3)
C(17)–Ru(2)–C(18)	39.5(3)	O(1)–Ru(2)–C(23)	174.6(3)
C(17)–Ru(2)–C(23)	104.7(3)	C(18)–Ru(2)–C(23)	101.0(3)
O(1)–Ru(2)–C(24)	137.7(3)	C(17)–Ru(2)–C(24)	100.1(3)
C(18)–Ru(2)–C(24)	121.6(3)	C(23)–Ru(2)–C(24)	38.1(3)
O(1)–Ru(2)–C(25)	107.4(3)	C(17)–Ru(2)–C(25)	121.7(3)
C(18)–Ru(2)–C(25)	156.9(3)	C(23)–Ru(2)–C(25)	67.3(3)
C(24)–Ru(2)–C(25)	37.6(3)	O(1)–Ru(2)–C(26)	90.1(3)
C(17)–Ru(2)–C(26)	150.3(3)	C(18)–Ru(2)–C(26)	166.8(3)
C(23)–Ru(2)–C(26)	85.0(3)	C(24)–Ru(2)–C(26)	70.1(3)
O(1)–Ru(2)–C(27)	86.1(3)	C(17)–Ru(2)–C(27)	161.8(3)
C(18)–Ru(2)–C(27)	129.4(3)	C(23)–Ru(2)–C(27)	91.2(3)
C(24)–Ru(2)–C(27)	97.8(3)	O(1)–Ru(2)–C(28)	104.5(3)
C(17)–Ru(2)–C(28)	138.1(3)	C(18)–Ru(2)–C(28)	98.7(3)
C(23)–Ru(2)–C(28)	75.9(3)	C(24)–Ru(2)–C(28)	103.6(3)
C(25)–Ru(2)–C(26)	36.3(3)	C(25)–Ru(2)–C(27)	72.3(3)
C(26)–Ru(2)–C(27)	38.0(3)	C(25)–Ru(2)–C(28)	97.6(3)
C(26)–Ru(2)–C(28)	71.2(3)	C(27)–Ru(2)–C(28)	37.3(3)
Ru(2)–O(1)–C(1)	113.3(5)	Ru(1)–O(4)–C(16)	113.6(5)
Ru(1)–C(2)–C(1)	115.6(6)	Ru(1)–C(2)–C(3)	70.0(4)
Ru(1)–C(2)–C(17)	105.8(5)	Ru(1)–C(3)–C(2)	70.4(4)
Ru(1)–C(3)–C(4)	116.1(5)	Ru(1)–C(8)–C(9)	67.8(6)
Ru(1)–C(8)–C(15)	112.3(7)	Ru(1)–C(9)–C(8)	73.7(6)
Ru(1)–C(9)–C(10)	76.1(7)	Ru(1)–C(10)–C(9)	67.0(6)
Ru(1)–C(10)–C(11)	72.7(6)	Ru(1)–C(11)–C(10)	71.8(6)
Ru(1)–C(11)–C(12)	68.6(6)	Ru(1)–C(12)–C(11)	73.9(6)
Ru(1)–C(12)–C(13)	72.0(6)	Ru(1)–C(13)–C(12)	70.4(6)
Ru(1)–C(13)–C(14)	113.6(9)	Ru(2)–C(17)–C(2)	105.6(5)
Ru(2)–C(17)–C(16)	116.1(5)	Ru(2)–C(17)–C(18)	70.0(4)
Ru(2)–C(18)–C(17)	70.5(4)	Ru(2)–C(18)–C(19)	117.8(5)
Ru(2)–C(23)–C(24)	68.2(4)	Ru(2)–C(23)–C(30)	112.0(6)
Ru(2)–C(24)–C(23)	73.7(5)	Ru(2)–C(24)–C(25)	76.0(5)
Ru(2)–C(25)–C(24)	66.3(4)	Ru(2)–C(25)–C(26)	71.0(5)
Ru(2)–C(26)–C(25)	72.7(5)	Ru(2)–C(26)–C(27)	68.9(5)
Ru(2)–C(27)–C(26)	73.1(5)	Ru(2)–C(27)–C(28)	72.9(5)
O(1)–C(1)–C(2)	120.2(7)	O(1)–C(1)–C(6)	119.7(7)

Table 8. Selected Bond Angles (deg) for **3** (continued)

O(2)–C(4)–C(5)	119.3(7)	O(2)–C(4)–C(3)	124.5(7)
O(3)–C(5)–C(4)	111.8(7)	O(3)–C(5)–C(6)	125.2(7)
O(4)–C(16)–C(17)	119.4(7)	O(4)–C(16)–C(21)	121.0(8)
O(5)–C(19)–C(18)	123.5(9)	O(5)–C(19)–C(20)	120.0(8)
O(6)–C(20)–C(19)	110.9(8)	O(6)–C(20)–C(21)	126.5(9)
C(1)–C(2)–C(3)	120.6(7)	C(1)–C(2)–C(17)	114.3(7)
C(1)–C(6)–C(5)	120.4(7)	C(2)–C(1)–C(6)	120.1(7)
C(2)–C(3)–C(4)	119.5(7)	C(2)–C(17)–C(16)	114.7(7)
C(2)–C(17)–C(18)	120.2(7)	C(3)–C(2)–C(17)	120.4(7)
C(3)–C(4)–C(5)	116.2(7)	C(4)–C(5)–C(6)	123.0(7)
C(5)–O(3)–C(7)	117.2(6)	C(8)–C(9)–C(10)	121.6(1)
C(8)–C(15)–C(14)	107.0(9)	C(9)–C(8)–C(15)	122.3(9)
C(9)–C(10)–C(11)	127.9(1)	C(10)–C(11)–C(12)	133.1(1)
C(11)–C(12)–C(13)	132.0(1)	C(12)–C(13)–C(14)	126.6(1)
C(13)–C(14)–C(15)	108.1(9)	C(16)–C(17)–C(18)	120.3(7)
C(16)–C(21)–C(20)	120.9(8)	C(17)–C(16)–C(21)	119.6(7)
C(17)–C(18)–C(19)	120.0(7)	C(18)–C(19)–C(20)	116.5(7)
C(19)–C(20)–C(21)	122.5(8)	C(20)–O(6)–C(22)	117.5(8)
C(23)–C(24)–C(25)	121.2(8)	C(24)–C(23)–C(30)	121.3(8)
C(24)–C(25)–C(26)	125.7(8)	C(25)–C(26)–C(27)	135.0(8)

monometallic *p*-biquinone complex can easily capture a second ruthenium by an appropriately located chelation system which was fixed by the first chelation, and as a result, a more stable bimetallic species **3** is formed. Although several transition metal *p*-quinone complexes have been synthesized so far, such a *p*-biquinone-coordinated bimetallic complex is unprecedented, to the best of our knowledge.

In contrast to the case of complex **1**, reactions of Ru(η^4 -cod)(η^6 -cot) (cod = 1,5-cyclooctadiene), which is a precursor of **1**, with *p*-quinones and *p*-biquinone gave only insoluble materials and did not afford **2** or **3** at all, respectively. This suggests that a π -acidic dimethyl fumarate ligand in **1** is required to control the electron density of ruthenium during substitution by *p*-quinones or *p*-biquinone. In the case of Ru(η^4 -cod)(η^6 -cot), the relatively electron-rich ruthenium center may donate the *d*-electrons and reduce the coordinated *p*-quinone to a semiquinone anion or a hydroquinone dianion species.

Conclusion

Novel zerovalent ruthenium complexes **2** and **3**, bearing either *p*-quinone or *p*-biquinone as π -acceptors, were synthesized by simple and selective ligand exchange of **1**. Since complexes **2** and **3** are a potentially electron-rich species and also have electron-accepting systems, versatile catalytic activities are expected. Complex **3** has two electron-rich reaction sites located close together without a metal–metal bond, and this unique structure should provide novel catalytic reactions.

Experimental Section

Materials and Methods. All manipulations were performed under an argon atmosphere using standard Schlenk techniques. $\text{Ru}(\eta^6\text{-cot})(\text{dmfm})_2$ (**1**) was synthesized as we reported previously.²³ All solvents were distilled under argon over appropriate drying reagents (sodium, calcium hydride, sodium-benzophenone, or calcium chloride). 5,5'-Dimethoxy-2,2'-*p*-biquinone was prepared as reported in the literature.²⁶

Physical and Analytical Measurements. NMR spectra were recorded on JEOL EX-400 (FT, 400 MHz (^1H), 100 MHz (^{13}C)) and AL-300 (FT, 300 MHz (^1H), 75 MHz (^{13}C)) spectrometers. Chemical shift values (δ) for ^1H and ^{13}C are referenced to internal solvent resonances and reported relative to SiMe_4 . NMR data for **2a–g** are summarized in Table 2 (^1H) and Table 3 (^{13}C). IR spectra were recorded on a Nicolet Impact 410 FT-IR spectrometer. Melting points were determined under argon on a Yanagimoto micro melting point apparatus. HR-MS spectra were recorded on a JEOL SX102A spectrometer with *m*-nitrobenzyl alcohol (*m*-NBA) as a matrix.

Synthesis of $\text{Ru}(\eta^6\text{-cot})(p\text{-quinone})$ (2a–g**).** All of the *p*-quinone complexes **2a–g** were synthesized in a similar manner. The following procedure

for **2a** is representative.

Ru(η^6 -cot)(*p*-benzoquinone) (2a). A mixture of 100 mg (0.20 mmol) of Ru(η^6 -cot)(dmfm)₂ (**1**), 24 mg (0.22 mmol) of *p*-benzoquinone, and 5 mL of Et₂O was stirred at room temperature for 2 h. The resulting pale yellow precipitate was filtered, rinsed with Et₂O (5 mL \times 5), and dried under vacuum to give the title complex (67 mg, 98%), mp 122 °C dec. IR (CHCl₃): 1600, 1573 cm⁻¹. HR-MS (FAB-*m*NBA): *m/z* 317.0114 (M + H)⁺, calcd for C₁₄H₁₅O₂Ru 317.0116.

Ru(η^6 -cot)(*p*-toluquinone) (2b). Pale yellow solid, mp 117 °C dec. IR (CHCl₃): 1597, 1568 cm⁻¹. HR-MS (FAB-*m*NBA): *m/z* 331.0246 (M + H)⁺, calcd for C₁₅H₁₇O₂Ru 331.0272.

Ru(η^6 -cot)(2,6-dimethyl-*p*-benzoquinone) (2c). Pale yellow solid, mp 144 °C dec. IR (KBr disk): 1583, 1558, 1551 cm⁻¹. HR-MS (FAB-*m*NBA): *m/z* 345.0457 (M + H)⁺, calcd for C₁₆H₁₉O₂Ru 345.0429.

Ru(η^6 -cot)(2,5-diphenyl-*p*-benzoquinone) (2d). Pale yellow solid, mp 233 °C dec. IR (KBr disk): 1606, 1584 cm⁻¹. HR-MS (FAB-*m*NBA): *m/z* 469.0766 (M + H)⁺, calcd for C₂₆H₂₃O₂Ru 469.0742.

Ru(η^6 -cot)(2,5-dichloro-*p*-benzoquinone) (2e). Brown solid, mp 221 °C dec. IR (KBr disk): 1604 cm⁻¹. HR-MS (FAB-*m*NBA): *m/z* 384.9356 (M + H)⁺, calcd for C₁₄H₁₃Cl₂O₂Ru 384.9336.

Ru(η^6 -cot)(2,6-dimethoxy-*p*-benzoquinone) (2f). Pale yellow solid, mp 172 °C dec. IR (KBr disk): 1579, 1545 cm⁻¹. HR-MS (FAB-*m*NBA): *m/z* 377.0312 (M + H)⁺, calcd for C₁₆H₁₉O₄Ru 377.0327.

Ru(η^6 -cot)(*p*-naphthoquinone) (2g). Brown solid, mp 300 °C dec. IR (nujol): 1567 cm⁻¹. HR-MS (FAB-*m*NBA): *m/z* 367.0291 (M + H)⁺, calcd for C₁₈H₁₇O₂Ru 367.0272.

Synthesis of {Ru(η^6 -cot)}₂(5,5'-dimethoxy-2,2'-*p*-biquinone) (3). To an Et₂O suspension (5 mL) of 5,5'-dimethoxy-2,2'-*p*-biquinone (69 mg, 0.25 mmol) was added a CH₂Cl₂ solution (5 mL) of **1** (248 mg, 0.50 mmol) dropwise

at 0 °C. The reaction mixture immediately turned black and was warmed to room temperature. After stirring for 1 h, the solvent was removed, and then CH₂Cl₂ (1.5 mL) and Et₂O (18 mL) were added for recrystallization. The resulting black powder was filtered, washed with Et₂O (3 mL × 2), and dried under vacuum to give complex **3** (109 mg, 63%), mp 225–227 °C dec. IR (CHCl₃): 1672, 1621 cm⁻¹. ¹H NMR (400 MHz, CDCl₃): δ 6.66 (dd, *J* = 8.8 and 5.3 Hz, CH of cot, 2H), 6.17 (t, *J* = 8.8 Hz, CH of cot, 2H), 5.52 (m, CH of cot, 2H), 5.25 (s, CH at 6 and 6'-positions of biquinone, 2H), 4.74 (t, *J* = 9.3 Hz, CH of cot, 2H), 4.33 (t, *J* = 6.6 Hz, CH of cot, 2H), 3.68 (s, CH at 3 and 3'-positions of biquinone, 2H), 3.60 (s, OCH₃, 6H), 2.70 (q, *J* = 7.3 Hz, CH of cot, 2H), 2.17 (m, CHH of cot, 2H), 1.64 (m, CHH of cot, 2H), 1.02 (m, CHH of cot, 2H), -0.64 (m, CHH of cot, 2H). ¹³C NMR (100 MHz, CDCl₃): δ 202.2, 191.4, 161.9, 105.9, 105.0, 101.6, 92.2, 87.0, 86.2, 69.3, 66.0, 56.4, 53.6, 33.2, 25.3. HR-MS (FAB-*m*NBA): *m/z* 690.0134 (M)⁺, calcd for C₃₀H₃₀O₆Ru₂ 690.0129.

Crystallographic Study of Complexes 2f and 3. Single crystals of complexes **2f** and **3** obtained by recrystallization from CHCl₃/pentane (**2f**) or CH₂Cl₂/pentane (**3**) were subjected to X-ray crystallographic analysis. The crystal data and experimental details for **2f** and **3** are summarized in Table 4. All measurements were made on a Rigaku RAXIS imaging plate area detector with graphite monochromated Mo Kα radiation (λ = 0.71069 Å). The structures were solved by direct methods using SIR92²⁷ and expanded using Fourier techniques, DIRDIF99.²⁸ The non-hydrogen atoms were refined anisotropically, except for an oxygen atom of a lattice water in **2f**, which was refined isotropically. Hydrogen atoms were refined using the riding model. Neutral atom-scattering factors were taken from Cromer and Waber.²⁹ Anomalous dispersion effects were included in F_{calc} ³⁰; the values for $\Delta f'$ and $\Delta f''$ were those of Creagh and McAuley.³¹ The values for the mass attenuation coefficients were those of Creagh and Hubbell.³² All calculations were performed using the CrystalStructure^{33,34} crystallographic software package. In Figures 1 and 3,

thermal ellipsoids are shown at the 30% probability level and hydrogen atoms are omitted for clarity.

References

- (1) Sternberg, H. W.; Markby, R.; Wender, I. *J. Am. Chem. Soc.* **1958**, *80*, 1009.
- (2) (a) Schrauzer G. N.; Thyret, H. *J. Am. Chem. Soc.* **1960**, *82*, 6420. (b) Schrauzer G. N.; Thyret, H. *Z. Naturforsch.* **1961**, *16b*, 353. (c) Schrauzer G. N.; Thyret, H. *Z. Naturforsch.* **1962**, *17b*, 73. (d) Schrauzer G. N.; Thyret, H. *Angew. Chem., Int. Ed.* **1963**, *2*, 478.
- (3) Schrauzer G. N.; Dewhirst, K. C. *J. Am. Chem. Soc.* **1964**, *86*, 3265.
- (4) Glick, M. D.; Dahl, L. F. *J. Organomet. Chem.* **1965**, *3*, 200.
- (5) (a) Aleksandrov, G. G.; Gusev, A. I.; Khandkarova, V. S.; Struchkov, Yu. T.; Gubin, S. P. *J. Chem. Soc. D* **1969**, 748. (b) Aleksandrov, G. G.; Struchkov, Yu. T.; Khandkarova, V. S.; Gubin, S. P. *J. Organomet. Chem.* **1970**, *25*, 243.
- (6) Uchtman, V. A.; Dahl, L. F. *J. Organomet. Chem.* **1972**, *40*, 403.
- (7) Slocum, D. W.; Engelmann, T. R. *J. Am. Chem. Soc.* **1972**, *94*, 8596.
- (8) (a) Dickson, R. S.; Kirsch, H. P. *Aust. J. Chem.* **1974**, *27*, 61. (b) Dickson, R. S.; Johnson, S. H. *Aust. J. Chem.* **1976**, *29*, 2189. (c) Corrigan, P. A.; Dickson, R. S. *Aust. J. Chem.* **1981**, *34*, 1401.
- (9) Bodner, G. M.; Engelmann, T. R. *J. Organomet. Chem.* **1975**, *88*, 391.
- (10) Minematsu, H.; Takahashi, S.; Hagihara, N. *J. Organomet. Chem.* **1975**, *91*, 389.
- (11) (a) Fairhurst, G.; White, C. *J. Organomet. Chem.* **1978**, *160*, C17. (b) Fairhurst, G.; White, C. *J. Chem. Soc., Dalton Trans.* **1979**, 1531.
- (12) (a) Chetcuti, M. J.; Howard, J. A. K.; Pfeffer, M.; Spencer, J. L.; Stone, F. G. A. *J. Chem. Soc., Dalton Trans.* **1981**, 276. (b) Chetcuti, M. J.; Herbert,

- J. A.; Howard, J. A. K.; Pfeffer, M.; Spencer, J. L.; Stone, F. G. A.; Woodward, P. *J. Chem. Soc., Dalton Trans.* **1981**, 284.
- (13) Hiramatsu, M.; Shiozaki, K.; Fujinami, T.; Sakai, S. *J. Organomet. Chem.* **1983**, 246, 203.
- (14) (a) Jewell, C. F., Jr.; Liebeskind, L. S.; Williamson, M. *J. Am. Chem. Soc.* **1985**, 107, 6715. (b) Liebeskind, L. S.; Jewell, C. F., Jr. *J. Organomet. Chem.* **1985**, 285, 305. (c) Cho, S. H.; Wirtz, K. R.; Liebeskind, L. S. *Organometallics* **1990**, 9, 3067.
- (15) Le Bras, J.; Amouri, H.; Vaissermann, J. *Organometallics* **1998**, 17, 1116.
- (16) Klein, H.-F.; Auer, E.; Dal, A.; Lemke, U.; Lemke, M.; Jung, T.; Rohr, C.; Florke, U.; Haupt, H.-J. *Inorg. Chim. Acta* **1999**, 287, 167.
- (17) Cooke, J.; Takats, J. *J. Am. Chem. Soc.* **1997**, 119, 11088.
- (18) Rosete, R. O.; Cole-Hamilton, D. J.; Wilkinson, G. *J. Chem. Soc., Dalton Trans.* **1979**, 1618.
- (19) (a) Oh, M.; Carpenter, G. B.; Sweigart, D. A. *Angew. Chem., Int. Ed.* **2001**, 40, 3191. (b) Oh, M.; Carpenter, G. B.; Sweigart, D. A. *Organometallics* **2002**, 21, 1290.
- (20) Davidson, J. L.; Green, M.; Stone, F. G. A.; Welch, A. J. *J. Chem. Soc., Dalton Trans.* **1976**, 738.
- (21) Le Bras, J.; Amouri, H.; Vaissermann, J. *J. Organomet. Chem.* **1998**, 553, 483.
- (22) Sun, S.; Carpenter, G. B.; Sweigart, D. A. *J. Organomet. Chem.* **1996**, 512, 257.
- (23) Mitsudo, T.; Suzuki, T.; Zhang, S.-W.; Imai, D.; Fujita, K.; Manabe, T.; Shiotsuki, M.; Watanabe, Y.; Wada, K.; Kondo, T. *J. Am. Chem. Soc.* **1999**, 121, 1839.
- (24) (a) Suzuki, T.; Shiotsuki, M.; Wada, K.; Kondo, T.; Mitsudo, T. *Organometallics* **1999**, 18, 3671. (b) Suzuki, T.; Shiotsuki, M.; Wada, K.; Kondo, T.; Mitsudo, T. *J. Chem. Soc., Dalton Trans.* **1999**, 4231. (c)

- Shiotsuki, M.; Suzuki, T.; Kondo, T.; Wada, K.; Mitsudo, T. *Organometallics* **2000**, *19*, 5733.
- (25) Koelle, U.; Weisschadel, Chr.; Englert, U. *J. Organomet. Chem.* **1995**, *490*, 101.
- (26) Jacob, P., III; Callery P. S.; Shulgin A. T.; Castagnoli, N., Jr. *J. Org. Chem.* **1976**, *41*, 3627.
- (27) Altomare, A.; Cascarano, G.; Giacovazzo, C.; Guagliardi, A.; Burla, M.; Polidori, G.; Camalli, M. *J. Appl. Cryst.* **1994**, *27*, 435.
- (28) Beurskens, P. T.; Admiraal, G.; Beurskens, G.; Bosman, W. P.; de Gelder, R.; Israel, R.; Smits, J. M. M. *The DIRDIF-99 program system*; Technical Report of the Crystallography Laboratory: University of Nijmegen, Netherlands, **1999**.
- (29) Cromer, D. T.; Waber, J. T. *International Tables for X-ray Crystallography*; The Kynoch Press: Birmingham, England, Vol. IV, **1974**.
- (30) Ibers, J. A.; Hamilton, W. C. *Acta Crystallogr.* **1964**, *17*, 781.
- (31) Creagh, D. C.; McAuley, W. J. *International Tables for X-ray Crystallography*; Kluwer Academic Publishers, Boston, Vol. C, **1992**.
- (32) Creagh, D. C.; Hubbell, J. H. *International Tables for X-ray Crystallography*; Kluwer Academic Publishers, Boston, Vol. C, **1992**.
- (33) CrystalStructure 2.00, *Crystal Structure Analysis Package*, Rigaku and MSC, **2001**.
- (34) Watkin, D. J.; Prout, C. K.; Carruthers, J. R.; Betteridge, P. W. *CRYSTALS Issue 10*; Chemical Crystallography Laboratory: Oxford, UK.

Chapter 5

Synthesis of Novel Zerovalent Ruthenium η^6 -Arene Complexes via Direct Displacement of a 1,3,5-Cyclooctatriene Ligand by Arenes

Abstract

Novel zerovalent arene complexes bearing two dimethyl fumarate ligands, Ru(η^6 -arene)(dimethyl fumarate)₂ [arene = benzene (**2a**), toluene (**2b**), *p*-xylene (**2c**), mesitylene (**2d**), hexamethylbenzene (**2e**), *t*-butylbenzene (**2f**), anisole (**2g**), *N,N*-dimethylaniline (**2h**), biphenyl (**2i**), methyl benzoate (**2j**), or naphthalene (**2k**)], were synthesized via the direct ligand-exchange reaction of Ru(η^6 -cot)-(dimethyl fumarate)₂ [**1**; cot = 1,3,5-cyclooctatriene] with arenes. The detailed structures of **2g** and **2h** were determined by the X-ray crystallography, which revealed that the coordination geometry can be represented by a highly distorted trigonal bipyramid, and confirmed that these complexes are zerovalent complexes.

Introduction

Many ruthenium η^6 -arene complexes have been synthesized and investigated so far, since these complexes are of great interest in catalysis.^{1,2} Most of them are divalent complexes, and there are comparatively few examples of *zerovalent* arene complexes. There are three well-known methods for the practical preparation of zerovalent ruthenium η^6 -arene complexes. One is the cyclotrimerization of alkynes on a metal center.³⁻⁵ Although this procedure can use various alkynes, a mixture of regiomers is formed with an asymmetric alkyne.^{4,5} The second method is the reduction of divalent ruthenium arene complexes.⁶⁻²⁹ Divalent arene complexes are reduced by the appropriate reagents such as alkali metal,⁶⁻⁹ sodium naphthalide,¹⁰⁻¹² sodium borohydride,¹³⁻¹⁵ carbonate/alcohol,¹⁶⁻¹⁸ Grignard reagent,¹⁹ zinc,²⁰ etc., which efficiently generates zerovalent ruthenium arene complexes. However, this method has been established only for a certain divalent ruthenium arene complex. The third method is the ligand-exchange reaction of zerovalent ruthenium complexes with arenes. Pertici and co-workers found that $\text{Ru}(\eta^4\text{-cod})(\eta^6\text{-arene})$ complexes could be obtained by reacting $\text{Ru}(\eta^4\text{-cod})-(\eta^6\text{-cot})$ (cod = 1,5-cyclooctadiene, cot = 1,3,5-cyclooctatriene) with arenes under a hydrogen atmosphere.³⁰ They also found that the same complexes could be obtained via the exchange of a naphthalene moiety of $\text{Ru}(\eta^4\text{-cod})(\eta^6\text{-naphthalene})$ with arenes in the presence of acetonitrile.³¹ In these reactions, the additives are essential, and there has been no previous report of a simple and direct ligand-exchange reaction of zerovalent ruthenium complexes with arenes.

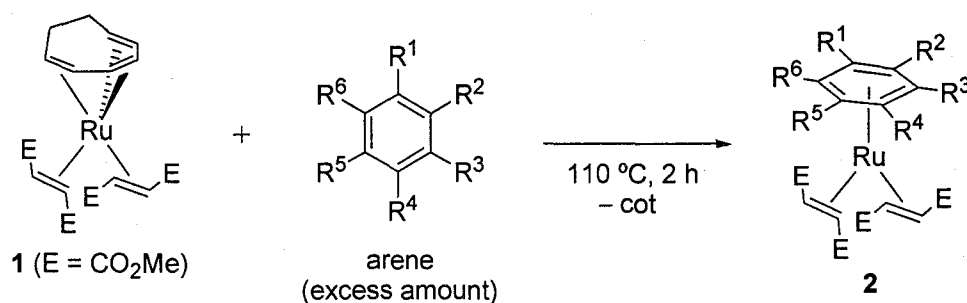
Recently, we reported a novel zerovalent ruthenium complex $\text{Ru}(\eta^6\text{-cot})-(\text{dmfm})_2$ [**1**; dmfm = dimethyl fumarate]. Complex **1** shows very high catalytic activity in a unique dimerization of 2,5-norbornadiene to afford a novel half-cage compound.³² During our investigation of the reactivity of **1**,³³⁻³⁶ we found that reactions of **1** with arenes gave novel zerovalent ruthenium arene

complexes via the direct ligand-exchange of cyclooctatriene with arenes. We report here the synthesis and structures of these complexes bearing two olefinic π -acceptor ligands; i.e., dimethyl fumarate.

Results and Discussion

Complex **1** reacted with various aromatic compounds to give a series of novel zerovalent ruthenium η^6 -arene complexes $\text{Ru}(\eta^6\text{-arene})(\text{dmfm})_2$ (**2**) in good yields by ligand exchange between the tridentate ligands, 1,3,5-cycloocta-

Table 1. Reactions of **1** with Arenes



entry	arenes	compound	yield (%) ^a
1 ^b	benzene	2a	66
2	toluene	2b	64
3	<i>p</i> -xylene	2c	67
4	mesitylene	2d	40
5 ^c	hexamethylbenzene	2e	31
6	<i>t</i> -butylbenzene	2f	61
7	anisole	2g	59
8	<i>N,N</i> -dimethylaniline	2h	77
9	biphenyl	2i	61
10	methyl benzoate	2j	13
11	naphthalene	2k	60

^a Isolated yield. ^b The reaction was carried out in an autoclave.

^c Hexamethylbenzene (5 equiv) and diglyme (as a solvent) were used.

Table 2. ^1H NMR Data of **2a–k** (δ , ppm)^a

	dimethyl fumarate		aromatic ligand	
	=CH	Me	aromatic protons	others
2a^b	4.27 (d, 9.9, 2H), 2.02 (d, 9.9, 2H)	3.72 (s, 6H), 3.60 (s, 6H)	5.72 (s, 6H)	
2b	4.07 (d, 9.8, 2H), 2.04 (d, 9.8, 2H)	3.72 (s, 6H), 3.60 (s, 6H)	6.16 (m, 1H), 5.40–5.37 (m, 3H), 5.17 (d, 5.9, 1H)	2.41 (s, 3H)
2c^b	3.85 (d, 9.7, 2H), 2.03 (d, 9.7, 2H)	3.71 (s, 6H), 3.60 (s, 6H)	5.24 (d, 5.9, 2H), 5.14 (d, 5.9, 2H)	2.42 (s, 6H)
2d	3.71 (d, 9.8, 2H), 2.04 (d, 9.8, 2H)	3.70 (s, 6H), 3.58 (s, 6H)	5.24 (s, 3H)	2.17 (s, 9H)
2e	2.98 (d, 9.8, 2H), 2.07 (d, 9.8, 2H)	3.66 (s, 6H), 3.56 (s, 6H)		2.00 (s, 18H)
2f	4.34 (d, 9.8, 2H), 1.99 (d, 9.8, 2H)	3.71 (s, 6H), 3.59 (s, 6H)	6.58 (vt, 5.7, 1H), 5.39 (d, 6.4, 1H), 5.27 (d, 6.4, 1H), 5.21 (vt, 6.2, 1H), 5.16 (vt, 6.0, 1H)	1.45 (s, 9H)
2g	3.98 (d, 9.7, 2H), 2.08 (d, 9.7, 2H)	3.97 (s, 6H), 3.75 (s, 6H)	6.10 (t, 5.8, 1H), 5.65 (t, 5.8, 1H), 5.34 (dd, 6.4, 2.0, 1H), 5.06 (dd, 6.4, 2.0, 1H), 4.94 (t, 5.8, 1H)	3.97 (s, 3H)
2h	3.96 (d, 9.8, 2H), 2.03 (d, 9.8, 2H)	3.70 (s, 6H), 3.58 (s, 6H)	5.99 (t, 5.8, 1H), 5.74 (ddd, 6.6, 5.4, 1.2, 1H), 5.07 (dd, 6.6, 2.2, 1H), 4.71 (dd, 6.6, 2.2, 1H), 4.62 (ddd, 6.6, 5.4, 1.2, 1H)	3.18 (s, 6H)
2i	4.21 (d, 10.3, 2H), 2.06 (d, 10.3, 2H)	3.71 (s, 6H), 3.20 (s, 6H)	7.63–7.61 (m, 2H), 7.45–7.40 (m, 3H), 6.45 (d, 6.9, 1H), 6.23 (t, 6.2, 1H), 6.00 (t, 6.6, 1H), 5.32 (d, 6.9, 1H), 4.94 (t, 5.9, 1H)	
2j	4.30 (d, 9.8, 2H), 2.04 (d, 9.8, 2H)	3.72 (s, 6H), 3.63 (s, 6H)	6.75 (t, 5.7, 1H), 6.08 (d, 5.9, 1H), 5.73 (d, 6.3, 1H), 5.51 (t, 5.9, 1H), 5.28 (t, 6.1, 1H)	4.06 (s, 3H)
2k	4.46 (d, 9.9, 2H), 1.84 (d, 9.9, 2H)	3.56 (s, 6H), 3.55 (s, 6H)	7.81(br, 2H), 7.61 (br, 1H), 7.60 (br, 1H), 6.77 (t, 5.9, 1H), 5.74 (d, 5.9, 1H), 5.68 (t, 5.9, 1H), 5.54 (d, 6.3, 1H)	

^a Measured in CDCl_3 at room temperature and 400 MHz. Legend: s = singlet, d = doublet, t = triplet, vt = virtual triplet, m = multiplet, br = broad. Values in parentheses are the coupling constants, J (Hz). ^b 300 MHz.

Table 3. ^{13}C NMR Data of **2a–k** (δ , ppm)^a

	dimethyl fumarate			aromatic ligand	
	C=O	=CH	Me	aromatic carbons	others
2a ^b	177.1, 173.1	47.6, 41.4	51.3, 51.2	96.4	
2b	176.7, 173.1	48.1, 42.5	51.4, 51.2	112.7, 97.1, 97.0, 95.9, 95.8, 94.4	19.0
2c ^b	177.0, 173.4	48.3, 43.8	51.2, 51.0	111.0, 97.8, 95.5	18.7
2d	176.3, 173.8	47.3, 41.3	51.2, 51.0	109.5, 96.6	18.1
2e	175.3, 174.4	47.4, 41.4	51.1, 50.9	106.0	15.2
2f	177.5, 173.3	47.0, 40.0	51.3, 51.2	126.8, 103.4, 100.3, 92.5, 92.2, 88.8	35.3, 30.6
2g	176.9, 173.4	48.6, 43.5	51.4, 51.2	142.1, 94.9, 94.8, 92.7, 85.6, 77.9	56.5
2h	177.6, 174.3	46.5, 39.7	51.1, 51.0	136.3, 94.5, 92.2, 92.1, 78.8, 69.6	39.5
2i	175.2, 172.7	48.8, 42.3	51.2, 50.8	133.2, 129.2, 128.7, 128.5, 128.4, 127.9, 112.2, 97.5, 96.4, 95.0, 95.0, 92.7	
2j	176.5, 172.3	50.2, 44.1	51.7, 51.5	104.1, 103.3, 94.9, 94.5, 92.3, 91.4	164.6, 53.3
2k	176.7, 172.7	48.7, 44.2	51.1, 50.9	131.8, 130.8, 128.7, 127.5, 105.7, 104.7, 98.5, 97.2, 91.5, 90.7	

^a Measured in CDCl_3 at room temperature and 100 MHz. ^b 75 MHz.

triene and arene (Table 1). Arenes were used as solvents in all the reactions except in the case of complex **2e**. Benzene (entry 1), alkyl-substituted arenes (entries 2–6), and arenes with electron-donating or electron-withdrawing group such as anisole (entry 7), *N,N*-dimethylaniline (entry 8), or biphenyl (entry 9) were efficient. In the case of biphenyl, only a mononuclear ruthenium η^6 -biphenyl complex was obtained and no binuclear complex was formed. The reaction with methyl benzoate gave the desirable complex **2j** in low yield (entry 10). The use of naphthalene also gave a naphthalene complex in η^6 -fashion (entry 11).

The structures of **2a–k** were deduced based on ^1H and ^{13}C NMR spectroscopic analyses (Tables 2 and 3). The signals for the aromatic protons of the coordinated arenes in **2a–k** appear at 4.6–6.8 ppm in the ^1H NMR spectra,

which are shifted to a higher magnetic field by around 1–2 ppm compared to those of free arenes. These values are similar to those of reported zerovalent Ru(η^6 -arene) complexes.^{3–31} One of the signals for the olefinic protons of dimethyl fumarates in **2a–k** constantly appears at around 2.0 ppm as a doublet, and another doublet signal is observed at 3.0–4.5 ppm. This chemical shift value strongly depends on the substituents on the coordinated aromatic ring. In particular, as far as **2a–e** are concerned, the olefinic proton signal shifts to a higher field, i.e., δ 4.27 (**2a**), 4.07 (**2b**), 3.85 (**2c**), 3.71 (**2d**), and 2.98 (**2e**), respectively, as the number of the methyl substituents on the aromatic ring increases. This higher shift may be attributable to shielding by the methyl groups.

As for the ^{13}C NMR signals for aromatic carbons in **2b** and **2f–j** (mono-substituted arene complexes), six non-equivalent peaks appear within the range of 70–142 ppm. This suggests that no symmetrical plane exists in these complexes and thus the two dimethyl fumarate ligands coordinate to the ruthenium center on the same enantiofaces, as in **1**.³² The two signals for the olefinic carbons of dimethyl fumarates in **2a–k** are shifted to a higher field (40–44 ppm and 47–50 ppm) and both of the chemical shift values are almost constant, in contrast to the signals of the olefinic protons in the ^1H NMR spectra described above.

The structures of **2g** and **2h** were confirmed by X-ray crystallography and the ORTEP drawings of **2g** and **2h** are shown in Figures 1 and 2. The crystal data and experimental details for **2g** and **2h** are summarized in Table 4. Lists of the selected bond angles and bond lengths of **2g** and **2h** are given in Tables 5–8, respectively. The coordination geometry of these complexes can be represented by a highly distorted trigonal bipyramid. In complex **2g**, one of the dimethyl fumarate ligands [C(1)–C(2)] and an aromatic olefin moiety [C(17)–C(18)] occupy the axial positions, while the other dimethyl fumarate [C(7)–C(8)] and two residual aromatic olefin moieties [C(13)–C(14), C(15)–C(16)] are located at

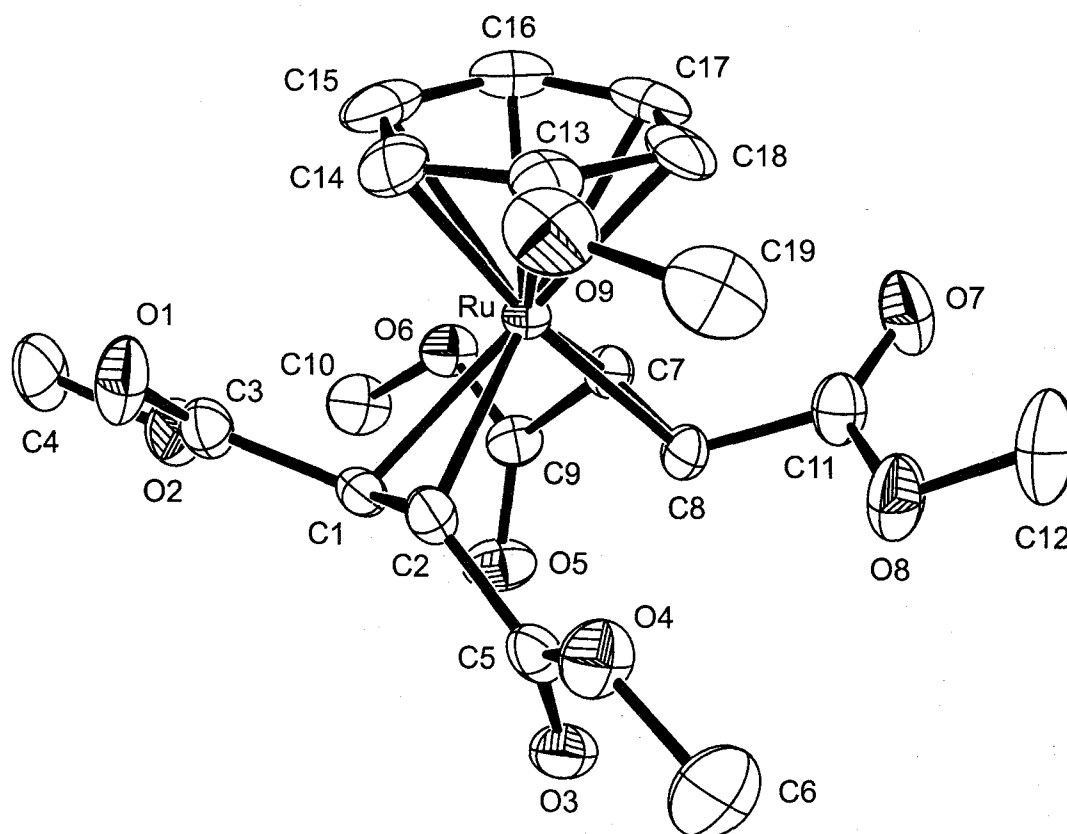


Figure 1. ORTEP drawing of **2g**.

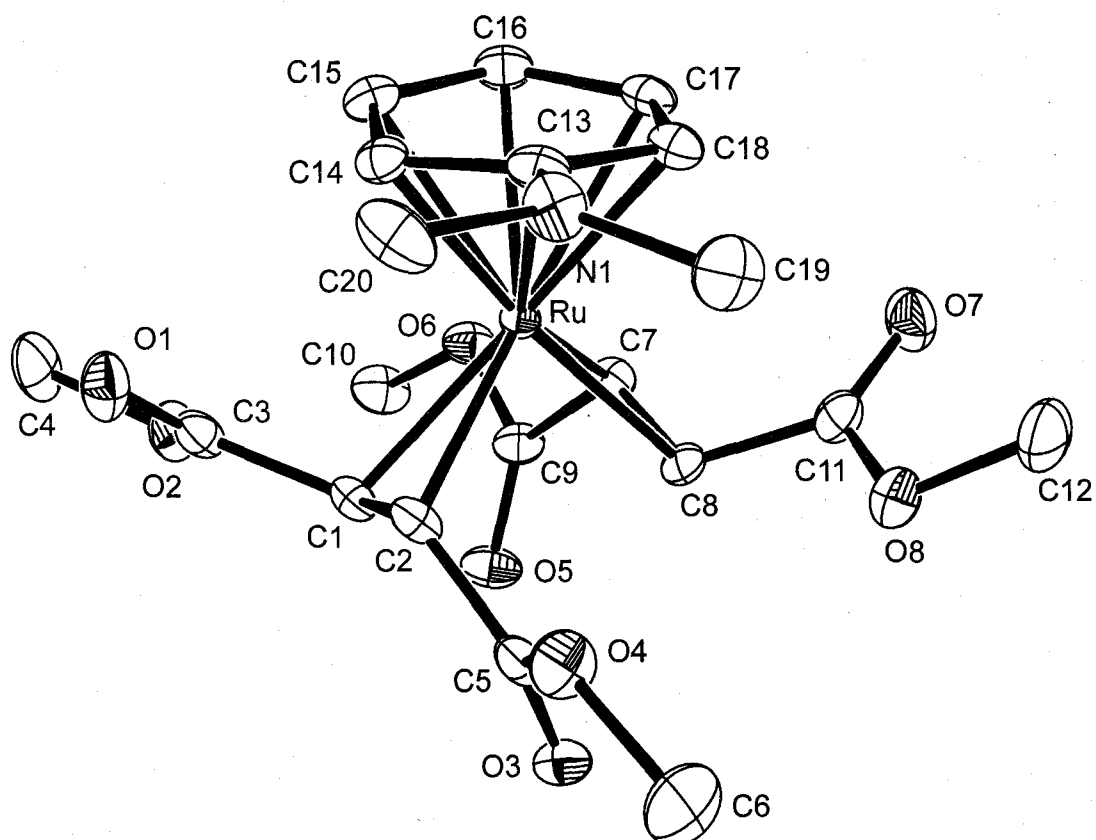


Figure 2. ORTEP drawing of **2h**.

Table 4. Summary of Crystal Data, Collection Data, and Refinement of **2g** and **2h**

	2g	2h
formula	C ₁₉ H ₂₄ O ₉ Ru	C ₂₀ H ₂₇ NO ₈ Ru
fw	497.46	510.51
crystal color	yellow	yellow
crystal system	monoclinic	monoclinic
space group	<i>P</i> 2 ₁	<i>P</i> 2 ₁
<i>a</i> (Å)	7.7075(8)	7.6613(4)
<i>a</i> (Å)	16.088(1)	15.9060(5)
<i>c</i> (Å)	8.1884(6)	8.6199(5)
β (deg)	96.341(6)	96.612(2)
<i>V</i> (Å ³)	1009.1(2)	1043.44(9)
<i>Z</i>	2	2
<i>D</i> _{calcd} (g/cm ³)	1.637	1.625
<i>T</i> (°C)	−180	−180
μ (Mo K α) (cm ^{−1})	8.26	7.99
$2\theta_{\max}$ (deg)	54.6	54.9
no. of measd rflns	8451	9976
no. of obsd rflns	2125	2441
residuals: <i>R</i> ; <i>R</i> _w	0.029; 0.033	0.023; 0.037
GOF	1.39	3.64

Table 5. Selected Bond Lengths (Å) for **2g**

Ru–C(1)	2.153(5)	Ru–C(2)	2.164(5)
Ru–C(7)	2.157(5)	Ru–C(8)	2.128(6)
Ru–C(13)	2.322(6)	Ru–C(14)	2.214(7)
Ru–C(15)	2.275(7)	Ru–C(16)	2.293(7)
Ru–C(17)	2.221(5)	Ru–C(18)	2.297(6)
O(1)–C(3)	1.183(9)	O(2)–C(3)	1.348(8)
O(2)–C(4)	1.437(9)	O(3)–C(5)	1.186(8)
O(4)–C(5)	1.350(7)	O(4)–C(6)	1.42(1)
O(5)–C(9)	1.211(7)	O(6)–C(9)	1.344(8)
O(6)–C(10)	1.431(8)	O(7)–C(11)	1.196(8)
O(8)–C(11)	1.340(8)	O(8)–C(12)	1.44(1)
O(9)–C(13)	1.336(9)	O(9)–C(19)	1.46(2)
C(1)–C(2)	1.419(8)	C(1)–C(3)	1.492(9)
C(2)–C(5)	1.482(9)	C(7)–C(8)	1.409(8)
C(7)–C(9)	1.478(8)	C(8)–C(11)	1.485(9)
C(13)–C(18)	1.41(1)	C(13)–C(14)	1.43(1)
C(14)–C(15)	1.38(1)	C(15)–C(16)	1.41(1)
C(16)–C(17)	1.38(2)	C(17)–C(18)	1.42(1)

Table 6. Selected Bond Angles (deg) for **2g**

C(1)–Ru–C(2)	38.4(2)	C(1)–Ru–C(7)	90.2(2)
C(1)–Ru–C(8)	90.7(2)	C(1)–Ru–C(13)	117.8(3)
C(1)–Ru–C(14)	96.8(3)	C(1)–Ru–C(15)	102.3(3)
C(1)–Ru–C(16)	129.5(3)	C(1)–Ru–C(17)	165.0(5)
C(1)–Ru–C(18)	151.4(2)	C(2)–Ru–C(7)	113.3(2)
C(2)–Ru–C(8)	91.1(3)	C(2)–Ru–C(13)	88.3(2)
C(2)–Ru–C(14)	86.7(3)	C(2)–Ru–C(15)	113.0(3)
C(2)–Ru–C(16)	149.0(3)	C(2)–Ru–C(17)	151.2(2)
C(2)–Ru–C(18)	115.0(2)	C(7)–Ru–C(8)	38.4(2)
C(7)–Ru–C(13)	151.2(3)	C(7)–Ru–C(14)	154.1(3)
C(7)–Ru–C(15)	118.3(3)	C(7)–Ru–C(16)	91.6(3)
C(7)–Ru–C(17)	90.6(3)	C(7)–Ru–C(18)	115.6(2)
C(8)–Ru–C(13)	128.1(3)	C(8)–Ru–C(14)	164.7(3)
C(8)–Ru–C(15)	154.1(3)	C(8)–Ru–C(16)	119.6(3)
C(8)–Ru–C(17)	99.1(4)	C(8)–Ru–C(18)	101.9(3)
C(13)–Ru–C(14)	36.7(3)	C(13)–Ru–C(15)	64.8(3)
C(13)–Ru–C(16)	76.0(3)	C(13)–Ru–C(17)	64.2(3)
C(13)–Ru–C(18)	35.6(3)	C(14)–Ru–C(15)	35.8(3)
C(14)–Ru–C(16)	64.8(3)	C(14)–Ru–C(17)	76.4(4)
C(14)–Ru–C(18)	65.7(3)	C(15)–Ru–C(16)	36.1(3)
C(15)–Ru–C(17)	64.4(5)	C(15)–Ru–C(18)	77.1(3)
C(16)–Ru–C(17)	35.6(5)	C(16)–Ru–C(18)	65.3(3)
C(17)–Ru–C(18)	36.6(3)	C(2)–C(1)–C(3)	121.0(6)
C(1)–C(2)–C(5)	120.7(6)	C(7)–C(8)–C(11)	120.6(6)
C(8)–C(7)–C(9)	120.9(6)	C(14)–C(13)–C(18)	118.5(7)
O(9)–C(13)–C(14)	117.0(9)	O(9)–C(13)–C(18)	124.5(9)
C(13)–O(9)–C(19)	118.8(9)		

Table 7. Selected Bond Lengths (Å) for **2h**

Ru–C(1)	2.149(5)	Ru–C(2)	2.171(5)
Ru–C(7)	2.166(5)	Ru–C(8)	2.137(5)
Ru–C(13)	2.389(5)	Ru–C(14)	2.232(5)
Ru–C(15)	2.287(6)	Ru–C(16)	2.289(6)
Ru–C(17)	2.220(4)	Ru–C(18)	2.292(5)
N(1)–C(13)	1.358(7)	N(1)–C(19)	1.479(9)
N(1)–C(20)	1.462(8)	O(1)–C(3)	1.221(8)
O(2)–C(3)	1.346(7)	O(2)–C(4)	1.454(8)
O(3)–C(5)	1.207(7)	O(4)–C(5)	1.353(7)
O(4)–C(6)	1.452(8)	O(5)–C(9)	1.222(7)
O(6)–C(9)	1.355(7)	O(6)–C(10)	1.448(7)
O(7)–C(11)	1.208(7)	O(8)–C(11)	1.359(7)
O(8)–C(12)	1.438(8)	C(1)–C(2)	1.422(7)
C(1)–C(3)	1.477(8)	C(2)–C(5)	1.477(8)
C(7)–C(8)	1.420(8)	C(7)–C(9)	1.484(7)
C(8)–C(11)	1.482(8)	C(13)–C(14)	1.451(8)
C(13)–C(18)	1.418(8)	C(14)–C(15)	1.421(7)
C(15)–C(16)	1.402(8)	C(16)–C(17)	1.41(1)
C(17)–C(18)	1.430(8)		

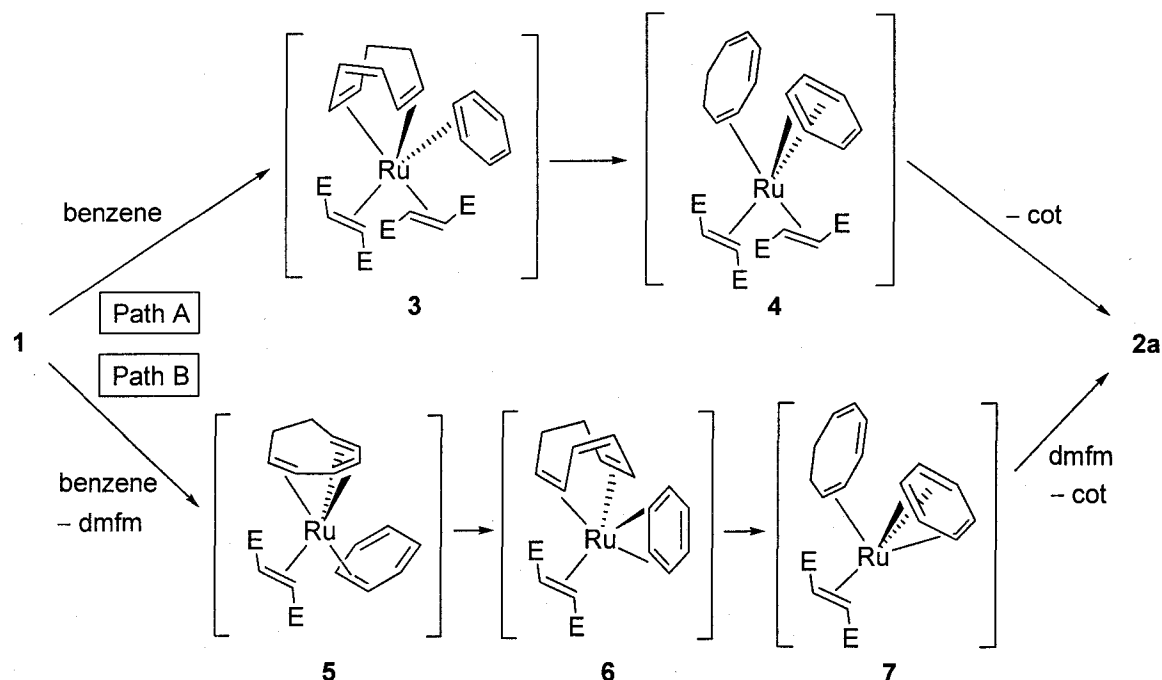
Table 8. Selected Bond Angles (deg) for **2h**

C(1)–Ru–C(2)	38.4(2)	C(1)–Ru–C(7)	89.9(2)
C(1)–Ru–C(8)	89.4(2)	C(1)–Ru–C(13)	119.5(2)
C(1)–Ru–C(14)	97.7(2)	C(1)–Ru–C(15)	102.5(2)
C(1)–Ru–C(16)	128.6(2)	C(1)–Ru–C(17)	165.0(3)
C(1)–Ru–C(18)	152.5(2)	C(2)–Ru–C(7)	113.5(2)
C(2)–Ru–C(8)	90.5(2)	C(2)–Ru–C(13)	89.1(2)
C(2)–Ru–C(14)	85.8(2)	C(2)–Ru–C(15)	112.2(2)
C(2)–Ru–C(16)	147.9(2)	C(2)–Ru–C(17)	152.2(2)
C(2)–Ru–C(18)	115.6(2)	C(7)–Ru–C(8)	38.5(2)
C(7)–Ru–C(13)	149.7(2)	C(7)–Ru–C(14)	155.6(2)
C(7)–Ru–C(15)	119.0(2)	C(7)–Ru–C(16)	91.9(2)
C(7)–Ru–C(17)	89.4(2)	C(7)–Ru–C(18)	114.5(2)
C(8)–Ru–C(13)	127.4(2)	C(8)–Ru–C(14)	163.3(2)
C(8)–Ru–C(15)	155.4(2)	C(8)–Ru–C(16)	121.2(2)
C(8)–Ru–C(17)	99.3(3)	C(8)–Ru–C(18)	101.9(2)
C(13)–Ru–C(14)	36.4(2)	C(13)–Ru–C(15)	64.8(2)
C(13)–Ru–C(16)	75.8(2)	C(13)–Ru–C(17)	64.2(2)
C(13)–Ru–C(18)	35.2(2)	C(14)–Ru–C(15)	36.6(2)
C(14)–Ru–C(16)	65.2(2)	C(14)–Ru–C(17)	77.3(2)
C(14)–Ru–C(18)	65.5(2)	C(15)–Ru–C(16)	35.7(2)
C(15)–Ru–C(17)	65.0(3)	C(15)–Ru–C(18)	77.3(2)
C(16)–Ru–C(17)	36.5(3)	C(16)–Ru–C(18)	65.9(2)
C(17)–Ru–C(18)	36.9(2)	C(2)–C(1)–C(3)	120.7(5)
C(1)–C(2)–C(5)	122.5(5)	C(7)–C(8)–C(11)	117.8(5)
C(8)–C(7)–C(9)	122.7(5)	C(14)–C(13)–C(18)	117.2(5)
N(1)–C(13)–C(14)	121.6(5)	N(1)–C(13)–C(18)	121.1(6)
C(13)–N(1)–C(19)	119.4(5)	C(13)–N(1)–C(20)	120.6(6)
C(19)–N(1)–C(20)	117.9(5)		

the three equatorial positions. As mentioned above, two dimethyl fumarates coordinate to ruthenium C_2 -symmetrically to avoid the steric hindrance. The bond lengths between ruthenium and the four olefinic carbons of dimethyl fumarates in **2g** [Ru–C(1), C(2), C(7), and C(8)] are in the range of 2.128(6)–2.164(5) Å, and are thus slightly shorter than those of the corresponding bonds in **1** [2.155(5)–2.204(5) Å].³² The C–C double-bond lengths of the dimethyl fumarates in **2g** [1.409(8) and 1.419(8) Å] are almost as long as those in **1** [1.408(8) and 1.431(7) Å].³²

Although the displacement mechanism has not yet been clarified, two pathways can be considered (Scheme 1). *Path A* shows a straightforward exchange mechanism between cyclooctatriene and arene without dissociation of

Scheme 1. Possible Displacement Mechanisms



dimethyl fumarate. On the other hand, in *Path B*, the release of a dimethyl fumarate ligand is followed by displacement of the *cot* ligand with arene and re-coordination of dimethyl fumarate to give **2**. While the intermediates **3–7** have not yet been detected, monodentate amine- and phosphine-ligated analogues of **5**, i.e., $\text{Ru}(\eta^6\text{-cot})(\text{dmfm})(\text{NR}_3)^{33\text{b}}$ and $\text{Ru}(\eta^6\text{-cot})(\text{dmfm})(\text{PR}_3)^{34}$ have been obtained by reacting **1** with corresponding ligands. The analogues of **6**, $\text{Ru}(\eta^4\text{-cot})(\text{dmfm})(\text{N}\text{N})^{33\text{a}}$ (NN = 2,2-bipyridyl or 1,10-phenanthroline) and $\text{Ru}(\eta^4\text{-cot})(\text{dmfm})(\text{dppm})^{35}$ [dppm = bis(diphenylphosphino)methane] have also been synthesized in a similar manner. Thus, one of the two dimethyl fumarate ligands in **1** was found to be labile. In addition, the re-coordination of dimethyl fumarate has been demonstrated. The reaction of **1** with excess pyridine (py) first gave $\text{Ru}(\eta^6\text{-cot})(\text{dmfm})(\text{py})$ at room temperature, which was then converted into $\text{Ru}(\text{dmfm})_2(\text{py})_3$ at 115 °C.^{33c} The reaction of **1** with tridentate nitrogen ligands (NNN) gave a mixture of stereoisomers of $\text{Ru}(\text{dmfm})_2(\text{N}\text{N}\text{N})$ via the ligand exchange from *cot* to a tridentate nitrogen ligand. The stereoisomers are different from each other at the coordinated

enantiofaces of one of the dimethyl fumarate ligands, which means that the cot ligand is not directly substituted by a tridentate nitrogen ligand.^{33c} Considering these facts, while we can not rule out *Path A*, *Path B* is more likely.

Conclusion

A novel additive-free displacement of cyclooctatriene by arenes on zerovalent ruthenium was achieved. X-ray crystallography of Ru(η^6 -anisole)-(dmfm)₂ and Ru(η^6 -*N,N*-dimethylaniline)(dmfm)₂ revealed that the coordination geometry of both complex can be represented by a highly distorted trigonal bipyramid, and confirmed that each of these complexes is a zerovalent complex following the 18-electron rule. Further studies on the stoichiometric and catalytic reactivity of these complexes are expected.

Experimental Section

Materials and Methods. All manipulations were performed under an argon atmosphere using standard Schlenk techniques. Ru(cot)(dmfm)₂ (**1**) was synthesized as we reported previously.³² All solvents were distilled under argon over appropriate drying reagents (sodium, calcium hydride, sodium-benzophenone or calcium chloride).

Physical and Analytical Measurements. NMR spectra were recorded on JEOL EX-400 (FT, 400 MHz (¹H), 100 MHz (¹³C)) and AL-300 (FT, 300 MHz (¹H), 75 MHz (¹³C)) spectrometers. Chemical shift values (δ) for ¹H and ¹³C are referenced to internal solvent resonances and reported relative to SiMe₄. NMR data for **2a–k** are summarized in Table 1 (¹H) and Table 2 (¹³C). IR spectra were recorded on a Nicolet Impact 410 FT-IR spectrometer. Melting points were determined under argon on a Yanagimoto micro melting point apparatus. HR-MS spectra were recorded on JEOL SX102A spectrometers with

m-nitrobenzyl alcohol (*m*-NBA) as a matrix. Elemental analyses were performed at the Microanalytical Center of Kyoto University.

Synthesis of Ru(η^6 -benzene)(dmfm)₂ (2a). A mixture of Ru(cot)(dmfm)₂ [1; 0.30 g, 0.61 mmol] and 5.0 mL of benzene was placed in a 50 mL stainless steel autoclave equipped with a glass liner and a magnetic stirring bar. The mixture was stirred at 110 °C for 2 h, and then chromatographed on alumina. Elution with CHCl₃ gave a yellow solution, from which the solvent was evaporated and the residue was recrystallized from Et₂O to give **2a** as pale-yellow microcrystals (0.19 g, 66%).

Complex **2a**: mp 185–187 °C dec. IR (KBr disk): 1738 cm⁻¹. HR-MS (FAB-*m*NBA): *m/z* 469.0420 (M + H)⁺, calcd for C₂₀H₂₇O₈Ru 469.0436.

Synthesis of Ru(η^6 -toluene)(dmfm)₂ (2b). A suspension of Ru(cot)-(dmfm)₂ [1; 0.50 g, 1.0 mmol] in 5.0 mL of toluene was stirred at 110 °C for 2 h, and then chromatographed on alumina. Elution with CHCl₃ gave a yellow solution, from which the solvent was evaporated and the residue was recrystallized from Et₂O to give **2b** as pale-yellow microcrystals (0.31 g, 64%).

Complex **2b**: mp 156–159 °C dec. IR (KBr disk): 1689 cm⁻¹. HR-MS (FAB-*m*NBA): *m/z* 483.0630 (M + H)⁺, calcd for C₁₉H₂₅O₈Ru 483.0593.

Synthesis of Ru(η^6 -*p*-xylene)(dmfm)₂ (2c). A suspension of Ru(cot)-(dmfm)₂ [1; 0.50 g, 1.0 mmol] in 5.0 mL of *p*-xylene was stirred at 110 °C for 2 h, and then chromatographed on alumina. Elution with CHCl₃ gave a yellow solution, from which the solvent was evaporated and the residue was recrystallized from Et₂O to give **2c** as pale-yellow microcrystals (0.35 g, 66%).

Complex **2c**: mp 152–153 °C dec. IR (KBr disk): 1691, 1710 cm⁻¹. HR-MS (FAB-*m*NBA): *m/z* 497.0735 (M + H)⁺, calcd for C₂₀H₂₇O₈Ru 497.0749.

Synthesis of Ru(η^6 -mesitylene)(dmfm)₂ (2d). A suspension of Ru(cot)-(dmfm)₂ [1; 0.50 g, 1.0 mmol] in 5.0 mL of mesitylene was stirred at 110 °C for 2 h, and then chromatographed on alumina. Elution with CHCl₃ gave a yellow solution, from which the solvent was evaporated and the residue was

recrystallized from Et₂O to give **2d** as pale-yellow microcrystals (0.38 g, 74%).

Complex **2d**: mp 114–116 °C dec. IR (KBr disk): 1709 cm⁻¹. Anal. Calcd for C₂₁H₂₈O₈Ru: C, 49.50; H 5.54. Found: C, 49.30; H, 5.54.

Synthesis of Ru(η^6 -hexamethylbenzene)(dmfm)₂ (2e). A mixture of Ru(cot)(dmfm)₂ [**1**; 0.39 g, 0.78 mmol], hexamethylbenzene (0.20 g, 0.94 mmol) and 5.0 mL of diglyme was stirred at 110 °C for 2 h, and then chromatographed on alumina. Elution with CHCl₃ gave a yellow solution, from which the solvent was evaporated and the residue was recrystallized from Et₂O to give **2e** as brown microcrystals (0.13 g, 30%).

Complex **2e**: mp 231–233 °C dec. IR (KBr disk): 1686 cm⁻¹. HR-MS (FAB-*m*NBA): *m/z* 553.1371 (M + H)⁺, calcd for C₂₄H₃₅O₈Ru 553.1375.

Synthesis of Ru(η^6 -*t*-butylbenzene)(dmfm)₂ (2f). A suspension of Ru(cot)(dmfm)₂ [**1**; 0.25 g, 0.50 mmol] in 5.0 mL of *t*-butylbenzene was stirred at 110 °C for 2 h, and then chromatographed on alumina. Elution with CHCl₃ gave a yellow solution, from which the solvent was evaporated and the residue was recrystallized from Et₂O to give **2f** as pale-yellow microcrystals (0.16 g, 61%).

Complex **2f**: mp 125–126 °C dec. IR (KBr disk): 1693 cm⁻¹. HR-MS (FAB-*m*NBA): *m/z* 525.1053 (M + H)⁺, calcd for C₂₀H₂₇O₈Ru 525.1062.

Synthesis of Ru(η^6 -anisole)(dmfm)₂ (2g). A suspension of Ru(cot)(dmfm)₂ [**1**; 0.35 g, 0.71 mmol] in 6.0 mL of anisole was stirred at 110 °C for 2 h, and then chromatographed on alumina. Elution with CHCl₃ gave a yellow solution, from which the solvent was evaporated and the residue was recrystallized from Et₂O to give **2g** as pale-yellow microcrystals (0.20 g, 59%).

Complex **2g**: mp 204–206 °C dec. IR (KBr disk): 1691 cm⁻¹. HR-MS (FAB-*m*NBA): *m/z* 499.0564 (M + H)⁺, calcd for C₁₉H₂₅O₉Ru 499.0542.

Synthesis of Ru(η^6 -*N,N*-dimethylaniline)(dmfm)₂ (2h). A suspension of Ru(cot)(dmfm)₂ [**1**; 0.35 g, 0.71 mmol] in 5.0 mL of *N,N*-dimethylaniline was stirred at 110 °C for 2 h, and then chromatographed on alumina. Elution with

CHCl₃ gave a yellow solution, from which the solvent was evaporated and the residue was recrystallized from Et₂O to give **2h** as pale-yellow microcrystals (0.27 g, 77%).

Complex **2h**: mp 166–168 °C dec. IR (KBr disk): 1690 cm⁻¹. HR-MS (FAB-*m*NBA): *m/z* 512.0850 (M + H)⁺, calcd for C₂₀H₂₈NO₈Ru 512.0858.

Synthesis of Ru(η^6 -biphenyl)(dmfm)₂ (2i). A mixture of Ru(cot)(dmfm)₂ [**1**; 0.50 g, 1.0 mmol] and biphenyl (2.0 g) was stirred at 110 °C for 2 h, and then chromatographed on alumina. Elution with CHCl₃ gave a yellow solution, from which the solvent was evaporated and the residue was recrystallized from Et₂O to give **2i** as pale-yellow microcrystals (0.33 g, 61%).

Complex **2i**: mp 162–163 °C dec. IR (KBr disk): 1703 cm⁻¹. HR-MS (FAB-*m*NBA): *m/z* 545.0772 (M + H)⁺, calcd for C₂₄H₂₇O₈Ru 545.0749.

Synthesis of Ru(η^6 -methyl benzoate)(dmfm)₂ (2j). A suspension of Ru(cot)(dmfm)₂ [**1**; 0.25 g, 0.50 mmol] in 4.0 mL of methyl benzoate was stirred at 110 °C for 2 h, and then chromatographed on alumina. Elution with CHCl₃ gave a yellow solution, from which the solvent was evaporated and the residue was recrystallized from Et₂O to give **2j** as pale-yellow microcrystals (0.030 g, 13%).

Complex **2j**: mp 203–205 °C dec. IR (KBr disk): 1708 cm⁻¹. HR-MS (FAB-*m*NBA): *m/z* 527.0508 (M + H)⁺, calcd for C₂₀H₂₅O₁₀Ru 527.0491.

Synthesis of Ru(η^6 -naphthalene)(dmfm)₂ (2k). A mixture of Ru(cot)(dmfm)₂ [**1**; 0.30 g, 0.61 mmol] and naphthalene (2.0 g) was stirred at 110 °C for 2 h, and then chromatographed on alumina. Elution with CHCl₃ gave a yellow solution, from which the solvent was evaporated and the residue was recrystallized from Et₂O/pentane to give **2k** as brown microcrystals (0.19 g, 60%).

Complex **2k**: mp 183–185 °C dec. IR (KBr disk): 1691, 1702 cm⁻¹. HR-MS (FAB-*m*NBA): *m/z* 519.0604 (M + H)⁺, calcd for C₂₂H₂₅O₈Ru 519.0593.

Crystallographic Study of Complexes 2g and 2h. Single crystals of complexes **2g** and **2h** obtained by recrystallization from CHCl₃/pentane were subjected to X-ray crystallographic analyses. The crystal data and experimental details for **2g** and **2h** are summarized in Table 4. All measurements were made on a Rigaku RAXIS imaging plate area detector with graphite monochromated Mo K α radiation ($\lambda = 0.71069$ Å). The structures were solved by direct methods using SIR92³⁷ and expanded using Fourier techniques (DIRDIF99).³⁸ The non-hydrogen atoms were refined anisotropically and hydrogen atoms were refined isotropically. Neutral atom scattering factors were taken from Cromer and Waber.³⁹ Anomalous dispersion effects were included in F_{calc} ⁴⁰; the values for $\Delta f'$ and $\Delta f''$ were those of Creagh and McAuley.⁴¹ The values for the mass attenuation coefficients were those of Creagh and Hubbell.⁴² All calculations were performed using the CrystalStructure^{43,44} crystallographic software package. In Figures 1 and 2, thermal ellipsoids are shown at the 30% and 50% probability level, respectively, and all hydrogen atoms are omitted for clarity.

References

- (1) Le Bozec, H.; Touchard, D.; Dixneuf, P. H. *Adv. Organomet. Chem.* **1989**, *29*, 163.
- (2) Bennett, M. A. In *Comprehensive Organometallic Chemistry II*; Abel, E. W., Stone, F. G. A., Wilkinson, G., Eds.; Pergamon: Oxford, U.K., 1995; Vol. 7, p 549.
- (3) Itoh, K.; Mukai, K.; Nagashima, H.; Nishiyama, H. *Chem. Lett.* **1983**, 499.
- (4) Lucherini, A.; Porri, L. *J. Organomet. Chem.* **1978**, *155*, C45.
- (5) (a) Pertici, P.; Verrazzani, A.; Pitzalis, E.; Caporusso, A. M.; Vitulli, G. *J. Organomet. Chem.* **2001**, *621*, 246. (b) Pertici, P. Verrazzani, A.; Vitulli, G.; Baldwin, R.; Bennett, M. A. *J. Organomet. Chem.* **1998**, *551*, 37.
- (6) Fischer, E. O.; Elschenbroich, C. *Chem. Ber.* **1970**, *103*, 162.

- (7) Joslin, F. L.; Roundhill, D. M. *Organometallics* **1992**, *11*, 1749.
- (8) Bennett, M. A.; Matheson, T. W.; Robertson, G. B.; Smith, A. K.; Tucker, P. A. *J. Organomet. Chem.* **1976**, *121*, C18.
- (9) Hull, J. W.; Gladfelter, W. L. *Organometallics* **1984**, *3*, 605.
- (10) Bennett, M. A.; Neumann, H.; Thomas, M.; Wang, X. Q.; Pertici, P.; Salvadori, P.; Vitulli, G. *Organometallics* **1991**, *10*, 3237.
- (11) (a) Werner, H.; Roder, K. *J. Organomet. Chem.* **1989**, *367*, 339. (b) Werner, R.; Werner, H. *Chem. Ber.* **1982**, *115*, 3781. (c) Werner, H.; Werner, R. *J. Organomet. Chem.* **1979**, *174*, C63. (d) Werner, H.; Werner, R. *Angew. Chem., Int. Ed. Engl.* **1978**, *17*, 683.
- (12) tom Dieck, H.; Kollvitz, W.; Kleinwächter, I. *Organometallics* **1986**, *5*, 1449.
- (13) (a) Steed, J. W.; Tocher, D. A. *J. Chem. Soc., Dalton Trans.* **1993**, 3187. (b) Steed, J. W.; Tocher, D. A. *J. Organomet. Chem.* **1993**, *444*, C47.
- (14) Rybinskaya, M. I.; Kaganovich, V. S.; Kudinov, A. R. *J. Organomet. Chem.* **1982**, *235*, 215.
- (15) Jones, D.; Pratt, L.; Wilkinson, G. *J. Chem. Soc.* **1962**, 4458.
- (16) (a) Bennett, M. A.; Matheson, T. W. *J. Organomet. Chem.* **1978**, *153*, C25. (b) Bennett, M. A.; Huang, T. N.; Matheson, T. W.; Smith, A. K. *Inorg. Synth.* **1982**, *21*, 74.
- (17) Pertici, P.; Bertozzi, S.; Lazzaroni, R.; Vitulli, G.; Bennett, M. A. *J. Organomet. Chem.* **1988**, *354*, 117.
- (18) Bauer, A.; Englert, U.; Geyser, S.; Podewils, F.; Salzer, A. *Organometallics* **2000**, *19*, 5471.
- (19) Mueller, J.; Kreiter, C. G.; Merschenk, B.; Schmitt, S. *Chem. Ber.* **1975**, *108*, 273.
- (20) (a) Pertici, P.; Vitulli, G.; Paci, M.; Porri, L. *J. Chem. Soc., Dalton Trans.* **1980**, 1961. (b) Pertici, P.; Vitulli, G.; Porri, L. *J. Chem. Soc., Chem. Commun.* **1975**, 846.

- (21) Crocker, M.; Green, M.; Howard, J. A. K.; Norman, N. C.; Thomas, D. M. *J. Chem. Soc., Dalton Trans.* **1990**, 2299.
- (22) Luo, S.; Rauchfuss, T. B.; Wilson, S. R. *J. Am. Chem. Soc.* **1992**, *114*, 8515.
- (23) (a) Swann, R. T.; Hanson, A. W.; Boekelheide, V. *J. Am. Chem. Soc.* **1986**, *108*, 3324. (b) Swann, R. T.; Boekelheide, V. *Tetrahedron Lett.* **1984**, 899. (c) Grundy, S. L.; Maitlis, P. M. *J. Chem. Soc., Chem. Commun.* **1982**, 379.
- (24) Bennett, M. A.; Matheson, T. W.; Robertson, G. B.; Smith, A. K.; Tucker, P. A. *Inorg. Chem.* **1980**, *19*, 1014.
- (25) Rosa, P.; Ricard, L.; Mathey, F.; Le Floch, P. *Organometallics* **1999**, *18*, 3348.
- (26) Crocker, M.; Froom, S. F. T.; Green, M.; Nagle, K. R.; Orpen, A. G.; Thomas, D. M. *J. Chem. Soc., Dalton Trans* **1987**, 2803.
- (27) Müller, J.; Qiao, K.; Siewing, M.; Westphal, B. *J. Organomet. Chem.* **1993**, *458*, 219.
- (28) Hull, J. W.; Gladfelter, W. L. *Organometallics* **1982**, *1*, 1716.
- (29) Koola, J. D.; Roddick, D. M. *J. Am. Chem. Soc.* **1991**, *113*, 1450.
- (30) (a) Pertici, P.; Vitulli, G.; Bertozzi, S.; Lazzaroni, R. *Inorg. Chim. Acta* **1988**, *149*, 235. (b) Pertici, P.; Vitulli, G.; Lazzaroni, R.; Salvadori, P.; Barili, P. L. *J. Chem. Soc., Dalton Trans.* **1982**, 1019. (c) Pertici, P.; Simonelli, G.-P.; Vitulli, G.; Deganello, G.; Sandrini, P.-L.; Mantovani, A. *J. Chem. Soc., Chem. Commun.* **1977**, 132.
- (31) Vitulli, G.; Pertici, P.; Salvadori, P. *J. Chem. Soc., Dalton Trans.* **1984**, 2255.
- (32) Mitsudo, T.; Suzuki, T.; Zhang, S.-W.; Imai, D.; Fujita, K.; Manabe, T.; Shiotsuki, M.; Watanabe, Y.; Wada, K.; Kondo, T. *J. Am. Chem. Soc.* **1999**, *121*, 1839.
- (33) (a) Suzuki, T.; Shiotsuki, M.; Wada, K.; Kondo, T.; Mitsudo, T.

- Organometallics* **1999**, *18*, 3671. (b) Suzuki, T.; Shiotsuki, M.; Wada, K.; Kondo, T.; Mitsudo, T. *J. Chem. Soc., Dalton Trans.* **1999**, 4231. (c) Shiotsuki, M.; Suzuki, T.; Iida, K.; Ura, Y.; Wada, K.; Kondo, T.; Mitsudo, T. *Organometallics*, in press.
- (34) Shiotsuki, M.; Suzuki, T.; Kondo, T.; Wada, K.; Mitsudo, T. *Organometallics* **2000**, *19*, 5733.
- (35) Shiotsuki, M.; Miyai, H.; Ura, Y.; Suzuki, T.; Kondo, T.; Mitsudo, T. *Organometallics* **2002**, *21*, 4960.
- (36) Ura, Y.; Sato, Y.; Shiotsuki, M.; Suzuki, T.; Wada, K.; Kondo, T.; Mitsudo, T. *Organometallics*, **2003**, *22*, 77.
- (37) Altomare, A.; Cascarano, G.; Giacovazzo, C.; Guagliardi, A.; Burla, M.; Polidori, G.; Camalli, M. *J. Appl. Cryst.* **1994**, *27*, 435.
- (38) Beurskens, P. T.; Admiraal, G.; Beurskens, G.; Bosman, W. P.; de Gelder, R.; Israel, R.; Smits, J. M. M. *The DIRDIF-99 program system*; Technical Report of the Crystallography Laboratory: University of Nijmegen, Netherlands, **1999**.
- (39) Cromer, D. T.; Waber, J. T. *International Tables for X-ray Crystallography*; The Kynoch Press: Birmingham, England, Vol. IV, **1974**.
- (40) Ibers, J. A.; Hamilton, W. C. *Acta Crystallogr.* **1964**, *17*, 781.
- (41) Creagh, D. C.; McAuley, W. J. *International Tables for X-ray Crystallography*; Kluwer Academic Publishers, Boston, Vol. C, **1992**.
- (42) Creagh, D. C.; Hubbell, J. H. *International Tables for X-ray Crystallography*; Kluwer Academic Publishers, Boston, Vol. C, **1992**.
- (43) CrystalStructure 2.00, *Crystal Structure Analysis Package*, Rigaku and MSC, **2001**.
- (44) Watkin, D. J.; Prout, C. K.; Carruthers, J. R.; Betteridge, P. W. *CRYSTALS Issue 10*; Chemical Crystallography Laboratory: Oxford, UK.

General Conclusion

The synthesis of novel zerovalent ruthenium complexes derived from $\text{Ru}(\eta^6\text{-cot})(\text{dmfm})_2$ [**1**; cot = 1,3,5-cyclooctatriene, dmfm = dimethyl fumarate] and their detailed reactivity were described in this thesis, which consists of five chapters.

Chapter 1 dealt the reactions of **1** with mono- or bidentate phosphorus ligands. Novel ruthenium(0) phosphine complexes, $\text{Ru}(\eta^6\text{-cot})(\text{dmfm})(\text{L})$ [L = triphenylphosphine, diphenylmethylphosphine, dimethylphenylphosphine, and triethylphosphine], were prepared in high yields by the reaction of **1** with monodentate tertiary phosphine ligands. The NMR spectra of these complexes show fluxionality in solution, and the X-ray crystallography elucidated that the difference of coordination mode of the cot ligand depends on a sort of coordinated phosphine ligand. These results indicated that the fluxionality is based on the rotation of the cot ligand. On the other hand, the reaction of **1** with a bidentate phosphine ligand, dppe [dppe = 1,2-bis(diphenylphosphino)ethane], gave two kinds of novel complexes, $\text{Ru}(\text{dmfm})(\text{dppe})_2$ and $\text{Ru}(\text{alkenyl})(\text{alkyl})(\text{dppe})$, according to the amount of dppe. $\text{Ru}(\text{dmfm})(\text{dppe})_2$ is formed via the dissociation of cot and one of the dmfm ligands followed by the coordination of two moles of dppe. $\text{Ru}(\text{alkenyl})(\text{alkyl})(\text{dppe})$ is generated by the activation of the sp^2 carbon–hydrogen bond of dimethyl fumarate, and then the insertion of the other dimethyl fumarate into the formed ruthenium–hydrogen bond. The treatment of $\text{Ru}(\text{alkenyl})(\text{alkyl})(\text{dppe})$ with 1 atm of carbon monoxide afforded $\text{Ru}(\text{alkenyl})(\text{alkyl})(\text{dppe})(\text{CO})$ by the dissociation of the carbonyl oxygen of the β -methoxycarbonylalkyl ligand. Further, the reaction of $\text{Ru}(\text{alkenyl})(\text{alkyl})(\text{dppe})$ with 60 atm of carbon monoxide gave dimers of dimethyl fumarate and $\text{Ru}(\text{CO})_3(\text{dppe})$ via reductive elimination. A series of the reactions are considered as a model stepwise reaction of catalytic dimerization of olefinic compounds, which includes the $\text{Ru}(\text{alkenyl})(\text{alkyl})$ species.

In Chapter 2, the synthesis and reactivity of a zerovalent ruthenium aqua complex were discussed in detail. The reaction of **1** with dppe in the presence of excess water afforded $\text{Ru}(\text{dmfm})_2(\text{dppe})(\text{H}_2\text{O})$, which is a quite rare example of a stable and isolable ruthenium(0) aqua complex. There have been no reports about an isolable zerovalent ruthenium aqua complex. The X-ray crystallography of this complex indicated that coordination of a water molecule to the ruthenium center is stabilized by two hydrogen bonds with the carbonyl oxygen atoms of the dmfm ligands. In the case of the reaction of **1** with dppm [dppm = bis(diphenylphosphino)methane], the product was not an aqua complex such as $\text{Ru}(\text{dmfm})_2(\text{dppm})(\text{H}_2\text{O})$ even in the presence of excess water, but a novel zerovalent complex, $\text{Ru}(\eta^4\text{-cot})(\text{dmfm})(\text{dppe})$, was obtained via the dissociation of one of dmfm and one of cot's olefinic bond followed by the coordination of dppm. This complex is considered as a model complex of the intermediate in the formation reaction of $\text{Ru}(\text{dmfm})_2(\text{dppe})(\text{H}_2\text{O})$. The reactivity of $\text{Ru}(\text{dmfm})_2(\text{dppe})(\text{H}_2\text{O})$ toward carbon monoxide was examined, and it reacted with 1 atm of carbon monoxide to give $\text{Ru}(\text{CO})_2(\text{dmfm})(\text{dppe})$ via the dissociation of H_2O and one of the dmfm ligands followed by the coordination of two carbon monoxide molecules. The NMR spectra fully elucidated the dynamic behavior of this complex in solution, which is based on the ligand rearrangement between *cis* and *trans* isomers.

Chapter 3 presented the synthesis and structure of novel zerovalent ruthenium complexes with three pyridine ligands or tridentate pyridyl ligands. Complex **1** reacted with an excess amount of pyridine to give a novel ruthenium(0) complex, $\text{Ru}(\text{dmfm})_2(\text{pyridine})_3$. Tridentate pyridyl ligands (N-N'-N) such as 2,2':6',2''-terpyridine (terpy), 2,6-bis(imino)pyridyl ligands, and 2,6-bis[(4*S*)-(-)-isopropyl-2-oxazolin-2-yl]pyridine (*i*-Pr-Pybox), reacted with **1** to give a novel ruthenium(0) complex, $\text{Ru}(\text{dmfm})_2(\text{N-N'-N})$. The NMR spectra revealed that the products are mixtures of two isomers, respectively; one of which is different from the other by the coordinating enantioface of one of the

dmfm ligands. The X-ray crystallography elucidated that the structures of these complexes can be rationalized as a distorted trigonal bipyramid, in which the outer coordinative moieties of N-N'-N occupy axial sites, and the central pyridyl moiety of N-N'-N and two dmfm ligands locate equatorial positions. These complexes are the first example of an isolable zerovalent ruthenium complex with three moles of a nitrogen ligand and tridentate nitrogen ligands. Since they are a new kind of zerovalent complex with both strong π -acceptor and σ -donor ligands, a novel characteristic reactivity is expected.

Chapter 4 depicted the synthesis of novel *p*-quinone coordinated ruthenium(0) complexes, $\text{Ru}(\eta^6\text{-cot})(p\text{-quinone})$, which was formed via the reaction of **1** with *p*-quinones. The structure of $\text{Ru}(\eta^6\text{-cot})(2,6\text{-dimethoxy-}p\text{-quinone})$ was determined by X-ray crystallography to be represented by a highly distorted trigonal bipyramid, in which the *p*-quinone ligand coordinated with two olefinic bonds. In the ^{13}C NMR spectrum, however, the carbonyl carbons of *p*-quinones were shifted upfield by ~ 30 ppm, as reported for other *p*-quinone complexes. The infrared spectra show that the $\nu(\text{C}=\text{O})$ bands of the quinone ligands appeared at $1550\sim 1610\text{ cm}^{-1}$, which are shifted to a lower wavenumber by $50\sim 100\text{ cm}^{-1}$ compared with those of the corresponding free quinones. This shift is attributable to π -back donation from ruthenium, and also supports some contribution from the resonance structure of semiquinone and hydroquinone complexes. The reaction of **1** with *p*-biquinone gave a novel bimetallic zerovalent complex $\{\text{Ru}(\eta^6\text{-cot})\}_2(p\text{-biquinone})$. The structure of the *p*-biquinone complex was determined by X-ray crystallography, in which *p*-biquinone coordinates to two isolated $\text{Ru}(\text{cot})$ moieties with a unique mode and the two $\text{Ru}(\text{cot})$ groups are located at endo positions.

Chapter 5 displayed the synthesis of novel zerovalent arene complexes bearing two dimethyl fumarate ligands, $\text{Ru}(\eta^6\text{-arene})(\text{dmfm})_2$ [arene = benzene, toluene, *p*-xylene, mesitylene, hexamethylbenzene, *t*-butylbenzene, anisole, *N,N*-dimethylaniline, biphenyl, methyl benzoate, naphthalene] by the direct

ligand-exchange reaction of **1** with arenes. This synthetic method does not need any additives which are essential to the conventional synthesis of zerovalent ruthenium arene complexes. The X-ray crystallography of $\text{Ru}(\eta^6\text{-anisole})(\text{dmfm})_2$ and $\text{Ru}(\eta^6\text{-}N,N\text{-dimethylaniline})(\text{dmfm})_2$ revealed that the coordination geometry of both complexes is represented by a highly distorted trigonal bipyramid, and confirmed that these complexes are zerovalent complexes following the 18-electron rule.

As described above, a various kind of zerovalent ruthenium complexes were synthesized from $\text{Ru}(\eta^6\text{-cot})(\text{dmfm})_2$ (**1**). The common feature of the obtained zerovalent complexes is the coordination of strong π -acceptor ligands such as dimethyl fumarate or *p*-quinones, which makes the active zerovalent complex stable and isolable. The π -acidity of the coordinated ligands is one of the factors determining the reactivity of the complex so that it is very important to control the π -acidity of the ligands. In this sense, the newly prepared complexes in this thesis, for instance, $\text{Ru}(\text{dmfm})_2(\text{N-N'-N})$ that has both of strong σ -donor and π -acceptor ligands, are expected to have distinctive features in both stoichiometric and catalytic reactivity. The author strongly believes that these new complexes lead us to a new frontier of organometallic chemistry.

List of Publications

- Chapter 1 **Reaction of Ru(1-6- η -cyclooctatriene)(η^2 -dimethyl fumarate)₂ with Monodentate and Bidentate Phosphines: A Model Reaction of Catalytic Dimerization of Alkenes**
Masashi Shiotsuki, Toshiaki Suzuki, Teruyuki Kondo, Kenji Wada, and Take-aki Mitsudo
Organometallics **2000**, *19*, 5733–5743.
- Chapter 2 **Synthesis, Structure, and Reactivity of a Stable Zerovalent Ruthenium Aqua Complex**
Masashi Shiotsuki, Hiroshi Miyai, Yasuyuki Ura, Toshiaki Suzuki, Teruyuki Kondo, and Take-aki Mitsudo
Organometallics **2002**, *21*, 4960–4964.
- Chapter 3 **Synthesis and Structure of Novel Zerovalent Ruthenium Complexes with Three Pyridine Ligands or Tridentate Pyridyl Ligands**
Masashi Shiotsuki, Toshiaki Suzuki, Kazuo Iida, Yasuyuki Ura, Kenji Wada, Teruyuki Kondo, and Take-aki Mitsudo
Organometallics **2003**, in press.
- Chapter 4 **Synthesis and Structures of Novel Zerovalent Ruthenium *p*-Quinone Complexes and a Bimetallic *p*-Biquinone Complex**
Yasuyuki Ura, Yoshitaka Sato, Masashi Shiotsuki, Toshiaki Suzuki, Kenji Wada, Teruyuki Kondo, and Take-aki Mitsudo
Organometallics **2003**, *22*, 77.

Chapter 5 **Synthesis of Novel Zerovalent Ruthenium η^6 -Arene Complexes via Direct Displacement of a 1,3,5-Cyclooctatriene Ligand by Arenes**

Yasuyuki Ura, Masashi Shiotsuki, Kazuo Sadaoka, Toshiaki Suzuki, Teruyuki Kondo, and Take-aki Mitsudo
Organometallics, submitted.

The following publications are not included in this dissertation

- (1) **Novel Ruthenium Complex-Catalyzed Dimerization of 2,5-Norbornadiene to Pentacyclo[6.6.0.0^{2,6}.0^{3,13}.0^{10,14}]tetradeca-4,11-diene Involving Carbon–Carbon Bond Cleavage**
Take-aki Mitsudo, Toshiaki Suzuki, Shi-Wei Zhang, Daisuke Imai, Ken-ichi Fujita, Takao Manabe, Masashi Shiotsuki, Yoshihisa Watanabe, Kenji Wada, and Teruyuki Kondo
J. Am. Chem. Soc. **1999**, *121*, 1839–1850.
- (2) **Syntheses and Structures of Novel Zerovalent 2,2'-Bipyridyl or 1,10-Phenanthroline Ruthenium Complexes**
Toshiaki Suzuki, Masashi Shiotsuki, Kenji Wada, Teruyuki Kondo, and Take-aki Mitsudo
Organometallics **1999**, *18*, 3671–3678.
- (3) **Syntheses and Structures of Novel Zerovalent Ruthenium Monodentate Amine Complexes**
Toshiaki Suzuki, Masashi Shiotsuki, Kenji Wada, Teruyuki Kondo, and Take-aki Mitsudo
J. Chem. Soc., Dalton Trans. **1999**, 4231–3237.

- (4) **Rapid Ruthenium-Catalyzed Synthesis of Pyranopyrandiones by Reconstructive Carbonylation of Cyclopropenones Involving C–C Bond Cleavage**
Teruyuki Kondo, Yushi Kaneko, Yoshinori Taguchi, Ayako Nakamura, Takumi Okada, Masashi Shiotsuki, Yasuyuki Ura, Kenji Wada, and Take-aki Mitsudo
J. Am. Chem. Soc. **2002**, *124*, 6824–6825.
- (5) **Novel Synthesis of Benzenepolycarboxylates by Ruthenium-Catalyzed Cross-Benzannulation of Acetylenedicarboxylates with Allylic Compounds**
Teruyuki Kondo, Yushi Kaneko, Fumiaki Tsunawaki, Takumi Okada, Masashi Shiotsuki, Yasuhiro Morisaki, and Take-aki Mitsudo
Organometallics **2002**, *21*, 4564–4567.
- (6) **Palladium-Catalyzed Allylic Alkylation Using Chiral Hydrazones as Ligands**
Takashi Mino, Masashi Shiotsuki, Nozomi Yamamoto, Tomoe Suenaga, Masami Sakamoto, Tsutomu Fujita, and Masakazu Yamashita
J. Org. Chem. **2001**, *66*, 1795–1797.
- (7) **Synthesis of Novel Ruthenium and Rhodium Complexes with a Silsesquioxane-Based Phosphine Ligand**
Kenji Wada, Daisuke Izuhara, Masashi Shiotsuki, Teruyuki Kondo, and Take-aki Mitsudo
Chem. Lett. **2001**, 734–735.

(8) **Synthesis of Alkenylene-Bridged Macrocyclic Silsesquioxanes
by Ruthenium or Rhodium-Catalyzed Ring-Closing Reactions
of Bis(allyldimethylsilyl) Groups**

Kenji Wada, Daisuke Izuhara, Koichi Yamada, Masashi Shiotsuki,
Teruyuki Kondo, and Take-aki Mitsudo

Chem. Commun. **2001**, 1802–1803.